THE UNIVERSITY
of EDINBURGH

This thesis has been submitted in fulfilment of the requirements for a postgraduate degree (e.g. PhD, MPhil, DClinPsychol) at the University of Edinburgh. Please note the following terms and conditions of use:

This work is protected by copyright and other intellectual property rights, which are retained by the thesis author, unless otherwise stated.
A copy can be downloaded for personal non-commercial research or study, without prior permission or charge.
This thesis cannot be reproduced or quoted extensively from without first obtaining permission in writing from the author.
The content must not be changed in any way or sold commercially in any format or medium without the formal permission of the author.
When referring to this work, full bibliographic details including the author, title, awarding institution and date of the thesis must be given.

Facility Location Problems and Games

Thomas Byrne

Doctor of Philosophy
University of Edinburgh
2020

For maman and Vati

Declaration

I declare that this thesis was composed by myself and that the work contained therein is my own, except where explicitly stated otherwise in the text.

(*Thomas Byrne*)

Abstract

We concern ourselves with facility location problems and games wherein we must decide upon the optimal locating of facilities. A facility is considered to be any physical location to which customers travel to obtain a service, or from which an agent of the facility travels to customers to deliver a service. We model facilities by points without a capacity limit and assume that customers obtain (or are provided with) their service from the closest facility. Throughout this thesis we consider distance to be measured exclusively using the Manhattan metric, a natural choice in urban settings and also in scenarios arising from clustering for data analysis with heterogeneous dimensions. Additionally we always model the demand for the facility as continuously and uniformly distributed over some convex polygonal demand region $\mathcal{P}$ and it is only within $\mathcal{P}$ that we consider locating our facilities.

We first consider five facility location problems[1] where n facilities are present in a convex polygon in the rectilinear plane, over which continuous and uniform demand is distributed and within which a convex polygonal barrier is located (removing all demand and preventing all travel within the barrier), and the optimal location for an additional facility is sought. We begin with an in-depth analysis of the representation of the bisectors of two facilities affected by the barrier and how it is affected by the position of the additional facility. Following this, a detailed investigation into the changes in the structure of the Voronoi diagram caused by the movement of this additional facility, which governs the form of the objective function for numerous facility location problems, yields a set of linear constraints for a general convex barrier that partitions the market space into a finite number of regions within which the exact solution can be found in polynomial time. This allows us to formulate an exact polynomial-time algorithm that makes use of a triangular decomposition of the incremental Voronoi diagram and the first order optimality conditions.

Following this we study competitive location problems in a continuous setting, in which the first player ("White") places a set of n points in a rectangular domain $\mathcal{P}$ of width p and height q, followed by the second player ("Black"), who places the same number of points. Players cannot place points atop one another, nor can they move a point once it has been placed, and after all $2n$ points have been played each player wins the fraction of the board for which one of their points is closest. The goal for each player in the One-Round Voronoi Game is to score more than half of the area of $\mathcal{P}$, and that of the One-Round Stackelberg Game is to maximise one's total area. Even in the more diverse setting of Manhattan distances, we determine a complete characterisation for the One-Round Voronoi Game wherein White can win only if $\frac{p}{q} \geq n$, otherwise Black wins, and we show each player's winning strategies. For the One-Round Stackelberg Game we explore arrangements of White's points in which the Voronoi cells of individual facilities are equalised with respect to a number of attractive geometric properties such as fairness (equally-sized Voronoi cells) and local optimality (symmetrically balanced Voronoi cell areas), and explore each player's best strategy under certain conditions.

[1] These are the Conditional Median Problem, the Conditional Antimedian Problem, the Conditional Centre Problem, the Market Share Problem, and the Conditional Maximal Covering Location Problem.

Lay Summary

The problem of finding optimal locations for service facilities is of strategic importance. The optimal placement of a fire station could save a forest from destruction, that of a hospital could save numerous lives, and that of a supermarket could save thousands of minutes in customers' travel times. Although an increasing number of models have been proposed, an adequate representation of demand is often crucially neglected. In most models customer demand is assumed to be discrete and aggregated to a relatively small number of points. However, in many applications the number of potential customers can be in the millions, and representing every customer residence as a separate demand point is usually infeasible. Therefore it may be more accurate to represent customer demand as continuously distributed over some region.

Furthermore, the region of demand and the region over which a facility can be feasibly located are often assumed to be convex polygons. However, this supposition is not realistic for real-world applications. Moreover, in urban settings the predominantly used straight-line distance does not adequately represent the realised distance for the customer. Further problems arise when we introduce untraversable areas (e.g. rivers or parks) since this fundamentally alters the way we measure distances between facilities and their demand.

In this thesis we go some way in plugging the holes in such facility location models. Given a convex polygonal market region within which we have some existing facilities, constant demand, and one convex polygonal barrier, we firstly explore facility location problems where we find the best location Z of a new facility in order to optimise one of five objectives:

- to minimise the average distance between customers and their closest facility – ideal for facilities providing a service for many customers, such as hospitals;
- to maximise the average distance between customers and their closest facility – ideal for facilities which are considered undesirable to reside close to, such as refuse tips;
- to minimise the maximum distance between customers and their closest facility – ideal for facilities which must be close enough to all customers, such as fire stations;
- to maximise the number of customers serviced by chosen facilities – ideal for competitive scenarios with facilities such as shops;
- to maximise the total demand captured within a certain radius of each facility – ideal for facilities with a limited reach of service, such as 5G masts.

A great difficulty of applying these problems to our model is that the representation of these objectives changes erratically depending on where in the market region we are considering locating Z; an issue we manage to resolve by finding a partition of the market region into cells such that, for placements of Z within a cell, the objective remains stable. We can thus solve the subproblems within these cells and ultimately find the desired global optimum.

We follow this up with a study of an adaptation of the fourth problem described above in a competitive two-person game setting. In a similar manner to the set-up of the abovementioned problems, we consider demand distributed, in this instance, across a rectangular playing arena. In our formulation the leader places their points within the playing arena and the follower responds by playing the same number of points. Each player is said to control the area to which one of their points is the closest point and their score is exactly this area. We begin by considering the game where the winner is the player with the highest score (so each player wants to control over half of the playing arena) and determine which player will win depending on the aspect ratio of the playing arena. We conclude this research by pursuing a more general game where each player wishes to maximise their score (not merely win!) and discovering optimal strategies for both players.

Publications and Presentations

Some portions of material in this thesis are drawn from the following papers:

- Byrne, T., & Kalcsics, J. (2020). Conditional facility location problems with continuous demand and a polygonal barrier. *European Journal of Operational Research [under revision].*
- Byrne, T., Fekete, S. P., Kalcsics, J., & Kleist, L. (2021). Competitive location problems: balanced facility location and the one-round Manhattan Voronoi game. In *International Conference and Workshops on Algorithms and Computations (WALCOM) [to appear].* A full version can be found at arXiv: 2011.13275 (Byrne, Fekete, Kalcsics, & Kleist, 2020).

Much of the material has been curated (reordered and edited) to ensure a coherent narrative structure. Section 3.3 roughly corresponds to the main body of Byrne and Kalcsics (2020) while Chapter 4 and the outline of Chapter 6 are contained in Byrne, Fekete, Kalcsics, and Kleist (2021). Other material (notably Section 5.1) is yet to be submitted for publication, and generalises or improves op. cit., while some additions (in particular Section 3.2) provide a valuable introduction to the problems and our approaches.

I have presented this research in its many phases of development at the following events:

- Nanzan University OR Seminar Series, online, June 2020: presented *'Breaking Down Barriers – Conditional Location Problems with Continuous Demand and Polygonal Barriers'* [presenting the complete approach and proofs in Section 3.3]
- International Symposium on Locational Decisions XV and EURO Working Group on Locational Analysis XXVI, Hamburg, June 2020 [postponed due to pandemic]: aimed to present work on a new heuristic for facility location problems with continuous demand and rectilinear distances [research related to thesis] with funding from the EURO Working Group on Locational Analysis
- EURO Working Group on Locational Analysis XXV, Brussels, June 2019: presented *'Game of Zones: The One-Round Voronoi Game Played on the Rectilinear Plane'* [presenting the complete theory in Chapter 4]
- European Chapter on Combinatorial Optimisation XXXII, St Julian's, May 2019: presented *'Game of Zones: The One-Round Voronoi Game Played on the Rectilinear Plane'* [presenting the complete theory in Chapter 4]
- International Workshop on Locational Analysis and Related Problems IX, Cadiz, January 2019: presented *'The One-Round Voronoi Game Played on the Rectilinear Plane'* [covering early findings in Chapter 4]
- The OR Society Annual Conference, Lancaster, September 2018: presented *'Diamonds are a Facility Locator's Best Friend: Location Problems with Continuous Demand on a Polygon with Holes'* [presenting the complete algorithm in Section 3.2 followed by an analysis of its approach and introduction to the ideas in Section 3.3] with funding from Edinburgh Research Group in Optimisation
- European Conference of Operational Research XXIX, Valencia, July 2018: presented *'Location Problems with Continuous Demand on a Polygon with Holes: Characterising Structural Properties of Geodesic Voronoi Diagrams'* [presenting the complete algorithm in Section 3.2]

- European Chapter on Combinatorial Optimisation XXXI, Fribourg, June 2018: presented *'Location Problems with Continuous Demand on a Polygon with Holes: Characterising Structural Properties of Geodesic Voronoi Diagrams'* [presenting the complete algorithm in Section 3.2] with funding from the Laura Wisewell Travel Scholarship
- EURO Working Group on Locational Analysis XXIV, Edinburgh, May 2018: co-organised conference, produced conference book, and presented *'Location Problems with Continuous Demand on a Polygon with Holes: Characterising Structural Properties of Geodesic Voronoi Diagrams'* [presenting the complete algorithm in Section 3.2]
- International Symposium on Locational Decisions XIV, Toronto, August 2017: chaired Continuous Location III session and presented *'Location Problems with Continuous Demand on a Polygon with Holes: Characterising Structural Properties of Geodesic Voronoi Diagrams'* [introducing findings in Section 3.2] with funding from the Laura Wisewell Travel Scholarship and Principal's Go Abroad Fund.

Acknowledgements

I feel fortunate to have gained so much enjoyment from my research topic and I feel it has ideally suited my strengths and interests. The topic was introduced to me during my Master's course at the University of Edinburgh when my future supervisor, Jörg Kalcsics, approached me to ask if I would be interested in studying this challenging but rewarding area under him. It is for this reason among many others that I would like to thank Jörg first and foremost. He has been a source of bountiful knowledge and donated considerable time to my development during the early years of my PhD. I could always rely upon him to give sound advice, and to ensure that I did not forget the big picture while immersed in the nitty-gritty. I would also like to thank him for enduring my frequent jokes for four years. I just hope he doesn't regret picking me!

A visit to Edinburgh, under Jörg's invitation, by Sándor P. Fekete brought with it an offer to join another exciting research venture which has ultimately accounted for over half of the material in this thesis. I would therefore like to thank Sándor for selecting me to join the project and for presenting this new problem to me, as well as for introducing me to Linda Kleist whom I also wish to thank immensely for her inspiration and assistance in breaking the deadlock which released a deluge of results that has made the end of my PhD a riveting flurry of writing.

I would like to record my appreciation towards the Edinburgh Research Group in Optimisation (ERGO) for providing such a nurturing and congenial community. Among staff I would like to note the friendship and support of my second supervisor Sergio García Quiles and of Julian Hall, Jacek Gondzio, and Miguel F. Anjos who have been more actively invested in my future endeavours than I could have asked.

The completion of my PhD would not have been possible without the support of my EPSRC Standard Research Studentship (EP/N509644/1), and I would also like to acknowledge ERGO, the School of Mathematics, and the University of Edinburgh for the funding so generously provided to me in order to enable my attendance at important conferences and courses.

I am greatly indebted to the Optimisation and Operational Research PhD cohort at the University of Edinburgh for providing the first community of mathematicians that I truly felt a part of. My biggest thanks go to Saranthorn "Mookimooj" Phusingha, the best PhD twin sister I could have asked for. It has been a joy to spend five years studying together with both Mook and Minerva Martin Del Campo Barraza as we have grown side by side from innocent babies (Master's students) to hormonal poorly-proportioned teenagers (PhD students). I am also particularly grateful for the friendship of Filip Hanzely who was the best office mate I could have imagined. I lament that we were not able to continue our PhDs together. Regretfully, owing to lack of space, I cannot give each member of the OR (and wider) community at the University of Edinburgh (and beyond) the sentence of praise and rose-tinted recollection that they deserve, but I treasure our many happy memories.

Last, but certainly not least, I wish to express my deepest gratitude to my family. I appreciate the advice my uncle Martin has freely provided throughout my academic career; but most importantly I owe so very much to my parents. They have supported me unconditionally throughout my highs and lows of the past four years (and before then too). I owe them both a boatload of thanks for the hours they have poured into poring over my work: to my father for bravely venturing into the deep dark depths of CGAL/C++ programming, and to my mother for being a devoted editor without whom this thesis would look very much more untidy (thank you for clearing up my dangling participles!).

And I suppose thank you to my sister Anna, for staying out of my way.

Contents

Chapter 1

Introduction

Problems of optimal location are arguably among the most important in a wide range of fields, such as economics, engineering, and biology, as well as in mathematics and computer science. In recent years, they have gained a tremendous amount of importance through clustering problems in artificial intelligence. In all scenarios, the task is to choose a set of positions from a given domain, such that some optimality criteria with respect to the resulting distances to a set of demand points are satisfied.

The task of determining optimal locations for a set of facilities is of strategic importance and so, naturally, a vast number of models and algorithms have appeared in the literature; see the classic book of Drezner (1995a) with over 1200 citations, or the more recent book by Laporte, Nickel, and Saldanha da Gama (2019). It all started with the seminal works of Launhardt (1900) and Weber (1909), who were the first to study the problem in an industrial context (finding an optimal location for a plant on the plane in the presence of a single market and two suppliers); see Wesolowsky (1993) for a good discussion. In the 1960s, location problems in other domains evolved, namely on networks (Hakimi, 1964) and discrete location problems (Manne, 1964). But ever since the works of Launhardt and Weber, planar location problems have received considerable and ongoing attention in the literature: see Drezner and Hamacher (2002).

Nevertheless, despite the attention these topics garner, an adequate representation of demand is often crucially neglected. Many location problems can be modelled as optimisation problems on weighted graphs and, furthermore, the most dominant type of model by far is a purely discrete one; in most models customer demand is assumed to be discrete and aggregated to a relatively small number of points. However, the real world, being geometric in nature, gives rise to a whole range of scenarios which beset us with continuous choices over continuous data. In many urban applications the number of potential customers can be in the millions, and representing every customer residence as a separate demand point is usually infeasible. Therefore it may be more accurate to represent customer demand as continuously distributed over some region. Moreover, the uncertainty and sporadic nature of some demands lends itself much better to a continuous distribution over certain areas.

Whilst problems upon weighted graphs contain the inter-facility distances inherent in their construction, for continuous location models we must give careful consideration to our measure of distance. The most prevalent metric used in research is the Euclidean (straight line) distance. However, in a multitude applications it is simply not feasible to travel unobstructed between origin and destination, and often travel must be restricted to a network of passageways. For this reason we consider the Manhattan (rectilinear) distance, a metric ideally suited, but not limited, to urban scenarios, and implement the geodesic Manhattan metric if there are known obstacles to travel.

It is these two properties which form the common theme of this research: continuous location with continuous demand, and in the l_1 norm.

1.1 Facility location problems

In the first half of this thesis we will consider five well-known location problems (though the methodology is applicable to a range of continuous demand location problems): the median and antimedian problems, the centre problem, the market share problem, and the maximal covering problem. The objectives are: in the median (antimedian) problem, to minimise (maximise) the combined distance that all customers travel; in the centre problem, to minimise the maximum distance that any customer travels; in the market share problem, to maximise the total demand captured by a selected company's facilities (supposing that the selected company owns the new facility and the others belong to the company or its competitors); and in the maximal covering problem, to maximise the demand of all customers captured within a particular coverage radius from a facility.

The vast majority of planar location problems rely on the assumptions that the demand of customers is represented by a finite set of discrete points and that the placement of facilities on the plane as well as travel across the plane is not restricted, as is evidenced by the three abovementioned books.

In an industrial context, as laid out by Launhardt and Weber, a discrete set of demand points often adequately reflects the problem. For commercial and public service facilities in an urban environment, however, there can be millions of potential customers, and it is impracticable to represent every customer site as a separate demand point. One option to deal with such a situation is to aggregate customers into a smaller number of meta-customers, e.g. by postal codes, census tracts, or wards. This, however, introduces various kinds of aggregation errors to the problem, which can be quite pronounced (Drezner, 1995b; Francis & Lowe, 2019). A second, more accurate approach is to model customer demand as continuously distributed over the specified area. Moreover, the uncertain and sporadic nature of some demands lends itself much better to a continuous distribution over the region under consideration than to a discrete one. The first treatment of a location problem with continuous demand (and Euclidean distances) is due to Lösch (1954). Since then, a significant amount of research has been dedicated to planar location problems with continuous demand distributions: see Newell (1973); Erlenkotter (1989); Fekete, Mitchell, and Beurer (2005); Averbakh, Berman, Kalcsics, and Krass (2015) and references therein.

Concerning the second assumption, the region of demand and the region over which a facility can be feasibly located are often assumed to be the whole plane or, at least, convex polygons. However, this supposition is not a realistic one for many real-world applications, as there are often obstacles in cities which restrict the placement of facilities as well as travel, for example, rivers, lakes, parks, hills, or highways and rail tracks. Location problems containing forbidden areas that can be traversed, but where placement is not allowed, have been studied, e.g. in Aneja and Parlar (1994); Hamacher and Nickel (1995). If the traversal of these areas is also not allowed, then we can no longer use 'straight-line' distances and must instead revert to geodesic distances; these areas are usually called barriers. One of the first works on barrier location problems is Katz and Cooper (1981), who consider a circular barrier. Since then, barrier location problems have received ongoing attention in the literature: see Larson and Sadiq (1983); Aneja and Parlar (1994); Klamroth (2001); Bischoff and Klamroth (2007); Canbolat and Wesolowsky (2012); Oğuz, Bektaş, and Bennell (2018) and references therein.

However, to the best of our knowledge, so far continuous demand and barrier problems have only been studied independently of one another, and this is the first work that combines both of them into a single model. The added value of combining both is immediately apparent since the setting in which spatially distributed demand is most appropriate, namely in an urban environment, is also the one where barriers have the biggest impact on facility placement and, especially, on travelling. A current example, owing to the COVID-19 pandemic, is optimally locating roadside testing facilities to reduce the spread of infection and save lives: such facilities seek to serve a large population (requiring continuous demand to model) and customers (patients) travel (approximately according to rectilinear distance) to the facilities within an urban area full of barriers. Given its urban environment, this is a scenario which critically requires an algorithm dealing with continuous demand, rectilinear distances, and barriers.

Solving either of the two extensions independently is challenging, but both combined is even more so. Moving from discrete demand points to a continuous demand distribution significantly changes the structure of the problem. Planar location problems with discrete demand and Euclidean distances can be solved analytically, without having to investigate any geometric properties of the problem (Weiszfeld, 1937; Xue, Rosen, & Pardalos, 1996). For the Manhattan norm, one can even discretise the solution space and pose the problem as an equivalent discrete location problem (Francis & White, 1974). Not so for continuous demand distributions with multiple facilities. Following stipulation of the locations of all p facilities, the demand space has to be subdivided into areas known as *Voronoi cells*; the resulting partition is called the *Voronoi diagram*. Moreover, in order to solve the problem, merely calculating the Voronoi diagram based on the facility locations is insufficient. Instead, it is essential to study the *structure* of the Voronoi diagram, i.e. the position and the geometry of the cell boundaries, and how it changes dynamically when one or more of the facilities 'move around' on the plane. Unfortunately, this structure can alter dramatically, which makes it generally nigh impossible to represent the objective function of the problem in closed form, and renders the formulation of the underlying optimisation problems very challenging (Averbakh et al., 2015).

The following example gives an idea of these difficulties of representation (even before the addition of a barrier). Figure 1.1 shows the current facilities A_1, A_2, A_3, and A_4 and their Voronoi cells representing the trading regions of these facilities within the market space $\mathcal{P}$ along with a barrier $\mathcal{B}$. Regarding the two potential locations Z and Z', we notice that their Voronoi cells have significantly different shapes despite the proximity of the trial facilities. Hence, computing the demand for the market share problem (or any other objective function) over these Voronoi cells would result in functional expressions that differ considerably, making it very challenging to optimise the location of Z over the market region.

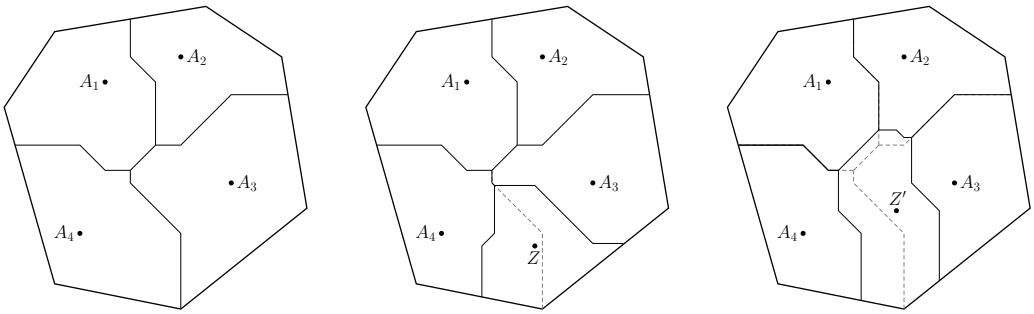

Figure 1.1: The market areas of four facilities within a polygonal market region and changes when a new facility Z or Z' is added.

These difficulties are exacerbated when we introduce barriers. In this case, we have to replace the regular 'straight-line' distances with their geodesic counterparts. While some solution methods for barrier location problems with discrete demand require the calculation of the barrier-restricted Voronoi diagram, this is always the Voronoi diagram of the set of fixed demand points, and thus is static and not affected by the locations of the facilities (Dearing, Hamacher, & Klamroth, 2002; Dearing, Klamroth, & Segars, 2005). Moreover, since we are working with continuous demand we cannot even derive such Voronoi diagrams based on discrete customer locations in the first place. This is a stark contrast to models for continuous customer demand and invalidates any exact solution method for discrete demand barrier problems.

One exemplary instance of this is an imaginary scenario with which I usually begin my talks when I have presented this research at conferences in the past, and which has proven very popular with audiences. The situation presented is one in which I am living in a convex polygonal city within which existing facilities (let us say restaurants) are located, as in Figure 1.2a. To my delight, my favourite restaurant has decided to open up a branch in the city in which I live, and greater excitement is aroused when they decide to use current facility location techniques to decide on the optimal location to set up this restaurant. This location is shown in Figure 1.2b and the proximity to my location increases the width of my smile.

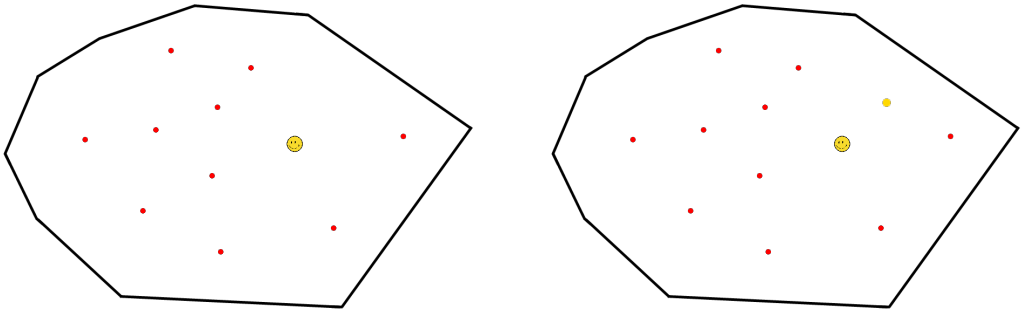

(a) The barrier-free location problem setting. (b) The barrier-free location problem solution.

Figure 1.2: The barrier-free location problem where existing facilities (red points) are located within a convex polygonal city. I, an interested customer, am represented by a smiley face.

However, returning to reality, the city within which I live is Edinburgh, full of beautiful and historic barriers, as shown from the satellite view in Figure 1.3a. Perhaps the most famous of these is Arthur's Seat, an extinct volcano to the east of the city centre. This barrier removes all demand that it covers and is also an obstacle to passage. When we add this barrier to the original barrier-free location problem setting as in Figure 1.3b, we can see that the optimal location found in Figure 1.2b falls drastically short by a large margin in the barrier-restricted case, and is no longer a recommended place to locate the restaurant.

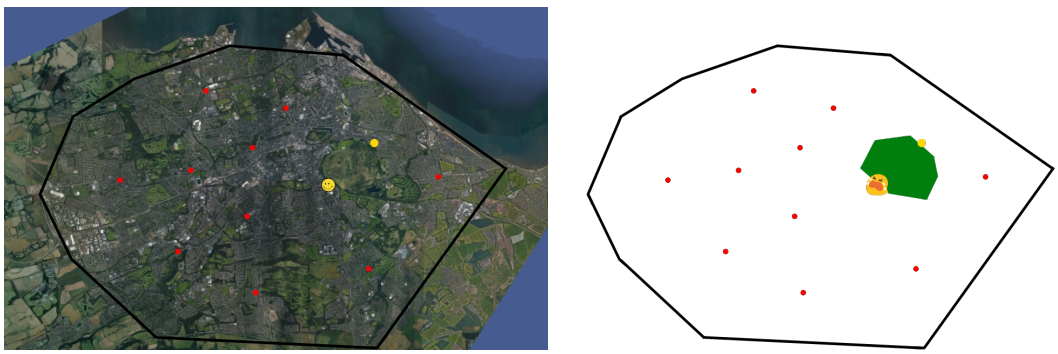

(a) The reality of the barrier-free location problem setting. (b) The barrier-restricted location problem setting.

Figure 1.3: The barrier-restricted location problem where existing facilities (red points) are located within a convex polygonal city containing a convex polygonal barrier (green area). I, an interested customer, am represented by a smiley face until I realise the barrier-free location problem solution is pitiful in the barrier-restricted problem.

To empirically demonstrate the additional difficulties we are facing due to the barrier, we present an example where we are given five existing locations for facilities and we want to find an optimal location for a sixth facility, with the goal of maximising the area of its Voronoi cell, i.e. maximising its market share for a uniform demand distribution. Figure 1.4a shows the five existing facilities A_1, ..., A_5 within a convex polygonal area and what could well be the optimal location, Z. We show the parts of the Voronoi diagram of the five existing facilities that disappeared after the addition of Z in dashed grey.

Moreover, if the real-life situation happened to include barriers which were not included in the modelling, then a multitude of shortcomings could befall the valuation of this location Z. A simple one is that Z may not be feasible in the barrier-restricted problem, because we cannot locate in the barrier and Z may lie within the barrier. Even if Z is still feasible, the barrier can severely affect the originally calculated captured demand, because the area captured may in reality be much less than promised in the barrier-free case if the barrier swallows up

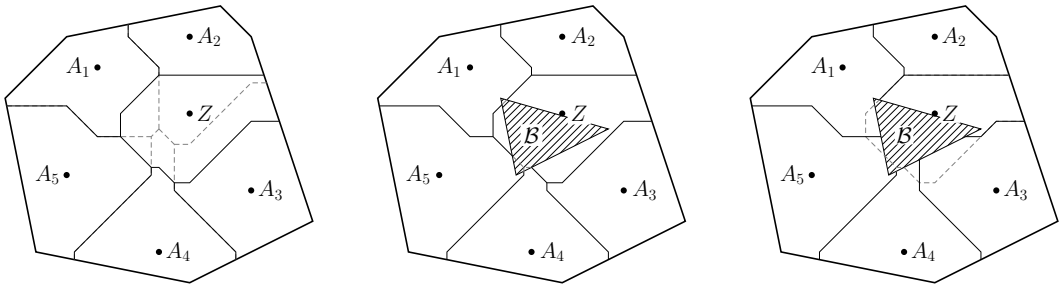

(a) A solution to a barrier-free facility location problem.

(b) The barrier-free solution in the presence of a barrier.

(c) The equivalent barrier-restricted solution.

Figure 1.4: Demonstration of some drawbacks of sharing solutions between barrier-free and barrier-restricted location problems.

much of the Voronoi cell of Z. We can see in Figure 1.4b that a large proportion of what we were previously awarding to Z is swallowed by $\mathcal{B}$, so the captured demand in the original Voronoi cell of Z is much less in the barrier-restricted problem. Furthermore, we can see that the barrier has cut off the leftmost area of the original Voronoi cell of Z. It no longer makes any sense to assign this isolated area to Z. Additionally, the barrier now enforces that, in order to access the bottommost area of the original Voronoi cell of Z, one must travel around the rightmost vertex of $\mathcal{B}$. Because the barrier warps distance, it is nonsensical to still assign the area within the barrier-free Voronoi cell of Z to Z in the barrier-restricted problem. The barrier can greatly influence the Voronoi diagram and Figure 1.4c shows that the barrier-restricted cell of the barrier-free optimum can easily be drastically different, and lead to a particularly poor solution. These shortcomings befall not only the market share problem, but any such facility location problem.

The ideas here become increasingly prevalent when one considers the fact that a barrier-free modelling of a barrier-restricted problem will contain a large area wherein facilities are not located (because of the barrier) and so optimal solutions of the barrier-free problem may be even more likely to be placed in or near the barrier and so be very significantly affected by the barrier's reintroduction.

1.2 Facility location games

Additionally, what makes facility location problems particularly challenging is that often they are not one-person optimisation problems, in which a single agent can aim for optimal choices in an isolated manner, but happen in a *competitive* setting, in which two or more players contend for the best locations. This change to competitive, multi-player versions can have a serious impact on the algorithmic difficulty of optimisation problems: for example, the classic Travelling Salesman Problem is known to be NP-hard, while the competitive two-player variant is known to be PSPACE-complete (Fekete, Fleischer, Fraenkel, & Schmitt, 2004).

In the second half of this thesis, we consider problems of competitive facility location under Manhattan distances; while rectilinear distances have been studied in location theory and applications (e.g. see Batta, Ghose, and Palekar (1989); Kolen (1981); Kusakari and Nishizeki (1997); Larson and Sadiq (1983); Wesolowsky and Love (1971a, 1971b, 1972)), they have received limited attention in a setting in which facilities compete for customers. In this context, see also von Hohenbalken and West (1984).

We study a natural scenario in which facilities have to be placed within a rectangular playing arena $\mathcal{P}$ with width p and height q. In this setting, a facility dominates the set of points for which it is closer than any other facility, i.e. the respective Voronoi cell, subject to the applicable metric. While for Euclidean distances a bisector (the set of points that have equal distance to two facilities) is precisely the boundary of the Voronoi cells so its two-dimensional measure disappears, this is not necessarily the case for Manhattan distances: as will be demonstrated in

Figure 2.3 there may be bisectors of positive area. Accounting for fairness and local optimality, we consider arrangements of points for which the respective Voronoi cells are equalised.

Exploiting the geometric nature of Voronoi cells, we completely resolve a classic problem of competitive location theory for the previously open case of Manhattan distances. In the *One-Round Voronoi Game*, first player *White* and then player *Black* each place n points in $\mathcal{P}$. Each player scores all the points for which one of its facilities is closer than any other facility, with care taken to explore several distinct potential strategies for the allocation of demand between points which contribute degenerate bisectors to the Voronoi diagram; Figure 1.5 illustrates an example.

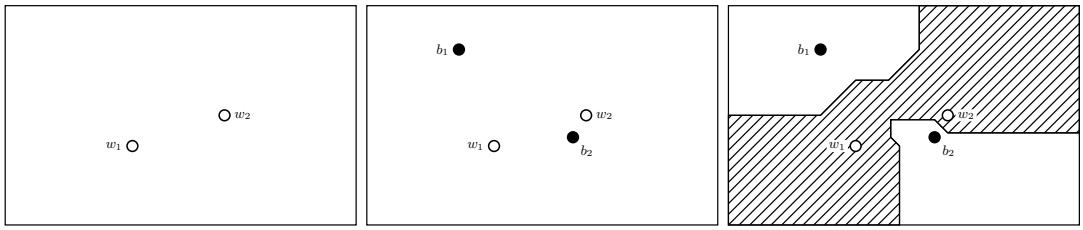

(a) White places two points. (b) Black places two points. (c) $\mathcal{P}$ is divided up.

Figure 1.5: Demonstration of the One-Round Voronoi Game for $n = 2$ (White wins).

The goal for each player in the Voronoi game is to obtain the higher score. Owing to the different nature of the Manhattan metric, both players may dominate strictly less than $\frac{1}{2}Area(\mathcal{P})$ depending on the chosen rule for the allocation of bisectors of non-zero area.

Meanwhile the objective for each player in the *Stackelberg game*, a game formulated identically to that of the Voronoi game, is to maximise their score. The focus of this game is subtly different to that of the Voronoi game which can be seen as a 'subgame' of the Stackelberg game, in that the winning player in the Voronoi game does not simply settle with a solution which claims over half of the area of $\mathcal{P}$. In this case the winner explores how to adapt their arrangement in order to control the largest proportion of $\mathcal{P}$, while the loser attempts to minimise their losses in finding the placements that protect most of their territory from capture.

1.3 Organisation of the thesis

Having introduced all of the problems we will explore, we will outline the structure of the thesis thus.

This introduction is followed by six chapters. Chapter 2 contains a tailored tour of the definitions, notation, and basic results we rely upon within this thesis; it is the best preparation for the reader's journey through the dense but wondrous forest of results this document contains. We present bisectors under the Manhattan norm and how they contribute to the construction of the Voronoi diagram. We introduce barriers into this theory and demonstrate how they can distort the properties that research relied upon without their addition. The facility location problems are then formulated, along with formal statements of the games.

Our first class of problems is covered in Chapter 3. In this chapter we extend the structural properties of classic Voronoi diagrams to geodesic rectilinear distances and show how to use them to identify sub-regions within which we can obtain a closed form of the objective function for our location problems. Two approaches to determine this partition are presented. The first approach (Section 3.2) fixes the additional facility within a certain portion of $\mathcal{P}$ and finds all possible partitioning lines for any barrier by exploring every possible interaction of the two. Not only is this work very labour-intensive, but the results are not particularly intuitive. It does, however, act as an effective introduction to our second method (Section 3.4) which delves into what it means for a facility to be located upon one of these partitioning lines. In addition, once this partition is found, we discuss how to determine efficiently the parametric representation of the objective function over each region and how to solve the resulting non-linear optimisation problem. Thus an algorithm is born which finds an exact optimum of the conditional median,

antimedian, centre, market share, and maximal covering facility location problems in polynomial time.

Chapter 4 brings with it a change of scene as we turn towards the One-Round Voronoi Game. Our work in this area begins with the identification of two crucial properties in any winning arrangement of White's points: *fairness* (in that area is shared equally between White's points); and *local optimality* (in that area is distributed symmetrically about White's point within each Voronoi cell). This promotes the exploration of certain properties of White's cells which brings us to deriving our main result: a full characterisation of the possible outcomes assuming optimal play by each player. We show that White has a winning strategy if and only if $\frac{p}{q} \geq n$; for all other cases, we give a winning strategy for Black.

On the back of this success we tackle the One-Round Stackelberg Game in Chapters 5 and 6. We discuss what arrangements adhering to the properties discussed in the previous chapter would resemble and see how they fare in the Stackelberg game. This leads us to consider separately White's grid arrangements and non-grid arrangements (hence the two chapters, respectively). For cases wherein White plays a grid arrangement we discern Black's best single point and propose optimal (or at least effective) arrangements in response to White's play. Owing to the lack of structure and infinite number of White's potential non-grid arrangements, we explore non-grid arrangements satisfying the attractive fairness and local optimality conditions defined earlier, finding all such arrangements for certain (small) values of n and designing such non-grid arrangements for almost all n.

To conclude, the seventh chapter summarises the notable results presented within this thesis, and provides a smorgasbord of open questions to inspire readers to take our theory to even greater heights.

Chapter 2

General Theory

2.1 Bisectors, barriers, and Voronoi diagrams

Between any two points $P = (p_x, p_y)$ and $Q = (q_x, q_y)$ in $\mathbb{R}^2$, the *rectilinear distance* is $l_1(P,Q) = |p_x - q_x| + |p_y - q_y|$ and the *bisector* (the set of points that are equidistant from P and Q) is $B(P,Q) = \{Z \in \mathbb{R}^2 | l_1(P,Z) = l_1(Q,Z)\}$. Let $B^{\leq}(P,Q) = \{Z \in \mathbb{R}^2 | l_1(P,Z) \leq l_1(Q,Z)\}$. The relative positions of P and Q decide the bisector's shape. These positions are defined by the following three expressions: $|p_x - q_x| \diamond |p_y - q_y|$, $p_x \diamond q_x$, and $p_y \diamond q_y$ where $\diamond \in \{\leq, \geq\}$. For fixed P, fixing an inequality for each of the three relations gives a set of points Q called a *configuration cone*. The first one is defined as $\mathcal{CC}^1(P) := \{Q \in \mathbb{R}^2 | p_x \leq q_x, p_y \leq q_y, p_x - q_x \leq p_y - q_y\}$ with the other cones $\mathcal{CC}^2(P), \ldots, \mathcal{CC}^8(P)$ created analogously and labelled anticlockwise as displayed in Figure 2.1. The *configuration lines* $\mathcal{CL}^k(P) := \mathcal{CC}^k(P) \cap \mathcal{CC}^{k-1}(P), k = 1, \ldots, 8$ bound the configuration cones (where $\mathcal{CC}^0(P) := \mathcal{CC}^8(P)$) and, together, $\mathcal{CC}^{2k-1}(P) \cap \mathcal{CC}^{2k}(P)$ make up the *kth quadrant* of P for $k = 1, \ldots, 4$.

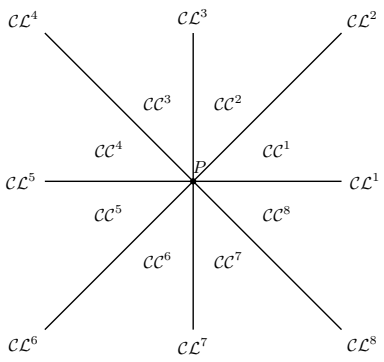

Figure 2.1: The eight configuration cones of P.

The bisector $B(P,Q)$ is piecewise linear with exactly three pieces if $Q \in \text{int}(\mathcal{CC}^k(P))$ (where $\text{int}(\star)$ is the interior of $\star$). These line segments are referred to as *bisector parts* or *breaklines* and the vertices where they meet are *breakpoints*. Crucially (as we will discover) the representations of the breakpoints, and therefore also of the breaklines, are linear in the coordinates of P and Q. There exist four distinct shapes of these bisectors for $p_y \leq q_y$, for Q in either $\mathcal{CC}^1(P)$, $\mathcal{CC}^2(P)$, $\mathcal{CC}^3(P)$, or $\mathcal{CC}^4(P)$, as displayed from left to right in Figure 2.2. Identical plots are obtained for the other configuration cones with $p_y \geq q_y$, only with P and Q exchanged. If $Q \in \text{int}(\mathcal{CC}^k(P))$ then we call $B(P,Q)$ a $\mathcal{CC}^k(P)$ *bisector* or a $\mathcal{CC}^k$ *bisector of* P.

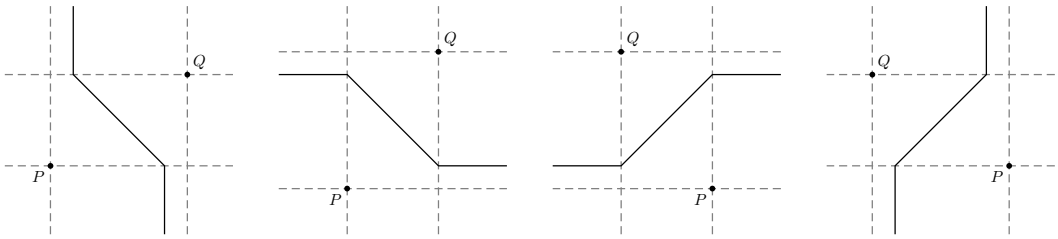

Figure 2.2: The four different shapes for non-degenerate bisectors for $p_y \leq q_y$.

Alternatively, if $Q \in \mathcal{CL}^k(P)$, for $k = 1, 3, 5, 7$, then the bisector is a straight line oriented vertically if $k = 1$ or $k = 5$ or horizontally if $k = 3$ or $k = 7$. If $Q \in \mathcal{CL}^k(P), k = 2, 4, 6, 8$, then the bisector consists of two quarterplanes (representing infinite areas of points which are equidistant from both P and Q) connected by a diagonal (note that a diagonal line is considered to be one with a gradient of ± 1) and we call these bisectors *degenerate*; cf. Okabe, Boots, Sugihara, and Chiu (2000); Aurenhammer, Klein, and Lee (2013). An example of such a degenerate bisector is shown in Figure 2.3 for $Q \in \mathcal{CL}^2(P)$ and it can be rotated anticlockwise in turn by 90° to obtain the equivalent bisectors of $Q \in \mathcal{CL}^k(P)$ for $k = 4$, $k = 6$, and then $k = 8$.

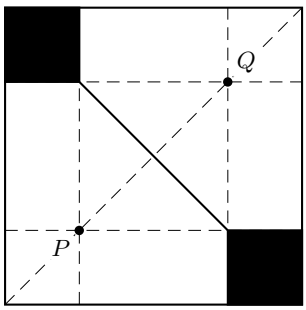

Figure 2.3: A degenerate bisector.

We shall now introduce additive bisectors (Okabe et al., 2000) which will prove abundantly useful in our barrier-restricted research. The *additive bisector* between *active points* P and Q with additive constant c is $B_c^{add}(P, Q) = \{X \in \mathbb{R}^2 \,|\, l_1(P, X) = l_1(Q, X) + c\}$. These have six unique forms as shown in Figure 2.4, with the sixth being the empty cell if $|c| > l_1(P, Q)$. As we can see, a value of $c = 0$ gives the original bisector $B(P, Q)$.

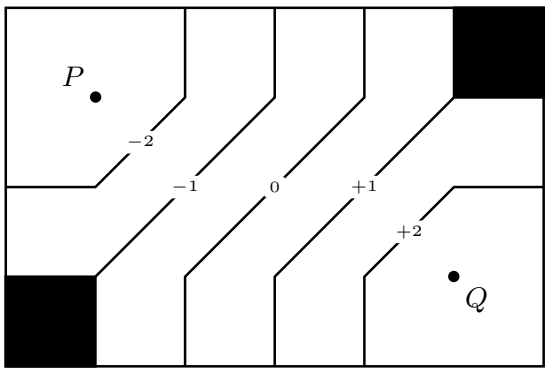

Figure 2.4: Additive bisectors $B_c^{add}(P, Q)$ for various values of c (as labelled) where $P = (0, 0)$ and $Q = (2, -1)$.

It is worth addressing the fact that two of these additive bisectors produce quarterplanes. This will only happen if $|c| = ||p_x - q_x| - |p_y - q_y||$ which is rare, but of course not impossible. We discuss how we can deal with the quarterplanes in bisectors (additive or otherwise) for facility location problems and games within Sections 2.2.2 and 2.4 respectively. It is also important to note that the breakpoints (and therefore the edges) of additive bisectors are linear in the coordinates of original facilities: Q contributes linearly to c ($= l_1^{\mathcal{B},+}(B_i, Q)$ or $= l_1^{\mathcal{B},-}(B_i, Q)$) which has a linear effect on the additive bisector's breakpoints.

Now we shall briefly introduce the theory of Voronoi diagrams; see Okabe et al. (2000) and the surveys by Aurenhammer and Klein (2000) for a more in-depth review. For a set $\{A_1, \ldots, A_n\} \in \mathbb{R}^2$ of $n \geq 2$ distinct points, define the *Voronoi cell* of A_i to be $V(A_i) = \bigcap_{j=1}^{n} B^{\leq}(A_i, A_j) = \{Q \in \mathbb{R}^2 | l_1(Q, A_i) \leq l_1(Q, A_j) \forall j \in \{1, \ldots, n\}\}$ and we say A_i is the *generator* of $V(A_i)$. The *Voronoi diagram* for $\{A_1, \ldots, A_n\}$ is denoted by $\mathcal{VD}(A_1, \ldots, A_n) = \{V(A_1), \ldots, V(A_n)\}$ (or sometimes $\mathcal{VD}$ for short if it is clear from which points the Voronoi diagram is computed).

The perimeter of a Voronoi cell $V(A_i)$ is composed entirely of pieces of bisectors $B(A_i, A_j)$ for some values of j and so, since the representation of the breakpoints and breaklines of these bisectors is linear in the coordinates of A_i and A_j, the representation of the vertices and edges of this perimeter is linear in the coordinates of the generators (noting that the intersection between two line segments, both having representation that is linear in the facility coordinates, also has representation that is linear in these coordinates). Hence the vertices and edges of $\mathcal{VD}(A_1, \ldots, A_n)$ have representations that are linear in the coordinates of A_1 to A_n.

This unrestricted Voronoi diagram $\mathcal{VD}$ has $\mathcal{O}(n)$ edges and $\mathcal{O}(n)$ vertices and can be computed in $\mathcal{O}(n \log n)$ time (Lee & Wong, 1980). Additionally, the line between A_i and each vertex of the Voronoi cell is wholly contained inside the polygon, a critical property called *star-shaped*. Due to the shape of non-degenerate bisectors it is obvious that the Voronoi cells are not generally convex; however, they are connected.

Furthermore, we only consider the Voronoi diagram within the market region/playing arena, $\mathcal{P}$. Let $\mathcal{P} \subset \mathbb{R}^2$ be a compact convex m-sided polygon with vertices $P_i = (p_{i_x}, p_{i_y})$ and suppose $A_1, \ldots, A_n \in \mathcal{P}$. We redefine the Voronoi cells $V(A_i) := V(A_i) \cap \mathcal{P}$. According to Finke and Hinrichs (1995) the overlay of two simply connected planar subdivisions, with $\mathcal{O}(a)$ and $\mathcal{O}(b)$ edges respectively, has $\mathcal{O}(a + b)$ edges (and vertices) and can be calculated in $\mathcal{O}(a + b)$ time. Therefore $\mathcal{VD}(A_1, \ldots, A_n) = \{V(A_1) \cap \mathcal{P}, \ldots, V(A_n) \cap \mathcal{P}\}$ has $\mathcal{O}(n + p)$ edges and vertices. Moreover, since $\mathcal{P}$ is convex, every $V(A_i)$ is still star-shaped, connected, and compact.

After adding the new generator A_{n+1} to the existing facilities $\{A_1, \ldots, A_n\}$, we call the new Voronoi diagram $\mathcal{VD}(A_1, \ldots, A_{n+1})$ the *incremental Voronoi diagram*. Some new edges and vertices that were not present in $\mathcal{VD}(A_1, \ldots, A_n)$ may appear in $\mathcal{VD}(A_1, \ldots, A_{n+1})$ and, vice versa, some old edges and vertices in $\mathcal{VD}(A_1, \ldots, A_n)$ may disappear when evaluating $\mathcal{VD}(A_1, \ldots, A_{n+1})$. It is important that we understand how these changes affect the representation of the objective function as shown in the Introduction. If there is an area of the solution space $\mathcal{P}$ over which the representation of the objective function remains the same, then we are able to find extreme values over this area. To ease notation we will abbreviate $\mathcal{VD}(A_1, \ldots, A_n)$ as $\mathcal{VD}$.

In the first half of the thesis we introduce a convex p-sided polygonal *barrier* $\mathcal{B}$ with vertices $B_i = (b_{i_x}, b_{i_y})$ within which there is zero demand, and across which travel is not permitted. Now that a barrier exists, the distance between P and Q is no longer the rectilinear distance l_1, but the distance of the shortest rectilinear path from P to Q around the barrier, say $l_1^{\mathcal{B}}(P, Q)$. Since the barrier alters the measuring of distances between points, it can affect the bisectors and therefore the Voronoi diagram (Mitchell, 1992). As we have glimpsed in Figure 1.4, the new Voronoi cell of A_i, $V(A_i) = \{Q \in \mathcal{P} \setminus int(\mathcal{B}) \,|\, l_1^{\mathcal{B}}(Q, A_i) \leq l_1^{\mathcal{B}}(Q, A_j) \forall j \in \{1, \ldots, n\}\}$ can have a very different shape to the original Voronoi cell from the barrier-free problem since its perimeter is dictated by the barrier-influenced bisector $B^{\mathcal{B}}(P, Q) = \{Z \in \mathbb{R}^2 | l_1^{\mathcal{B}}(P, Z) = l_1^{\mathcal{B}}(Q, Z)\}$ which, as we will see in Section 2.3, can look very dissimilar to $B(P, Q)$. Whilst these new Voronoi cells and the overlying Voronoi diagram could be described with the qualifier 'geodesic', in this thesis we will refer to them simply as Voronoi cells $V(A_i)$ in the Voronoi diagram, and will specify otherwise if required.

Now it may be sensible to ask how the properties of the Voronoi diagram in the barrier-constrained problem differ from that in the barrier-free problem. The properties of interest are the shapes of the cells and the number of edges and vertices in the Voronoi diagram. Through sketches such as Figure 1.4c (and as our foray into barrier-constrained bisectors – which contribute to the edges of the Voronoi diagram – will show in Section 2.3), we have seen that Voronoi cells are no longer star-shaped. However, they do remain connected: for any $P \in \mathcal{P}$ and facility A_i, if the shortest path between A_i and P passes through $P' \in int(V(A_j))$, say, then

$$l_1^{\mathcal{B}}(A_i, P) = l_1^{\mathcal{B}}(A_i, P') + l_1^{\mathcal{B}}(P', P) > l_1^{\mathcal{B}}(A_j, P') + l_1^{\mathcal{B}}(P', P) \geq l_1^{\mathcal{B}}(A_j, P)$$

so $P \notin V(A_i)$. We shall concern ourselves now with the number of vertices and edges of barrier-constrained Voronoi diagrams, as answered in the following lemma (advancing the existing result that the number of edges and the number of vertices in barrier-free Voronoi diagrams, not confined to market regions, are each $\mathcal{O}(n)$ (Lee & Wong, 1980)).

Lemma 2.1.1. *For facilities $A_1, \ldots, A_n$ and a p-sided convex barrier $\mathcal{B}$ located with an m-sided convex polygon $\mathcal{P}$, the number of edges and the number of vertices in $\mathcal{VD}(A_1, \ldots, A_n)$ are each $\mathcal{O}(m + n + p)$.*

Proof. For this proof we utilise the dual graph (or the Delaunay triangulation) of the Voronoi diagram. We obtain this by taking the facilities A_1 to A_n as our vertices and we draw an edge between two vertices if their facilities' Voronoi cells neighbour one another. Since each Voronoi cell is connected, this graph is a planar graph (no two edges must cross as this would prevent one of the neighbouring conditions – the edge between A_i and A_j can be drawn through only $V(A_i)$ and $V(A_j)$, allowing curves) with n vertices, and so Euler's formula gives the maximum number of edges of the dual graph as $3n - 6$ for $n > 2$, and 1 if $n = 2$.

Each edge of this graph corresponds to a bisector between two facilities. As seen above, the bisector in the barrier-free problem, composed of three line segments, is changed by the addition of the barrier whenever an extreme vertex of $\mathcal{B}$ becomes an active extreme vertex, and each change causes a shift in the original bisector, or a horizontal or vertical to become a diagonal, or a diagonal to become a horizontal or vertical, increasing the edge count by at most one. The barrier itself can also intersect the bisector once, splitting an edge into two, so creating another edge. There are a maximum of four extreme vertices of $\mathcal{B}$ so the maximum number of edges of a bisector is $3 + 4 + 1 = 8$. Therefore every edge in the dual graph corresponds to a bisector within the Voronoi diagram of at most eight edges.

Finally, the edges of $\mathcal{B}$ and $\mathcal{P}$ must be included in the Voronoi diagram. According to Finke and Hinrichs (1995), there are then $\mathcal{O}(m + n + p)$ edges in $\mathcal{VD}(A_1, \ldots, A_n)$. It follows from the fact that the number of vertices cannot exceed the number of edges that we also have $\mathcal{O}(m + n + p)$ vertices in $\mathcal{VD}(A_1, \ldots, A_n)$. □

Regarding the algorithmic complexities of computing the barrier-restricted Voronoi diagram itself, the barrier-restricted Voronoi diagram for the existing facilities can be calculated in $\mathcal{O}((n + p)\log^2(n + p))$ time using a 'continuous Dijkstra' technique of 'wavefront' propagation as in Mitchell (1992), and its overlay with the market region $\mathcal{P}$ can then be calculated in $\mathcal{O}(m + n + p)$ time (Finke & Hinrichs, 1995).

2.2 Facility location problems

2.2.1 Problem definitions

We will consider uniform demand over $\mathcal{P}$ and assume that each demand point is served by the closest facility. Whilst uniform demand could be seen to be a simplifying assumption, even with this restrictive condition the problem is extremely difficult. Now we shall formally state the five location models chosen to be examined, each one focusing on finding the optimal location for the additional facility $A_{n+1} \in \mathcal{P}$ as stated in their original (barrier-free) formulation in Averbakh et al. (2015).

In the *Conditional Median Problem* we seek the location A_{n+1} that minimises the total distance travelled

$$F_{CM}(A_{n+1}) = \int\int_{(u,v)\in\mathcal{P}} \min_{i=1,\ldots,n+1} l_1(A_i,(u,v))dudv$$

(cf. Cavalier and Sherali (1986)). This is clearly appropriate for desirable facilities, though maximising the total distance travelled $F_{CM}(A_{n+1})$ is necessary when locating an undesirable facility (such as a rubbish dump). This is the *Conditional Antimedian Problem*. We note that it is clearly optimal to locate A_{n+1} at an existing facility so constrict the distance between the new and existing facilities to be no less than $D > 0$, as suggested by Berman and Huang (2008).

In the *Conditional Centre Problem* we seek the location A_{n+1} that minimises the maximum distance travelled by a customer

$$F_{CC}(A_{n+1}) = \max_{(u,v)\in\mathcal{P}} \min_{i=1,\ldots,n+1} l_1(A_i,(u,v))$$

(cf. Suzuki and Drezner (1996)). This is important for facilities such as the emergency services.

In the *Market Share Problem* we seek the location A_{n+1} which, given $A_1,\ldots,A_k$ competitor facilities and $A_{k+1},\ldots,A_n$ facilities of our own, maximises the total demand attracted by our facilities

$$F_{MS}(A_{n+1}) = \int\int_{(u,v)\in\{(u,v)\in\mathcal{P}|\,\min_{i>k} l_1((u,v),A_i)\leq\min_{i\leq k} l_1((u,v),A_i)\}} 1dudv$$

(cf. Eiselt, Pederzoli, and Sandblom (1985)). This relies on the assumption that a customer will always have a preference for the nearest facility, choosing ours in the case of a tie.

In the *Conditional Maximal Covering Location Problem* we seek the location A_{n+1} which maximises the total demand captured of all customers no more than a certain distance away from a facility

$$F_{MCL}(A_{n+1}) = \int\int_{(u,v)\in\{(u,v)\in\mathcal{P}|\,\min_{i=1,\ldots,n+1} l_1((u,v),A_i)\leq R\}} 1dudv$$

(cf. Matisziw and Murray (2009b)), where we assume that $R > 0$ is the maximum distance that a customer is willing to travel. For future ease let us define the *unit ball* of radius R about A_i to be $B_R(A_i)$.

We shall now reformulate these objectives for use in the barrier-restricted setting and provide a more geometric interpretation by way of their recapitulation in the Voronoi diagram environment, for which we will utilise the term $Area(*)$ to denote the area of the structure $*$. The Conditional Median and Antimedian Problems then become

$$\begin{aligned} F_{CM}(A_{n+1}) &= \int\int_{(u,v)\in\mathcal{P}\setminus int(\mathcal{B})} \min_{i=1,\ldots,n+1} l_1^{\mathcal{B}}(A_i,(u,v))dudv \\ &= \sum_{i=1}^{n+1} \int\int_{Q=(u,v)\in V(A_i)} l_1^{\mathcal{B}}(A_i,Q)dudv\,. \end{aligned} \tag{2.2.1}$$

The Conditional Centre Problem becomes

$$\begin{aligned} F_{CC}(A_{n+1}) &= \max_{(u,v)\in\mathcal{P}\setminus int(\mathcal{B})} \min_{i=1,\ldots,n+1} l_1^{\mathcal{B}}(A_i,(u,v)) \\ &= \max_{i=1,\ldots,n+1} \max_{Q=(u,v)\in V(A_i)} l_1^{\mathcal{B}}(A_i,Q) \end{aligned} \tag{2.2.2}$$

The Market Share Problem becomes

$$\begin{aligned} F_{MS}(A_{n+1}) &= \int\int_{(u,v)\in\{(u,v)\in\mathcal{P}\setminus int(\mathcal{B})|\,\min_{i>k} l_1^{\mathcal{B}}((u,v),A_i)\leq \min_{i\leq k} l_1^{\mathcal{B}}(Q,A_i)\}} 1 du dv \\ &= \sum_{i=k+1}^{n+1} \int\int_{Q=(u,v)\in V(A_i)} 1 du dv \\ &= \sum_{i=k+1}^{n+1} Area(V(A_i))\,. \end{aligned} \tag{2.2.3}$$

And the Conditional Maximal Covering Location Problem becomes

$$\begin{aligned} F_{MCL}(A_{n+1}) &= \int\int_{(u,v)\in\{(u,v)\in\mathcal{P}\setminus int(\mathcal{B})|\,\min_{i=1,\dots,n+1} l_1^{\mathcal{B}}((u,v),A_i)\leq R\}} 1 du dv \\ &= \sum_{i=1}^{n+1} \int\int_{Q=(u,v)\in V(A_i)\cap B_R(A_i)} 1 du dv \\ &= \sum_{i=1}^{n+1} Area(V(A_i)\cap B_R(A_i))\,. \end{aligned} \tag{2.2.4}$$

It may be interesting to note that $F_{CC}(A_{n+1})$ requires only the distances from each generator to the vertices of its Voronoi cell while $F_{MS}(A_{n+1})$ and $F_{MCL}(A_{n+1})$ rely merely on the areas of the Voronoi cells, restricted to the unit ball in the latter's case. Meanwhile the geometry of the entire Voronoi diagram must be understood to compute $F_{CM}(A_{n+1})$. These qualities afford us different solution approaches and therefore varying degrees of difficulty when solving each problem; it is commonly agreed that each problem presented within this paragraph is increasingly challenging (for both the barrier-free case and their adaptation to the barrier-restricted case). For a better idea of the intricacies that each solution method demands in the barrier-free scenario, we will explain these procedures in Section 2.2.2. From this we can imagine how introducing a barrier may further complicate means, issues that are resolved in Section 3.4 where we present the processes that solve such problems in the barrier-restricted setting.

2.2.2 Solution methodology for the barrier-free problems

After defining the problems under consideration, the natural next question would concern how best to evaluate their objectives given $\mathcal{VD}(A_1,\dots,A_{n+1})$ and to optimise these objectives. Before we begin, recall from Section 2.1 that the vertices of the Voronoi diagram are linear in the coordinates of the facilities. This will prove to be a crucial property for our work.

Summarising the approaches suggested in Averbakh et al. (2015), firstly, it was found through a centroid triangulation of $\mathcal{VD}$ (a partition of each $V(A_i)$ into triangles, each with one vertex at the generator, being possible due to the star-shaped property of barrier-free Voronoi cells, as depicted in Figure 2.5) that $F_{CM}(A_{n+1})$ is cubic in the coordinates of A_{n+1}. The partial derivatives are therefore quadratic and, via computing the determinant of Sylvester's matrix (Cohen, 1993), their solution amounts to solving a quartic with at most four real-valued roots that can be derived in closed form; cf. Abramowitz and Stegun (1972).

Next, $F_{CC}(A_{n+1})$ is easy to assess. For a polygonal Voronoi diagram, the point furthest away from any generator within its Voronoi cell will be a vertex of the Voronoi cell, so we need only determine the largest of distances between vertices of $\mathcal{VD}$ and the generator of the cells that contain them. Since the $\mathcal{O}(m+n+p)$ vertices of $\mathcal{VD}$ are linear in the coordinates of A_{n+1}, the distance between vertices and generators will also be linear in the coordinates of A_{n+1} and so $F_{CC}(A_{n+1})$ is the upper envelope of $\mathcal{O}(m+n+p)$ linear functions. The minimum of this can be found by solving the linear programming problem which can be done in $\mathcal{O}(m+n+p)$ time (Megiddo, 1983).

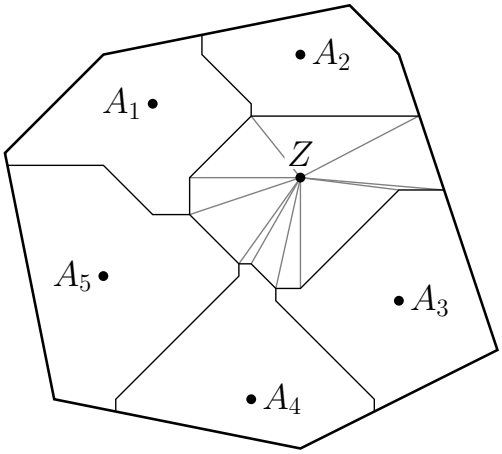

Figure 2.5: An example of centroid triangulation for $V(Z)$ in Figure 1.4a.

To calculate $F_{MS}(A_{n+1})$ and $F_{MCL}(A_{n+1})$ we must quantify the areas of Voronoi cells, or of the union of Voronoi cells and the unit ball. For this we will make use of Gauss's area formula. If a simple polygon $\mathcal{D}$ has the vertices $D_1, \ldots, D_j$ with $D_i = (D_i^x, D_i^y)$, then Gauss's area formula states that

$$Area(\mathcal{D}) \;=\; \sum_{i=1}^{j} \left(D_i^x \, D_{i+1}^y \;-\; D_{i+1}^x \, D_i^y \right) .$$

Applying this to $\mathcal{D} = V(A_i)$ and $\mathcal{D} = V(A_i) \cap B_R(A_i)$ (which are both simple polygons), because the coordinates of $D_1, \ldots, D_j$ are linear in the coordinates of A_{n+1} it is the case that $Area(V(A_i) \cap B_R(A_i))$ and $Area(V(A_i) \cap B_R(A_i))$ are quadratic functions in the coordinates of A_{n+1}. Consequently, in maximising the objective, the first-order conditions are easy to solve, as a system of two linear equations with two unknowns.

These representations, however, are usually only valid in a small neighbourhood around A_{n+1}. For example, see Figure 2.6 wherein the perturbation in Figure 2.6b introduces changes in the coordinate values of the vertices in $\mathcal{VD}$ but not in their representation, whereas the perturbation in Figure 2.6c introduces changes in both the coordinate values and representation of the vertices in $\mathcal{VD}$.

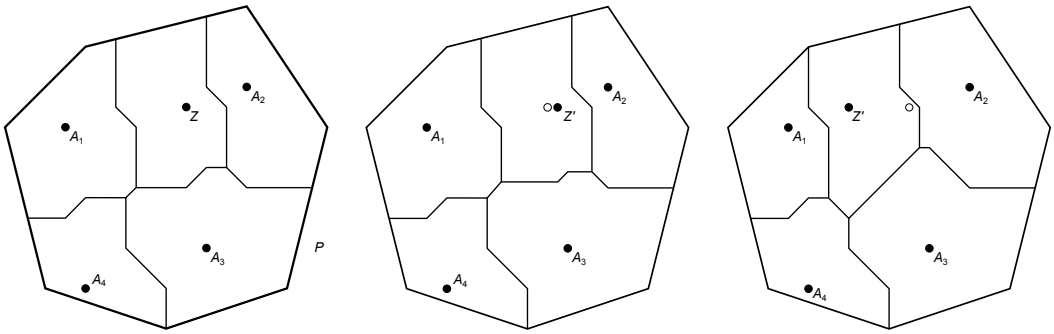

(a) The original $\mathcal{VD}$. (b) No change in representation. (c) A change in representation.

Figure 2.6: Demonstration of changes in the coordinate values and representation of the vertices of $\mathcal{VD}$ (adapted from Averbakh et al. (2015)).

In Averbakh et al. (2015), *structural identity* (concisely, the property of the Voronoi diagram having the same number of edges and vertices generated by the same points) was enough to guarantee the preservation of the representation of the barrier-free objectives. It was found that, after determining the Voronoi diagram for $\mathcal{P}$, three sets of lines induce a partition of $\mathcal{P}$ within which the representation of the objective function remains unchanged. These lines are:

- configuration lines: these are the lines $\mathcal{CL}^k(A_i)$ for every $i \in \{1, \ldots, n\}$ and every $k = 1, \ldots, 8$ which, as we have already seen in Figure 2.2, affect the configuration of the bisectors;

- quadrant lines: these are the lines $x = p_{ix}$ and $x = p_{ix}$ (the horizontal and vertical lines through the vertices of $\mathcal{P}$) and they affect the centroid triangulation;

- intersection lines: these lines govern when and how a bisector intersects a bisector within $\mathcal{VD}(A_1, \ldots, A_n)$ and so which breakpoints and breaklines are present within $\mathcal{VD}$, but they are more difficult to represent in a closed form so we shall demonstrate how they can be found in the following example (Kalcsics, 2012).

Returning to the example shown in Figure 2.6, we can better understand exactly how the Voronoi diagram in Figure 2.6c comes to have different representations of vertices from the original Voronoi diagram in Figure 2.6a. Figure 2.7 displays the underlying bisectors of both the Voronoi diagrams depicted in Figures 2.6a and 2.6c so that we may discern which different breaklines are intersecting, thereby causing the changes in representation.

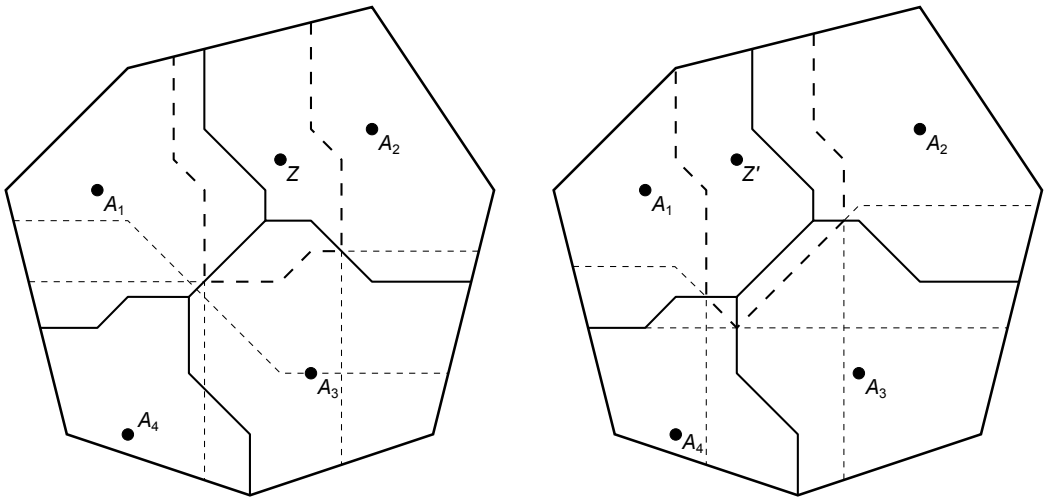

(a) Bisectors in original placement.

(b) Bisectors in perturbed placement.

Figure 2.7: Illustration of the structural differences between the Voronoi cells for Z and Z'.

From Figure 2.7 we can identify many alterations in the intersections of bisector parts. For example, the lower vertical breakline of $B(Z, A_2)$ intersects the diagonal bisector part of $B(A_2, A_3)$ in Figure 2.7a but not in Figure 2.7b. Let us explore this further to obtain the intersection lines associated with this intersection.

For $A_2 = (7, 7)$, $A_3 = (6, 3)$, and $Z = (x, y)$, consider the intersection of the bisector part $\overline{E_2E_3} = \overline{(7, 4.5)(6, 5.5)}$ of $\mathcal{VD}$ with the lower breakline L of $B(Z, A_2)$ as displayed in Figure 2.8:

$$L \;=\; \overline{(0.5\,(x-y)+7, y)(0.5\,(x-y)+7, -\infty)}\,.$$

The intersection point of the underlying lines has the coordinates

$$(0.5\,(x-y)+7,\; 0.5\,(y-x)+4.5)\,.$$

Hence, we obtain the following conditions for an intersection (from requiring the lower breakpoint of $B(Z, A_2)$ to be above $\overline{E_2E_3}$ and for the lower breakline to fall between E_2 and E_3):

$$9 \;\leq\; x+y \quad \text{and} \quad -2 \;\leq\; x-y \;\leq\; 0\,.$$

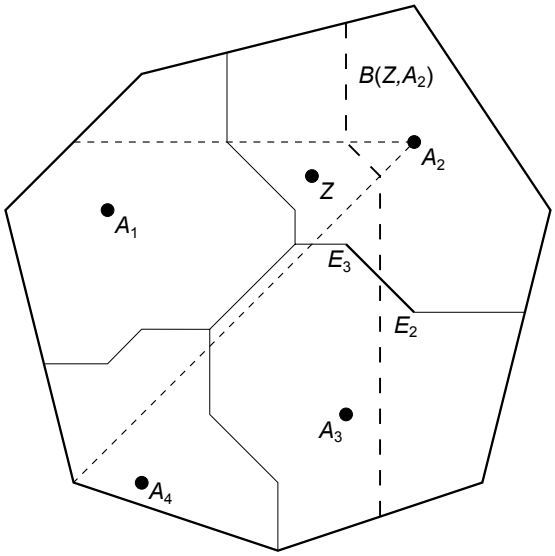

Figure 2.8: A closer look at the example in Figure 2.6a where $A_2 = (7, 7)$ and $A_3 = (6, 3)$.

Along with the configuration lines this generates the subset of points for which L and $\overline{E_2E_3}$ intersect, shown in Figure 2.9a, and we can continue finding the intersection lines for the remaining bisector intersections in order to obtain the partition cell in Figure 2.9b such that, if Z is placed within it, $\mathcal{VD}(A_1, \ldots, A_4, Z)$ has identical intersections (and is structurally identical).

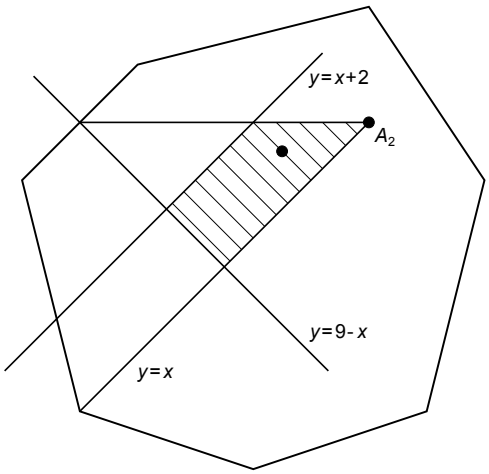

(a) Subset of points for which L and $\overline{E_2E_3}$ intersect.

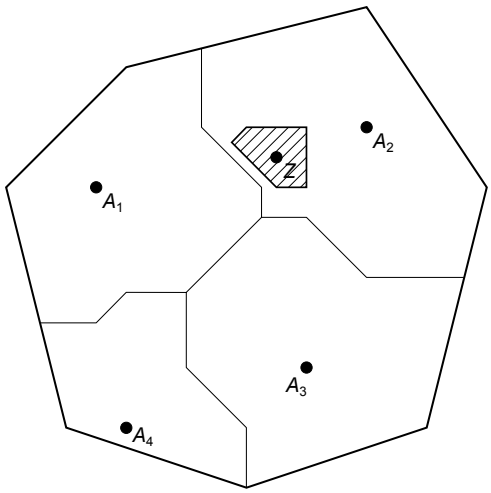

(b) Partition of points for which $\mathcal{VD}$ is structurally identical.

Figure 2.9: Areas of $\mathcal{P}$ within which at least some structure is identical.

There are $8n$ configuration lines, $2p$ quadrant lines, and it was found in Averbakh et al. (2015) that there are $\mathcal{O}((n+m)^2)$ intersection lines. Hence this partitions $\mathcal{P}$ into $\mathcal{O}((n+m)^2)$ cells within which the Voronoi diagram is structurally identical. Therefore we have a polynomial number of cells over which we are able to find the optimal location A_{n+1} for a consistent demand function over the cells by exploiting first order methods (taking care to find the optima over the interior of each cell as well as in the interior of any partition edge).

However, these partitioning lines are not sufficient to ensure structural identity if a barrier is present. When a barrier is introduced in $\mathcal{P}$ we are almost guaranteed not to have representation identity within the partition provided by these lines. For a simple demonstration of the difference in representation within the partition obtained from Averbakh et al. (2015), consider one facility $A_1 = (0, 0)$ in a simple rectangular market region $\mathcal{P}$ within which a triangular barrier sits. Since

$\mathcal{P}$ is a rectangle, the quadrant lines follow the perimeter of $\mathcal{P}$. For ease let us define

$$R(P,Q) = \left\{(x,y) \in \mathbb{R}^2 | \min[p_x, q_x] \leq x \leq \max[p_x, q_x], \min[p_y, q_y] \leq y \leq \max[p_y, q_y]\right\}$$

to be the rectangle with opposite corners $P = (p_x, p_y)$ and $Q = (q_x, q_y)$, and $\Delta(A, B, C)$ to be the triangle with vertices A, B, and C. Furthermore, since there is only one initial facility A_1, there are no bisectors within $\mathcal{VD}(A_1)$ to provide intersection lines. Therefore there are only configuration lines contributing to the partition. Figure 2.10 shows four placements of Z within the same partition cell (partitioning lines shown dashed) but with clearly different Voronoi diagram structures.

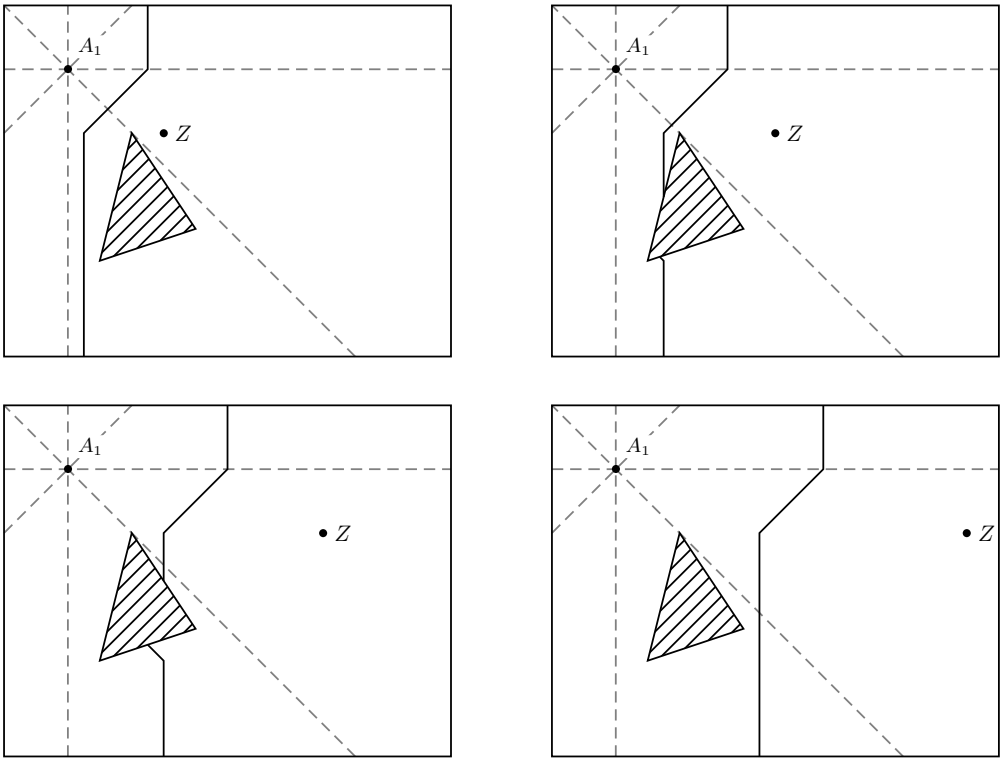

Figure 2.10: Four placements of Z within a rectangular $\mathcal{P} = R((-1, -3.5), (6, 0.5))$ with one existing facility $A_1 = (0, 0)$ and a triangular barrier $\mathcal{B} = \Delta((0.5, -3), (1, -1), (2, -2.5))$.

Thus we require more partitioning lines to be found in order to obtain a partition where the representation of the objective function is identical no matter where Z is located within each cell.

Before moving on we have to address the possibility that the bisectors produce a quarterplane and how we overcome the issues that this may bring. As we have seen, quarterplanes can exist in bisectors in l_1, even without the inclusion of a barrier's interaction, if the two facilities are on the same diagonal, and they may also occur in additive bisectors. While we may comment that in practice this case need not occur since one can appeal to measurement error (in order to be allowed to perturb an 'offending' point by some negligible amount so as to avoid the production of a quarterplane) and we do assume that no existing facilities lie on diagonal configuration lines of one another, for completeness we must still choose how to deal with such a bisector if the new facility is located on a diagonal configuration line of an existing facility. Does the original facility maintain the custom, or do the customers fall for the attraction of what's shiny and new?

The choice is made simpler by the realisation that we require an exact solution for our algorithm. If it is decided that the original facility keeps the demand in the quarterplane then one can easily see that we could have the case where, within a cell of structural identity, the area of $V(Z)$ will increase as it approaches the point on one of the edges at which a quarterplane would be created. This maximisation would therefore have a supremum, but not a maximum as we require. Therefore we do require the demand within the quarterplane to go to the new facility. One can interpret this as meaning that our customers are curious creatures, intrigued by novelty.

The Voronoi cells to which these bisectors would contribute remain star-shaped and connected, so the effect that this choice has upon our work is simply that, within the partition, we must also consider a degenerate placement of A_{n+1} on each diagonal configuration line of A_i for $i = 1, \ldots, n$.

2.3 Barrier-constrained bisectors and geodesic Voronoi diagrams

This motivates us to investigate constraints on the coordinates of Z such that the representation of the objective function is preserved. But before we can begin to look at such a thing we must properly understand how the barrier affects the Voronoi cells. To help classify the interaction between Z and $\mathcal{B}$, and to discuss these candidate partitioning cells for Z later, we introduce the following definitions (Larson & Sadiq, 1983).

Definition 2.3.1. *In a space with barriers, two points are considered visible from one another with respect to a norm if the shortest distance between the points is the same in the unconstrained and constrained space. The visible area of a space from a given point is the set of all points visible from that point, and the non-visible area is exactly its complement.*

Now that we have a notion of visibility, we will outline a particular area created by $\mathcal{B}$ which plays with this visibility.

Definition 2.3.2. *For a p-sided polygonal barrier $\mathcal{B}$ with vertices $(b_{1x}, b_{1y}), \ldots, (b_{p_x}, b_{p_y})$, define its shadow in the l_1 norm to be*

$$Shadow(\mathcal{B}) = \left\{ (x, y) \in \mathbb{R}^2 : \min_i b_{ix} \leq x \leq \max_i b_{ix}, \min_i b_{iy} \leq y \leq \max_i b_{iy} \right\}.$$

We call the leftmost, rightmost, topmost, and bottommost vertices of $\mathcal{B}$ the *extreme* points of $\mathcal{B}$ (and not just any vertex of $\mathcal{B}$ as in the classical definition) and it is these extreme points which dictate the dimensions of $Shadow(\mathcal{B})$. Further, denote the corners of $Shadow(\mathcal{B})$ to be $C_1 = (\min_i b_{ix}, \max_i b_{iy})$, $C_2 = (\max_i b_{ix}, \max_i b_{iy})$, $C_3 = (\max_i b_{ix}, \min_i b_{iy})$, and $C_4 = (\min_i b_{ix}, \min_i b_{iy})$. We will find that the bisectors between two facilities interact not only with $\mathcal{B}$ but with $Shadow(\mathcal{B})$ and with the visible–non-visible boundary. We will use this term to describe the occurrence of certain bisectors, and it is important to understand the effect of this visibility as portrayed in Figure 2.11.

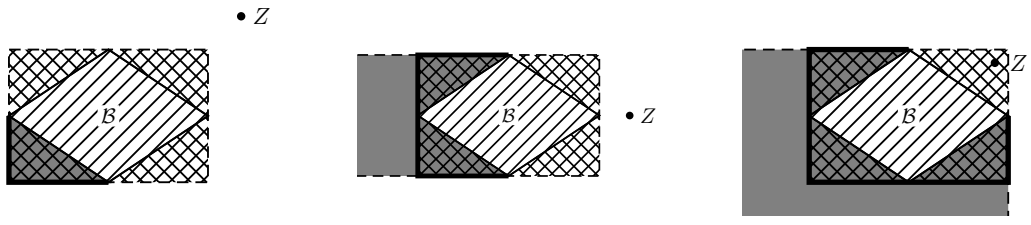

(a) Facility diagonal to $Shadow(\mathcal{B})$. (b) Facility adjacent to $Shadow(\mathcal{B})$. (c) Facility within $Shadow(\mathcal{B})$.

Figure 2.11: Visible areas of the space from different locations. Here a general barrier $\mathcal{B}$ is represented by a diamond. Grey areas are not visible from the facility.

To understand the effect that $\mathcal{B}$ has on the Voronoi diagram we need to know how it can change the bisector between two facilities. Now we introduce two important results regarding these bisectors in the barrier-constrained problem which we will make use of in our exploration. First of all we may want to ask if, or when, the bisector is unchanged despite the addition of a barrier. Our first lemma sheds light on this.

Lemma 2.3.1. *For a fixed trial location of the additional facility, any point on the bisector in the barrier-free facility location problem that lies in the visible areas as shown in Figure 2.11 for the existing and additional facility is a point on the bisector in the barrier-constrained facility location problem.*

Proof. In the barrier-free facility location problem, the boundary between the Voronoi cells of two facilities represents the set of points in the space that are equidistant from both facilities. If a point on this bisector lies in the visible area of a facility then it remains at the same distance from the facility as in the barrier-free problem. Therefore if a point on the bisector lies in both visible areas of the facilities then it is still equidistant from both facilities, and is thus a point on the bisector in the barrier-constrained facility location problem. □

Next we may wonder in how many instances a barrier can interact with one placement of Z, or rather how many times a bisector can intersect a barrier (though we will discover other interactions). The following lemma answers exactly this.

Lemma 2.3.2. *A bisector between any two facilities will intersect $\mathcal{B}$ twice or not at all (counting touches as not intersecting).*

Proof. Suppose the bisector intersects $\mathcal{B}$ $n \geq 3$ times. If all these bisector parts begin at $\mathcal{B}$ and extend to $\mathcal{P}$ then they partition the space into n regions, each region being a Voronoi cell of either facility P or Q. Each region will have exactly two neighbouring regions and be bounded by exactly one continuous boundary with each neighbour, a section of $\mathcal{B}$, and a section of $\mathcal{P}$. Since two Voronoi cells of the same facility must not be neighbours, n must be even. Therefore there must be at least two Voronoi cells of each facility, although this means that at least one Voronoi cell will not contain its respective facility (i.e. the shortest path to a point in the Voronoi cell of Q must travel through a Voronoi cell of P and so contain points that are, by definition, closer to P than Q). This is a clear contradiction.

Alternatively, if not all bisector parts extend to $\mathcal{P}$ then at least one bisector part must intersect $\mathcal{B}$ at both ends. From an identical argument to that above, this region must contain a facility and, since it is surrounded by Voronoi cells of another facility, this becomes the only Voronoi cell, contradicting the supposition that the bisector intersects $\mathcal{B}$ more than twice.

Thus, the bisector may only intersect $\mathcal{B}$ twice or not at all. □

This lemma hints at one of the largest changes brought about by introducing a barrier. When the bisector intersects the barrier it splits into two different parts. Each of these parts corresponds to the shortest paths from at least one of the facilities travelling either way around the barrier. That is, in the presence of a barrier there is now a choice of paths: one travels clockwise about the barrier, and the other anticlockwise (note that for many destinations these paths will be the same, otherwise it is not even sensible to think of the paths travelling around the barrier). This gives rise to two potential contributions to the bisectors for $B^{\mathcal{B}}(P, Q)$: the line of equidistance of paths travelling clockwise from P and anticlockwise from Q; and anticlockwise from P and clockwise from Q.

It is easy to discern the two when the bisector intersects $\mathcal{B}$. However, these bisector parts still exist when no intersection occurs. An example of this is shown in Figure 2.12. Here we see the 'upper' bisector part in Figure 2.12a formed using the shortest path from Q anticlockwise about $\mathcal{B}$ and the 'lower' bisector part in Figure 2.12b from the clockwise path – note that these bisectors are piecewise linear and do not always partition the space. For this let us define $l_1^{\mathcal{B},+}(P, Q)$ and $l_1^{\mathcal{B},-}(P, Q)$ to be the shortest distances from P to Q in the geodesic l_1 norm clockwise or anticlockwise about $\mathcal{B}$ respectively. These are combined in Figure 2.12c to create the full bisector, where the dotted line shows the points at which the shortest paths from Q clockwise and anticlockwise about $\mathcal{B}$ are of equal length, i.e. $l_1^{\mathcal{B},+} = l_1^{\mathcal{B},-}$; we define this to be the line of equidistance from Q around $\mathcal{B}$. Importantly, its vertices are linear in the coordinates

of Q (and therefore so are its line segments). It is always along this line that the bisector swaps from the 'upper' part to the 'lower' part.

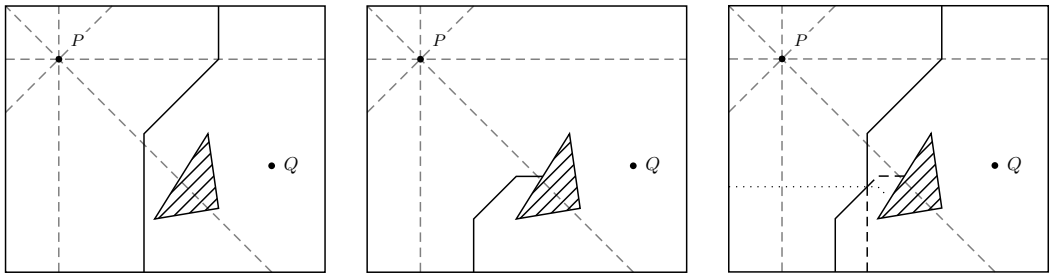

(a) Upper bisector part $l_1^{\mathcal{B}}(P,X) = l_1^{\mathcal{B},-}(Q,X)$.

(b) Lower bisector part $l_1^{\mathcal{B}}(P,X) = l_1^{\mathcal{B},+}(Q,X)$.

(c) $B^{\mathcal{B}}(P,Q)$.

Figure 2.12: The different bisector parts and their combination for the placement of $Q = (4,-2)$ within $\mathcal{P} = R((-1,-3.5),(5,0.5))$ with one existing facility $P = (0,0)$ and $\mathcal{B} = \Delta((1.8,-3),(2.8,-1.4),(3,-2.8))$. The line of equidistance from Q about $\mathcal{B}$ is shown in Figure 2.12c as a dotted line.

Therefore to understand the bisector we must understand the bisector parts since the bisector will change its representation only when the bisector parts change representation or when the line of equidistance about $\mathcal{B}$ intersects a different segment of the bisector part. So how do these bisector parts behave? We know from Lemma 2.3.1 that the bisector will remain unchanged if it is visible from both facilities, and this is also true for the bisector parts. Therefore we will explore how the bisector parts look when they venture into non-visible areas. When the bisector part enters a non-visible area, the shortest path from one of the facilities must always pass by an extreme point of $\mathcal{B}$ (see Figure 2.11). This extreme point then acts as one of the facilities for the bisector part beyond this point, but rather than the bisector part being the set of points that are equidistant from the visible facility and the extreme point (according to the certain shortest path orientation about $\mathcal{B}$), it is the set of points that are closer to the extreme point than to the visible facility by a magnitude of exactly twice the distance between the extreme point and the non-visible facility. These are the additive bisectors we showed in Section 2.1.

Thus, when the bisector part between P and Q enters a non-visible area from Q (i.e. the shortest paths must all pass by an extreme point B_i of $\mathcal{B}$) the bisector part in this non-visible area will be the additive bisector between P and B_i with c equal to the distance the shortest path has travelled from Q to B_i. In the barrier-constrained setting taking, for example, the bisector part from the clockwise path from P and anticlockwise from Q, we have the geodesic additive bisector $B_c^{add,+}(P,B_i) = \{Z \in \mathbb{R}^2 | l_1^{\mathcal{B},+}(P,Z) = l_1^{\mathcal{B},-}(B_i,Z) + c\}$ where $c = l_1^{\mathcal{B},-}(B_i,Q)$. The analogous definition for the 'lower' part $B_c^{add,-}(P,B_i)$ is clear from this. Using Figure 2.12b for a numerical example, the bottommost vertex of $\mathcal{B}$, $B = (1.8,-3)$, acts as the new active point within the additive bisector. Here $c = l_1(Q,B) = 3.2$ so Figure 2.12b displays $B_{3.2}^{add,-}(P,B) = \{Z \in \mathbb{R}^2 | l_1^{\mathcal{B},-}((0,0),Z) = l_1^{\mathcal{B},+}((1.8,-3),Z) + 3.2\}$.

This gives us a clearer idea of how the bisector part looks when it enters a non-visible area from either of the original facilities. This can obviously be extended to how it looks whenever it enters any new non-visible areas from any of the active points of the bisector part (facilities or extreme points from which the additive bisector is acting) as it will simply create a new additive bisector. Thus the bisector parts are a concatenation of the original bisector and additive bisectors, becoming a new additive bisector whenever the current one enters an area not visible from either one of the active points. An example of these bisector parts contributing to the final bisector is shown in Figure 2.13 (observe that an additive bisector may even have its own additive bisector).

So we have defined all potential Voronoi cells through the bisector parts of their bisectors. The exact production of the specific bisectors is studied in more detail in Section 3.3.1 and the configuration lines used to determine the expression of the additive bisector (as shown in Figure 2.4) are derived in Section 3.3.

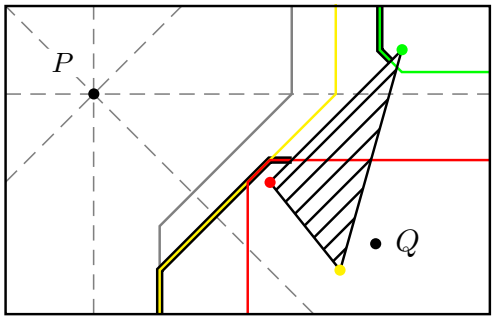

Figure 2.13: Bisectors and additive bisectors for the facilities $P = (0, 0)$ and $Q = (3.2, -1.7)$ in the presence of $\mathcal{B} = \Delta((2, -1), (2.8, -2), (3.5, 0.5))$. Each additive bisector $B_c^{add}(P, B_i)$, for B_i a vertex of $\mathcal{B}$ and $c = l_1^{\mathcal{B}}(B_i, Q)$, is colour-coded to match B_i; the bisector in the original barrier-free problem is shown in grey; and the overall barrier-constrained bisector is highlighted with a black border.

It is interesting to note that, when the bisector part between two active points P and Q enters an area of $\mathbb{R}^2$ that is not visible from P but visible from facility Q, it will change its direction by 45° (by the continuity of the additive bisector), choosing the bearing that travels equidistant from the vertex of $\mathcal{B}$ most recently passed on the shortest path from P. That is, a horizontal/vertical or a diagonal part will become a diagonal or horizontal/vertical part respectively. Otherwise a bisector part's direction remains unchanged. The only possibility for a different situation to arise would be if the bisector moves from an area visible to both facilities to one non-visible from both, but this is impossible (except in the degenerate quarterplane case which has already been addressed) for a convex $\mathcal{B}$ and convex $\mathcal{P}$ (for convex $\mathcal{P}$ only vertices of $\mathcal{B}$ can become active points). This can be seen by realising that a vertex becomes the new active point when the bisector crosses either the horizontal or vertical through it. If the bisector were to move into an area non-visible from both current active points, two new active points P and Q would have to be found (and at the same vertical or horizontal to the bisector), and of course they must be either side of the bisector. If these active points lie on the same horizontal or vertical as one another, then by the convexity of $\mathcal{B}$ the line PQ must be contained in $\mathcal{B}$, so there is no such area for the bisector to enter. For the other case, suppose that the bisector hits the horizontal of P and the vertical of Q. For P to act as an active point the bisector must travel vertically before hitting the horizontal of P. However, identically for Q the bisector must travel horizontally before hitting the vertical of Q, which is clearly a contradiction.

Therefore a bisector will only change direction by 45° unless it is crossing the line of equidistance around $\mathcal{B}$ (where the bisector part being used changes) in which case it can also change by 90°. We know that the angle can never be 135° by noticing that the line of equidistance about $\mathcal{B}$, since it is simply an additive bisector of sorts, is composed of only horizontal, vertical, and diagonal line segments. Now, suppose for contradiction that there is a change in direction of the bisector of 135°. As explained above, a bisector part can only change direction by 45° so this must be the point at which the upper and lower bisector parts meet (without loss of generality the shortest paths from Q must travel either side of $\mathcal{B}$, say). Therefore the line of equidistance from Q around $\mathcal{B}$ intersects the bisector (travelling from one side of the bisector to the other) at the point of this 135° direction change. However, as the line of equidistance enters the Voronoi cell of P containing the acute angle, it must, for however long, travel along the bisector itself since these bisector line segments are themselves diagonal, horizontal, or vertical. This is impossible. One can see this as, for small enough ε, travelling ε perpendicularly from the line of equidistance will move ε closer to Q, much as moving ε perpendicular to a bisector into a cell will move ε closer to the cell's facility. On the line segment shared by the line of equidistance and the bisector, venturing ε into $V(P)$ perpendicular to these lines will move both ε closer to P and ε closer to Q, and so this should also be contained in the bisector.

It is worth noting that even though the bisector parts may be affected by the barrier their combination to form the bisector may not be. Further more detailed exploration of the bisectors can be found later in Section 3.3.

For our facility location problems, the representation of the objective function changes if the representation of the Voronoi diagram changes. Therefore, using the knowledge obtained above, we explore the different structures that the Voronoi diagram can take, and look for a way to categorise these and identify the partition lines across which these changes take place.

2.4 Facility location games

In the formulation of the games we study, just as in Fekete and Meijer (2005), $\mathcal{P}$ is the rectangular playing board with width p and height q. Both players have $n > 1$ points to play and a player plays them all when it is their turn, where points cannot lie upon each other; W denotes the n points played by White (the 'leader'), while B is the set of n points played by Black (the 'follower'). After all of the $2n$ points have been played, each player receives a score equal to the area of $\mathcal{P}$ to which one of their points is the closest point. All distances are measured according to the l_1 norm.

Therefore each player receives a score equal to the area of the Voronoi cells of their points. That is, White and Black have respective scores

$$\mathcal{W} = \sum_{w \in W} Area(V(w))$$
$$\mathcal{B} = \sum_{b \in B} Area(V(b))$$

where the Voronoi diagram of the points played $\mathcal{VD}(W \cup B) = \{V(x) : x \in W \cup B\}$.

In the *Voronoi game* each player wishes to score the larger amount (so $> \frac{1}{2} Area(\mathcal{P})$) and in the *Stackelberg game* (a name coined following the seminal paper by von Stackelberg (1952)) each player aims to maximise their score. The subtlety dividing these games lies in the fact that the Voronoi game needs only a good enough strategy from the winning player whereas the Stackelberg game requires the best strategies from both players. In this way the Voronoi game uses a simpler arbitration to determine the effectiveness of each player's strategies, and the Stackelberg game can be considered a more in-depth and advanced extension of the Voronoi game.

To combat the possible confusion between Voronoi cells of the Voronoi diagram at different stages in the game, we introduce the following notation (for $b \in B$):

$$\mathcal{VD}(W) = \{V^{\circ}(x) : x \in W\}$$
$$\mathcal{VD}(W \cup b) = \{V^{+}(x) : x \in W \cup b\}$$
$$\mathcal{VD}(W \cup B) = \{V(x) : x \in W \cup B\}$$

At this point we may wonder how to score each player in the presence of degenerate bisectors between any $w \in W$ and $b \in B$; are the quarterplanes shared equally between both players, or should there perhaps be a first-come-first-served rule (these areas are *loyal* and remain with White), or finders-keepers rule (these areas are *curious* and transfer to Black) implemented for such cases, or should it even be declared that if White and Black won't stop fighting then no one gets them (simply *discard* the quarterplanes)? We shall answer this question by demonstrating that whichever option we choose either makes the game a trivial one in the Voronoi game or causes Black never to locate on a diagonal configuration line through one of White's points, thereby allowing us to forget all concerns of degenerate bisectors between white and black points.

Given White's arrangement W, we must explore how Black can fare by locating on a diagonal configuration line through one of White's points under the abovementioned modus operandi. Firstly, if the areas in question are curious then, by placing on the diagonal sufficiently close to one of White's points w, Black can capture over $75(1-\varepsilon)\%$ of $V^{\circ}(w)$ for any w and $\varepsilon > 0$. Therefore Black can always win the Voronoi game by playing each of their points as close to each of White's points upon a diagonal configuration line through these points. On the other

hand, if the areas are loyal then Black will never seek to locate on the diagonal through one of White's points. In this case, placing on the diagonal loses control of both quarterplanes whereas perturbing off this diagonal will gain one whole quarterplane at the expense of a strip bordering the other quarterplane. Provided that the gained quarterplane has non-zero area, this perturbation can be small enough to always improve the solution. Therefore Black will never choose to play on the diagonal.

Finally, if the quarterplanes are to be shared then diagonals are still never profitable for Black. If one quarterplane is larger than the other then if Black perturbs their point horizontally or vertically off the diagonal moving closer to the larger quarterplane, they will capture it all and so improve their solution. If both quarterplanes are the same area then such a perturbation will not decrease the solution value since the size and direction of the perturbation can always be chosen to balance any possible area change due to the slivers of area lost and gained on either side of the new non-degenerate bisector. In a similar vein, Black will never decrease their score by perturbing off the diagonal if the quarterplanes are discarded.

Therefore the optimal strategies are trivial in the curious case (see also the discussion beginning at Chapter 6) and in all other cases, though the supremum may often be on the diagonal, Black's optimal solution will never produce a degenerate bisector. For ease of exposition we shall say that if a point is placed upon a diagonal configuration line through a point of another colour, the player who placed their point last can choose which quarterplane they occupy (for example, if $b \in \mathcal{CC}^2(w)$ then Black can choose the bisector type of $b \in \mathcal{CC}^1$ or $b \in \mathcal{CC}^2(w)$). If readers do not enjoy this treatment of degenerate cases they may prefer to imagine the points lying on these diagonal configuration lines perturbed by a negligible amount to the appropriate side of the diagonal.

Depending on the chosen rule, we must not discount that it may be advantageous for White (or Black) to deliberately play a degenerate bisector among its own points. An advanced discussion of these degenerate bisectors between White's points is contained in Chapter 6.

Equipped with this background knowledge and a strong foundation of results, we can commence with the meat of this thesis.

Chapter 3

Conditional Facility Location Problems

In this chapter, we will explore the five previously mentioned location problems over a convex polygonal market region in the rectilinear plane containing one known convex polygonal barrier outside of which some facilities are already fixed within the space. Furthermore, we assume that the demand is continuous and uniform, with customers being served by the nearest facility only. We concentrate on conditional location problems where we wish to find the optimal location for an additional facility, the location of which has no restriction within the traversable polygon.

Our goal is to develop an algorithm to work with this continuous demand and an arbitrary convex polygonal barrier. To that end, in this chapter we derive the structural properties of geodesic Voronoi diagrams with rectilinear distances. This enables us to solve the overlying optimisation problem itself by restricting the location of the new facility to a sub-region where the resulting geodesic Voronoi diagram is structurally identical for every point in the region. Given such regions, we derive a parametric representation of the objective function which is valid for any location in the region. By this means we optimise the location of the new facility over this region using classical non-linear programming techniques, and the best optimal location of each sub-region is the optimal solution to the problem.

A summary of relevant literature is provided in Section 3.1. The issue of finding partitioning lines to preserve the representation is introduced in Section 3.2 and we outline a simple procedure to find all such partitioning lines in the presence of a barrier, followed by an analysis of this process. In response to this review, a more involved but ultimately more intuitive, undemanding, and satisfying method is derived in Section 3.3 wherein we identify seven distinct classifications of our partition lines. In Section 3.4 we compute the objective functions for the five conditional location problems previously defined.

3.1 Literature review

As alluded to in the Introduction, there is some literature on facility location problems with continuous demand, but it is meagre in comparison to that for discrete demand problems. The first discussion of location problems with continuous demand and rectilinear distances appears in Marucheck and Aly (1981) where a branch-and-bound algorithm is proposed for a rectangular market region model over which demand is distributed uniformly. An unbounded market region with uniform demand is studied in the general optimal market area model in Erlenkotter (1989) with l_1, l_2, and block norms, which also includes facility costs. Different supply area shapes of each facility are trialled (circle, square, diamond, and hexagon) and closed-form expressions for the optimal size of the supply area are derived, offering the opportunity to assess the sensitivity of non-optimally sized, or shaped, supply areas. All five problems we will explore are addressed in Averbakh et al. (2015) with uniform demand over a convex polygon with rectilinear distances. After identifying a partition of the market area which preserves the structural identity of the Voronoi diagram, they devise an exact polynomial algorithm for all five problems.

Exact polynomial algorithms solving the median problem for a single facility are proposed in Fekete et al. (2005) for straight-line rectilinear and geodesic distances and continuous demand, an approach they assert to be further applicable to multifacility problems if the boundaries of the Voronoi regions can be suitably represented. This is performed for polygonal market areas with and without holes; with holes it is shown to be NP-hard for multiple facilities whose number is part of the input. The two-facility problem is considered with l_1 and l_2 distances in Murat, Verter, and Laporte (2011). The problem is displayed as a two-dimensional boundary value problem with optimality conditions found, and is solved by means of a two-dimensional shooting algorithm.

Addressing the centre problem, Suzuki and Drezner (1996) derive upper and lower bounds for the p-centre problem for a convex polygonal area with uniform demand in Euclidean space by proposing a random-start heuristic based on Cooper's location-allocation algorithm. This is extended in Wei, Murray, and Xiao (2006) to cover non-convex demand regions with holes, wherein they apply their heuristic in order to find a preferable location for warning sirens.

With regard to market share problems, Okabe and Suzuki (1987) and Okabe and Aoyagi (1993) explore the equilibrium arrangements of competitive firms under a variety of premises (e.g. about the number of facilities or the market area's shape) by running simulations involving techniques such as the gradient descent method where each facility is permitted to relocate once in each time interval.

Regarding maximal covering location problems, Matisziw and Murray (2009a) describe the extension of their earlier study on discs to arbitrarily-shaped demand spaces. Murray and Tong (2007) solve the problem with a demand defined by points, line segments, or polygons with Euclidean distance. Murray, O'Kelly, and Church (2008) suggest partitioning the demand space into regular polygons for location set covering problems, using the Euclidean metric in their warning siren study.

There have been few forays into facility location problems with barriers, and we are not aware that any have broached the continuous demand problem. Katz and Cooper (1981) study the Weber problem for a given discrete set of demand points, a circular barrier, and Euclidean distances. They first show how to calculate the geodesic Euclidean distance between two points on the plane. Afterwards, to solve the problem, they propose to convert the non-linear constraint minimisation problem into a sequence of non-linear unconstrained minimisation problems. Aneja and Parlar (1994) consider the same setting, but with polygonal forbidden regions as well as with polygonal barriers. For the former, they show that either the optimal solution coincides with the optimal solution of the unconstrained problem, or it lies on the boundary of a forbidden region. For the latter, they propose a simulated annealing heuristic. Larson and Sadiq (1983) study the p-median problem with Manhattan distances and arbitrary barriers. Analysing the geometry of shortest geodesic paths, they identify a finite set of points on the plane that contains an optimal solution.

Given a discrete set of existing customers and convex polyhedral barriers, Klamroth (2001) find the location of a facility to optimise any convex objective function in the distances between the facility and customers by partitioning the space into smaller subproblems. Dearing et al. (2002) discuss the 1-centre problem in l_1 for discrete demand and a set of convex polyhedral barriers, and show that the optimal location is found in the set of intersection points between barrier-restricted bisectors. This is extended in Dearing et al. (2005) to the case of general block distances. In a more recent paper Oğuz et al. (2018) discretise not only the location space but the shortest-path space, in that the traversable region is reduced to a network as opposed to continuous space. The use of these discretisations to calculate the distances between the customer demand points and the potential new facility site transforms the continuous multi-facility Weber problem into a discrete problem formulated as a mixed-integer linear programming problem. Furthermore, both deterministic and probabilistic barriers are considered in this formulation. Regarding heuristics, Bischoff and Klamroth (2007) design a genetic algorithm for the 1-Weber problem with discrete demand and convex polyhedral barriers in a general metric space, which determines iteratively the subproblems (as noted above) to solve. For weighted geometric problems in the presence of obstacles, see Choi, Shin, and Kim (1998).

Finally we refer the reader to Canbolat and Wesolowsky (2012) for a novel and hands-on approach to solving such discrete problems. In their paper the Varignon frame method is adapted to the barrier-restricted 1-Weber problem in l_2 with discrete demand and one convex barrier, using physical weights and strings to find the optimal solution mechanically. We encourage any keen reader with time to spare to enjoy recreating some of these spidery contraptions.

3.2 Preliminary findings in partitions

3.2.1 Conditions on the preservation of the representation of the objective function for the 1+1 case

Before we tackle the general notion of extending the intersection lines in Averbakh et al. (2015) to the polygonal barrier case, we study how the bisectors can be affected by the existence of a barrier by looking at the $1 + 1$ case. In this section we consider one existing facility A_1 within a large rectangular $\mathcal{P}$ (so the polygonal space $\mathcal{P}$ becomes irrelevant) and within which there is a convex polygonal barrier $\mathcal{B}$. Since we are concerned merely with the shape of the partition we can, without loss of generality, take $A_1 = (0, 0)$. Additionally, whilst our pictorial examples involve only triangles for ease, the stated results are true for general convex polygonal barriers.

For our facility location problems, the representation of the objective function changes if the representation of the Voronoi diagram changes. Therefore we explore the different structures that the Voronoi diagram can take, and look for a way to categorise these and identify in what locations of Z these structures are found. After experimenting with placements of Z for a specific $\mathcal{B}$ example, one could divide up the space into regions that, if Z is placed within the region, share the same representation of the bisector.

In Figure 2.10 we saw a simple example of the different structures a Voronoi diagram can take in the presence of a barrier. These figures provide the ideal subject to dissect in order to demonstrate the explorations to which we refer, so we shall now produce a part of the partition for one existing facility $A_1 = (0, 0)$ within a rectangular $\mathcal{P} = R((-1, -3.5), (6, 0.5))$ with a triangular barrier $\mathcal{B} = \Delta(B_1, B_2, B_3) = \Delta((0.5, -3), (1, -1), (2, -2.5))$.

For the purposes of this example we shall consider only $Z = (x, y) \in \mathcal{CC}^8(A_1)$ positioned above $\mathcal{B}$, the bisector types of which are displayed in Figure 2.10. For these bisectors it is only the lower vertical bisector part which intersects (or does not intersect) the barrier edge, and we can differentiate between each bisector type by noting which top edge of $\mathcal{B}$ it intersects, or to which side of $\mathcal{B}$ the bisector falls if not intersecting $\mathcal{B}$ at all. Therefore we want to find when the lower vertical bisector part intersects the barrier edge $\overline{B_1B_2}$ (Figure 3.1a) and when it intersects the barrier edge $\overline{B_2B_3}$ (Figure 3.1b).

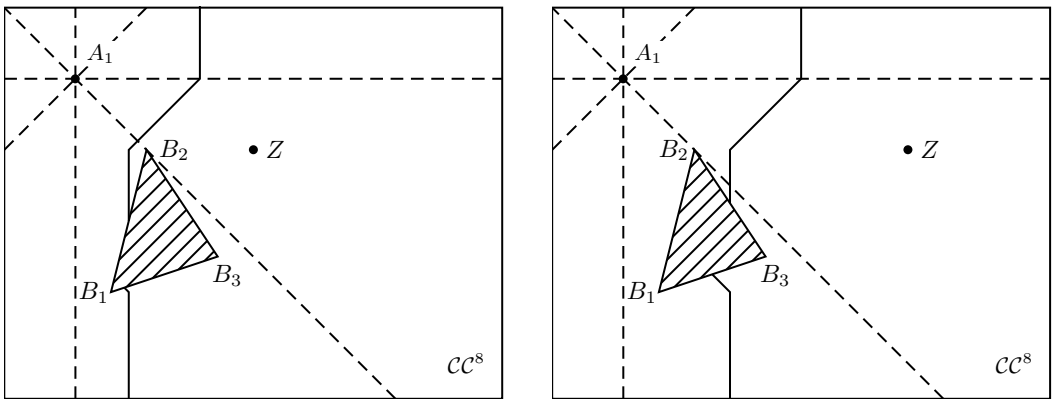

(a) $B(A_1, Z)$ intersects $\overline{B_1B_2}$.

(b) $B(A_1, Z)$ intersects $\overline{B_2B_3}$.

Figure 3.1: The two structures of a bisector that intersects $\mathcal{B} = \Delta((0.5, -3), (1, -1), (2, -2.5))$ for $A_1 = (0, 0)$ and $Z \in \mathcal{CC}^8(A_1)$.

In the uv plane, the lower vertical bisector part is the line

$$u = \frac{x-y}{2} + y = 0.5(x+y).$$

Hence, we obtain the following condition for this to intersect $\overline{B_1B_2} = \overline{(0.5,-3)(1,-1)}$ from above:

$$0.5 \;\leq\; 0.5(x+y) \;\leq\; 1\,,$$

and the following condition for an intersection with $\overline{B_2B_3} = \overline{(1,-1)(2,-2.5)}$:

$$1 \;\leq\; 0.5(x+y) \;\leq\; 2\,.$$

Thus we have the following partition lines in $\mathcal{CC}^8(A_1)$ (remembering the condition that Z lies above $\mathcal{B}$):

$$y = -1 \qquad x+y = 1 \qquad x+y = 2 \qquad x+y = 4$$

These lines give us the beginning of a partitioning of $\mathcal{P}$ into cells wherein each cell has structurally identical Voronoi diagrams $\mathcal{VD}(\{A_1, Z\})$ for Z located there, as shown in Figure 3.2.

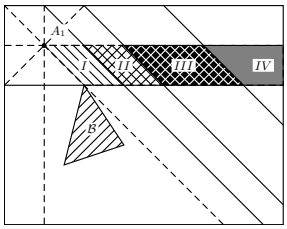

Figure 3.2: The beginning of a partition of $\mathcal{P}$.

An example of a complete partition is shown in Figure 3.3.

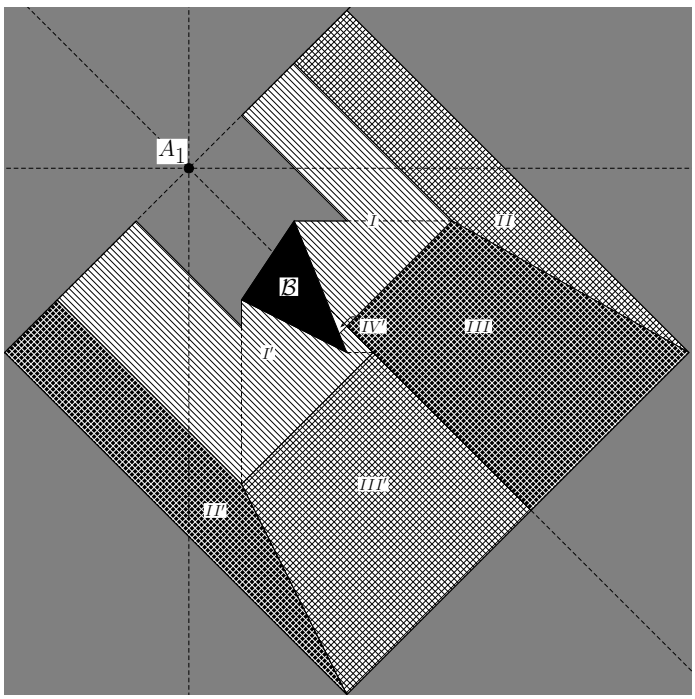

Figure 3.3: The complete partition of a large $\mathcal{P}$ with one existing facility $A_1 = (0,0)$ and a barrier $\mathcal{B}$ with vertices $(2,-5)$, $(4,-2)$, and $(6,-7)$.

Every cell in this partition corresponds to a different Voronoi diagram representation (the solid grey space covers the area over which the Voronoi diagram is not affected by the barrier). That is, if Z is placed in a different partition region of the space then it will produce a different bisector, and so a different Voronoi diagram. These Voronoi diagrams are shown in Figure 3.4. It is then within these regions that the placement of Z gives objective functions taking the same form, and thus it is over these regions that we can optimise. We ask, for any barrier $\mathcal{B}$, how do we find all of these lines which partition the space?

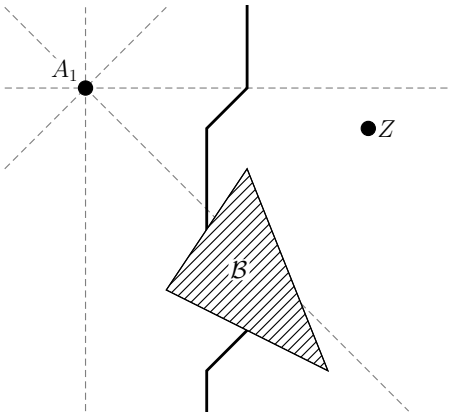

(a) Voronoi diagram for Z in Section I.

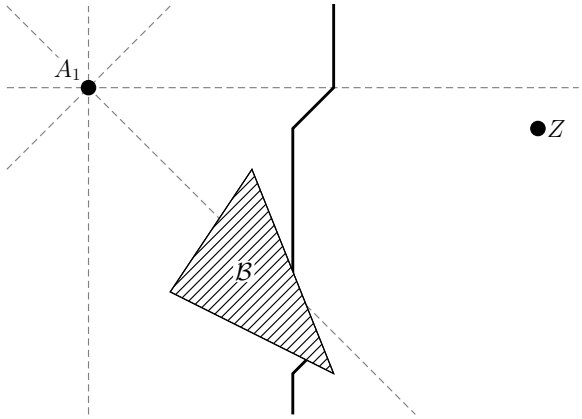

(b) Voronoi diagram for Z in Section II.

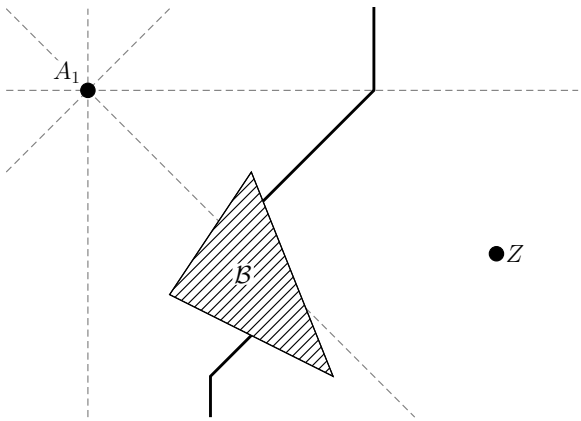

(c) Voronoi diagram for Z in Section III.

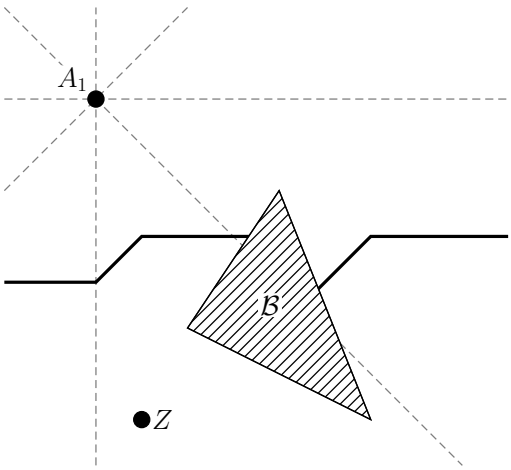

(d) Voronoi diagram for Z in Section I'.

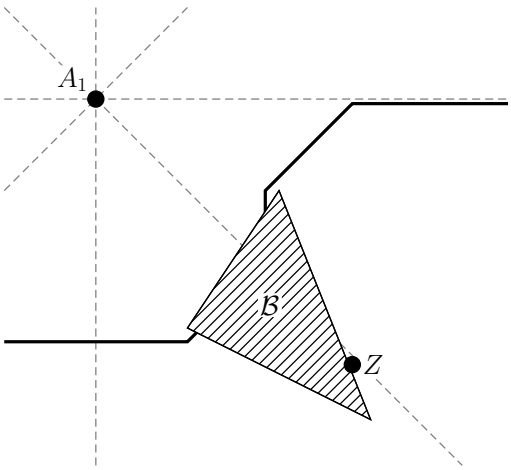

(e) Voronoi diagram for Z in Section IV'.

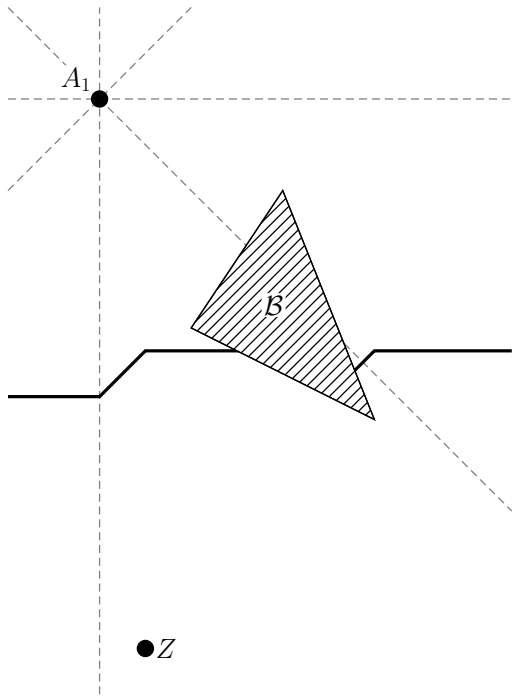

(f) Voronoi diagram for Z in Section II'.

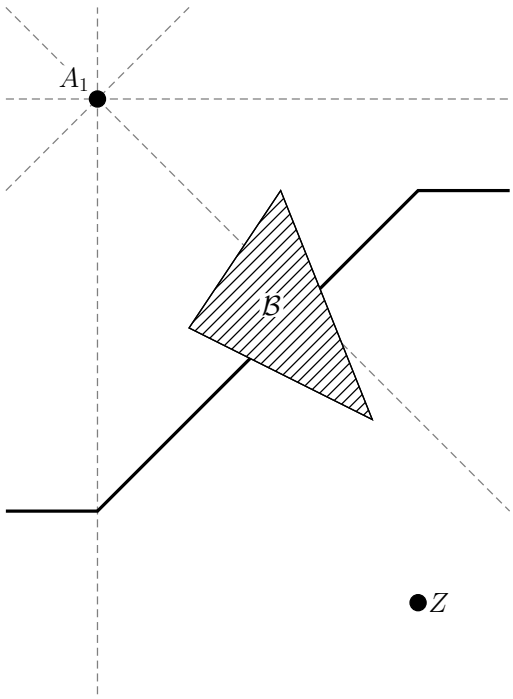

(g) Voronoi diagram for Z in Section III'.

Figure 3.4: All possible Voronoi diagram types for one existing facility $A_1 = (0, 0)$ and a barrier $\mathcal{B}$ with vertices $(2, -5)$, $(4, -2)$, and $(6, -7)$ within a large $\mathcal{P}$, where each section references those displayed in Figure 3.3.

An obvious approach to obtaining this partition would be to investigate the structures the Voronoi diagram can take when Z is limited to being located within certain areas only with respect to A_1 and $\mathcal{B}$, with the hope that these investigations can be extended to placing Z anywhere within $\mathcal{P}$. In this way we hope to be able to characterise the bisector types and notice when the bisectors change.

For our explorations we need only consider one existing facility A_1 and focus on locating Z in $\mathcal{CC}^8(A_1)$; since the results in $\mathcal{CC}^8$ are invariant under a rotation by 90° about A_1 and under a reflection in the horizontal or vertical axis, they carry over to the whole plane. Additionally the results hold for problems including multiple initial facilities $\{A_1, \ldots, A_n\}$ because, though adding another initial facility complicates the Voronoi diagram, the lines in $\mathcal{VD}$ are obtained purely from the bisectors between Z and exactly one existing facility, independent of other facilities. Therefore our partition will consist of the lines found for $B(A_1, Z)$ and these lines adapted appropriately for $B(A_i, Z)$ for all $i \in \{1, ..., n\}$. Additionally, given $\mathcal{VD}(A_1, \ldots, A_n)$, we must investigate the interaction not only between $B(Z, A_i)$ and $\mathcal{B}$ but with the lines within $\mathcal{VD}(A_1 m \ldots, A_n)$, much in the same way we have already seen. This theory can easily be applied to any of the general location problems since the partition is independent of any objective function.

We approach the difficulty that the barrier presents by observing how the bisector is affected by the addition of the barrier when we consider the placement of the new facility with respect to the barrier-free bisector. We will do this by investigating the bisector changes when the additional facility is placed in Sections I to $VIII$ as described in Figure 3.5, and also when placed within $Shadow(\mathcal{B})$ itself. Since we are only considering facilities $Z = (x, y) \in CC^8$ (whose bisector lies further right of the original facility A_1) we can discount Sections VI, VII, and $VIII$ as the barrier will not affect any shortest paths to the bisector. This corresponds to the constraint

$$x \geq \min_i b_{x_i} .$$

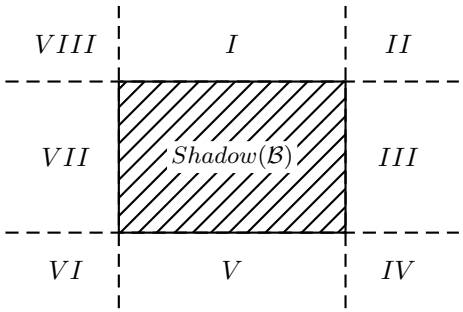

Figure 3.5: Sections respective to the barrier $\mathcal{B}$.

We need only investigate barriers entering either one or both of the first and fourth quadrants of the existing facility since the shortest paths between the facilities and the bisector travel, in the bisector-free scenario, in these quadrants (when we speak of quadrants, these will always refer to those with respect to A_1 unless otherwise stated).

3.2.2 Facilities within $Shadow(\mathcal{B})$

Firstly we shall investigate the bisector types if Z lies within the $Shadow(\mathcal{B})$. We shall split this section into the following four investigations: Z in the top left, top right, bottom left, and bottom right of $Shadow(\mathcal{B})$. It is clear that this is exhaustive and that Z can lie in one and only one of these.

Facilities within the top left of $Shadow(\mathcal{B})$

If Z lies in the top left of $Shadow(\mathcal{B})$ then $\mathcal{B}$ must enter the fourth quadrant and not the second quadrant. It is also clear that all of the second quadrant with respect to Z and the top left of $Shadow(\mathcal{B})$ is visible from both A_1 and Z. This contains the whole upper bisector part which is identical to the original bisector, whose intersection with $\mathcal{B}$ is classified by the lines (3.2.7) from Sections I and II as we will see. By Lemma 2.3.1 the only possible difference may come from the lower bisector part.

If the lower vertical bisector part falls to the left of $\mathcal{B}$ then the bisector takes the exact form of the original bisector. This is if $\frac{x+y}{2} < \min_i\{b_{x_i}\}$. Otherwise the lower vertical bisector hits an upward-facing edge of $\mathcal{B}$ and there must be a second bisector part. The lower vertical breakline (of this first ('upper') bisector part) hits a vertex B' of $\mathcal{B}$ if $b'_x < x$ and $b'_y \geq \min_i b_{iy}$ (so B' is an upward-facing vertex of $\mathcal{B}$), and if

$$\frac{x+y}{2} = b'_x\,. \tag{3.2.1}$$

The second ('lower') bisector part will consist of the points Q at which the distance from A_1 travelling anticlockwise around $\mathcal{B}$ is equal to the distance from Z travelling clockwise around $\mathcal{B}$: $l_1^{\mathcal{B},-}(A_1,Q) = l_1^{\mathcal{B},+}(Z,Q)$. This bisector part can intersect the bottom side of $\mathcal{B}$ creating a bisector in the way we have already seen, or the right side of $\mathcal{B}$ potentially creating a horizontal-type bisector (which will be discussed later). In order to determine when the structure of the Voronoi diagram changes according to these intersections with $\mathcal{B}$, we need to find the lines upon which $B(A_1,Z)$ intersects the vertices of $\mathcal{B}$ (since either side of such a line corresponds to intersecting each barrier edge incident to this vertex). These lines of intersection are found below in Lemma 3.2.1. Note that the shortest path from A_1 will always pass the leftmost vertex of $\mathcal{B}$ and the shortest path from Z will always pass the topmost vertex of $\mathcal{B}$.

Lemma 3.2.1. *Given a convex polygonal barrier $\mathcal{B}$ with vertices $B_i = (b_{ix}, b_{iy}) \in \mathbb{R}^2$, choose any vertex $B' = (b'_x, b'_y)$ on the upper right side or bottom side of $\mathcal{B}$. If $Z = (x, y)$ lies in the top left-hand corner of Shadow($\mathcal{B}$) then the bisector $B(A_1, Z)$ intersects B' if Z lies on one of the lines, if $\mathcal{B}$ enters the third quadrant,*

$$\begin{aligned} y &= -x + 2\max_i b_{ix} + 2\min b_{ix} + 2\max_i b_{iy} - 2\min_i b_{iy} - 2b'_x + 2b'_y \\ y &= -x + 2\max_i b_{ix} + 2\min b_{ix} + 2\max_i b_{iy} + 2\min_i b_{iy} - 2b'_x - 2b'_y \\ y &= -x - 2\max_i b_{ix} + 2\min b_{ix} + 2\max_i b_{iy} + 2\min_i b_{iy} + 2b'_x - 2b'_y \end{aligned} \tag{3.2.2}$$

or, otherwise,

$$\begin{aligned} y &= -x + 2\max_i b_{ix} + 2\max_i b_{iy} - 2\min_i b_{iy} - 2b'_x + 2b'_y \\ y &= -x + 2\max_i b_{ix} + 2\max_i b_{iy} + 2\min_i b_{iy} - 2b'_x - 2b'_y \\ y &= -x - 2\max_i b_{ix} + 2\max_i b_{iy} + 2\min_i b_{iy} + 2b'_x - 2b'_y \end{aligned} \tag{3.2.3}$$

for B' on the bottom left, bottom right, and top right of $\mathcal{B}$ respectively.

Proof. At this lower breakline, both the distance from A_1 to B' along the bottom of $\mathcal{B}$ and the distance from Z to B' along the top of $\mathcal{B}$ must be equal. We have the following distances displayed in Table 3.1 conditional on the position and shape of $\mathcal{B}$ and for B' on the bottom side or upper right side (where the path from A_1 to B' will have to pass the leftmost vertex if and only if $\mathcal{B}$ enters the third quadrant).

Vertices passed:			Distance between Z and B' ($l_1^{\mathcal{B},+}(Z, B')$)
topmost	bottommost	rightmost	
✓			$b'_x - x + 2\max_i b_{iy} - y - b'_y$
✓		✓	$2\max_i b_{ix} - x - b'_x + 2\max_i b_{iy} - y - b'_y$
✓	✓	✓	$2\max_i b_{ix} - x - b'_x + 2\max_i b_{iy} - y - 2\min_i b_{iy} + b'_y$

Vertices passed:			Distance between A_1 and B' ($l_1^{\mathcal{B},-}(A_1, B')$)
leftmost	rightmost	bottommost	
			$b'_x - b'_y$
		✓	$b'_x - 2\min_i b_{iy} + b'_y$
	✓	✓	$2\max_i b_{ix} - b'_x - 2\min_i b_{iy} + b'_y$
✓			$-2\min b_{ix} + b'_x - b'_y$
✓		✓	$-2\min b_{ix} + b'_x - 2\min_i b_{iy} + b'_y$
✓	✓	✓	$2\max_i b_{ix} - 2\min b_{ix} - b'_x - 2\min_i b_{iy} + b'_y$

Table 3.1: Distances to B' from A_1 and Z along opposite sides of $\mathcal{B}$.

Equating each of the three distances in the first table with the six in the other table gives eighteen lines. However, since the route following the shortest path from A_1 to B' and then from B' to Z travels below $\mathcal{B}$, only one of the shortest paths must pass by the bottommost vertex and the rightmost vertex of $\mathcal{B}$, so as before we can choose the distances to equate.

Therefore we have nine lines. If B' is on the bottom left of $\mathcal{B}$ then

$$\begin{aligned} 2\max_i b_{ix} - x - b'_x + 2\max_i b_{iy} - y - 2\min_i b_{iy} + b'_y &= b'_x - b'_y \\ \Rightarrow y &= -x + 2\max_i b_{ix} + 2\max_i b_{iy} - 2\min_i b_{iy} - 2b'_x + 2b'_y \end{aligned}$$

or, if $\mathcal{B}$ enters the third quadrant,

$$\begin{aligned} 2\max_i b_{ix} - x - b'_x + 2\max_i b_{iy} - y - 2\min_i b_{iy} + b'_y &= -2\min b_{ix} + b'_x - b'_y \\ \Rightarrow y &= -x + 2\max_i b_{ix} + 2\min b_{ix} + 2\max_i b_{iy} - 2\min_i b_{iy} - 2b'_x + 2b'_y\,. \end{aligned}$$

Otherwise, if B' is on the bottom right of $\mathcal{B}$ then

$$\begin{aligned} 2\max_i b_{ix} - x - b'_x + 2\max_i b_{iy} - y - b'_y &= b'_x - 2\min_i b_{iy} + b'_y \\ \Rightarrow y &= -x + 2\max_i b_{ix} + 2\max_i b_{iy} + 2\min_i b_{iy} - 2b'_x - 2b'_y \end{aligned}$$

or, if $\mathcal{B}$ enters the third quadrant,

$$\begin{aligned} 2\max_i b_{ix} - x - b'_x + 2\max_i b_{iy} - y - b'_y &= -2\min b_{ix} + b'_x - 2\min_i b_{iy} + b'_y \\ \Rightarrow y &= -x + 2\max_i b_{ix} + 2\min b_{ix} + 2\max_i b_{iy} + 2\min_i b_{iy} - 2b'_x - 2b'_y \,. \end{aligned}$$

Otherwise, if B' is on the top right of $\mathcal{B}$ then

$$\begin{aligned} b'_x - x + 2\max_i b_{iy} - y - b'_y &= 2\max_i b_{ix} - b'_x - 2\min_i b_{iy} + b'_y \\ \Rightarrow y &= -x - 2\max_i b_{ix} + 2\max_i b_{iy} + 2\min_i b_{iy} + 2b'_x - 2b'_y \end{aligned}$$

or, if $\mathcal{B}$ enters the third quadrant,

$$\begin{aligned} b'_x - x + 2\max_i b_{iy} - y - b'_y &= 2\max_i b_{ix} - 2\min b_{ix} - b'_x - 2\min_i b_{iy} + b'_y \\ \Rightarrow y &= -x - 2\max_i b_{ix} + 2\min b_{ix} + 2\max_i b_{iy} + 2\min_i b_{iy} + 2b'_x - 2b'_y \,. \end{aligned}$$

□

Now that we have discerned all of the possible intersections between $B(A_1, Z)$ and $\mathcal{B}$, we must consider how the bisector parts behave after intersection – i.e. do they remain a $\mathcal{CC}^8$ bisector type? The answer is no, not necessarily. If the lower bisector part intersects the top right of $\mathcal{B}$ then we obtain the additive bisector with active points being the topmost and rightmost vertices of $\mathcal{B}$; if the lower bisector part intersects the bottom right of $\mathcal{B}$ then we obtain the additive bisector with active points being the rightmost and bottommost vertices of $\mathcal{B}$; and if the lower bisector part intersects the bottom left of $\mathcal{B}$ then we obtain the additive bisector with active points being the bottommost and leftmost vertices of $\mathcal{B}$. As we have seen, the structure of additive bisectors $B_c^{add}(P, Q)$ depends heavily on the value of c, and the structure will change when the value of c is such that the distance from P to a non-vertex corner of $R(P, Q)$ is equal to the distance from Q to that same corner plus c. In our situation, this means our structure will change when the additive bisector crosses the corners of C_2, C_3, or C_4 of $Shadow(\mathcal{B})$ (for each of our possible additive bisectors described above, respectively). Therefore the partitioning lines are exactly the lines upon which Z is the same distance away from C_i as A_1 is from C_i, for $i = 2, 3, 4$. These are found in Lemma 3.2.2.

Lemma 3.2.2. *Given a convex polygonal barrier $\mathcal{B}$ with vertices $B_i = (b_{ix}, b_{iy}) \in \mathbb{R}^2$, if $Z = (x, y)$ lies in the top left-hand corner of $Shadow(\mathcal{B})$ then the bisector $B(A_1, Z)$ intersects C_2 if Z lies on the line*

$$y = -x + \min_i b_{ix} - |\min_i b_{ix}| + 2\min_i b_{iy} \,, \tag{3.2.4}$$

intersects C_3 if Z lies on the line

$$y = -x + \min_i b_{ix} - |\min_i b_{ix}| + 2\max_i b_{iy} \,, \tag{3.2.5}$$

and intersects C_4 if Z lies on the line

$$y = -x + 2\max_i b_{ix} - \min_i b_{ix} - |\min_i b_{ix}| + 2\max_i b_{iy} \,. \tag{3.2.6}$$

Proof. The calculations to determine when $B(A_1, Z)$ intersects each C_i are more straightforward than those shown in Lemma 3.2.1 since we know which extreme vertices of $\mathcal{B}$ must be passed on

the shortest path from A_1 and from Z. These distances are shown in Table 3.2.

i	$l_1^{\mathcal{B},+}(Z, C_i)$
2	$\max_i b_{ix} - x + \max_i b_{iy} - y$
3	$\max_i b_{ix} - x + 2\max_i b_{iy} - \min_i b_{iy} - y$
4	$2\max_i b_{ix} - \min_i b_{ix} - x + 2\max_i b_{iy} - \min_i b_{iy} - y$

i	$l_1^{\mathcal{B},-}(A_1, C_i)$
2	$\max_i b_{ix} - \min_i b_{ix} + \lvert\min_i b_{ix}\rvert + \max_i b_{iy} - 2\min_i b_{iy}$
3	$\max_i b_{ix} - \min_i b_{ix} + \lvert\min_i b_{ix}\rvert - \min_i b_{iy}$
4	$\lvert\min_i b_{ix}\rvert - \min_i b_{iy}$

Table 3.2: Distances to C_i from A_1 and Z along opposite sides of $\mathcal{B}$.

Equating each of these three distances give us our required lines.

Therefore the line associated with C_2 is

$$\begin{aligned}\max_i b_{ix} - x + \max_i b_{iy} - y = \max_i b_{ix} - \min_i b_{ix} + \lvert\min_i b_{ix}\rvert + \max_i b_{iy} - 2\min_i b_{iy}\\ \Rightarrow y = -x + \min_i b_{ix} - \lvert\min_i b_{ix}\rvert + 2\min_i b_{iy},\end{aligned}$$

the line associated with C_3 is

$$\begin{aligned}\max_i b_{ix} - x + 2\max_i b_{iy} - \min_i b_{iy} - y = \max_i b_{ix} - \min_i b_{ix} + \lvert\min_i b_{ix}\rvert - \min_i b_{iy}\\ \Rightarrow y = -x + \min_i b_{ix} - \lvert\min_i b_{ix}\rvert + 2\max_i b_{iy}\,,\end{aligned}$$

and the line associated with C_4 is

$$\begin{aligned}2\max_i b_{ix} - \min_i b_{ix} - x + 2\max_i b_{iy} - \min_i b_{iy} - y = \lvert\min_i b_{ix}\rvert - \min_i b_{iy}\\ \Rightarrow y = -x + 2\max_i b_{ix} - \min_i b_{ix} - \lvert\min_i b_{ix}\rvert + 2\max_i b_{iy}\,.\end{aligned}$$

□

Thus we have found the partitioning lines (3.2.2), (3.2.3), (3.2.4), (3.2.5), and (3.2.6) (as well as lines (3.2.7), the exploration of which we have postponed until the more appropriate Section 3.2.3) which completely partition the top left corner of $Shadow(\mathcal{B})$ into our desired cells.

Facilities within the top right, bottom left, and bottom right of $Shadow(\mathcal{B})$

For the remainder of the corners of $Shadow(\mathcal{B})$ we observe a simple property that will greatly reduce the workload (to nothing in fact) to find the partitioning lines.

For Z in the top right corner of $Shadow(\mathcal{B})$, the shortest path from A_1 to Z can travel past the topmost vertex of $\mathcal{B}$ if travelling anticlockwise, and must travel past the rightmost vertex of $\mathcal{B}$ if travelling clockwise. Note also that any point within the top right corner of $Shadow(\mathcal{B})$ remains at the same distance from the topmost and rightmost vertices of $\mathcal{B}$ as it moves (remaining within $Shadow(\mathcal{B})$) diagonally in the northeasterly (or southwesterly) direction. Therefore, since it is these distances that dictate the form of the bisector, the bisector $B(A_1, Z)$ is identical for all Z on this diagonal (with gradient 1) within the corner of $Shadow(\mathcal{B})$. This bisector is therefore identical to the bisector of Z on the edge of $Shadow(\mathcal{B})$ (where the diagonal meets the perimeter of $Shadow(\mathcal{B})$). This means that any partitioning lines in Sections I and III that meet the edge of $Shadow(\mathcal{B})$ in the top right corner can be continued in a diagonal into the top right corner of $Shadow(\mathcal{B})$. Therefore, once we know the partitioning lines in Sections I and III, we know the partitioning lines in the top right corner of $Shadow(\mathcal{B})$.

An identical argument can be used for the bottom left and bottom right corners, using northeasterly and northwesterly diagonal lines respectively. This sufficiently partitions the remaining corners and we need not explore any more lines within $Shadow(\mathcal{B})$.

3.2.3 Facilities in Sections I and Sections II

For an additional facility in Sections I and II, since it is above the barrier, only the lower vertical of the bisector might change (by Lemma 2.3.1) – as we have seen in Figure 2.10. Therefore we investigate how the bisectors can change as the lower vertical of the upper bisector part and the lower bisector part intersect different parts of $\mathcal{B}$.

The barrier is constrained to the third and fourth quadrant (by the Section I and II conditions and $\mathcal{CC}^8$ condition along with convexity of $\mathcal{B}$), entering the third quadrant only if it is also in the fourth quadrant. If intersecting the barrier, the bisector enters a top-facing edge (so visible from both facilities) of $\mathcal{B}$ and leaves from a bottom-facing edge (so not visible from both facilities) of $\mathcal{B}$ by Lemmas 2.3.1 and 2.3.2, meaning we need only consider conditions on which edge each bisector part touches. If Z lies in Section I or II of a barrier then the triangles in Figure 3.6 display all of the possible cases of intersection (note that the bisector in Figure 3.6f is not possible if Z lies in Section I).

Each of the bisector types in Figures 3.6a, 3.6b, 3.6d, and 3.6f are defined by where the lower vertical breakline of the upper bisector part falls down to meet the barrier. Therefore it is clear that they are partitioned in part by the lines induced by the vertical breaklines intersecting a vertex of the triangle. That is, for a vertex $B' = (b'_x, b'_y) \in \mathbb{R}^+ \times \mathbb{R}^-$ on the top side of $\mathcal{B}$ and $Z = (x, y) \in \mathcal{CC}^8$, exactly the line:

$$|b'_x| = \frac{1}{2}(|x| + |y|) - |y| \Rightarrow y = 2b'_x - x\,. \tag{3.2.7}$$

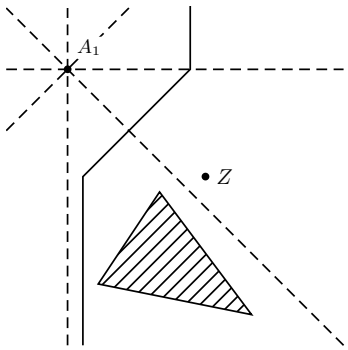

(a) Bisector line not intersecting the barrier, passing to the left.

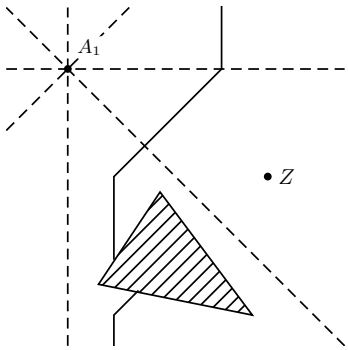

(b) Vertical bisector line intersecting the leftmost visible barrier edge.

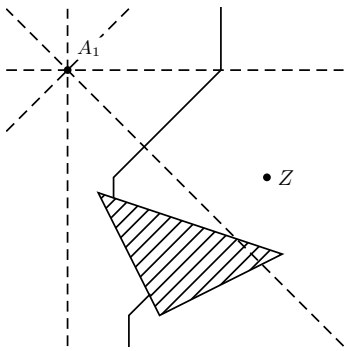

(c) Vertical bisector line intersecting the leftmost non-visible barrier edge.

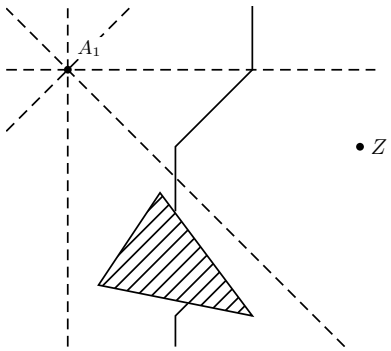

(d) Vertical bisector line intersecting the rightmost visible barrier edge.

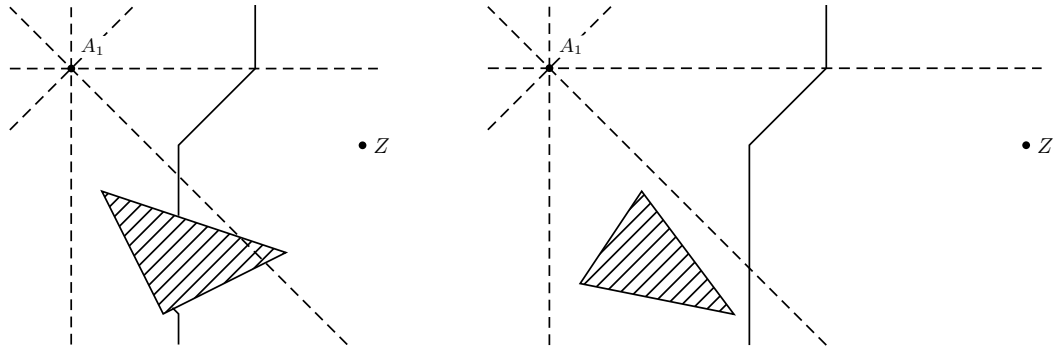

(e) Vertical bisector line intersecting the rightmost non-visible barrier edge.

(f) Bisector line not intersecting the barrier, passing to the right.

Figure 3.6: All bisector types for placement of Z in Sections I and II.

The bisectors in Figures 3.6c and 3.6e depend on where the vertical breakline of the lower bisector part rises up in relation to the barrier. This is where the vertical breakline diagonalises to intersect the vertex from below. For a barrier contained solely in the third and fourth quadrant with non-empty intersection with the fourth quadrant, and facilities in Section I or II, Lemma 3.2.3 lists the lines upon which the vertical breakline rises to meet a barrier vertex.

Lemma 3.2.3. *Given a polygonal barrier $\mathcal{B}$ with vertices $B_i = (b_{ix}, b_{iy}) \in \mathbb{R} \times \mathbb{R}^-$, choose any vertex $B' = (b'_x, b'_y)$ on the bottom side of $\mathcal{B}$. The bisector between the Voronoi cells of A_1 and Z intersects vertex B' if $Z = (x, y)$ lies on one of the lines, if Z is in Section I,*

$$\begin{aligned} y &= x - 2\max_i b_{ix} + |\min_i b_{ix}| - \min_i b_{ix} + 2\min_i b_{iy} + 2b'_x - 2b'_y \\ y &= x - 2\max_i b_{ix} + |\min_i b_{ix}| - \min_i b_{ix} - 2\min_i b_{iy} + 2b'_x + 2b'_y\,, \end{aligned} \tag{3.2.8}$$

and, if Z is in Section II,

$$\begin{aligned} y &= -x + |\min_i b_{ix}| - \min_i b_{ix} + 2\min_i b_{iy} + 2b'_x - 2b'_y \\ y &= -x + |\min_i b_{ix}| - \min_i b_{ix} - 2\min_i b_{iy} + 2b'_x + 2b'_y\,. \end{aligned} \tag{3.2.9}$$

Proof. At the lower vertical breakline, both the distances $l_1^{\mathcal{B},-}(A_1, B')$ and $l_1^{\mathcal{B},+}(Z, B')$ are equal. We have the following distances displayed in Table 3.3 conditional on the position and shape of $\mathcal{B}$.

Vertices of $\mathcal{B}$ passed: bottommost	$l_1^{\mathcal{B},-}(A_1, B')$
	$\lvert\min_i b_{ix}\rvert + b'_x - \min_i b_{ix} - b'_y$
✓	$\lvert\min_i b_{ix}\rvert + b'_x - \min_i b_{ix} - 2\min_i b_{iy} + b'_y$

Vertices of $\mathcal{B}$ passed: bottommost	$l_1^{\mathcal{B},+}(Z, B')$
	$\lvert x - \max_i b_{ix}\rvert + \max_i b_{ix} - b'_x + y - b'_y$
✓	$\lvert x - \max_i b_{ix}\rvert + \max_i b_{ix} - b'_x + y - 2\min_i b_{iy} + b'_y$

Table 3.3: Distances to B' from A_1 and Z along the bottom side of $\mathcal{B}$.

Note that the shortest path from A_1 to a vertex on the underbelly of $\mathcal{B}$, passing by the left of $\mathcal{B}$, must (or can be made to) pass the leftmost vertex (since the leftmost vertex is not above A_1 otherwise there would be no Section I or II in $\mathcal{CC}^8$), and similarly for Z passing by the right of $\mathcal{B}$.

Equating each of the two distances in one table with each of the two in the other table gives four lines. However, since the route consisting of the shortest path from A_1 to B' anticlockwise around $\mathcal{B}$ and then the shortest path from B' to Z anticlockwise around $\mathcal{B}$ travels below $\mathcal{B}$, exactly one of the shortest paths must pass by the bottommost vertex of $\mathcal{B}$; both of them travelling by the bottommost vertex equates to B' being the bottommost vertex ($\mathcal{B}$ is convex so two vertices can be the bottommost vertex only if there lies an edge of $\mathcal{B}$ between the two vertices, and both distances in the table are correct for this case).

Therefore we have two lines. If B' is to the left of the bottommost vertex then

$$\begin{aligned} |\min_i b_{ix}| + b'_x - \min_i b_{ix} - b'_y &= |x - \max_i b_{ix}| + \max_i b_{ix} - b'_x + y - 2\min_i b_{iy} + b'_y \\ \Rightarrow y &= -|x - \max_i b_{ix}| - \max_i b_{ix} + |\min_i b_{ix}| - \min_i b_{ix} + 2\min_i b_{iy} + 2b'_x - 2b'_y. \end{aligned}$$

If Z is in Section I then we have the line

$$y = x - 2\max_i b_{ix} + |\min_i b_{ix}| - \min_i b_{ix} + 2\min_i b_{iy} + 2b'_x - 2b'_y$$

and if Z is in Section II then we have the line

$$y = -x + |\min_i b_{ix}| - \min_i b_{ix} + 2\min_i b_{iy} + 2b'_x - 2b'_y.$$

Otherwise, if B' is to the right of the bottommost vertex then

$$\begin{aligned} |\min_i b_{ix}| + b'_x - \min_i b_{ix} - 2\min_i b_{iy} + b'_y &= |x - \max_i b_{ix}| + \max_i b_{ix} - b'_x + y - b'_y \\ \Rightarrow y &= -|x - \max_i b_{ix}| - \max_i b_{ix} + |\min_i b_{ix}| - \min_i b_{ix} - 2\min_i b_{iy} + 2b'_x + 2b'_y. \end{aligned}$$

If Z is in Section I then we have the line

$$y = x - 2\max_i b_{ix} + |\min_i b_{ix}| - \min_i b_{ix} - 2\min_i b_{iy} + 2b'_x + 2b'_y$$

and if Z is in Section II then we have the line

$$y = -x + |\min_i b_{ix}| - \min_i b_{ix} - 2\min_i b_{iy} + 2b'_x + 2b'_y.$$

□

We have found partitioning lines (3.2.7), (3.2.8), and (3.2.9) of where the bisector intersects each edge of $\mathcal{B}$ from above and from below. For a facility Z in Section I or II it is clear that these are the only possible representations of the bisector; if the bisector intersects the barrier then, by Lemmas 2.3.1 and 2.3.2, it must touch the barrier on exactly one upward-facing edge and exactly one downward-facing edge. Therefore we have defined the partition boundaries for all bisector representations for Z in Section I or II.

3.2.4 Facilities in Section III

Now we consider facilities in Section III. To find all partitioning lines within Section III we will have to investigate the possible barrier intersections of the upper bisector part, the possible barrier intersections of the lower bisector part, and the possible intersections of the upper and lower bisector parts, and then finally determine how the structures of each bisector part can change. The barrier must enter the third and/or fourth quadrant for Section III to occur in $\mathcal{CC}^8$ and if it does not enter the fourth quadrant then it must be enter all of the first, second, and third quadrants in order to affect the bisector.

We shall consider how the upper bisector part can be influenced by the barrier.

If $\mathcal{B}$ does not enter both the first and second quadrants then the vertical breakline in the barrier-free bisector is visible from both A_1 and Z (or at least some ray of it is) and so, for the most part, the upper bisector part resembles the bisector in the barrier-free problem. In this case the upper bisector differs from the barrier-free case only if the topmost vertex of $\mathcal{B}$ lies within the

first or fourth quadrants. If the topmost vertex lies within the first quadrant (i.e. $\max_i b_{iy} > 0$) then, at $y = \max_i b_{iy}$, the vertical breakline will become a diagonal, travelling equidistant to the topmost vertex until it intersects $\mathcal{B}$ or until it hits the ray descending vertically from the leftmost (or rightmost) vertex of $\mathcal{B}$ (at which point it will become a horizontal until intersecting $\mathcal{B}$) or until it intersects the horizontal through A_1 (or Z) (at which point it will become a vertical indefinitely or until intersecting the lower bisector part). Instead, if the topmost vertex lies within the fourth quadrant (i.e. $\max_i b_{iy} < 0$) then: if, at $y = \max_i b_{iy}$, the bisector is left of the topmost vertex of $\mathcal{B}$ then it will become a vertical, continuing indefinitely or until it hits $\mathcal{B}$ or the lower bisector part; otherwise it will continue diagonally until it hits $\mathcal{B}$, the lower bisector part, the horizontal line through Z (at which point it will become a vertical (this is exactly the bisector in the barrier-free problem) and continue indefinitely or until it hits $\mathcal{B}$ – it will not intersect the lower bisector part before $\mathcal{B}$ by Lemma 2.3.1), or the vertical ray descending from the rightmost vertex of $\mathcal{B}$ (at which point it will become a horizontal and again continue until an intersection with either $\mathcal{B}$ or the lower bisector part – since Z is in Section III the point at which the bisector part becomes horizontal is itself within Section III and travelling towards $\mathcal{B}$ so it will intersect $\mathcal{B}$ if not the lower bisector part).

The representation of the bisector will change when the bisector intersects a new edge of $\mathcal{B}$ or when its orientation changes as described above. The following lemma finds the lines dictating the intersections of the upper bisector part with $\mathcal{B}$ for a barrier $\mathcal{B}$ which does not enter the second quadrant.

Lemma 3.2.4. *Given a convex polygonal barrier $\mathcal{B}$ with vertices $B_i = (b_{ix}, b_{iy}) \in \mathbb{R}^2$ such that $\mathcal{B} \cap (\mathbb{R}^- \times \mathbb{R}^+) = \emptyset$, choose any vertex $B' = (b'_x, b'_y)$ of $\mathcal{B}$. Let $Z = (x, y)$ lie in Section III. The bisector $B(A_1, Z)$ intersects vertex B' if Z lies on one of the lines*

$$\begin{aligned} y &= x - 2b'_x + 2\max_i b_{iy} \\ y &= x - 2b'_x + 2b'_y - \max_i b_{iy} - |\max_i b_{iy}| \\ y &= x + 2b'_y - 2\max_i b_{ix} - \max_i b_{iy} - |\max_i b_{iy}|\,. \end{aligned} \tag{3.2.10}$$

Proof. In a similar approach to that in the proof of Lemma 3.2.3, we shall investigate the distances which comprise the upper bisector part, $l_1^{\mathcal{B},+}(A_1, B')$ and $l_1^{\mathcal{B},-}(Z, B')$, and equate them. The table below contains the various forms these distances can take depending on B''s location upon $\mathcal{B}$. For $\mathcal{B}$ not entering the second quadrant, the uppermost part of the upper bisector part will be identical to the original bisector and all of the second quadrant will belong in $V(A_1)$ while all of Section II will belong in $V(Z)$. Therefore the upper bisector part can only ever intersect the top side of $\mathcal{B}$ or the bottom side of $\mathcal{B}$ to the right of the bottommost vertex, and only points above Z. For this reason the shortest paths to B' from A_1 and Z are only possibly restricted by the rightmost and topmost vertices respectively.

Vertices passed: rightmost	Vertices passed: topmost	$l^{\mathcal{B},+}(A_1, B')$
		$b'_x - b'_y$
	✓	$b'_x + \max_i b_{iy} + \lvert\max_i b_{iy}\rvert - b'_y$
✓	✓	$2\max_i b_{ix} - b'_x + \max_i b_{iy} + \lvert\max_i b_{iy}\rvert - b'_y$

Vertices passed: topmost	$l^{\mathcal{B},-}(Z, B')$
	$x - b'_x + b'_y - y$
✓	$x - b'_x + 2\max_i b_{iy} - y - b'_y$

Table 3.4: Distances to B' from A_1 and Z along opposite sides of $\mathcal{B}$.

Equating each of the three distances in one table with each of the two in the other table gives six lines. However, since the route consisting of the shortest path from A_1 to B' anticlockwise around $\mathcal{B}$ and then the shortest path from B' to Z anticlockwise around $\mathcal{B}$ travels above $\mathcal{B}$,

exactly one of the shortest paths must pass by the topmost vertex of $\mathcal{B}$; both of them travelling by the topmost vertex equates to B' being the topmost vertex ($\mathcal{B}$ is convex so two vertices can be the topmost vertex only if there lies an edge of $\mathcal{B}$ between the two vertices, and both distances in the table are correct for this case). Therefore we need only equate distances from travelling via the topmost vertex with distances from not travelling via the topmost vertex. Equating appropriate distances from Table 3.4, we obtain three lines.

If B' is on the top side of $\mathcal{B}$ to the left of the topmost point then

$$\begin{aligned} b'_x - b'_y &= x - b'_x + 2\max_i b_{iy} - y - b'_y \\ &\Rightarrow y = x - 2b'_x + 2\max_i b_{iy}\,. \end{aligned}$$

If B' is on the top side of $\mathcal{B}$ to the right of the topmost point then

$$\begin{aligned} b'_x + \max_i b_{iy} + |\max_i b_{iy}| - b'_y &= x - b'_x + b'_y - y \\ \Rightarrow y &= x - 2b'_x + 2b'_y - \max_i b_{iy} - |\max_i b_{iy}|\,. \end{aligned}$$

If B' is on the bottom side of $\mathcal{B}$ to the right of the bottommost point then

$$\begin{aligned} 2\max_i b_{ix} - b'_x + \max_i b_{iy} + |\max_i b_{iy}| - b'_y &= x - b'_x + b'_y - y \\ \Rightarrow y &= x + 2b'_y - 2\max_i b_{ix} - \max_i b_{iy} - |\max_i b_{iy}|\,. \end{aligned}$$

□

This next lemma proves an equivalent result for $\mathcal{B}$ entering the second quadrant.

Lemma 3.2.5. *Given a convex polygonal barrier $\mathcal{B}$ with vertices $B_i = (b_{ix}, b_{iy}) \in \mathbb{R}^2$ such that $\mathcal{B} \cap (\mathbb{R}^- \times \mathbb{R}^+) \neq \emptyset$, choose any vertex $B' = (b'_x, b'_y)$ of $\mathcal{B}$. Let $Z = (x, y)$ lie in Section III. If $\mathcal{B}$ enters the third quadrant then the bisector $B(A_1, Z)$ intersects vertex B' if Z lies on one of the lines*

$$\begin{aligned} y &= x - 2\min_i b_{ix} + 2b'_x + 2\max_i b_{iy} + 2\min_i b_{iy} - 2b'_y \\ y &= x + 2\min_i b_{ix} - 2b'_x + 2\max_i b_{iy} + 2\min_i b_{iy} - 2b'_y \\ y &= x + 2\min_i b_{ix} - 2b'_x - 2\max_i b_{iy} + 2\min_i b_{iy} + 2b'_y\,. \end{aligned} \tag{3.2.11}$$

Otherwise the bisector $B(A_1, Z)$ intersects vertex B' if Z lies on one of the lines

$$\begin{aligned} y &= x + 2\min_i b_{ix} - 2b'_x + 2\max_i b_{iy} - 2b'_y \\ y &= x + 2\min_i b_{ix} - 2b'_x - 2\max_i b_{iy} + 2b'_y \\ y &= x - 2\max_i b_{ix} + 2\min_i b_{ix} - 2\max_i b_{iy} + 2b'_y\,. \end{aligned} \tag{3.2.12}$$

Proof. The proof is analogous to that in Lemma 3.2.4. See Table 3.5 for the distances in question, where $l_1^{\mathcal{B},+}(A_1, B')$ must pass the bottommost vertex if $\mathcal{B}$ enters the third quadrant. Note also that $l_1^{\mathcal{B},+}(A_1, B')$ cannot be the shortest path if it passes both the bottommost and rightmost vertices of $\mathcal{B}$ since this would mean it passes all four extreme vertices of $\mathcal{B}$, in which case $l_1^{\mathcal{B},-}(A_1, B')$ must be the shortest path instead. It is also useful to realise that $B(A_1, Z)$ cannot intersect B' if $b'_y \leq y$ so we only consider $y \leq b'_y$.

One distance has been omitted here and that is $l_1^{\mathcal{B},+}(A_1, B')$ passing by only the bottommost vertex (and so not the leftmost vertex), only utilised in the special case of barriers where the rightmost and leftmost vertices of $\mathcal{B}$ are closer to Z and so $\mathcal{B}$ enters the third quadrant. This has length

$$l_1^{\mathcal{B},+}(A_1, B') = -b'_x + b'_y - 2\min_i b_{iy}\,.$$

Vertices passed: bottommost	topmost	rightmost	$l_1^{\mathcal{B},+}(A_1, B')$
			$b'_x - 2\min_i b_{ix} + b'_y$
	✓		$b'_x - 2\min_i b_{ix} + 2\max_i b_{iy} - b'_y$
	✓	✓	$2\max_i b_{ix} - 2\min_i b_{ix} - b'_x + 2\max_i b_{iy} - b'_y$
✓			$b'_x - 2\min_i b_{ix} + b'_y - 2\min_i b_{iy}$
✓	✓		$b'_x - 2\min_i b_{ix} + 2\max_i b_{iy} - 2\min_i b_{iy} - b'_y$

Vertices passed: topmost	leftmost	$l_1^{\mathcal{B},-}(Z, B')$
		$x - b'_x + b'_y - y$
✓		$x - b'_x + 2\max_i b_{iy} - b'_y - y$
✓	✓	$x - 2\min_i b_{ix} + b'_x + 2\max_i b_{iy} - y - b'_y$

Table 3.5: Distances to B' from A_1 and Z along opposite sides of $\mathcal{B}$ (where every $l_1^{\mathcal{B},+}(A_1, B')$ passes by the leftmost vertex of $\mathcal{B}$).

Equating each of the five distances in one table (and the single equation above) with each of the three in the other table gives fifteen lines but, as before, we will give careful consideration to which lines we equate. Also as before, exactly one of the shortest paths must pass the topmost vertex. Therefore we only have four lines.

If B' is on the bottom side of $\mathcal{B}$ to the left of the bottommost point (so it must be our special case described above else B' would be closer to A_1 than to Z) then

$$\begin{aligned} -b'_x + b'_y - 2\min_i b_{iy} &= x - 2\min_i b_{ix} + b'_x + 2\max_i b_{iy} - y - b'_y \\ \Rightarrow y &= x - 2\min_i b_{ix} + 2b'_x + 2\max_i b_{iy} + 2\min_i b_{iy} - 2b'_y\,. \end{aligned}$$

If B' is on the top side of $\mathcal{B}$ to the left of the topmost point then, if $\mathcal{B}$ enters the third quadrant,

$$\begin{aligned} b'_x - 2\min_i b_{ix} + b'_y - 2\min_i b_{iy} &= x - b'_x + 2\max_i b_{iy} - b'_y - y \\ \Rightarrow y &= x + 2\min_i b_{ix} - 2b'_x + 2\max_i b_{iy} + 2\min_i b_{iy} - 2b'_y \end{aligned}$$

or, otherwise,

$$\begin{aligned} b'_x - 2\min_i b_{ix} + b'_y &= x - b'_x + 2\max_i b_{iy} - b'_y - y \\ \Rightarrow y &= x + 2\min_i b_{ix} - 2b'_x + 2\max_i b_{iy} - 2b'_y\,. \end{aligned}$$

If B' is on the top side of $\mathcal{B}$ to the right of the topmost point then, if $\mathcal{B}$ enters the third quadrant,

$$\begin{aligned} b'_x - 2\min_i b_{ix} + 2\max_i b_{iy} - 2\min_i b_{iy} - b'_y &= x - b'_x + b'_y - y \\ \Rightarrow y &= x + 2\min_i b_{ix} - 2b'_x - 2\max_i b_{iy} + 2\min_i b_{iy} + 2b'_y \end{aligned}$$

or, otherwise,

$$\begin{aligned} b'_x - 2\min_i b_{ix} + 2\max_i b_{iy} - b'_y &= x - b'_x + b'_y - y \\ \Rightarrow y &= x + 2\min_i b_{ix} - 2b'_x - 2\max_i b_{iy} + 2b'_y\,. \end{aligned}$$

Finally, if B' is on the bottom side of $\mathcal{B}$ to the right of the bottommost point (so $\mathcal{B}$ does not enter the third quadrant) then

$$2\max_i b_{ix} - 2\min_i b_{ix} - b'_x + 2\max_i b_{iy} - b'_y = x - b'_x + b'_y - y$$
$$\Rightarrow y = x - 2\max_i b_{ix} + 2\min_i b_{ix} - 2\max_i b_{iy} + 2b'_y\,.$$

□

Thus we have found all lines (3.2.10), (3.2.11), and (3.2.12) upon which the upper bisector part of $B(A_1, Z)$ intersects a vertex of $\mathcal{B}$ for Z in Section III.

What remains to be found are the lines of intersection with the line of equidistance about $\mathcal{B}$ (which decides which bisector part is presented and from what line segment) and the lines determining the configuration of each additive bisector part for the upper bisector parts – lines which must also be found for the equivalent lower bisector part interactions.

This marks an appropriate point in time to pause to reflect on the work we have done and the work we still have to do in order to complete the general partition of $\mathcal{CC}^8(A_1)$.

3.2.5 Analysis of approach

One can see from the work shared thus far how the approach outlined here can be continued for the remaining lines in Section III and for Sections IV and V. This will provide all of the necessary partition lines, and it is clear that these partition lines will be linear since they amount to the intersection of a breakpoint or breakline of a bisector $B(Z, A_i)$ (linear in x and y) with an edge of $\mathcal{B}$, $\mathcal{P}$, $\mathcal{VD}(A_1, \ldots, A_n)$, or another fixed point such as C_i (constant in x and y), as we have seen. Adding these lines to those discovered in Averbakh et al. (2015) creates a finite partition, over the cells of which the representation of the objective function remains preserved. These cells are convex polygons and therefore we can look to find their extrema using first order methods. As there are only a finite number of vertices of $\mathcal{B}$, $\mathcal{P}$, and $\mathcal{VD}(A_1, \ldots, A_n)$ and each line involves only two vertices at most, there are a finite number of partitions. Hence there are similarly a polynomial number of partition cells. Therefore we have a polynomial partition consisting of linear boundaries which preserves the representation of the objective function and over which an extreme point can be found – the same situation as in Averbakh et al. (2015).

However, there are some noticeable drawbacks to this approach. First of all, we must calculate a vast number of line segments. Whilst only considering locating in $\mathcal{CC}^8$ in a rectangular $\mathcal{P}$ for one existing facility A_1, we have seen just a few lines. These represent the tip of the iceberg since there are even more complicated bisectors not yet explored (see Figure 3.7 for the possible bisectors in Section IV) and the lines of intersection with the line segments of $\mathcal{P}$ and $\mathcal{VD}$ would have to be found in a similar way. Once a general expression of these lines is found, it will have to be repeated for every section within every configuration cone of every existing facility. The work is not straightforward, and it is even harder to prove that all partition lines have been found and to determine how the number of lines relates to the number of facilities, or the number of vertices of $\mathcal{B}$ or $\mathcal{P}$ (which is crucial for algorithmic assessment). Moreover, it is rarely obvious from the form of one of these line segments what has occurred to produce this line, or what the bisector will resemble if Z were placed upon the line.

From studying the visualisation of our aim in Figure 3.3 we can see that, rather than having characteristics restricted to just one section within each configuration, many partition lines cross over section boundaries, and even venture across configuration cones. Rather than collecting many line segments that combine to create these partitioning line, it would be far preferable to understand what it means to lie on one of these partition lines. While Section 3.2 has served as a thorough introduction to the task of finding these partition lines, perhaps in the way previously described, we could instead consider characterising the lines in order to develop an approach with more manageable and intuitive results.

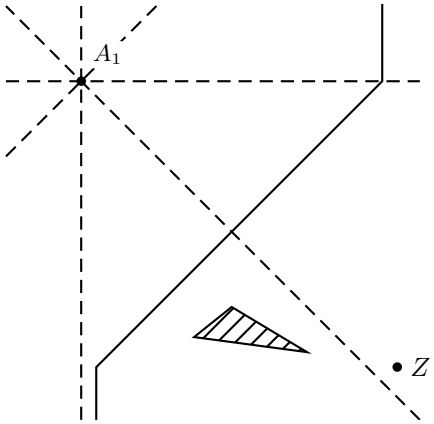

(a) Bisector line not intersecting the barrier, passing to the left.

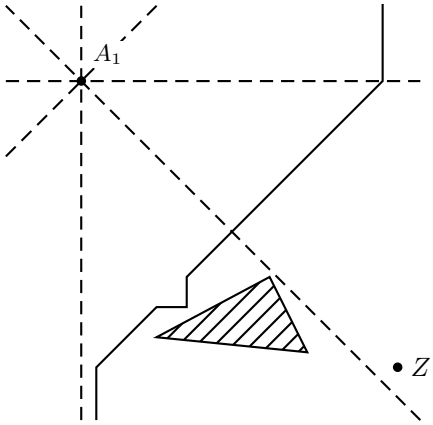

(b) Diagonal bisector line develops dent that lies above the barrier.

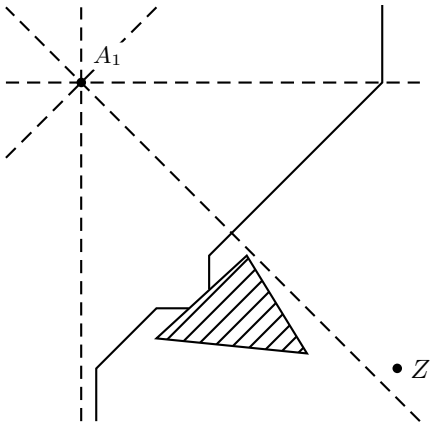

(c) Diagonal bisector line develops dent that intersects the barrier from above.

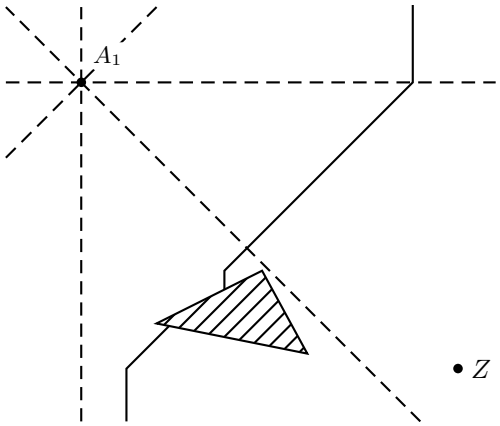

(d) Vertical bisector line intersecting the leftmost barrier edge while the diagonal intersects the bottom barrier edge.

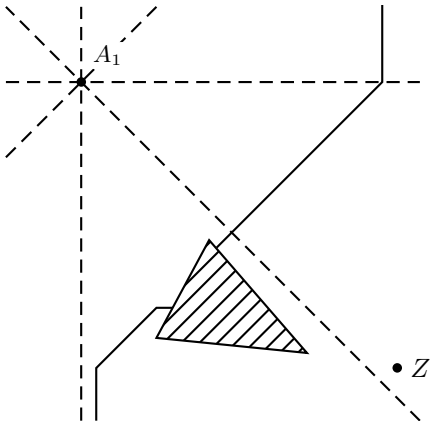

(e) Diagonal bisector line intersecting the rightmost barrier edge while the horizontal bisector line intersects the leftmost barrier edge.

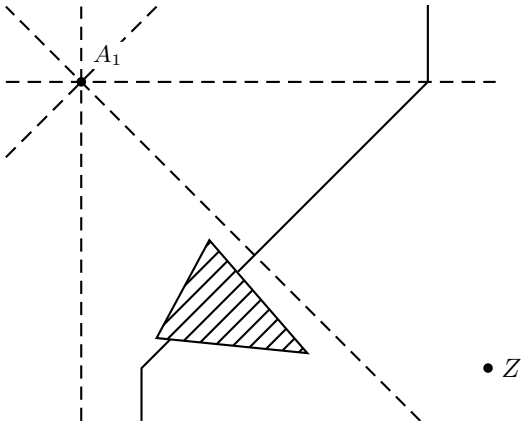

(f) Vertical bisector lines intersecting the rightmost and bottom barrier edges.

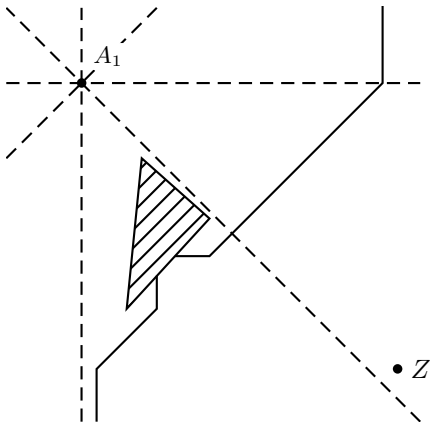

(g) Diagonal bisector line develops dent that intersects the barrier from below.

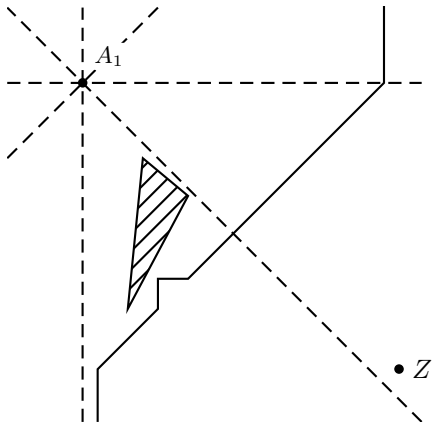

(h) Diagonal bisector line develops dent that lies below the barrier.

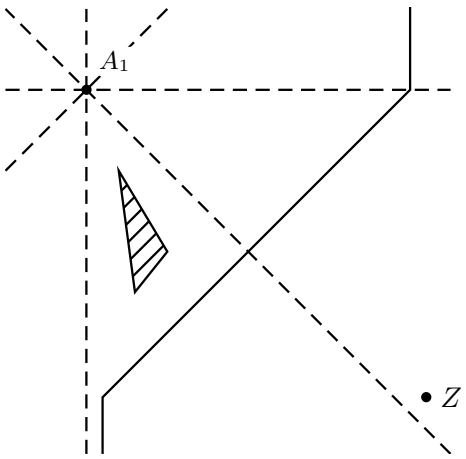

(i) Bisector line not intersecting the barrier, passing to the right.

Figure 3.7: All bisector types for placement of Z in Section IV.

3.3 Conditions on the preservation of the representation of the objective function

From sketches such as Figure 3.8, one can see that the effect of the barrier depends entirely on the location of Z with the bisector remaining unaffected if Z is located in a large area of $\mathcal{P}$. Equations were found for the partition lines depending on all of Z's possible positions in relation to A_1 and $\mathcal{B}$; however, this involves many separate cases even when restricted to the $1 + 1$ case. The simplicity and suggested patterns of diamond segments exhibited in Figure 3.8 hint at an easier solution. Therefore we are interested in how we can define the perimeter lines for each partition cell (specifically, what it means for Z to be located upon one of the lines) so that we can easily construct such a partition for any barrier $\mathcal{B}$.

Now the stage is set for us to introduce the categories of partition lines and their general forms.

Having investigated what it means for a facility to lie on a partitioning line, for any convex $\mathcal{P}$ with vertices $P_i = (p_{i_x}, p_{i_y})$ for $i = 1, \ldots, m$ and any convex $\mathcal{B}$ with vertices $B_i = (b_{i_x}, b_{i_y})$ for $i = 1, \ldots, p$ we can break the lines down into seven cases:

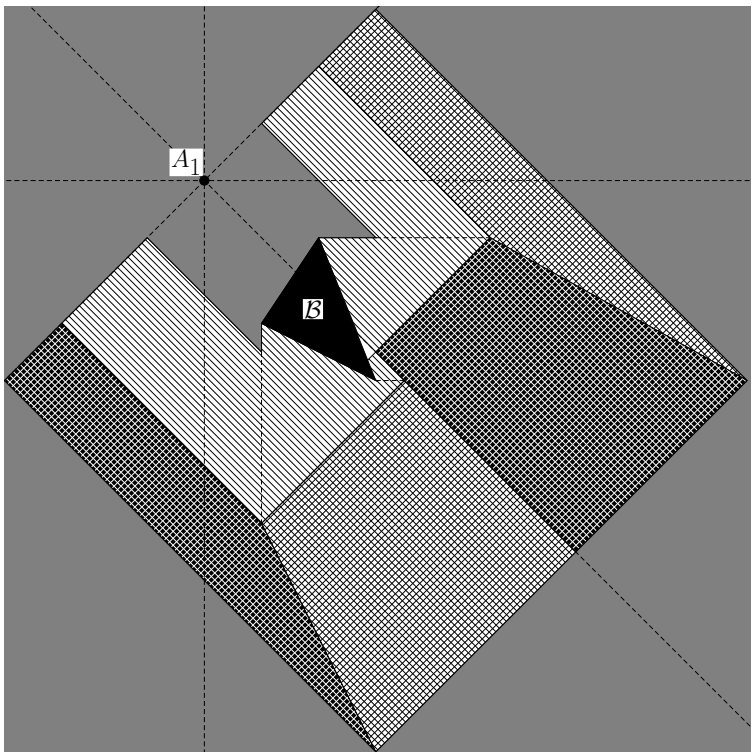

Figure 3.8: The partition of a large $\mathcal{P}$ with one existing facility $A_1 = (0, 0)$ and a barrier $\mathcal{B}$ with vertices $(2, -5)$, $(4, -2)$, and $(6, -7)$ wherein each cell has structurally identical Voronoi diagrams for Z located there.

- configuration lines of A_k;
- additive configuration lines of A_k;
- extreme lines of $\mathcal{B}$;
- geodesic diamonds centred on vertices of $\mathcal{VD}$;
- intersection lines of breakpoints and edges of $\mathcal{VD}$;
- kink lines of the corners of $Shadow(\mathcal{B})$;
- wrap-around lines of $\mathcal{B}$.

We will detail each of these lines separately, deriving general expressions for the lines with n existing facilities (without loss of generality we take $A_1 = (0, 0)$ for ease of calculation unless stated otherwise), and prove that they are necessary and sufficient for forming the full partition.

Configuration lines

It was shown in Averbakh et al. (2015) that these lines, stated below for $A_1 = (0, 0)$ for completeness:

$$y = 0\,,\ \ x = 0\,,\ \ y = x\,,\ \ y = -x\,,$$

were necessary for a full partition. Their use has been demonstrated earlier in Section 2.1, and illustrated in Figure 2.2. While we could include all of the lines identified in that paper for our partition (since the barrier-free problem can be seen as a problem contained in the barrier-constrained problems – for a barrier of negligible size, or one outside $\mathcal{P}$, say), equivalent such lines for all barrier-constrained problems have been found and so stating the other lines found in Averbakh et al. (2015) would be unnecessary and simply complicate the partition.

While, following on from the configuration lines for bisectors unobstructed by $\mathcal{B}$, this may seem a natural place to define additive configuration lines, the theory of the following lines proves useful in the derivation of additive configuration lines so we will return to these in Section 3.3.

Extreme lines

Our first new lines are the easiest to define. The extreme lines of $\mathcal{B}$ are simply

$$x = \min b_{ix}\,,\ x = \max b_{ix}\,,$$
$$y = \min b_{iy}\,,\ y = \max b_{iy}\,.$$

These lines delineate where the shortest path from Z to certain areas of $\mathcal{P}$ may now be restricted to pass by a vertex of $\mathcal{B}$ (since $\mathcal{B}$ is convex a shortest path will only have to pass a vertex of $\mathcal{B}$ if that vertex is an extreme one, and from an extreme point all points are visible until the next extreme point restricts it). Since the representation of the shortest paths changes, so can the bisector. We will show that these lines are necessary by way of an example shown in Figure 3.9, where the lower bisector breakpoint is on the same horizontal line as Z in Figure 3.9a, but not in Figure 3.9b. For any barrier $\mathcal{B}$ this gives exactly four lines.

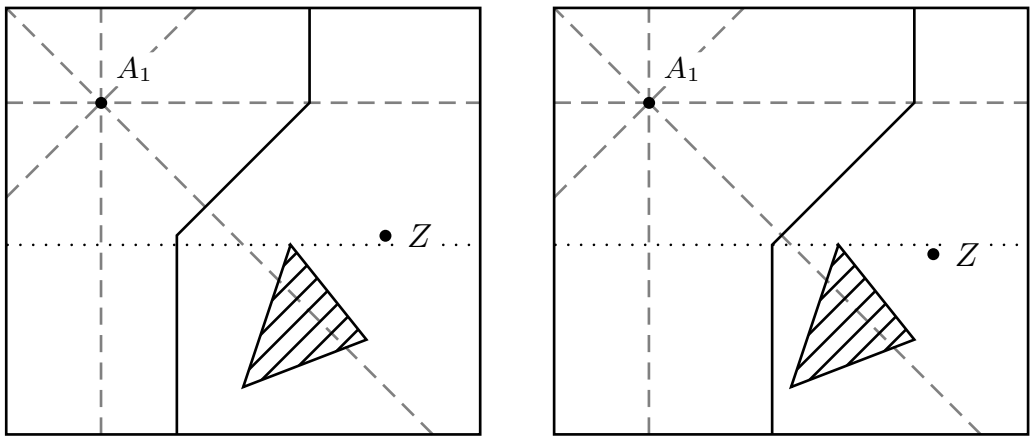

(a) Bisector with coordinates $(\frac{x+y}{2}, -3.5)$, $(\frac{x+y}{2}, y)$, $(\frac{x-y}{2}, 0)$, and $(\frac{x-y}{2}, 1)$.

(b) Bisector with coordinates $(\frac{x-y-3}{2}, -3.5)$, $(\frac{x-y-3}{2}, -1.5)$, $(\frac{x-y}{2}, 0)$, and $(\frac{x-y}{2}, 1)$.

Figure 3.9: Two placements of $Z = (x, y)$ within $\mathcal{P} = R((-1, -3.5), (4, 0.5))$ with one existing facility $A_1 = (0, 0)$ and $\mathcal{B} = \Delta((1.5, -3), (2, -1.5), (2.8, -2.5))$.

Geodesic diamonds

Next we will introduce geodesic diamonds, and explore them about vertices B_i of $\mathcal{B}$ – though the results for other vertices within $\mathcal{VD}$ follow identically.

While working with the l_1 norm, the gauge (lines of equidistance) is the diamond centred about its point of symmetry. Looking at existing partitions these diamonds now become blindingly obvious; however, importantly, not all are diamonds and some appear to have been distorted. This distortion is due to the barriers which, as we know all too well, can interrupt the shortest paths. In this way these partitioning lines are the geodesic gauges with their centre at a vertex of the barrier, and size given by the distance from that vertex to A_1.

We define the geodesic diamond centred on X to A_1 (as in, A_1 lies on the geodesic diamond) to be

$$\diamond_g^X(A_1) := \{Q \in \mathcal{P} \setminus \mathcal{B} : l_1^{\mathcal{B}}(Q, X) = l_1^{\mathcal{B}}(A_1, X)\}$$

where, here, we will take X to be one of the vertices of $\mathcal{VD}$.

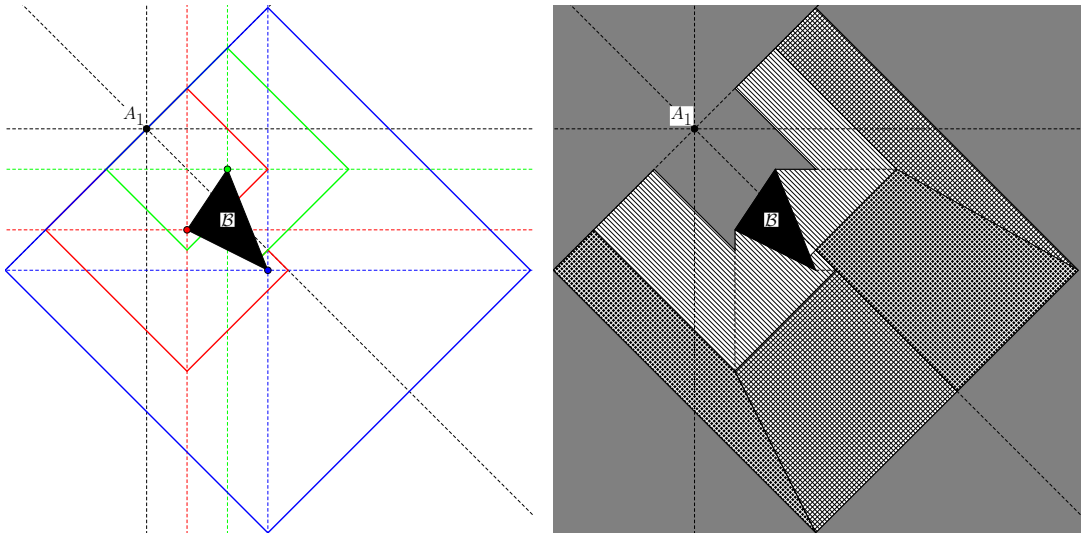

(a) Geodesic diamonds centred on each barrier vertex to A_1.

(b) Complete partition wherein each cell has structurally independent Voronoi diagrams.

Figure 3.10: The geodesic diamonds and complete partition of a large $\mathcal{P}$ with one existing facility $A_1 = (0, 0)$ and $\mathcal{B} = \Delta((2, -5), (4, -2), (6, -7))$.

It is on these diamonds that B_i is equidistant from A_1 and from Z and so, by definition, will belong on the bisector. Therefore they delineate where the bisector will intersect a new line (edge of $\mathcal{VD}$) and thus lead to a change in the cell structure. It is important to note that we need only concern ourselves, for any vertex of $\mathcal{VD}$, with the geodesic diamond to the facility generating the Voronoi cell within which the vertex lies, so each vertex of $\mathcal{VD}$ contributes exactly one geodesic diamond. From Figure 3.10 we can see that these geodesic diamonds contribute almost in their entirety to the majority of that partition. Indeed these geodesic l_1 gauges can be more colourful, as we see that they change direction by 90° whenever they hit a quadrant line of its centre vertex or an extreme line of $\mathcal{B}$.

We now include a lemma to count the maximum number of lines.

Lemma 3.3.1. *For a convex $\mathcal{B}$, geodesic diamonds have a maximum of seven edges.*

Proof. Let us first look at geodesic diamonds centred on vertices of $\mathcal{B}$. We will show the result is true by classifying the three cases of vertices of $\mathcal{B}$. A vertex of $\mathcal{B}$ can either be a corner of $Shadow(\mathcal{B})$, lie on one edge of $Shadow(\mathcal{B})$, or be neither (an 'interior' vertex). The possible geodesic diamonds for each of these vertices is shown in Figure 3.11 where the number of line segments of each diamond is labelled and can be seen never to exceed seven. This is because once the diamond enters a non-visible area of $\mathcal{P}$ it changes direction by a set angle, much like the bisector parts. This corresponds to a new vertex of $\mathcal{B}$ acting as an active point within the diamond (similarly to within additive bisectors). Once the diamond crosses a quadrant line of an active vertex it will then turn by 90°. Therefore as the geodesic diamond expands from the vertex, each time the intersection with $\mathcal{B}$ passes an extreme point it will introduce another line segment, with two produced from a corner vertex (a 'double' extreme point). Finally we observe, as expected, that the smallest number of line segments of a geodesic diamond centred on an interior vertex is three, on an edge vertex is four, and on a corner vertex is five, and the number of extreme points for the geodesic diamond still to reach is four, three, and two respectively. Therefore the maximum for each of these geodesic diamonds is seven.

This idea can easily be extended to geodesic diamonds centred on other vertices of $\mathcal{VD}$ since, beyond there being a geodesic diamond of four edges about every point, the possible geodesic diamonds are identical, and the theory does not rely on the vertex being connected to $\mathcal{B}$. □

Thus we obtain at most $\mathcal{O}(m + n + p)$ lines of this type: each $\mathcal{O}(m + n + p)$ vertex of $\mathcal{VD}$ contributes a geodesic diamond of at most seven edges.

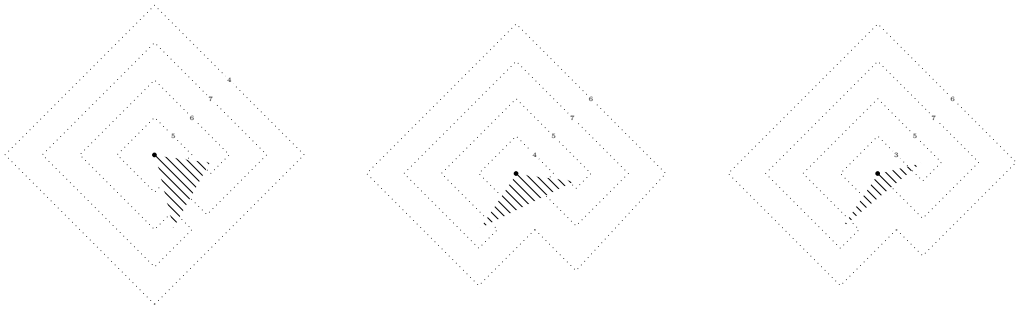

Figure 3.11: The possible geodesic diamonds centred at corner, edge, or interior vertices of $\mathcal{B}$.

Additive configuration lines

Just as the configuration lines are required to determine what orientation the bisector $B(A_i, Z)$ takes, we must find the additive configuration lines which dictate the type of additive bisector part present between facilities A_i and Z, as identified in Figure 2.4.

We wish to identify the lines across which the movement of an additional facility Z would change the type of additive bisector present (as portrayed in Figure 2.4). Fixing one facility, these lines correspond to the placement of the free facility so that the additive bisector creates a quarterplane (as this differentiates between the appropriate non-degenerate additive bisectors). Equivalently, for $B_c^{add}(P, Q)$, we find the points at which the non-active point corners of $R(P, Q)$ are equidistant from A_i and Z. It is important to note that the structure of the additive bisector can change in the way described only when we consider the additive bisector between active points which are visible from one another. We will split the additive bisectors possible in our set-up into three cases.

Firstly we examine additive bisectors between facilities A_i and Z whose active points B_j and B_k (respectively) are vertices of $\mathcal{B}$: $B^{add}_{l_1^{\mathcal{B}}(B_k,Z)}(B_j, B_k)$ (see Lemma 3.2.2 for a simple exploration of these for Z within the top-left corner of $Shadow(\mathcal{B})$). For this we require B_k to be non-visible from A_i and B_j to be non-visible from Z (else one of the facilities would be an active point). Since B_j and B_k are visible from one another and are extreme points of $\mathcal{B}$, $R(B_j, B_k)$ must share at least one corner $C_l \notin \{B_j, B_k\}$ with $Shadow(\mathcal{B})$. We must have $C_l \notin \mathcal{B}$ else there would be no such active points B_j or B_k. This C_l is unique unless $R(B_j, B_k) = Shadow(\mathcal{B})$, in which case we do not choose the corner in the interior of the visible region from A_i and Z. By the convexity of $\mathcal{B}$, this must be the only corner from which a quarterplane can begin (the shortest path from A_i or Z to the alternative corner – if it exists, i.e. the corner may lie within $\mathcal{B}$ – does not pass B_j or B_k respectively so cannot exist in $B^{add}_{l_1^{\mathcal{B}}(B_k,Z)}(B_j, B_k)$). Therefore the additive bisector creates a quarterplane if C_l is equidistant from A_i and Z. For a general A_i and $\mathcal{B}$ we require C_l to be either non-visible from A_i or on the boundary of A_i's visibility (for B_k to be non-visible from A_i). For $A_i \in Shadow(\mathcal{B})$ there can be as many as three such C_l, otherwise there are a maximum of two.

Thus, for any facility A_i, for a corner C_l either non-visible or on the boundary of the visible area from A_i we produce the lines

$$l_1^{\mathcal{B}}((x, y), C_l) = l_1^{\mathcal{B}}(A_i, C_l)\,.$$

This is a geodesic diamond $\diamond_g^{C_l}(A_i)$; however, we only require the segments contained within the area of $\mathcal{P}$ containing $Shadow(\mathcal{B})$ defined by the extreme lines through B_j and the adjacent extreme lines of $\mathcal{B}$ (since B_j must be non-visible from Z) and we only consider the segments of $\diamond_g^{C_l}(A_i)$ obtained by travelling in an opposite direction around $\mathcal{B}$ to travelling to A_i (since the shortest path to C_l from A_i and Z must travel in opposite directions around $\mathcal{B}$ for B_k to be closer to Z than to A_i). This amounts to a maximum of two line segments (as shown in the first example of Figure 3.10a): since the diagonal towards $\mathcal{B}$ from the opposite corner of $Shadow(\mathcal{B})$ to C_l makes up part of the line of equidistance from C_l around $\mathcal{B}$ and it cannot be crossed by this additive configuration line, this enforces a maximum of one extreme vertex of $\mathcal{B}$ to impede

the shortest path for this line and, in so doing, create another line segment. An example of such a case and its partitioning line is shown in Figure 3.12.

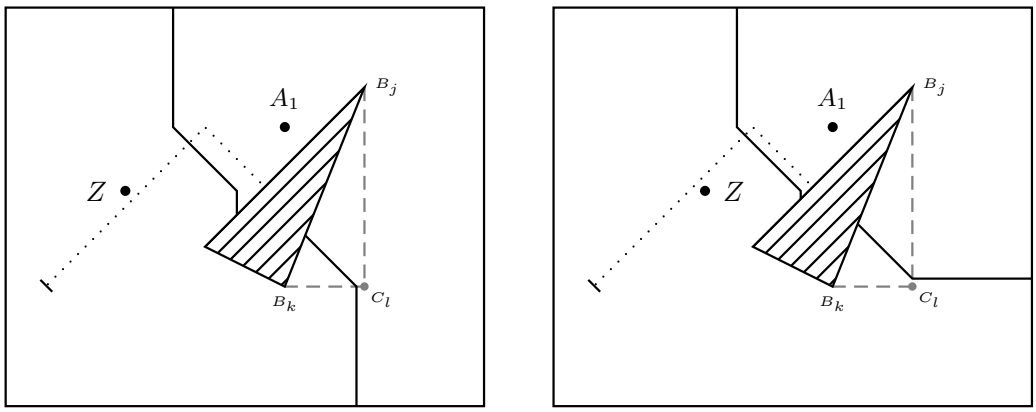

Figure 3.12: Two placements of Z within $\mathcal{P} = R((-1.5, 0), (4.5, 3))$ along with facility $A_1 = (2, 2.5)$ and $\mathcal{B} = \Delta((1, 1), (2, 0.5), (3, 2.5))$.

Secondly we will examine $B^{add}_{l_1^{\mathcal{B}}(B_j,Z)}(A_i, B_j)$, the barrier-constrained bisector between facilities A_i and Z where the additive bisector part acts between $A_i = (a_x, a_y)$ and the vertex $B_j = (b_x, b_y)$ of $\mathcal{B}$. For this we require B_j to be an extreme vertex of $\mathcal{B}$ visible from A_i (otherwise it would be a bisector of the previous type). Note that B_j can either lie on the perimeter of the non-visible area from Z or be non-visible from Z (being the second, or even third, active point which must be passed in the shortest path). Now since the active point A_i of this additive bisector is a facility, we will always have $c > 0$. This means that the additive bisector will always have a breakpoint on the longer edge of $R(A_i, B_j)$ adjacent to B_j and it remains to be shown whether the other breakpoint lies on the other longer edge or the other edge adjacent to B_j.

Therefore the corner of interest of $R(A_i, B_j)$ is the one closest to B_j, and this depends on the configuration cone of A_i within which B_j lies. If $B_j \in \mathcal{CC}^1(A_i) \cup \mathcal{CC}^4(A_i) \cup \mathcal{CC}^5(A_i) \cup \mathcal{CC}^8(A_i)$ then the corner of interest is (b_x, a_y), otherwise it is (a_x, b_y). If this corner is not visible from either of the active points due to $\mathcal{B}$ obscuring access (we need not concern ourselves with $\mathcal{P}$ as, whilst it may cut out the corner of interest, it does not affect the shortest paths so the following theory will still stand) then this additive bisector is not able to produce differing types of bisectors and we must explore the additive bisector between the new active points – the same is, or can be, true if the incident edge of $\mathcal{B}$ follows the perimeter of $Shadow(\mathcal{B})$. Thus, the corner must be visible from both A_i and B_j for the configuration to be able to change. Therefore additive bisector changes of this type can only occur for B_j, an extreme vertex lying on an extreme line of $\mathcal{B}$ which would separate $\mathcal{B}$ and A_i. For any A_i and $\mathcal{B}$ there can be at most two vertices of this type (since there are only a maximum of two extreme lines of $Shadow(\mathcal{B})$ which could separate A_i from $\mathcal{B}$ and an edge of $\mathcal{B}$ must not follow the outline of $Shadow(\mathcal{B})$ as described above).

Now, as before, for this corner to be on the bisector, $Z = (x, y)$ must satisfy

$$l_1^{\mathcal{B}}((x, y), (b_x, a_y)) = l_1^{\mathcal{B}}(A_i, (b_x, a_y)) = |b_x - a_x| \text{ or } l_1^{\mathcal{B}}((x, y), (a_x, b_y)) = l_1^{\mathcal{B}}(A_i, (a_x, b_y)) = |b_y - a_y|$$

depending on the location of B_j with respect to A_i as discussed above. Once more this is a geodesic diamond $\diamond_g^{(b_x,a_y)}(A_i)$ (or $\diamond_g^{(a_x,b_y)}(A_i)$) but it is composed of only the points for which the shortest paths from (b_x, a_y) (or (a_x, b_y)) must travel past B_j (so restricted by the extreme line $x = b_x$ or $y = b_y$ (respectively), the line of equidistance from (b_x, a_y) or (a_x, b_y) (respectively) around $\mathcal{B}$, and $\mathcal{B}$ itself). Now this shortest path may pass as many as three extreme vertices before it reaches the line of equidistance or $\mathcal{B}$ (passing four would cause it to enter an area visible from the starting point so it must have crossed the line of equidistance) so it consists of a maximum of three line segments. The effect of crossing this line is shown in Figure 3.13.

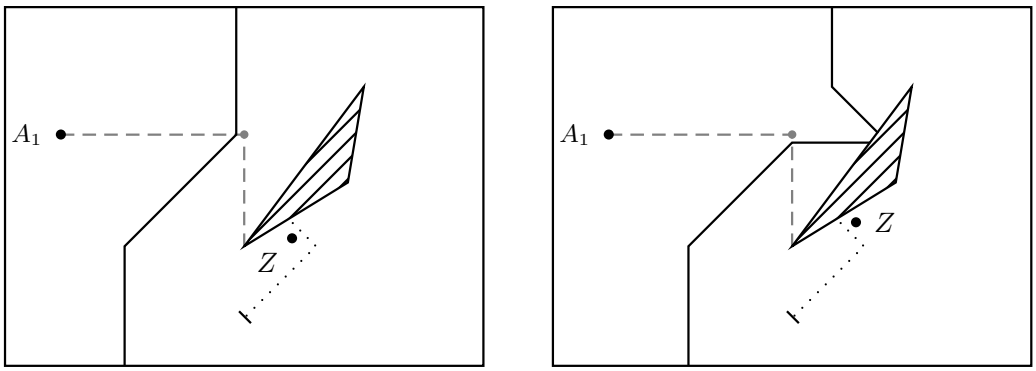

Figure 3.13: Two placements of Z within $\mathcal{P} = R((-1.5, 0), (4.5, 3.5))$ along with facility $A_1 = (-0.8, 2.4)$ and $\mathcal{B} = \Delta((1.5, 1), (2.8, 1.8), (3, 3))$.

Finally we will examine $B^{add}_{l_1^{\mathcal{B}}(A_i,B_j)}(Z, B_j)$, the barrier-constrained bisector between facilities A_i and Z where the additive bisector part acts between $Z = (x, y)$ and the vertex $B_j = (b_x, b_y)$ of $\mathcal{B}$. For this we require B_j to be an extreme vertex of $\mathcal{B}$ within or on the boundary of the non-visible area from A_i, or the previous active point (otherwise B_j is not an active point of the additive bisector), and we only consider Z visible from B_j and not from A_i. As before, since the active point Z of this additive bisector is a facility, we will always have $c > 0$ so we are interested in the locations of Z for which the bisector intersects the corner of $R(Z, B_j)$ closest to B_j. But since Z can move, this corner is the one lying on either the horizontal or the vertical through B_j depending on Z's location.

Therefore, for every half-line travelling horizontally or vertically from B_j, within or on the boundary of the non-visible area from A_i or the previous active point, we must consider Z being located such that the closest corner of $R(Z, B_j)$ to B_j lies on this line and the additive bisector travels through it. That is, for $Z = (x, y)$ lying in this area,

$$l_1^{\mathcal{B}}((x, y), (b_x, y)) = l_1^{\mathcal{B}}(A_i, (b_x, y)) \Rightarrow |y - b_y| = |x - b_x| - l_1^{\mathcal{B}}(A_i, B_j) \text{ or}$$
$$l_1^{\mathcal{B}}((x, y), (x, b_y)) = l_1^{\mathcal{B}}(A_i, (x, b_y)) \Rightarrow |y - b_y| = |x - b_x| + l_1^{\mathcal{B}}(A_i, B_j)$$

for the horizontal and vertical cases discussed respectively. While this gives the equation of eight lines, each one must lie in the non-visible area from A_i (or the previous active point if existing) and begin at the extreme lines through B_j, and thus only half of these at most will satisfy these conditions. Furthermore, each of these lines is only exhibited if the configuration cone $\mathcal{CC}^k(B_j)$ containing the line has $\left(\mathcal{CL}^k(B_j) \cup \mathcal{CL}^{k+1}(B_j)\right) \cap \mathcal{B} = \{B_j\}$ (else the bisectors will present the same since the bisector will intersect $\mathcal{B}$ before changing configuration) so, by the convexity of $\mathcal{B}$, this means we require a maximum of only three of these partition lines. The effect of crossing these lines is shown in Figure 3.14 in the lower bisector part of $B^{\mathcal{B}}(Z, A_1)$.

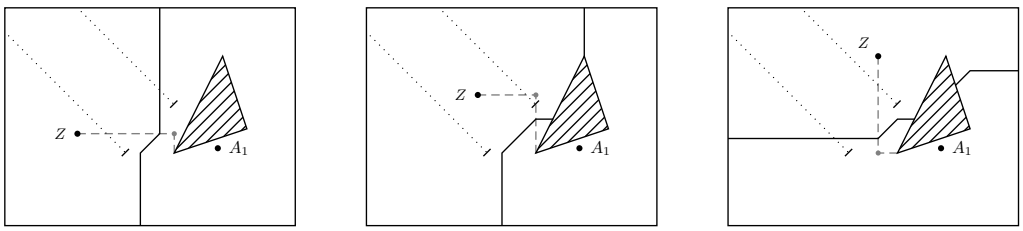

Figure 3.14: Three placements of Z within $\mathcal{P} = R((0.5, -0.5), (3.5, 4))$ along with facility $A_1 = (1.1, 2.9)$ and $\mathcal{B} = \Delta((1, 2), (1.5, 3.5), (3, 3))$.

Since these lines are important to categorise, we shall state them as a result as follows.

Lemma 3.3.2. *For a fixed facility $A_i = (a_x, a_y)$ and barrier $\mathcal{B}$, the additive configuration lines $\diamond_g^{C_l}(A_i)$ (for $C_k \notin \mathcal{B}$ non-visible or on the boundary of the visible area from A_i), $\diamond_g^{(b_x,a_y)}(A_i)$ or $\diamond_g^{(a_x,b_y)}(A_i)$ if $B_j \in \mathcal{CC}^1(A_i) \cup \mathcal{CC}^4(A_i) \cup \mathcal{CC}^5(A_i) \cup \mathcal{CC}^8(A_i)$ or otherwise (respectively) (for $B_j = (b_x, b_y)$ on an extreme line of $\mathcal{B}$ that separates A_i from $\mathcal{B}$), and $|y - b_y| = |x - b_x| \pm l_1^{\mathcal{B}}(A_i, B_j)$ (for any extreme vertex $B_j = (b_x, b_y)$ of $\mathcal{B}$) determine the identification of the additive bisectors between A_i and $Z = (x, y)$.*

These additive configuration lines contribute to an overall count of $\mathcal{O}(n)$ line segments – a maximum of two line segments from every line of the first case, for which a facility A_i has a maximum of three possible corners C_k with which to produce a line (so a maximum of $6n$ possible lines of the first case), and a maximum of three line segments from every line of the second case, for which a facility A_i has a maximum of two possible extreme vertices B_j with which to produce a line (so a maximum of $6n$ possible lines of the second case).

Breakpoint intersection lines

The next category of lines occurs when a breakpoint of the bisector intersects an edge of $\mathcal{VD}$. We will begin by demonstrating breakpoint intersection lines for when a breakpoint intersects an edge of $\mathcal{B}$.

A breakpoint occurs at either the same horizontal or vertical coordinate as one of the points between which the bisector lies (so A_1, Z, or an extreme point of $\mathcal{B}$ if an additive bisector part). Let us note, however, that the breakpoints of an additive bisector cannot intersect an edge of $\mathcal{B}$ at the same horizontal or vertical as the active point of $\mathcal{B}$ else this would contradict the convexity of $\mathcal{B}$. Therefore, for any point (b_x, b_y) on an edge of $\mathcal{B}$, the breakpoint of the bisector $B^{\mathcal{B}}(A_1, Z)$ will hit this point only if (b_x, b_y) is visible from Z and exclusively $x = b_x$ or $y = b_y$, or (b_x, b_y) is visible from A_1 and exclusively $b_x = 0$ or $b_y = 0$ and the distance $l_1^{\mathcal{B}}((b_x, b_y), Z)$ is identical to $l_1^{\mathcal{B}}((b_x, b_y), A_1)$ (note that it only needs to be visible from the facility on whose horizontal or vertical the breakpoint is lying to include additive bisectors).

Therefore, for $b_x = 0$ or $b_y = 0$ (so only for particular barriers), (b_x, b_y) is a site of intersection (without the active extreme point of $\mathcal{B}$ having this coordinate) if and only if

$$l_1^{\mathcal{B}}((b_x, b_y), Z) = |b_y|$$

with $sgn(y) = sgn(b_y)$ for $b_x = 0$, or

$$l_1^{\mathcal{B}}((b_x, b_y), Z) = |b_x|$$

with $sgn(x) = sgn(b_x)$ for $b_y = 0$, geodesic diamonds centred at (b_x, b_y).

When considering intersections at $b_x = x$ or $b_y = y$ for a fixed point (b_x, b_y) (so this breakpoint is visible from Z) it must be the case that Z lies on $(b_x, b_y \pm l_1^{\mathcal{B}}((b_x, b_y), A_1))$ or $(b_x \pm l_1^{\mathcal{B}}((b_x, b_y), A_1), b_y)$, depending on the side of $\mathcal{B}$ and the position of A_1 in relation to it. Our new partition lines are composed of these points so, for any adjacent vertices B_i and B_j of $\mathcal{B}$, the lines in question, since we can represent the edge as $y = \frac{b_{j_y} - b_{i_y}}{b_{j_x} - b_{i_x}} x - \frac{b_{i_x} * b_{j_y} - b_{i_x} * b_{i_y} - b_{j_x} * b_{i_y} + b_{i_x} * b_{i_y}}{b_{j_x} - b_{i_x}}$, are

$$\begin{aligned}
y &= \frac{b_{j_y} - b_{i_y}}{b_{j_x} - b_{i_x}} x - \frac{b_{i_x} b_{j_y} - b_{i_x} b_{i_y} - b_{j_x} b_{i_y} + b_{i_x} b_{i_y}}{b_{j_x} - b_{i_x}} \\
&\quad \pm l_1^{\mathcal{B}} \left(\left(x, \frac{b_{j_y} - b_{i_y}}{b_{j_x} - b_{i_x}} x - \frac{b_{i_x} b_{j_y} - b_{i_x} b_{i_y} - b_{j_x} b_{i_y} + b_{i_x} b_{i_y}}{b_{j_x} - b_{i_x}} \right), A_1 \right), \\
x &= \frac{b_{j_x} - b_{i_x}}{b_{j_y} - b_{i_y}} y + \frac{b_{i_x} b_{j_y} - b_{i_x} b_{i_y} - b_{j_x} b_{i_y} + b_{i_x} b_{i_y}}{b_{j_y} - b_{i_y}} \\
&\quad \pm l_1^{\mathcal{B}} \left(\left(\frac{b_{j_x} - b_{i_x}}{b_{j_y} - b_{i_y}} y + \frac{b_{i_x} b_{j_y} - b_{i_x} b_{i_y} - b_{j_x} b_{i_y} + b_{i_x} b_{i_y}}{b_{j_y} - b_{i_y}}, y \right), A_1 \right)
\end{aligned}$$

respectively. These lines are necessary since crossing them will cause a breakpoint to be created or removed, altering the Voronoi diagram as shown in Figure 3.15.

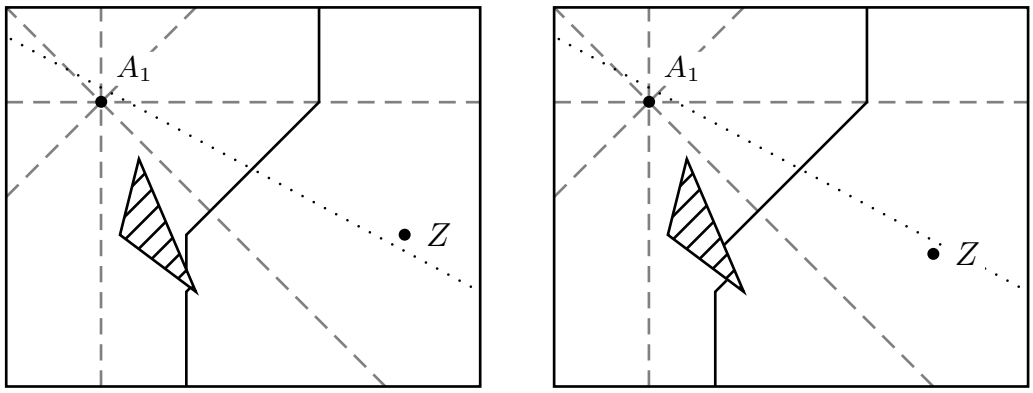

Figure 3.15: Two placements of $Z = (x, y)$ within $\mathcal{P} = R((-1, -2.5), (4, 0.5))$ with one existing facility $A_1 = (0, 0)$ and a barrier $\mathcal{B} = \Delta((0.2, -1.4), (0.4, -0.6), (1, -2))$ and breakpoint intersection line $7y = -13x + 38$.

The results are analogous for the intersection of breakpoints and the remaining edges of $\mathcal{VD}$ too, but for these we must also now consider the intersection of the breakpoint of an additive bisector part. This does not require much more thought. These breakpoints may only occur on a non-barrier edge of $\mathcal{VD}$ that is at the same x- or y-coordinate of the extreme vertex of $\mathcal{B}$ which is acting as an active point of the additive bisector.

We will phrase these lines in the context of an edge between adjacent vertices P_i and P_j of $\mathcal{P}$, but the same is true for any edge of $\mathcal{VD}$. A breakpoint of the additive bisector will occur, as before, on a horizontal or vertical line through one of the active points. We have calculated those partition lines for breakpoints sharing a horizontal or vertical with an active point that is a facility. Now we must do so for the extreme vertex which becomes an active point of the additive bisector. For an extreme vertex $B^* = (b_x^*, b_y^*)$, if we have an edge of $\mathcal{P}$ between adjacent vertices P_i and P_j that intersects, visibly, either $x' = b_x^*$ or $y' = b_y^*$, then there may be an intersection between the breakpoint of the bisector and the edge. These intersection points are $\left(b_x^*, \frac{(p_{i\,y} - p_{j\,y})b_x^* + p_{i\,x}p_{j\,y} - p_{i\,y}p_{j\,x}}{p_{i\,x} - p_{j\,x}}\right)$ and $\left(\frac{(p_{i\,x} - p_{j\,x})b_y^* + p_{i\,y}p_{j\,x} - p_{i\,x}p_{j\,y}}{p_{i\,y} - p_{j\,y}}, b_y^*\right)$ respectively and an intersection will occur only if

$$l_1^{\mathcal{B}}(Z, P^*) = l_1^{\mathcal{B}}(A_1, P^*)$$

where P^* is one of the two points identified above. Here we have a new geodesic diamond centred on P^* of radius $l_1^{\mathcal{B}}(A_1, P^*)$ for every intersection of the quadrant lines of an extreme point of $\mathcal{B}$ and an edge of $\mathcal{P}$ that is visible from the extreme point.

Each existing facility A_k will give as many of the first lines (geodesic diamonds about A_k for non-additive breakpoints on quadrant lines of A_k) as the number of times their quadrant lines intersect (visibly) an edge of $\mathcal{VD}$. Since $\mathcal{B}$ is convex, this amounts to a maximum of two partial geodesic diamonds per facility (only one visible intersection of each horizontal and vertical possible), and $\mathcal{P}$ can do this at most four times (since $A_k \in \mathcal{P}$ and $\mathcal{P}$ is convex). We must consider the bisector edges of $\mathcal{VD}$ a little differently by observing that the bisector between A_k and Z will only exist in the Voronoi diagram within $V(A_k)$. Thus the only bisector edges of $\mathcal{VD}$ that can produce one of these partial geodesic diamonds are those on the perimeter of $V(A_k)$, so this can happen a maximum of four times, analogously to the reasoning for $\mathcal{P}$. We also get a line (for non-additive breakpoints on quadrant lines of Z) for every edge of $\mathcal{VD}$. For the additive bisector breakpoint intersections (geodesic diamonds about intersection of edges and quadrant lines of extreme vertices), a new partition diamond is created each time $\mathcal{VD}$ intersects an extreme line of $\mathcal{B}$ – so eight from $\mathcal{P}$ and $4(n-1)$ from bisector edges in $\mathcal{VD}$ (using identical logic to the previous calculation) – or intersects a visible (i.e. not travelling through $\mathcal{B}$) quadrant half-line (so not an extreme line of $\mathcal{B}$) from an extreme vertex of $\mathcal{B}$. There are a maximum of four of these half-lines and $\mathcal{P}$ will intersect each of these while the remaining $\mathcal{O}(n)$ edges of $\mathcal{VD}$

can intersect all four of them a maximum of $2(n-1)$ times (this is the case where each Voronoi cell crosses each quadrant line, and the boundary between two neighbouring Voronoi cells cannot cross more than once). Therefore, by Lemma 3.3.1, we produce at most $\mathcal{O}(m+n+p)$ lines.

Kink lines

The next category of lines forms part of the diamonds described above but, rather than defining where the bisectors will intersect a new edge, they cause quite a different change, and so deserve their own section.

Recall the corners C_1, C_2, C_3, and C_4 of $Shadow(\mathcal{B})$. Now the kink lines of C_1, C_2, C_3, and C_4 are defined to be the set of $Z = (x, y)$ such that

$$l_1^{\mathcal{B}}(Z, C_k) = l_1^{\mathcal{B}}(A_i, C_k)$$

(alternatively $\diamond_g^{C_k}(A_i)$ – identical to the first case of additive configuration lines but later we shall see that they are different). For C_k visible from both A_1 and Z these lines are, respectively for C_k,

$$y = x - \min_i b_{ix} - |\min_i b_{ix}| + \max_i b_{iy} - |\max_i b_{iy}|,\ x \in \left(\min_i b_{ix}, \min_i b_{ix} + |\min_i b_{ix}| + |\max_i b_{iy}|\right)$$
$$y = -x + \max_i b_{ix} - |\max_i b_{ix}| + \max_i b_{iy} - |\max_i b_{iy}|,\ x \in \left(\max_i b_{ix} - |\max_i b_{ix}| - |\max_i b_{iy}|, \max_i b_{ix}\right)$$
$$y = x - \max_i b_{ix} + |\max_i b_{ix}| + \min_i b_{iy} + |\min_i b_{iy}|,\ x \in \left(\max_i b_{ix} - |\max_i b_{ix}| - |\min_i b_{iy}|, \max_i b_{ix}\right)$$
$$y = -x + \min_i b_{ix} + |\min_i b_{ix}| + \min_i b_{iy} + |\min_i b_{iy}|,\ x \in \left(\min_i b_{ix}, \min_i b_{ix} + |\min_i b_{ix}| + |\min_i b_{iy}|\right).$$

The effect of crossing these kink lines is shown in Figure 3.16.

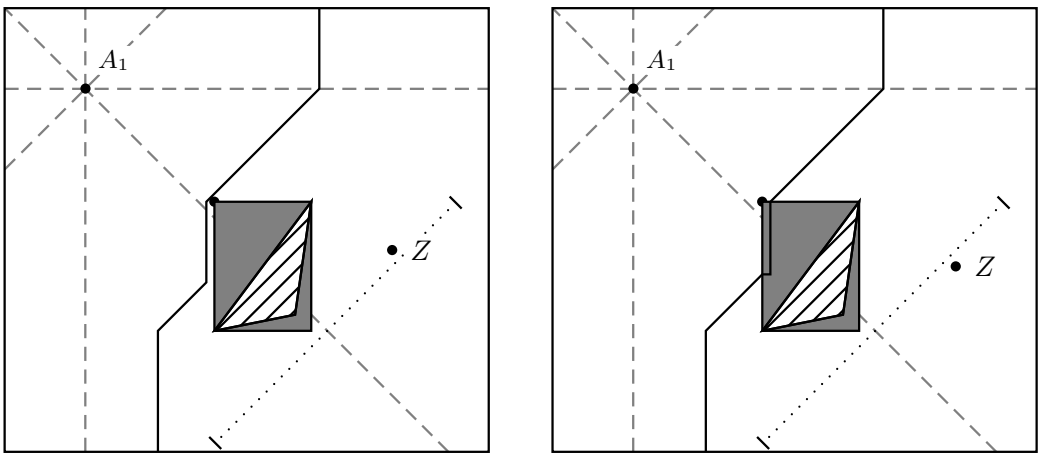

Figure 3.16: Two placements of Z within $\mathcal{P} = R((-1,-4.5),(5,0.5))$ with one existing facility $A_1 = (0,0)$ and $\mathcal{B} = \Delta((2.8,-1.4),(1.6,-3),(2.6,-2.8))$.

This could be described as a breakpoint hitting $Shadow(\mathcal{B})$ but the interactions are far more complex across these lines than across the breakpoint lines. When Z moves so that the bisector touches the corner of $Shadow(\mathcal{B})$ into an area that is not visible to one of the facilities and not already entered, the point of intersection of the clockwise and anticlockwise bisector parts enters $Shadow(\mathcal{B})$ (this must happen since a bisector part cannot leave $Shadow(\mathcal{B})$ once it has entered to intersect elsewhere – it will terminate at $\mathcal{B}$ or the other bisector part). It is because these bisector parts intersect within $Shadow(\mathcal{B})$ that we get a 'kink' since it is only here that the bisector parts can meet as a vertical and a horizontal.

Note that for these kink bisectors to occur we require the interior of the corner to be non-visible from one of the facilities and for the other facility to lie within the quarterplane

opposite to $\mathcal{B}$ formed by the extreme lines through the corner. This is due to the fact that we require both extreme points of $\mathcal{B}$ adjacent to the corner to act as an active point in each bisector part for one facility. This forces the other facility to access one active point clockwise about $\mathcal{B}$, and the other anticlockwise, from both active points (not acting through another barrier vertex) and outside the extreme lines in order to get a horizontal and vertical bisector part. Therefore these kink lines occur, given A_i, only for corners C_k for which the quarterplane opposite to or containing $\mathcal{B}$, formed by the extreme lines through C_k, contains A_i (and if A_i is in the quarterplane containing $\mathcal{B}$ then it must not be in the sub-area of $Shadow(\mathcal{B})$ containing C_k). Moreover, we need only the line segments of the geodesic diamonds contained solely within the opposite quarterplane (defined by the extreme lines through C_k) to A_i. The observant reader might wonder how these kink lines are any different to the first case of additive configuration lines. The answer lies exactly in these conditions discussed: while the two facilities in the first case of additive configuration lines must lie within the same quarterplane at C_k, the facilities in the kink construction must inhabit opposite quarterplanes.

Since for any A_i there are a maximum of two corners of $Shadow(\mathcal{B})$ at which these kinks can occur, and each geodesic diamond can contribute a maximum of two line segments (by the same argument as the first case of additive configuration lines), we then simply obtain a maximum of four line segments for each existing facility so a total contribution of $\mathcal{O}(n)$ lines.

Wrap-around lines

The final category is an extension of what we can see happening in the previous section. The kink facing A_k formed by crossing the lines described above will 'grow' the further Z travels away from the kink line. Once this touches $\mathcal{B}$ the connected bisector will separate into two parts, and thus the representation of the Voronoi cell will change.

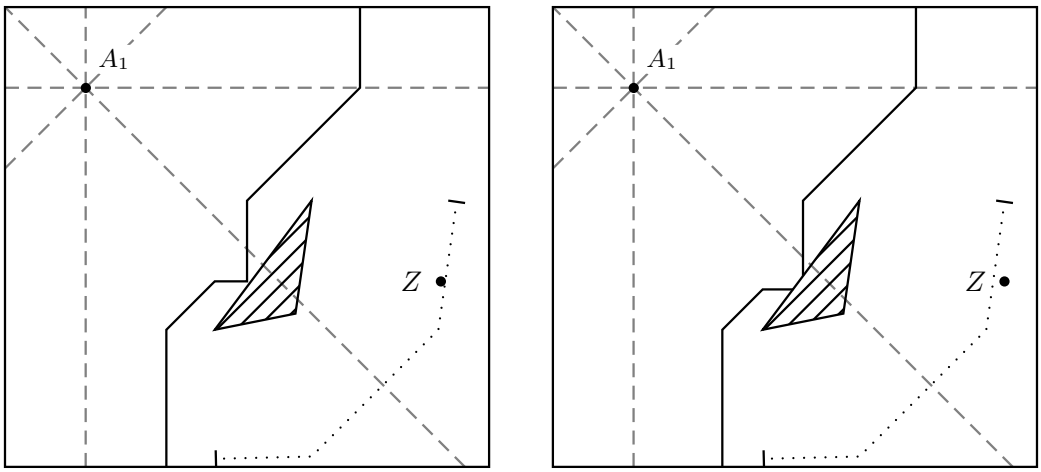

Figure 3.17: Two placements of Z within $\mathcal{P} = R((-1,-4.7),(5,0.5))$ with one existing facility $A_1 = (0,0)$ and $\mathcal{B} = \Delta((2.8,-1.4),(1.6,-3),(2.6,-2.8))$, showing the wrap-around line for $\overline{(2.8,-1.4)(1.6,-3)}$.

The tip of the kink will touch a specific point B' on an edge of $\mathcal{B}$ if the distances from B' to Z clockwise and anticlockwise about $\mathcal{B}$ are the same and are equal to $l_1^{\mathcal{B}}(B', A_1)$. Thus, for any given (b_x, b_y) on an edge of $\mathcal{B}$, we have $Z = (x, y)$ satisfying

$$l_1^{\mathcal{B},+}(Z,(b_x,b_y)) = l_1^{\mathcal{B},-}(Z,(b_x,b_y)) = l_1(A_1,(b_x,b_y))\,,$$

three equations in two unknowns so solvable (remembering from the previous discussion that, for this kink, A_1 must be visible from the corner of $Shadow(\mathcal{B})$ being crossed and outside the extreme lines of $\mathcal{B}$).

This formulation relies on the placement of Z in relation to $\mathcal{B}$ (and where $\mathcal{B}$ is located in relation to A_1) – recall that the point of intersection must be non-visible from Z. We will show a worked example for Z restricted to $x \geq \max b_{xi}$ and $\min b_{y_i} \leq y \leq \max b_{y_i}$, assuming that the edge between B_i and B_j is in the fourth quadrant of A_1, visible from A_1. In this instance, for (b_x, b_y) lying on $y' = \frac{b_{y_j} - b_{y_i}}{b_{xj} - b_{xi}} x' + \frac{b_{xj} b_{y_i} - b_{xi} b_{y_j}}{b_{xj} - b_{xi}}$ (the edge between B_i and B_j), $l_1^{\mathcal{B},+}(Z, (b_x, b_y)) = x + b_x - 2\min b_{xi} + y + b_y - 2\min b_{y_i}$, $l_1^{\mathcal{B},-}(Z, (b_x, b_y)) = x - b_x - y - b_y + 2\max b_{y_i}$, and $l_1^{\mathcal{B}}(A_1, (b_x, b_y)) = b_x - b_y$. Since the line must satisfy $l_1^{\mathcal{B},+}(Z, (b_x, b_y)) = l_1^{\mathcal{B},-}(Z, (b_x, b_y))$ we have

$$b_x = -y - b_y + \min b_{xi} + \min b_{y_i} + \max b_{y_i}\,.$$

Putting this into the equation of the edge between B_i and B_j we obtain

$$\begin{aligned} b_y &= \frac{b_{y_j} - b_{y_i}}{b_{xj} - b_{xi}} \left(-y - b_y + \min b_{xi} + \min b_{y_i} + \max b_{y_i}\right) + \frac{b_{xj} b_{y_i} - b_{xi} b_{y_j}}{b_{xj} - b_{xi}} \\ &\Rightarrow (b_{xj} - b_{xi} + b_{y_j} - b_{y_i}) b_y = -(b_{y_j} - b_{y_i}) y + (b_{y_j} - b_{y_i})(\min b_{xi} + \min b_{y_i} + \max b_{y_i}) + b_{xj} b_{y_i} - b_{xi} b_{y_j}\,. \end{aligned}$$

Now since $l_1^{\mathcal{B},+}(Z, (b_x, b_y)) = l_1^{\mathcal{B}}(A_1, (b_x, b_y))$ we have

$$b_y = \min b_{xi} + \min b_{y_i} - \frac{x + y}{2}\,.$$

Combining these two gives us the line

$$\begin{aligned} &(b_{xj} - b_{xi} + b_{y_j} - b_{y_i})(\min b_{xi} + \min b_{y_i} - \frac{x + y}{2}) \\ &\qquad = -(b_{y_j} - b_{y_i}) y + (b_{y_j} - b_{y_i})(\min b_{xi} + \min b_{y_i} + \max b_{y_i}) + b_{xj} b_{y_i} - b_{xi} b_{y_j} \\ &\qquad \Rightarrow y = \frac{b_{xj} - b_{xi} + b_{y_j} - b_{y_i}}{b_{y_j} - b_{y_i} - b_{xj} + b_{xi}} x + 2 \frac{(b_{y_j} - b_{y_i}) \max b_{y_i} - (b_{xj} - b_{xi})(\min b_{xi} + \min b_{y_i}) + b_{xj} b_{y_i} - b_{xi} b_{y_j}}{b_{y_j} - b_{y_i} - b_{xj} + b_{xi}}\,. \end{aligned}$$

This line contributes to the rightmost line segment in Figure 3.17 and the other segments are found similarly (using the appropriate representation of the shortest distance). These wrap-around lines give us a maximum of three line segments per edge since the line will only alter when an extreme line of $\mathcal{B}$ is crossed (thereby affecting the calculation of the shortest distance around $\mathcal{B}$). These lines take a variety of gradients as shown in Figure 3.18.

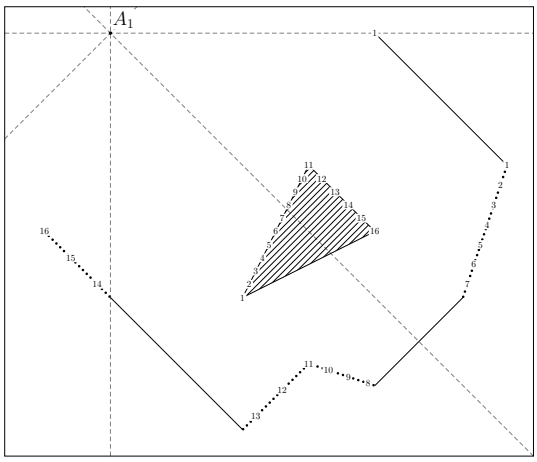

Figure 3.18: Possible placements of Z within $\mathcal{P} = R((-1, -6), (7, 1))$ with one existing facility $A_1 = (0, 0)$ and $\mathcal{B} = \Delta((20, -15), (10, -20), (15, -10))$ satisfying $l_1^{\mathcal{B},+}(Z, (b_x, b_y)) = l_1^{\mathcal{B},-}(Z, (b_x, b_y)) = l_1(A_1, (b_x, b_y))$ where the points (b_x, b_y) are specified on $\mathcal{B}$.

A particularly remarkable interaction occurs when a point on $\mathcal{B}$ is equidistant clockwise and anticlockwise around $\mathcal{B}$ to a corner of $Shadow(\mathcal{B})$. In Figure 3.18 this occurs with point 1,

somewhere between points 3 and 4, and point 6. There is not a unique position of Z at which the kink touches these points (as shown by the solid diagonal line). This is further exemplified when every point of the edge is the same distance away from A_1 (for example a diagonal facing A_1). As shown in Figure 3.19, the position of Z at which the kink intersects a specific part of $\mathcal{B}$ is not unique. It is in fact a diagonal line contained in $Shadow(\mathcal{B})$. This means that every point within the areas of $Shadow(\mathcal{B})$ not containing the diagonal facing A_1 forms a kink on this diagonal. While this does complicate the issue as we now have a kink block rather than a kink line (so the partitioning lines are the appropriate perimeter lines of $Shadow(\mathcal{B})$), it does mean that there may not be a unique optimal solution since multiple locations for Z give the same bisector (with A_1 at least).

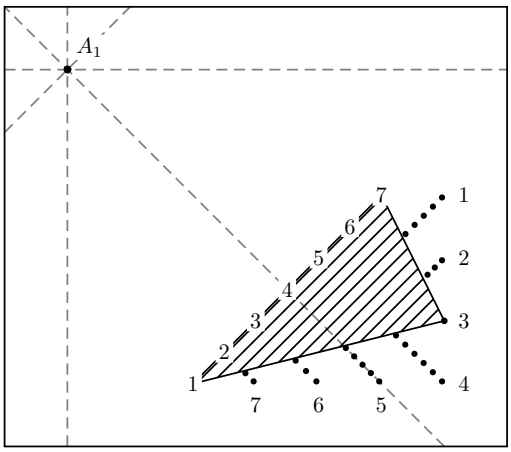

Figure 3.19: Possible placements of Z within $\mathcal{P} = R(-1, -5.5), (7, 0.5))$ with one existing facility $A_1 = (0, 0)$ and $\mathcal{B} = \Delta((5, -2), (6, -4), (2, -5))$ where the kink intersects the specified points on $\mathcal{B}$.

Finally there are also wrap-around lines where the shortest paths each way around $\mathcal{B}$ from A_1 are equal. Since A_1 is fixed, these are much simpler (being just one line segment) and they can only occur when a corner $C_i = (C_x, C_y)$ of $Shadow(\mathcal{B})$ is equidistant from A_1 both ways around $\mathcal{B}$. The kink will also only form along the diagonal line through C_i so we need no longer ask where the kink will intersect, but merely when. An example of this is shown in Figure 3.20.

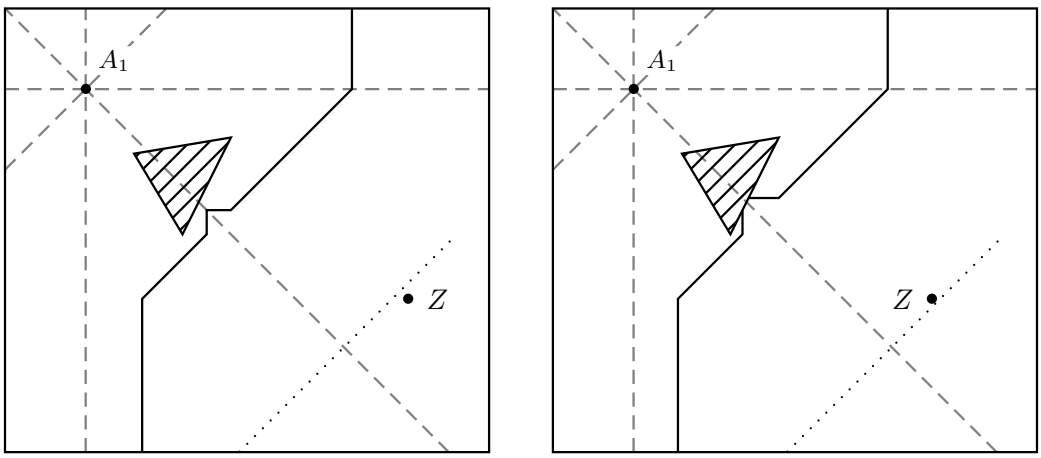

Figure 3.20: Two placements of Z within $\mathcal{P} = R((-1, -3), (5, 0.5))$ with one existing facility $A_1 = (0, 0)$ and $\mathcal{B} = \Delta((1.8, -0.6), (1.2, -1.8), (0.6, -0.8))$.

In this case, for the unique point (b_x, b_y) on $\mathcal{B}$ that is the first point of intersection of $\mathcal{B}$ on the same diagonal as C_i, the bisector intersects (b_x, b_y) if and only if Z lies on the line connecting $(C_x, C_y + sgn(C_y - b_y)(l_1^{\mathcal{B}}(A_1, (b_x, b_y)) - l_1(C_i, (b_x, b_y)))$ and $(C_x + sgn(C_x - b_x)(l_1^{\mathcal{B}}(A_1, (b_x, b_y)) - l_1(C_i, (b_x, b_y))), C_y)$. That is,

$$y = C_y + sgn(C_y - b_y)(l_1^{\mathcal{B}}(A_1, (b_x, b_y)) - l_1(C_i, (b_x, b_y)) - \frac{sgn(C_y - b_y)}{sgn(C_x - b_x)}(x - C_x)\,.$$

A barrier will produce a maximum of $p+n+8$ wrap-around line segments; each edge can only interact with the closest facility A_i to obtain a wrap-around line so the Voronoi diagram $\mathcal{VD}$ partitions the perimeter of $\mathcal{B}$ into at most $p + n$ edge segments, each one giving a wrap-around line while the (eight) intersections of these lines with the extreme lines of $\mathcal{B}$ cause another line segment to be created, as we have seen.

These being the last partitioning lines, we have a final total of a maximum number of lines to the order of $\mathcal{O}(m + n + p)$ in our partition.

We have introduced all of the partition lines which, from their algebraic formulation, are clearly unique, and have justified why they are necessary. We will next prove that these seven sets of lines are sufficient to partition the space into cells within which the Voronoi diagram is structurally identical.

3.3.1 Proof of the sufficiency of the partitioning lines

In order to prove that these lines are sufficient we need to note that a bisector will only change if the shortest path from either A_1 or Z in the barrier-free case is altered by the addition of $\mathcal{B}$. We will prove that this only happens, and so the bisector will only change its representation, when Z crosses a line that we have identified above.

It is important initially to realise that a barrier can affect the shortest path only in areas of $\mathcal{P}$ that are not visible from that facility, and that once a barrier has been placed there are now two different possible shortest path routes: one which travels clockwise about $\mathcal{B}$ and the other which travels anticlockwise. Owing to this latter property we can produce different bisectors when the clockwise distance becomes shorter than the anticlockwise distance, and vice versa.

Finally, before we begin our proof, let us recall Lemma 2.3.1. This result tells us that the bisector will only ever be different to the one in the barrier-free scenario if it enters an area of $\mathcal{P}$ not visible from A_1 or Z. We first argue that the bisector can only ever enter a non-visible part of $\mathcal{P}$ (from A_i, Z, or B_j) if it crosses a configuration line, additive configuration line, extreme line, geodesic diamond, intersection line, kink line, or wrap-around line: a collection of lines we will now refer to as *partitioning* lines.

Lemma 3.3.3. *If Z is moved so that the bisector $B(A_i, Z)$ in the barrier-free problem moves from outside to inside a non-visible area of $\mathcal{P}$ from either A_1 or Z, then it must have crossed a partitioning line.*

Proof. There are two ways in which the bisector can move into such a non-visible area. Either the visible area can change due to the placement of Z, or the change in Z will move the bisector into an area that is non-visible.

Firstly it is clear from Figure 2.11 that the visible area will only ever change (since A_1 and $\mathcal{B}$ are fixed) if Z crosses a horizontal or vertical line through the extreme vertices of $\mathcal{B}$ (the topmost, leftmost, bottommost, and rightmost). They are exactly quadrant lines through these vertices of $\mathcal{B}$, which we have recorded.

Now it remains to be seen when the bisector will be moved into a non-visible area from a visible area (with the visible area remaining unchanged). We assume that Z does not cross any configuration lines through A_1 (while this could change the bisector orientation to enter a non-visible part, it is already being recorded) so the bisector does not change shape for small changes of Z. Observing the possibilities in Figure 2.11 for a bisector to enter the non-visible part of $\mathcal{P}$, we see that the bisector will enter a non-visible area either by its intersection with $\mathcal{B}$ passing by an extreme vertex of $\mathcal{B}$ or by the bisector passing by the corner of $Shadow(\mathcal{B})$. This means that it must cross the lines on which the extreme vertex of $\mathcal{B}$ or the corner of $Shadow(\mathcal{B})$ is equidistant between A_1 and Z. These are exactly the geodesic diamonds centred on B_i and

the kink lines of the corners of $Shadow(\mathcal{B})$ (note that the kink lines are constrained to the range in which the chosen corner will be non-visible).

Therefore we have found all lines. □

Once a non-visible part is entered, the bisector no longer resembles that from the barrier-free problem. The bisector between A_i and A_j now becomes that of the additive bisector within the non-visible part, where the extreme vertex B_k of $\mathcal{B}$ which is casting the shadow for facility A_i (without loss of generality) now becomes the new facility replacing A_i with an additive value of $l_1(A_i, B_k)$.

Now that the barrier vertices are acting like facilities in the creation of (additive) bisectors, there are new non-visible areas that the bisector could enter, thereby creating additive bisectors of the additive bisector. Therefore we must also check that we are observing when the additive bisector parts are travelling into non-visible parts according to the new bisector points (the vertices of $\mathcal{B}$).

Lemma 3.3.4. *If Z is moved so that the bisector $B^{\mathcal{B}}(A_i, Z)$ moves into a new non-visible area of $\mathcal{P}$, thereby possibly affecting the bisector representation, then it must have crossed a partitioning line.*

Proof. By Lemma 3.3.3 we record when the bisector enters a non-visible part from a visible part. Once this happens, the bisectors behave as additive bisectors between a facility and a vertex of $\mathcal{B}$. This new bisector could change again once it enters a non-visible area with respect to the facility and the barrier vertex. Therefore we must check that we have recorded whenever a bisector enters a non-visible part of $\mathcal{P}$ according to any facility or any barrier vertex.

However, this is identical to the proof required in Lemma 3.3.3 since from the barrier vertex the visible area is still determined by the extreme vertices of $\mathcal{B}$ because $\mathcal{B}$ is convex. Therefore the bisector can enter a non-visible area from A_1, or the barrier vertex if the bisector passes an extreme vertex of $\mathcal{B}$, or the corner of $Shadow(\mathcal{B})$, thereby crossing the quadrant lines or kink lines. □

Not only do we require the knowledge of when a bisector enters a new non-visible area, thereby affecting the shortest path, but, due to the special quality of l_1 bisectors, once it enters this area we need to know how the bisector presents itself – i.e. how is it configured? The configuration lines in Averbakh et al. (2015) suitably carve up the space in the barrier-free case and this has been extended here to the additive configuration lines which provide the desired partition for each non-visible area into which the additive bisector may venture.

Now that we have proved when the bisector changes route due to the barrier, and how it would then naturally appear, we need to observe when it changes representation due to intersection with the edges of $\mathcal{VD}$. To prove that we have found all of the lines upon which the placement of Z causes the bisector to intersect a vertex of $\mathcal{VD}$ (since placing on either side of this line will result in an intersection on the edges either side of the vertex), we need only observe that, in order for the bisector to intersect a vertex, these lines are exactly the lines of equal distance about the vertex with distance equal to that from the vertex to the facility on the other side of the bisector. These are exactly the geodesic diamonds centred on vertices within $\mathcal{VD}$ to the facility A_k.

At an intersection we must also check what part of the bisector is intersecting these fixed edges, and so we need to know when a breakpoint intersects the edges of $\mathcal{VD}$. As we have learnt above, the bisector $B^{\mathcal{B}}(P, Q)$ will only change direction (create a breakpoint) once it hits either a vertical or horizontal line through P or Q, or a vertical or horizontal line through an extreme barrier vertex if this barrier vertex is acting as an anchor in an additive bisector, or when it enters a non-visible part from P, Q, or the barrier vertex mentioned. Once it enters a non-visible part it will again anchor on a barrier vertex so we need only examine the breakpoints at P, Q, and extreme vertices of $\mathcal{B}$. Breakpoints occur at the same horizontal or vertical coordinate as the points, and we have these exact lines in the intersection lines.

To prove, if it were in doubt, that these are the only intersections of $\mathcal{B}$ or $\mathcal{P}$, we use Lemma 2.3.2 which tells us that a barrier can have either zero or two intersections (with touches not counting as an intersection), and it is at these intersections that Z must lie on a partitioning line.

This result also brings us to our final point. The intersections divide the bisector into two parts: one part using the distances calculated travelling clockwise around $\mathcal{B}$ and the other part travelling anticlockwise around $\mathcal{B}$. Studying only one of these parts we see that, by Lemma 2.3.2, if it intersects $\mathcal{B}$ or $\mathcal{P}$ then the other part must also intersect $\mathcal{B}$ or $\mathcal{P}$. However, there is the possibility that these lines meet before intersecting the barrier or boundary at all, which gives us our final possible bisector deformation. This happens only when the clockwise and anticlockwise paths to a point are equidistant, and are equal to that distance from the point to the other facility. Thus we need to discover the lines upon which these bisector parts meet. These, by definition, are the wrap-around lines.

Thus we have identified every way in which the bisector can be changed by the barrier, and proved that we have shown the lines which preserve structural identity in this situation.

Theorem 3.3.1. *The set of configuration lines, additive configuration lines, extreme lines, geodesic diamonds, breakpoint intersection lines, kink lines, and wrap-around lines described above induces a partition of $\mathcal{P}$ into $\mathcal{O}(m+n+p)$ structurally identical cells.*

While we have described when and how each of the $\mathcal{O}(m+n+p)$ partitioning lines will appear in the partition, in practice it is sometimes the case that only a local maximum is sought. For example, the feasible region may be a subset of the market region if external regulations restrict the locating of the new facility to a certain geographical area. In this case we care less about the complete partition and concern ourselves only with the partition contained within the reduced feasible region, to which many partitioning lines will not contribute.

Which lines do and do not contribute to the partition, however, is inevitably specific to each individual scenario and very few claims can be made regarding how, generally, the complexity may be reduced in practical examples. There is no limit on the number of facilities a new facility may interact with, even if the location of this new facility is limited to one Voronoi cell of an existing facility; a problematic fact known all too well when exploring the structures of a new Voronoi cell in Section 4.2. Interestingly though, if the feasible region lies outside the geodesic diamonds centred on points in $\mathcal{VD} \cap \mathcal{B}$ then the problem is equivalent to the barrier-free problem (requiring $\mathcal{O}(m+n)$ partitioning lines). Analogously if the feasible region lies outside the geodesic diamonds centred on points in $\mathcal{VD} \cap \mathcal{P}$ then only $\mathcal{O}(n+p)$ partitioning lines are required. Beyond this, in theory and in practice, the number of required partitioning lines is still $\mathcal{O}(m+n+p)$.

3.4 Various conditional facility location problems

The partition derived in the previous section can be utilised to solve the five conditional planar facility location problems formulated earlier in Section 2.2.1 in equations (2.2.1), (2.2.2), (2.2.3), and (2.2.4). We first list them below, before investigating exact polynomial algorithms for solving each one.

The Conditional Median and Antimedian Problem (CMP and CAMP):

$$F_{CM}(Z) = \sum_{i=1}^{n+1} \int \int_{Q=(u,v)\in V(A_i)} l_1^{\mathcal{B}}(A_i, Q) du dv$$

The Conditional Centre Problem (CCP):

$$F_{CC}(Z) = \max_{i=1,\ldots,n+1} \max_{Q=(u,v)\in V(A_i)} l_1^{\mathcal{B}}(A_i, Q)$$

The Market Share Problem (MSP):

$$F_{MS}(Z) = \sum_{i=k+1}^{n+1} Area(V(A_i))$$

The Conditional Maximal Covering Location Problem (CMCLP):

$$F_{MCL}(Z) = \sum_{i=1}^{n+1} Area(V(A_i) \cap B_R(A_i))$$

3.4.1 Solving the Conditional Median and Antimedian Problems

The Conditional Median Problem requires the calculation of a more difficult integral. This is evaluated in Averbakh et al. (2015) using centroid triangulation, which is shown in Figure 3.21, and the notion of quadrant identity. However, in Averbakh et al. (2015) the Voronoi cells were always star-shaped while the inclusion of a barrier easily violates this property, as seen in Figure 3.22a (adapted from Figure 3.15[right]). Another issue is how the shortest path must be considered around $\mathcal{B}$, and so even some star-shaped Voronoi cells (taking out $\mathcal{B}$) need careful consideration, as shown in Figure 3.22b (taken from Figure 3.16[left]).

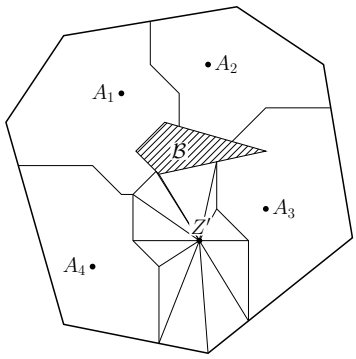

Figure 3.21: Centroid triangulation of a Voronoi cell $V(Z)$.

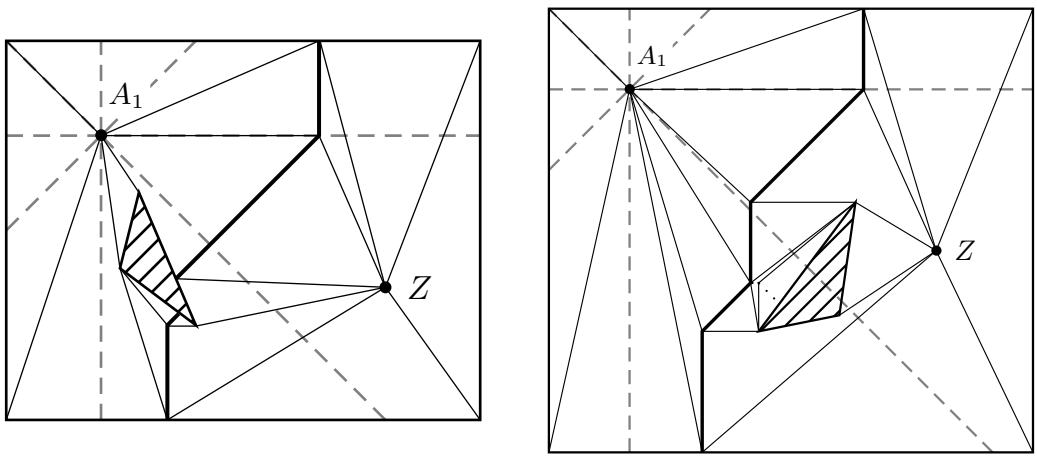

(a) Figure 3.15[right].

(b) Figure 3.16[left].

Figure 3.22: Two examples of non-star-shaped Voronoi cells.

Note that the shortest paths from each facility to each vertex of its Voronoi cell have been included in Figure 3.22, and for this in some cases we must include the lines of equidistance, shown in Figure 3.22b as the dotted line (this line is always piecewise linear). We include this in our subdivision as an edge of $V(A_k)$, thereby separating the areas of points reached travelling clockwise and anticlockwise about $\mathcal{B}$.

Whilst these Voronoi cells cannot be broken down using centroid triangulation, an adaptation of this method is easily found. To solve the issue we simply subdivide the cell into easily

manageable pieces using the quadrant lines through the vertices of $\mathcal{B}$. For centroid triangulation to work we need the area to be visible in l_2 from the facility. However, a vertex of $\mathcal{B}$ could easily block the line of sight (this need not always be an extreme vertex as we have explored before, since Euclidean visibility is reduced by a barrier to a much greater extent than l_1 visibility). Therefore we divide the Voronoi cell into subcells, each one designated to a vertex of $V(A_k)$ which could block l_2-sight from the facility and so become the acting centroid for the l_2-non-visible area of $V(A_k)$ – an additive centroid triangulation, if you will.

For any vertex of $V(A_k)$ on a reflex angle l_2-visible from A_k (these are the only vertices which could possibly interrupt line of sight), we partition $V(A_k)$ using the quadrant half-line from this vertex which is l_2-visible from A_k and travelling away from A_k (only one of which satisfies these conditions, unless the vertex and A_k are on the same horizontal or vertical lines in which case we ignore this vertex). Once these lines have been found, the partition cell of $V(A_k)$ containing A_k will be l_2-visible from A_k and so centroid triangulation will work and give the desired integral.

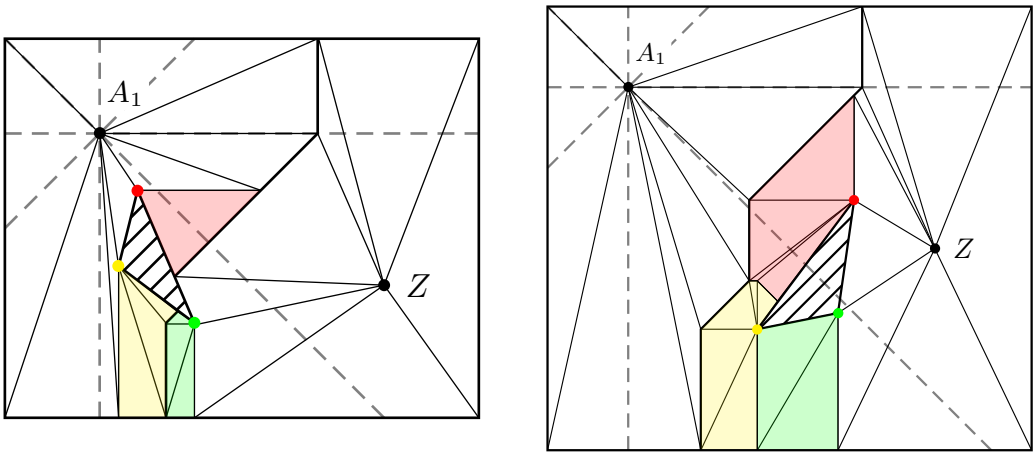

Figure 3.23: Two examples of additive centroid triangulation with blocking vertices and their partition cells colour-coded.

The remaining partition cells of $V(A_k)$ can be treated the same, with the blocking vertex acting in the place of A_k, and we partition the cells further into smaller cells in which we can use centroid triangulation until we are left with a cell which is wholly l_2-visible from the active vertex of the cell. Examples of this method are shown in Figure 3.23. Importantly, the shortest path between every point in each partition cell and A_k can pass by the acting centroid vertex of the cell (and subcells) in which it is contained. So, for every point Q in centroid triangle T in the partition cell of blocking vertex B', we have $l_1^{\mathcal{B}}(A_i, Q) = l_1^{\mathcal{B}}(A_i, B') + l_1^{\mathcal{B}}(B', Q)$. Thus the integral we require in this partition cell is

$$\int_{Q\in T} l_1^{\mathcal{B}}(A_i, Q)dQ = \int_{Q\in T} l_1^{\mathcal{B}}(B', Q)dQ + \int_{Q\in T} l_1^{\mathcal{B}}(A_i, B')dQ = \int_{Q\in T} l_1(B', Q)dQ + l_1^{\mathcal{B}}(A_i, B')Area(T)\,.$$

Therefore we can calculate the objective function for the Conditional Median Problem and find its maximiser, just as in the barrier-free case.

The representation of this partition of $V(A_k)$ will only change when Z crosses a quadrant line through one of these reflex vertices (thereby changing which quadrant half-line from this vertex is chosen to divide $V(A_k)$). These reflex vertices can only be vertices of $\mathcal{B}$ so this produces $2p$ lines. We must also have at most $2m$ lines from the quadrant lines of the vertices of $\mathcal{P}$ required for quadrant identity (the notion of which we have extended through our additive centroid triangulation), which is needed to ensure that the structure of the triangulation does not change. This leaves us with $\mathcal{O}(m+n+p)$ partition lines of $\mathcal{P}$, creating at most $\mathcal{O}((m+n+p)^2)$ partition cells.

Recalling the algorithmic complexities from Section 2.1, the barrier-restricted Voronoi diagram for the existing facilities can be calculated in $\mathcal{O}((n+p)\log^2(n+p))$ time (Mitchell, 1992) and its overlay with the market region $\mathcal{P}$ can be calculated in $\mathcal{O}(m+n+p)$ time (Finke & Hinrichs, 1995). Finally, as the objective is again cubic in x and y within each partition cell, from Averbakh et al. (2015), the minima in the interior of the cell and the minimum on any edge of the cell take a constant time to be found, so we obtain the following result.

Theorem 3.4.1. *The Conditional Median Problem can be solved in $\mathcal{O}((m+n+p)^2)$ time.*

The Conditional Antimedian Problem is addressed in Averbakh et al. (2015) by simply including all bounding lines of the l_1-disc of the specified radius about each A_i. We complete the same procedure in the barrier-constrained problem, except this time the l_1-disc is the geodesic diamond. This contributes at most $7n$ lines so the number of cells in the partition is again $\mathcal{O}((m+n+p)^2)$, giving us the following:

Theorem 3.4.2. *The Conditional Antimedian Problem can be solved in $\mathcal{O}((m+n+p)^2)$ time.*

3.4.2 Solving the Conditional Centre Problem

The solution to the Conditional Centre Problem can now also be found using the same reasoning as that offered in Averbakh et al. (2015), which relies solely on the vertices for the Voronoi cells being linear in the coordinates of Z. Using the fact that the number of vertices in the Voronoi diagram is $\mathcal{O}(m+n+p)$, an identical argument to that in Averbakh et al. (2015) gives:

Theorem 3.4.3. *The Conditional Centre Problem can be solved in $\mathcal{O}((m+n+p)^3)$ time.*

3.4.3 Solving the Market Share Problem

The objective function for the Market Share Problem is exactly the area of the Voronoi cells of the non-competitor facilities. Therefore we require the ability to calculate the area of a Voronoi cell. Remembering that $\mathcal{B}$ removes demand, we observe that $\mathcal{B}$ can be contained either entirely within $V(Z)$ or not at all (since $V(Z) \cap int(\mathcal{B}) = \emptyset$). First suppose the latter. Since $V(Z)$ is simple and polygonal, if the boundary of $V(Z)$ has vertices $D_1, \ldots, D_j$ then, from Gauss's area formula,

$$Area(V(Z)) = \sum_{i=1}^{j} \left(D_i^x \, D_{i+1}^y \; - \; D_{i+1}^x \, D_i^y \right).$$

The representations of the coordinates and of the line segments of the bisectors are clearly linear in the coordinates of the facilities to which the bisector belongs, so the vertices $D_1, \ldots, D_j$ are linear in the coordinates of Z. Thus $Area(V(Z))$ is a quadratic function in the coordinates of Z and can easily be maximised over its partition cell.

Alternatively, if $\mathcal{B}$ (with vertices $B_1, \ldots, B_l$) is contained entirely within $V(Z)$ then

$$Area(V(Z)) = \sum_{i=1}^{j} \left(D_i^x \, D_{i+1}^y \; - \; D_{i+1}^x \, D_i^y \right) - \sum_{i=1}^{l} \left(B_i^x \, B_{i+1}^y \; - \; B_{i+1}^x \, B_i^y \right)$$

which is likewise clearly quadratic and easily maximised.

Thus, using similar arguments to those in the Conditional Median Problem we obtain:

Theorem 3.4.4. *The Market Share Problem can be solved in $\mathcal{O}((m+n+p)^2)$ time.*

3.4.4 Solving the Conditional Maximal Covering Location Problem

The objective in the Conditional Maximal Covering Location Problem can be calculated by the same logic since $V(A_i) \cap B_R(A_i)$ remains simple and polygonal. However, while structural identity maintains the algebraic representation of $V(A_i)$, it is no longer sufficient to obtain an identical representation of $V(A_i) \cap B_R(A_i)$. To solve this, Averbakh et al. (2015) introduced the concept of sphere identity: two objects are sphere identical if they are either structurally identical, identical vertices of $B_R(A_i)$, or similar intersection points of the same edge of $B_R(A_i)$

and the similar segment of $\mathcal{VD}$. Following this they described spherical lines (each one of which ensures that a specific edge of $B_R(Z)$ intersects a specific segment of $B(A_i, Z)$) within the partition of which $V(A_i) \cap B_R(A_i)$ has an identical representation. We can follow their logic, extending the spherical lines to also include the intersection of the coverage dish with $\mathcal{B}$ through our geodesic formulations, introducing $\mathcal{O}(p)$ lines to give $\mathcal{O}(m + n + p)$ spherical lines overall. This leads us to our final theorem.

Theorem 3.4.5. *The Conditional Maximal Covering Location Problem can be solved in* $\mathcal{O}((m + n + p)^2)$ *time.*

Thus, after determining a partition of the market region into structurally identical cells, we have constructed exact polynomial time algorithms to solve the conditional median problem, conditional antimedian problem, conditional centre problem, market share problem, and conditional maximal covering location problem in the barrier-restricted facility location setting in rectlinear space.

Chapter 4

The Voronoi Game

Location is undoubtedly one of the most important issues when determining the success or failure of an operation. The distance between a proposed facility placement and its potential customer sites is perhaps the most natural way to discern the value of this position, and the need for effective facility locations becomes vital in competitive situations wherein customers will be gained or lost depending on whichever facility is closest. The importance of good location strategies is epitomised in the Voronoi game, a simple geometric model proposed in Ahn, Cheng, Cheong, Golin, and van Oostrum (2004).

We consider this competitive facility location problem with two players: White and Black. Players alternate placing points into the playing arena (beginning with White), until each of them has placed n points. It is assumed that no point that has been occupied can be changed or reused by either player. The arena is then subdivided according to the nearest-neighbour rule, creating the Voronoi diagram associated with the points W of White and B of Black together, and the winner is the player whose points control the larger area. But determining the winner is no easy feat as, even in a discrete graph setting, the problem is PSPACE-complete (Teramoto, Demaine, & Uehara, 2006).

This problem is the game theory interpretation of the market share problem where the optimal location of an additional facility in a region within which facilities already exist (including competitor facilities) is to be decided. The objective there is to maximise the total market share (demand captured) by the player's facilities. The exact location was proven to be found in Averbakh et al. (2015) with the l_1 norm in a convex market region. This problem is also related to work of a different type by Dehne, Klein, and Seidel (2005) using the Euclidean norm: they studied the problem of placing a single black point within the convex hull of a set of white points, such that the resulting black Voronoi cell in the unbounded Euclidean plane is maximised. They showed that there is a unique local maximum.

While some literature on this problem exists, there is a notable absence in the presentation of the game using the l_1 norm. The two-dimensional scenario was described to be the most natural one in Ahn et al. (2004), though it was solved only for the one-dimensional scenario in which a winning strategy for the second player, where the arena is a circle or a line segment, is presented for both variations where players can play more than one point at a time. It was shown that the first player can ensure that the second player wins by an arbitrarily small margin.

Cheong, Har-Peled, Linial, and Matousek (2004) provided interestingly differing results for the two- and higher-dimensional case with the Euclidean norm. For sufficiently large n and a square playing surface $\mathcal{P}$, Black has a winning strategy guaranteeing at least $\frac{1}{2} + \epsilon$ of the total area for some $\epsilon > 0$, though White can always win in a one-dimensional region. Their proof uses a combination of probabilistic arguments to show that Black will do well by playing a random point.

Optimal strategies for both players were found for a rectangular arena with Euclidean distance in Fekete and Meijer (2005) and it was ascertained that the particular values of n and the aspect ratio ρ of the arena determine which player wins: namely that Black can win if $n \geq 3$ and $\rho > \frac{\sqrt{2}}{n}$ or $n = 2$ and $\rho > \frac{\sqrt{3}}{2}$, otherwise White can win. This chapter proves a complementary characterisation in the l_1 case though, due to the different geometry, requiring a number of additional tools and having a number of considerably different outcomes.

The same game played on a polygon with holes was also tackled in Fekete and Meijer (2005) where it was found that, after White has played their point, it is NP-hard to find a position of black points that maximises the area that Black wins.

There is a considerable amount of other work on variants of the Voronoi game. Bandyapadhyay, Banik, Das, and Sarkar (2015) consider the one-round game in trees, providing a polynomial-time algorithm for the second player. As Fekete and Meijer (2005) have shown, the problem is NP-hard for polygons with holes, corresponding to a planar graph with cycles. For a spectrum of other variants and results, see Dürr and Thang (2007); Banik, Bhattacharya, Das, and Mukherjee (2013); Kiyomi, Saitoh, and Uehara (2011); Gerbner, Mészáros, Pálvölgyi, Pokrovskiy, and Rote (2013).

We start with a definition of our game. There are two players, White and Black, each having n points to play, where $n > 1$. The players alternate placing points on a rectangular playing area $\mathcal{P}$. Rather than the general multi-round game described above, we explore the simpler one-round game where a player places all of their points in one turn. As in chess, White starts the game, placing their n points within $\mathcal{P}$, followed by Black's placement of their n points. We assume that points cannot lie upon each other. Let W be the set of white points and B be the set of black ones. After all of the $2n$ points have been played, the arena is partitioned into the Voronoi diagram of $W \cup B$ using the l_1 metric and each player receives a score equal to the area of the Voronoi cells of their points, or rather their total market share. The player with the largest score wins.

The question we ask is *what is each player's best strategy?*

We answer this question for the one-round game, determining whether it is still chivalrous to play last, or it is first the worst, second the best.

The rest of this chapter is organised as follows. Preliminary (and vital) rules that White must adhere to are outlined in Section 4.1, laying down some crucial criteria for optimal strategies of both players. Section 4.2 advances these ideas and formulates the optimal strategy of White and the condition on $\mathcal{P}$ under which they can win.

4.1 Fairness and local optimality

Recall the notation introduced in Section 2.4 (for $b \in B$):

$$\begin{aligned}\mathcal{VD}(W) &= \{V^\circ(x) : x \in W\}\\ \mathcal{VD}(W \cup b) &= \{V^+(x) : x \in W \cup b\}\\ \mathcal{VD}(W \cup B) &= \{V(x) : x \in W \cup B\}\end{aligned}$$

To begin, we shall state one basic result that acts as a foundation upon which the decisions of both players in our game can be built.

Lemma 4.1.1. *For any arena $\mathcal{P}$, Black can place a point b within any bounded Voronoi cell $V^\circ(w)$ of White's in order to steal at least $50(1-\varepsilon)\%$ of $V^\circ(w)$ for any $\varepsilon > 0$.*

Proof. We utilise the fact that the l_1 bisector between two horizontal or vertical points is vertical or horizontal respectively.

Let $w = (w_x, w_y)$. Draw a horizontal line $y = w_y$ through w. If $Area(V^\circ(w) \cap \{(x,y) : y \geq w_y\}) > \frac{1}{2}Area(V^\circ(w))$ then it is clear that there exists y^* such that $Area(V^\circ(w) \cap \{(x,y) : y \geq y^*\}) = \frac{1}{2}Area(V^\circ(w))$. In this case, for any $0 < \delta \leq 2(y^* - w_y)$, placing $b = (w_x, w_y + \delta)$ will create a bisector at $y = w_y + \frac{\delta}{2} \in (w_y, y^*]$, cutting b more than 50% of $V^\circ(w)$.

If $Area(V^\circ(w) \cap \{y : y \geq w_y\}) < \frac{1}{2}Area(V^\circ(w))$ the same argument can be used with $Area(V^\circ(w) \cap \{(x,y) : y \leq y^*\}) = \frac{1}{2}Area(V^\circ(w))$.

Now we have the final case that $Area(V^\circ(w) \cap \{(x,y) : y \geq w_y\}) = \frac{1}{2}Area(V^\circ(w))$. Since $V^\circ(w)$ is bounded, there exists a finite x_{min} and x_{max} such that $V^\circ(w) \subset \{(x,y) : x_{min} \leq x \leq$

$x_{max}\}$. Therefore choosing $0 < \delta \leq \frac{\varepsilon Area(V^\circ(w))}{(x_{max}-x_{min})}$ and $b = (w_x, w_y + \delta)$ gives

$$\begin{aligned} Area(V^+(b) \cap V^\circ(w)) &\geq Area(V^\circ(w) \cap \{(x,y) : y \geq w_y\}) \\ &\quad - Area(V^\circ(w) \cap \{(x,y) : w_y \leq y \leq w_y + \frac{\varepsilon Area(V^\circ(w))}{2(x_{max}-x_{min})}\}) \\ &\geq \frac{Area(V^\circ(w))}{2} - \frac{\varepsilon Area(V^\circ(w))}{2(x_{max}-x_{min})} \times (x_{max}-x_{min}) \\ &= \frac{1-\varepsilon}{2} Area(V^\circ(w))\,. \end{aligned}$$

This gives a solution for b which will steal at least $50(1-\varepsilon)\%$ of $V^\circ(w)$ as required. □

We shall use the idea expressed in Lemma 4.1.1 in order to obtain the following properties for any of White's winning strategies.

In a competitive setting for facility location, it is a natural *fairness property* for a player to allocate the same amount of influence to each of their facilities in order to make each facility 'equally strong'. When aiming for efficient configurations in which demand points are assigned to the nearest facility, the implication is that the Voronoi cells of all of White's facilities should have the same area.

Lemma 4.1.2. *For any arena $\mathcal{P}$, if the Voronoi cells $V^\circ(w)$ have unequal area then Black can win.*

Proof. Following the positioning of White's points, if there are any unequally-sized Voronoi cells $V^\circ(w)$ then Black can steal $100(1-\delta)\%$ of the largest Voronoi cell $V^\circ(w_{max})$ by using two points sufficiently close to and either side of w_{max} (in the way shown in Lemma 4.1.1), and then position their remaining $n-2$ points within the next $n-2$ largest Voronoi cells, leaving the smallest Voronoi cell $V^\circ(w_{min})$ of White's uncontested. Black can choose their positions (i.e. choosing δ and ε) so that

$$\frac{\varepsilon pq}{2} < (1-2\delta+\varepsilon)Area(V^\circ(w_{max})) - (1-\varepsilon)Area(V^\circ(w_{min}))$$

as this gives

$$\begin{aligned} \sum_{b\in B} Area(V(b)) &\geq (1-\delta)Area(V^\circ(w_{max})) \\ &\quad + \frac{1-\varepsilon}{2}\left(\sum_{w\in W} Area(V^\circ(w)) - Area(V^\circ(w_{max})) - Area(V^\circ(w_{min}))\right) \\ &= \left(\frac{1-2\delta+\varepsilon}{2}\right) Area(V^\circ(w_{max})) + \frac{1-\varepsilon}{2} pq - \frac{1-\varepsilon}{2} Area(V^\circ(w_{min})) \\ &> \frac{\varepsilon pq}{2} + \frac{1-\varepsilon}{2} pq = \frac{pq}{2}\,, \end{aligned}$$

allowing Black to take over half of the arena's area. Thus the Voronoi cells of White must be identically sized. □

We shall refer to any arrangement W, Voronoi diagram $\mathcal{VD}(W)$, or Voronoi cell $V(x)$ within a Voronoi diagram, whose Voronoi cells satisfy Lemma 4.1.2 as *fair*.

A second *local optimality property* results from the selection of an effective location for a facility within its Voronoi cell. This property relates closely to the location-allocation algorithm (Cooper, 1963) and Lloyd's algorithm (Lloyd, 1982) for k-means clustering, both alternating methods for local optimisation which switch between solving an allocation problem (i.e. choose nearest neighbours for a given set of facilities or, rather, compute the Voronoi diagram) and solving a location problem (i.e. relocate the location clusters or, rather, optimise the location of each generator within its Voronoi cell).

Lemma 4.1.3. *For any arena $\mathcal{P}$, if any Voronoi cell $V^\circ(w)$ has unequal area either side of the horizontal or vertical through w then Black can win.*

Proof. Assuming all $V^\circ(w)$ are identically sized (else, by Lemma 4.1.2, Black can win), if there exists a $w' \in W$ where the area of $V^\circ(w')$ is distributed unequally either side of the horizontal or vertical lines through w' then Black can position a point b_1 within $V^\circ(w')$ that steals over half of the area of $V^\circ(w')$, say $\frac{1+\delta}{2}V^\circ(w')$ where $\delta > 0$. The remaining $n-1$ points can, by Lemma 4.1.1, be arranged close enough to the other points in $W \setminus \{w'\}$ with $\varepsilon < \frac{\delta}{n-1}$ as this gives

$$\begin{aligned}\sum_{b\in B} Area(V(b)) &\geq \frac{1+\delta}{2}Area(V^\circ(w')) + \frac{1-\varepsilon}{2}\sum_{w\in W\setminus\{w'\}} Area(V^\circ(w)) \\ &= \frac{1+\delta}{2}\frac{pq}{n} + \frac{1-\varepsilon}{2}(n-1)\frac{pq}{n} \\ &= \frac{pq}{2} + (\delta-(n-1)\varepsilon)\frac{pq}{2n} > \frac{pq}{2}\,,\end{aligned}$$

allowing Black to take over half of the arena's area. Thus the Voronoi cells of White must be 'area-symmetrical' in the horizontal and vertical planes. □

We shall refer to any arrangement W, Voronoi diagram $\mathcal{VD}(W)$, or Voronoi cell $V(x)$ within a Voronoi diagram, whose Voronoi cells satisfy Lemma 4.1.3 as *locally optimal*. Before continuing we shall state a simple and elegant property equivalent to being locally optimal.

Lemma 4.1.4. *Opposite quadrants of a locally optimal cell have the same area.*

These two properties give us the following definition.
A point set W in a rectangle $\mathcal{P}$ is *balanced* if the following conditions hold:

- *fairness/equal area*: for all $w_1, w_2 \in W$, the Voronoi cells $V^\circ(w_1)$ and $V^\circ(w_2)$ have the same area.
- *local optimality/area-symmetrical*: for all $w \in W$, w minimises the average distance to all points in $V^\circ(w)$ (this is equivalent to having equal area on either side of a horizontal or vertical divider through w (Fekete et al., 2005)).

Therefore the Voronoi cells in $\mathcal{VD}(W)$ must be balanced otherwise Black wins. We refer to Barvinok et al. (2003); Tamir and Mitchell (1998); Fekete and Meijer (2005) for other applications of this type of condition. This brings us to the derivation of a powerful result which will prove very useful for determining both players' optimal strategies.

Corollary 4.1.1. *Black wins if and only if they can place a point b that steals more than $\frac{pq}{2n}$ from White.*

Proof. Suppose Black wins. This means that $\sum_{b\in B} Area(V(b)) > \frac{pq}{2}$. Suppose for contradiction that there is no point $b \in B$ that steals more than $\frac{pq}{2n}$ from White. Therefore $\sum_{b\in B} Area(V(b)) \leq \sum_{b\in B} \frac{pq}{2n} = \frac{pq}{2}$ which is a clear contradiction.

Now suppose that there exists $b^* \in B$ such that $Area(V^+(b^*)) > \frac{pq}{2n}$. One property of l_1 bisectors is that the bisector between P and Q is contained in exactly one horizontal or vertical side of P and of Q. Therefore, relying on the fact from Lemma 4.1.3 that any $w \in W$ is positioned symmetrically within $V^\circ(w)$, Black can place a point b on the opposite side of w to b^* as described in Lemma 4.1.1 such that it steals $\frac{1-\varepsilon}{2}Area(V^\circ(w))$ and $V^+(b) \cap V^+(b^*) = \emptyset$ (i.e. it does not steal any area from b^*). If Black's remaining $n-1$ points are played in this way, say, next to $w_1, ..., w_{n-1}$, then their total area is

$$\begin{aligned}\sum_{b\in B} Area(V(b)) &= Area(V^+(b^*)) + \sum_{w\in\{w_1,\ldots,w_{n-1}\}} \frac{1-\varepsilon}{2}Area(V^\circ(w)) \\ &= Area(V^+(b^*)) + (n-1)\frac{1-\varepsilon}{2}\frac{pq}{n} = \frac{pq}{2} + Area(V^+(b^*)) - (1+\varepsilon(n-1))\frac{pq}{2n}\end{aligned}$$

using the fact from Lemma 4.1.2 that the Voronoi cells of White are identically sized. Thus, for any $\varepsilon < \frac{2nArea(V^+(b^*))-pq}{pq(n-1)}$ (so that $Area(V^+(b^*)) - (1+\varepsilon(n-1))\frac{pq}{2n} > 0$) the result is that Black wins. □

Now that we know how Black can react to certain weak placements of White's, we can better understand how White should play.

4.2 White's optimal strategy

Now we shall look closely into how a winning arrangement of White's could look. In order to be a winning strategy the points must be balanced; the Voronoi cells $V^\circ(w)$ must be of equal area (Lemma 4.1.2) and area-symmetrical (Lemma 4.1.3). For this, the corner cells seem to be a sensible place to start.

We start with a simple but useful result.

Lemma 4.2.1. *For rectangular arena $\mathcal{P}$ and any $n > 1$, if $V^\circ(w)$ contains a vertex of $\mathcal{P}$ then it also contains the rectangle with opposite vertices w and the vertex of $\mathcal{P}$. $V^\circ(w)$ can contain a maximum of two vertices of $\mathcal{P}$ and in this case they are consecutive and the distance between the edge upon which these vertices lie and w is $\frac{p}{2n}$ or $\frac{q}{2n}$ depending on whether this edge is vertical or horizontal respectively.*

Proof. Firstly, let $V^\circ(w)$ contain a corner P of $\mathcal{P}$. Suppose that there is a point x within the rectangle between w and P that is instead contained in $V^\circ(w')$. Then $l_1(w', P) \leq l_1(w', x) + l_1(x, P) < l_1(w, x) + l_1(x, P) = l_1(w, P)$ (since x is situated on a shortest path between w and P), clearly contradicting the fact that $P \in V^\circ(w)$.

Next, for any two points w_1 and w_2, rotating if necessary, all of the area to the left of w_1 (containing exactly two vertices of $\mathcal{P}$) is closer to w_1 and likewise all of the area to the right of w_2 (containing exactly two vertices of $\mathcal{P}$) is closer to w_2. Therefore no point can be closest to three vertices.

In the case where two vertices of $\mathcal{P}$ on a shared vertical (or horizontal) edge of $\mathcal{P}$ are contained in $V^\circ(w)$, from the above argument the rectangle containing these vertices obtained by cutting vertically (or horizontally) through w is contained in $V^\circ(w)$ and must, since W is balanced, have area $\frac{pq}{2n}$. Since the height (or width) of this rectangle is the height q (or width p) of $\mathcal{P}$ then the distance of w away from the edge of $\mathcal{P}$ must be $\frac{p}{2n}$ (or $\frac{q}{2n}$) as required. □

We shall investigate how Black can respond to White's placements in the vicinity of the corners of $\mathcal{P}$. For any $n > 1$ there will be between two and four points in W whose Voronoi cells in $\mathcal{VD}(W)$ contain a corner of $\mathcal{P}$. Picking any such point $w = (l, d)$ (the naming of which will make sense later) and rotating and/or reflecting $\mathcal{P}$ if necessary, we have the bottom left corner of $\mathcal{P}$ contained in $V^\circ(w)$ and the top left corner of $\mathcal{P}$ not contained in $V^\circ(w)$, an example of which is shown in Figure 4.1a.

We shall focus on the left half of $V^\circ(w)$ and how Black can steal enough of this and expand its borders upwards from this. If Black were to place a point at $b = (l - \delta, d + \delta)$ for some $\delta > 0$ then this point would be 2δ closer to every point on the top boundary of $V^\circ(w)$ up to $x = l - \delta$ and $2(l - x)$ closer to the boundary for $l - \delta \leq x \leq l$ (choosing the vertically-aligned $\mathcal{CC}^4(w)$ bisector – see the discussion in Section 2.4 on degenerate placements) and so would 'adopt' and advance this boundary. Since the left-hand boundary of $V^\circ(w)$ is composed entirely of $CC^3(w)$ bisectors (as it contains the vertex of $\mathcal{P}$) we can, in general, choose δ small enough so as not to change the orientation of bisectors contributing to this boundary and which segments are contributing. The only case in which this is not possible is when w lies on $\mathcal{CL}^7(w')$ for some neighbouring point $w' \in W$ in which case the originally horizontal bisector between w and w' will become a $CC^6(w')$ bisector between b and w', producing a diagonal segment with slope -1 from $x = l - \delta$ to $x = l$. Therefore the boundary of $V^+(b)$ will extend upwards a distance δ further than that of $V^\circ(w)$ from $x = 0$ to $x = l - \delta$ and then extend $l - x$ upwards from $x = l - \delta$ to $x = l$. This additional area is an increase of $l\delta - \frac{1}{2}\delta^2$.

On the other hand, the point $b = (l - \delta, d + \delta)$ will be further from all points within the left half of $V^\circ(w)$ between $x = l - \delta$ and $x = l$ that satisfy $y < x - l + d + \delta$. This leaves a total area of $d\delta + \frac{1}{2}\delta^2$ of $V^\circ(w)$ unclaimed. Both of these areas are shown in Figure 4.1b.

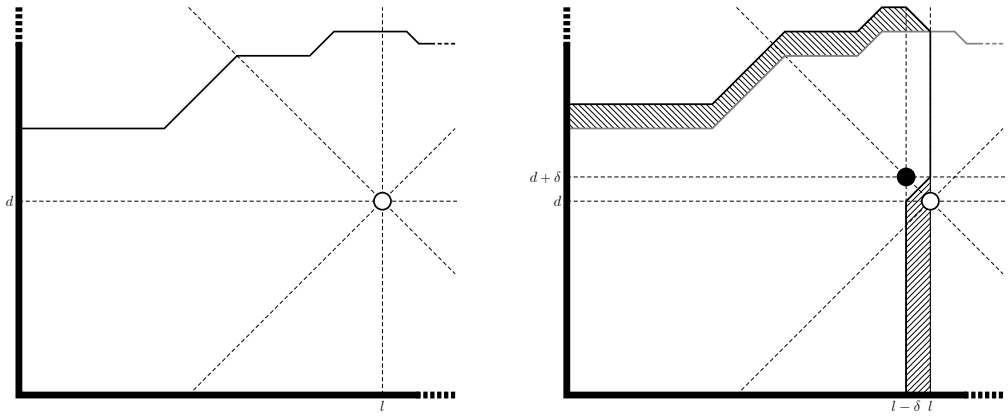

(a) An example corner cell. (b) A placement of b and the areas it gains and loses.

Figure 4.1: A corner cell and its contest.

This gives, for small δ,

$$\begin{aligned} Area(V^+(b)) &= \frac{1}{2}Area(V^\circ(w)) + l\delta - \frac{1}{2}\delta^2 - d\delta - \frac{1}{2}\delta^2 \\ &= \frac{pq}{2n} + (l-d)\delta - \delta^2 > \frac{pq}{2n} \Leftrightarrow \delta < (l-d)\,. \end{aligned}$$

Thus, as long as $l > d$ Black can always win by placing b close enough to w.

This is a very powerful result. It tells us that in any winning arrangement for White, if a Voronoi cell in $\mathcal{VD}(W)$ contains one corner of $\mathcal{P}$ then the generator must lie on the diagonal through that corner. Moreover, if a Voronoi cell in $\mathcal{VD}(W)$ contains two corners (without loss of generality let us say the bottom two corners labelled C_L and C_R, left to right) then its generator must lie outside the configuration cones $\mathcal{CC}^1(C_L)$ and $\mathcal{CC}^4(C_R)$. This is because the distance of the generator from the bottom edge of $\mathcal{P}$ must be greater than the distance to either of the vertical sides else, from the theory above, Black would win.

Not only this, but the same theory can be applied to a more general Voronoi cell. The crux of the theory lies in the fact that, from a position sufficiently close to one of White's points to take almost half of the point's cell, through a small adjustment of their point in a certain direction Black can sacrifice a small vertical (or horizontal) strip within this half of White's cell in order to gain a small horizontal (or vertical) strip atop this half of White's cell. If the horizontal (or vertical) strip has a greater area than the vertical (or horizontal) strip then this allows Black to adjust the point in order to steal an area greater than $\frac{pq}{2n}$ and thus win. This is summarised in the Lemma below which is preceded by a useful definition.

In order to allow us to more cleanly communicate these ideas and deliver our proofs let us define, for any cell $V(x) \in \mathcal{VD}(X)$, the arms of the cell to be the distances travelling either horizontally or vertically from the generator x to the boundary of $V(x)$. There are four such arms: the arm travelling vertically upwards of length u, the arm travelling horizontally rightwards of length r, the arm travelling vertically downwards of length d, and finally, unsurprisingly, the arm travelling horizontally leftwards of length l.

Lemma 4.2.2. *For any Voronoi cell $V^\circ(w)$ in a winning arrangement of White's, if one of the arms does not touch the boundary of $\mathcal{P}$ then the opposite arm parallel to this one is no shorter than the arms perpendicular to these arms.*

Proof. Take any Voronoi cell $V^\circ(w)$ and, for ease of notation, let us have the cell contained snugly in the first quadrant. That is, let $w = (l, d)$ using l and d as defined above. Again we shall focus on the left half of $V^\circ(w)$. As before, if Black were to place a point at $b = (l-\delta, d+\delta)$ for some $\delta > 0$ and choose the $\mathcal{CC}^4(w)$ bisector then this point would be 2δ closer to every point on the top boundary of $V^\circ(w)$ from $y = d + \delta$ up to $x = l - \delta$, $2(l - x)$ closer to the boundary for $l - \delta \leq x \leq l$, and $2(y - d)$ closer to the boundary for $d \leq y \leq d + \delta$.

Alternatively to the corner case, because all bisector types can occur to create the boundary of $V^\circ(w)$, we must consider more carefully how the perturbed position of b may change the boundary of $V^+(b)$. Regarding which bisector types are changed, we still have the result described above if w lies on $\mathcal{CL}^7(w')$. Analogously we have the same to the left if w lies on $\mathcal{CL}^1(w')$ for some neighbouring point w', where the vertical bisector will become a $\mathcal{CC}^5(b)$ bisector, producing a diagonal segment with slope -1 from $y = d + \delta$ to $y = d$. Finally we may be concerned if w lies on $\mathcal{CL}^2(w')$ for some neighbouring w' since the bisector will become a $\mathcal{CC}^6(b)$ bisector. However, these bisectors look identical within the bottom left of $V^\circ(w)$, and the area stolen within the top left of $V^\circ(w)$ can only increase with such a bisector change. All that is left to address is the fact that a new bisector may be present if two bisectors meet at 90° in the boundary of $V^\circ(w)$. The fact that this point may be equidistant from four of White's points is important because, though it does not present itself in the boundary of $V^\circ(w)$, it may present itself in the boundary of $V^+(b)$. This should be considered because the extension of the intersection of two perpendicular bisectors for $V^+(b)$ is 2δ further from the equivalent vertex of $V^\circ(w)$ and so could potentially give $V^+(b)$ even more area. Because of this there may well be a new bisector acting within this extra area (for this reason the space that the boundary of $V^+(b)$ could take is coloured in solid in such an area in Figure 4.2b). It is worth noting that these intersections only occur at $x = 0$ or $y = d$ (which will be useful in our area calculations) and, since we are exploring general cells, we will use the lower bound of the area in this case which, as before, is δ from the previous boundary of $V^\circ(w)$.

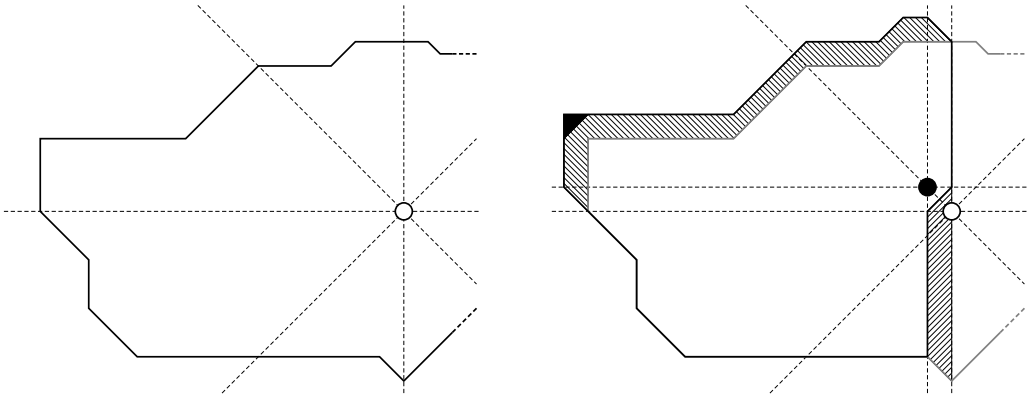

(a) An example general cell. (b) A placement of b and the areas it gains and loses.

Figure 4.2: A general cell and its contest.

Now that we are certain that, for small enough δ, the orientation of bisectors contributing to this boundary and which segments are contributing do not change except for the potential cases described above (not reducing the area), we can calculate the desired areas as highlighted in Figure 4.2b. As before, we have $l\delta - \frac{1}{2}\delta^2$ from extending the boundary upwards but, in contrast to the corner cell case, Black can also extend its area leftwards of the limits of $V^\circ(w)$. Therefore if there exists a total length of v vertical segments in the top left of $V^\circ(w)$ then this produces an additional area in the range $\left[v\delta, v\delta + \frac{1}{2}\delta^2\right]$ (this range encapsulates the effect of two bisectors intersecting at 90°). This brings the total extended area to lie within $\left[l\delta + v\delta - \frac{1}{2}\delta^2, l\delta + v\delta\right]$, or simply $l\delta - \frac{1}{2}\delta^2$ if $v = 0$.

The area in the left half of $V^\circ(w)$ not contained in $V^+(b)$ depends on the bisector composing the bottom boundary of $V^\circ(w)$. For this reason it lies in the range $\left[d\delta, d\delta + \frac{1}{2}\delta^2\right]$ (between the two extremes of a diagonal and horizontal lower boundary).

This gives, for small δ, a lower bound

$$\begin{aligned} Area(V^+(b)) &\geq \frac{1}{2}Area(V^\circ(w)) + l\delta - \frac{1}{2}\delta^2 - d\delta - \frac{1}{2}\delta^2 \\ &= \frac{pq}{2n} + (l-d)\delta - \delta^2 > \frac{pq}{2n} \Leftrightarrow \delta < (l-d) \end{aligned}$$

just as before. Thus, as long as $l > d$ Black can always win by placing b close enough to w.

Note that for this to work Black must be able to extend their cell into these new areas. For the lower bound we have required only that Black be able to extend upwards. If s of the upper boundary in the top left quadrant of $V^\circ(w)$ is shared with the boundary of $\mathcal{P}$ then this would reduce the area expansion by $s\delta$ $(= \frac{1}{2}\delta^2 + (s-\delta)\delta + \frac{1}{2}\delta^2)$ and in order for there to be a feasible δ we would require $s < l - d$. Therefore we require less than $l - d$ of the upper boundary of $V^\circ(w)$ within the top left quadrant to be on the boundary of $\mathcal{P}$.

Therefore, if any side of a Voronoi cell in a winning arrangement does not coincide sufficiently with the boundary of $\mathcal{P}$ then the arms parallel to this boundary must be no greater than the opposite perpendicular arm. Additionally, if any arm of the cell does not touch $\mathcal{P}$ then its perpendicular arms must be no greater than its opposite arm. □

Further to this, an alternative perspective on the scenario shown in Figure 4.2b yields yet another result.

Lemma 4.2.3. *For any Voronoi cell $V^\circ(w)$ in a winning arrangement of White's, if one of the arms does not touch the boundary of $\mathcal{P}$ then the arms perpendicular to this arm are equal.*

Proof. Let h be the total length of horizontal segments in the top left of $V^\circ(w)$ as depicted in Figure 4.2b. Using this notation and u as the length of the upwards arm (as above) we can represent the area extended by b as lying within the range $\left[u\delta + h\delta - \frac{1}{2}\delta^2, u\delta + h\delta\right]$, or simply $u\delta - \frac{1}{2}\delta^2$ if $h = 0$. This gives, for small δ, a lower bound

$$\begin{aligned} Area(V^+(b)) &\geq \frac{1}{2}Area(V^\circ(w)) + u\delta - \frac{1}{2}\delta^2 - d\delta - \frac{1}{2}\delta^2 \\ &= \frac{pq}{2n} + (u-d)\delta - \delta^2 > \frac{pq}{2n} \Leftrightarrow \delta < (u-d)\,. \end{aligned}$$

Thus, as long as $u > d$ Black can always win by placing b close enough to w.

As before, for this to hold, Black must be able to extend their cell leftwards so we require no more than $u - d$ of the left boundary of $V^\circ(w)$ within the top left quadrant to be on the boundary of $\mathcal{P}$.

Therefore, if any side of a Voronoi cell in a winning arrangement does not coincide sufficiently with the boundary of $\mathcal{P}$ then the parallel arms must be equal in length. That is, if any arm of the cell does not touch $\mathcal{P}$ (in this example that would be l) then its adjacent arms must be of equal length.

□

Using these two results, we can determine a very restrictive result about any cell that does not touch two opposite sides of $\mathcal{P}$.

Corollary 4.2.1. *For any Voronoi cell $V^\circ(w)$ in a winning arrangement of White's, if $V^\circ(w)$ does not touch opposite sides of $\mathcal{P}$ then its arms are all equal length.*

Proof. Since $V^\circ(w)$ does not touch opposite sides of $\mathcal{P}$, we have at least two adjacent (perpendicular) arms which do not touch $\mathcal{P}$. Without loss of generality let us say they are u and r. By Lemma 4.2.2 on u we have $d \geq l$ and $d \geq r$, and on r we have $l \geq u$ and $l \geq d$. By Lemma 4.2.3 on u we have $d \geq u$ and on r we have $l \geq r$. Thus all arms have equal length. □

Now we shall return to our corner cells. If a cell $V^\circ(w)$ contains exactly one corner then it cannot touch two opposite edges of $\mathcal{P}$ (because if it touches three edges of $\mathcal{P}$ then it must contain at least two corners of $\mathcal{P}$). Therefore by Corollary 4.2.1 its arms have equal length, l say. For the cell to be balanced the opposite quadrants of each cell must have identical area and since the quarter of the cell containing the corner is exactly the square with side length l, the opposite quadrant must also have area l^2 which, given arms of length l, restricts it to being the square of side length l also. Without loss of generality let us say that this is the bottom left corner of $\mathcal{P}$ – for reference see Figure 4.3a. In order to achieve a horizontal top boundary and vertical right boundary in this quadrant, the boundary (at least in this quadrant) must be composed of purely one $\mathcal{CC}^3(w)$ bisector and another $\mathcal{CC}^8(w)$ bisector.

In this case we shall focus on the right half of $V^\circ(w)$. If Black were to place a point at $b = (l + \delta, l + \delta)$ for some $\delta > 0$ and choose the $\mathcal{CC}^1(w)$ bisector then this point would be 2δ closer to every point on the top boundary of $V^\circ(w)$ from $x = l + \delta$ up to $y = l + \delta$, $2(x - l)$ closer to the boundary for $l \leq x \leq l + \delta$, and $2(y - l)$ closer to the boundary for $l \leq y \leq l + \delta$.

This is simply a special case of the one explored in the previous example shown in Figure 4.2, except that here we know the bisectors present in the extension areas (taking care to remember the possible diagonal bisector introduced in the perpendicular bisector intersection) and this is depicted in Figure 4.3b.

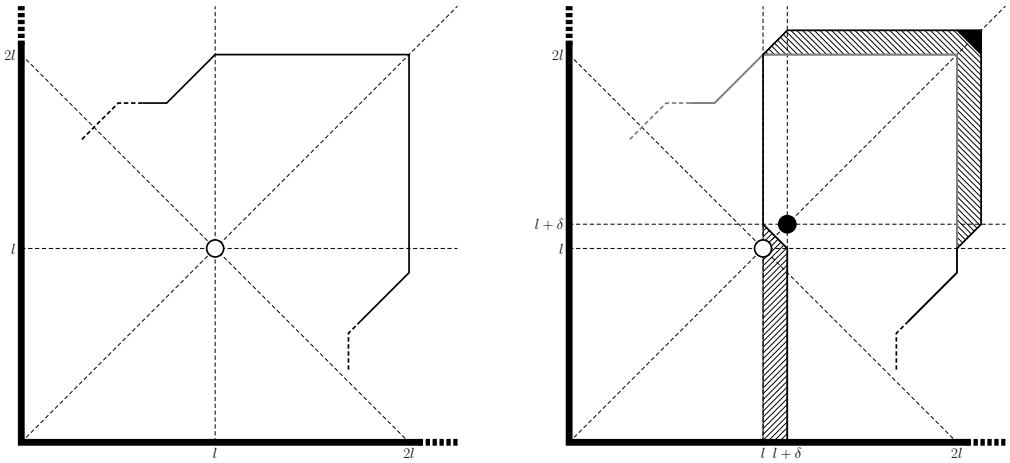

(a) A general cell containing exactly one corner. (b) A placement of b and the areas it gains and loses.

Figure 4.3: A general cell and its contest.

The area extended lies in the range $\left[2l\delta - \frac{1}{2}\delta^2, 2l\delta\right]$ and, since $V^\circ(w)$ contains the corner and no point lies on the boundary of $\mathcal{P}$, the area sacrificed is exactly $l\delta + \frac{1}{2}\delta^2$. This gives, for small δ, a lower bound

$$\begin{aligned} Area(V^+(b)) &\geq \frac{1}{2}Area(V^\circ(w)) + 2l\delta - \frac{1}{2}\delta^2 - l\delta - \frac{1}{2}\delta^2 \\ &= \frac{1}{2}Area(V^\circ(w)) + l\delta - \delta^2 > \frac{pq}{2n} \Leftrightarrow \delta < l\,. \end{aligned}$$

Therefore Black can always win if $V^\circ(w)$ contains exactly one corner.

This brings us to investigate cells containing two corners of $\mathcal{P}$ since these are the only remaining possible cells containing corners of $\mathcal{P}$ in a winning arrangement. Without loss of generality say the cell $V^\circ(w)$ contains the leftmost vertices C_D (bottom left) and C_U (top left). Firstly, since the rightwards arm from w does not touch $\mathcal{P}$, the upwards and downwards arms must be of equal length and so, since they stretch the height of $\mathcal{P}$, each must be $\frac{q}{2}$ (where q is the height of $\mathcal{P}$). As mentioned previously (but rotated here), the generator $w = (l, \frac{q}{2})$ of these cells lies in $\mathcal{CC}^1(C_D) \cap \mathcal{CC}^8(C_U)$. Therefore all of $\mathcal{P}$ to the left of $x = \frac{q}{2}$ is contained in the left half of this Voronoi cell. By Lemmas 4.1.2 and 4.1.3, $l = \frac{p}{2n}$ in order for the left half to have area $\frac{pq}{2n}$ and so we must have $\frac{q}{2} \leq \frac{p}{2n} \Rightarrow n \leq \frac{p}{q}$.

Finally, now that the only possible 'end' cells of $\mathcal{P}$ are found, we turn to the cells which do not contain a corner along with the condition that $\frac{p}{q} \geq n$ (so these cells are contained in a space bounded above and below by the boundary of $\mathcal{P}$ and on the left and right by the 'end' cells). If any one of the 'middle' cells were not to touch both horizontal edges of $\mathcal{P}$ then, in the same way as with cells containing exactly one corner, we would have $u = r = d = l$. Since $u + d < q$ then the area of this cell would be at most $(u + d) \times (l + r) < q \times q \leq \frac{pq}{n}$ which is less than the area required in order to satisfy Lemma 4.1.2. Therefore every 'middle' cell must touch both horizontal edges of $\mathcal{P}$ and, since $u = d$, lie on the line $y = \frac{q}{2}$. With all points lying on $y = \frac{q}{2}$, the only arrangement satisfying Lemma 4.1.2 is the regular $1 \times n$ orthogonal row where $w_i = (\frac{(2i-1)p}{2n}, \frac{q}{2})$ (where the bottom left vertex of $\mathcal{P}$ lies at $(0, 0)$).

Theorem 4.2.1. *The only winning arrangement for White is the $1 \times n$ arrangement for $\frac{p}{q} \geq n$. Otherwise Black wins.*

Proof. By the proof of Lemma 4.1.1, White will win if $n = 1$ by placing $w_1 = (\frac{p}{2}, \frac{q}{2})$ (arguably the 1×1 arrangement). Assume $n > 1$. As we have seen above, if $\frac{p}{q} < n$ then Black can win and if $\frac{p}{q} \geq n$ and White does not play the $1 \times n$ orthogonal row then Black can win. We explore Black's strategy against this $1 \times n$ orthogonal row given $\frac{p}{q} \geq n$.

We want to investigate the possible Voronoi diagrams $\mathcal{VD}(W \cup b_1)$ (in order to find the placement of b_1 so as to maximise $Area(V^+(b_1))$) as it is only when $Area(V^+(b_1)) > \frac{pq}{2n}$ that Black wins. To do this we aim to partition the arena into subsets within which the Voronoi diagram is structurally identical; that is, the vertices and line segments of the Voronoi diagram have the same algebraic representation in terms of the coordinates of b_1. We require this so that, once the algebraic representation of the area of $V^+(b_1)$ is found, we can maximise this over the partition to find the optimal placement of b_1 within that partition, thereby reducing Black's problem into many smaller more manageable subproblems. Since $\mathcal{P}$ is rectangular and all of White's bisectors are vertical then, from Averbakh et al. (2015), the partitioning lines are simply the configuration lines of each of White's points.

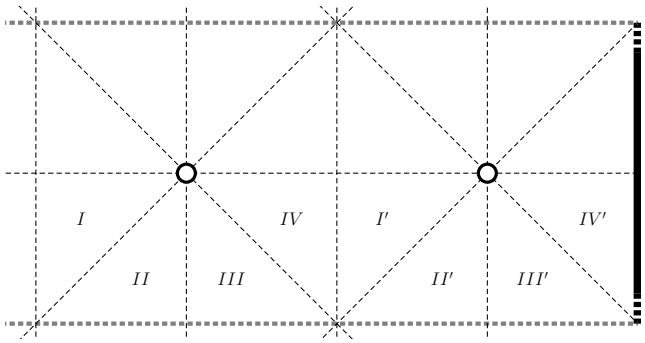

Figure 4.4: The partition of $\mathcal{P}$ about w_{n-1} and w_n for general n in a $\mathcal{P}$ of fixed width p and height q such that $\frac{p}{q} \geq n$. The dotted grey line depicts the upper and lower limits of $\mathcal{P}$ under this condition.

If we look at the Voronoi partition in the general case with $\frac{p}{q} \geq n$ we see that there are exactly eight cells that we must explore in $V^\circ(w_i)$ for each $i \in 1, ..., n$ (see Figure 4.4) since $\frac{p}{q} \geq n$ requires that $\frac{p}{2n} \geq \frac{q}{2}$, meaning that $V^\circ(w_i) \in \big(CC^4(w_{i+1}) \cup CC^5(w_{i+1})\big) \cap \big(CC^1(w_{i-1}) \cup CC^8(w_{i-1})\big)$ for $1 < i < n$. After ordering White's points $w_1, \ldots, w_n$ from left to right we note that $V^\circ(i)$ and $V^\circ(n+1-i)$ are identical by reflection through $x = \frac{p}{2}$, so we need only consider $V^\circ(\lceil \frac{n}{2} \rceil)$ to $V^\circ(n)$. Moreover, since $V^\circ(w_i) \in \big(CC^4(w_{i+1}) \cup CC^5(w_{i+1})\big) \cap \big(CC^1(w_{i-1}) \cup CC^8(w_{i-1})\big)$ for $1 < i < n$, $V^+(b_1)$ is contained in the white cell within which b_1 is placed and in the direct neighbours of this white cell, and the results after placing b_1 in Voronoi cell $V^\circ(i)$ are identical to the equivalent placement of b_1 in $V^\circ(j)$ for $1 < j < n$. Therefore we need only consider $V^\circ(n-1)$ and $V^\circ(n)$.

Each of $V(n-1)$ and $V(n)$ has eight partition cells but by reflective symmetry we need only consider four of these, the bottom four say. These are outlined in Figure 4.4. However, we can easily observe that every point in each cell in $V(n)$ is dominated by its equivalent cell in $V(n-1)$ since the areas won by b_1 in $V(n)$ are likely to have their space limited by the right edge of $\mathcal{P}$. Therefore the optimal location will lie in $V(n-1)$. Finally, we see that we only need to explore two of the cells of $V(n-1)$ due to reflective symmetry about $x = w_{n-1_x}$ and the irrelevance of the proximity to the right edge of $\mathcal{P}$.

We choose, without loss of generality, to investigate Section III and Section IV. For simplicity's sake take $w_{n-1} = (0, 0)$. The forms of these are shown in Figure 4.5.

Firstly we turn to Section III. The general form of $V^+(b_1)$ is shown in Figure 4.6.

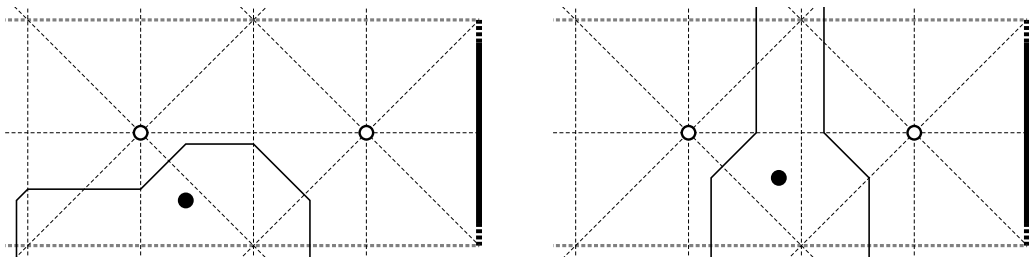

(a) Voronoi cell $V^+(b_1)$ for b_1 in Section III. (b) Voronoi cell $V^+(b_1)$ for b_1 in Section IV.

Figure 4.5: Voronoi cells $V^+(b_1)$ for b_1 in respective sections according to Figure 4.4.

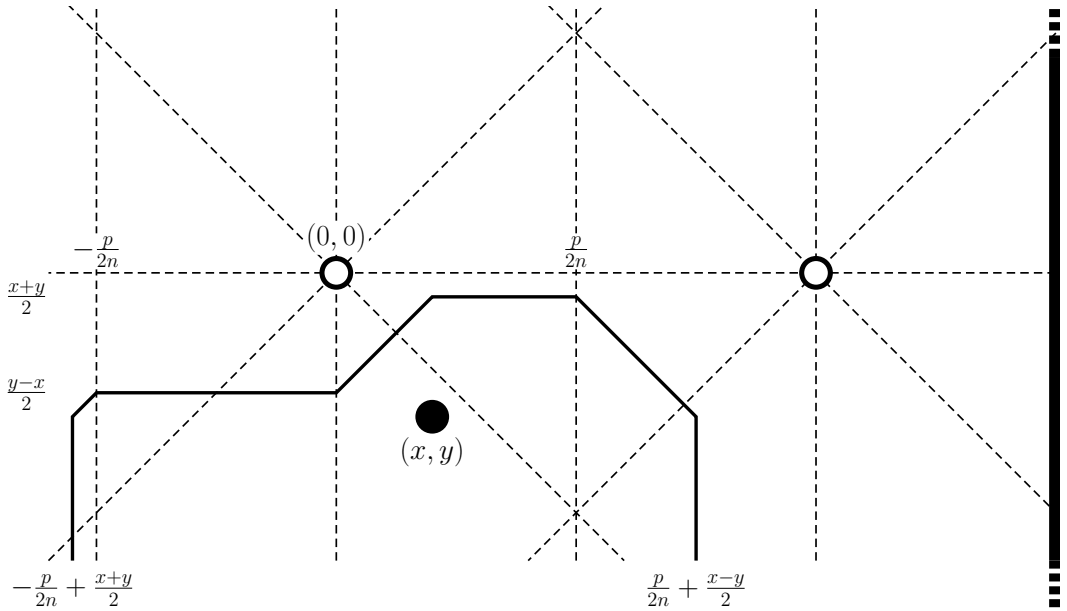

Figure 4.6: The Voronoi cell $V^+(b_1)$ for b_1 in Section III of $V^\circ(w_{n-1})$ for $n > 2$.

This has vertices, clockwise from bottom left, $(-\frac{p}{2n}+\frac{x+y}{2}, -\frac{q}{2})$, $(-\frac{p}{2n}+\frac{x+y}{2}, y)$, $(-\frac{p}{2n}, \frac{y-x}{2})$, $(0, \frac{y-x}{2})$, $(x, \frac{x+y}{2})$, $(\frac{p}{2n}, \frac{x+y}{2})$, $(\frac{p}{2n}+\frac{x-y}{2}, y)$, and $(\frac{p}{2n}+\frac{x-y}{2}, -\frac{q}{2})$ which give an area of

$$\begin{aligned}
Area(V^+(b_1)) &= (y+\frac{q}{2}) \times (\frac{p}{2n}+\frac{x-y}{2}+\frac{p}{2n}-\frac{x+y}{2}) + \frac{p}{2n} \times (\frac{y-x}{2}-y) \\
&\quad + (\frac{x+y}{2}-y) \times (\frac{p}{2n}+\frac{x-y}{2}-x) \\
&= (y+\frac{q}{2}) \times (\frac{p}{n}-y) - \frac{p}{2n} \times (\frac{x+y}{2}) + \frac{x-y}{2} \times (\frac{p}{2n}-\frac{x+y}{2}) \\
&= -\frac{x^2}{4} - \frac{3y^2}{4} + (\frac{p}{2n}-\frac{q}{2})y + \frac{pq}{2n}\,.
\end{aligned}$$

To find the maximum of this area over Section III we first use gradient methods

$$\begin{aligned}
\frac{\delta A}{\delta x} &= -\frac{x}{2} \\
\frac{\delta A}{\delta y} &= -\frac{3y}{2} + \frac{p}{2n} - \frac{q}{2}
\end{aligned}$$

to find that $Area(V^+(b_1))$ attains its maximum at $b_1^* = (0, \frac{p}{3n} - \frac{q}{3})$ with $Area(V^+(b_1^*)) = \frac{1}{2}(\frac{p}{2n}-\frac{q}{2})(\frac{p}{3n}-\frac{q}{3}) + \frac{pq}{2n}$. We have $V^+(b_1^*) > \frac{pq}{2n} \Leftrightarrow (\frac{p}{n}-q)^2 > 0 \Leftrightarrow \frac{p}{q} \neq n$. For b_1^* to be within

Section III we require that $-\frac{p}{n} \leq \frac{p}{3n} - \frac{q}{3} \leq 0 \Leftrightarrow \frac{n}{4} \leq \frac{p}{q} \leq n$ and so, since $\frac{p}{q} \geq n$ (and we have already found that $\frac{p}{q} \neq n$), this does not lie within Section III.

Therefore the maximum of $Area(V^+(b_1))$ must lie on the boundary of Section III, which we consider now.

- On the line $x = 0$, $Area(V^+(b_1)) = -\frac{3y^2}{4} + (\frac{p}{2n} - \frac{q}{2})y + \frac{pq}{2n}$ is maximised at $y = \frac{p}{3n} - \frac{q}{3} \geq 0$ (since $\frac{p}{n} \geq q$). Therefore the maximum on this boundary of Section III is achieved at $(0, 0)$ with $Area(V^+(0, 0)) = \frac{pq}{2n} \not> \frac{pq}{2n}$.

- On the line $x = -y$ we have the area $-y^2 + (\frac{p}{2n} - \frac{q}{2})y + \frac{pq}{2n}$ which reaches its maximum at $y = \frac{p}{4n} - \frac{q}{4}$. This gives $Area(V^+(-\frac{p}{4n} + \frac{q}{4}, \frac{p}{4n} - \frac{q}{4})) = (\frac{p}{4n} - \frac{q}{4})^2 + \frac{pq}{2n} > \frac{pq}{2n} \Leftrightarrow (\frac{p}{4n} - \frac{q}{4})^2 > 0 \Leftrightarrow \frac{p}{q} \neq n$. To check when $(-\frac{p}{4n} + \frac{q}{4}, \frac{p}{4n} - \frac{q}{4})$ lies on the boundary of Section III it must be the case that $-\frac{q}{2} \leq \frac{p}{4n} - \frac{q}{4} \leq 0 \Leftrightarrow \frac{p}{q} \leq n$ which is not valid (noting that we have already found $\frac{p}{q} \neq n$).

  Therefore we must check the endpoints $(0, 0)$ and $(\frac{q}{2}, -\frac{q}{2})$. $Area(V^+(0, 0))$ has already been calculated without success for Black. $Area(V^+(\frac{q}{2}, -\frac{q}{2})) = -(-\frac{q}{2})^2 - \frac{q}{2}(\frac{p}{2n} - \frac{q}{2}) + \frac{pq}{2n} = -\frac{pq}{4n} + \frac{pq}{2n} < \frac{pq}{2n}$ so no winning solution can be found on this boundary.

- Finally we investigate the boundary $y = -\frac{q}{2}$. At $y = -\frac{q}{2}$ the area has the form $-\frac{x^2}{4} + \frac{q^2}{16} + \frac{pq}{4n}$ which has the maximum at $x = 0$ giving $Area(V^+(0, -\frac{q}{2})) = \frac{q^2}{16} + \frac{pq}{4n} > \frac{pq}{2n} \Leftrightarrow \frac{p}{q} < \frac{n}{4}$ which contradicts our condition. Therefore there is no winning solution on this boundary if $\frac{p}{q} \geq n$.

Thus, if $\frac{p}{q} \geq n$, Black cannot find a point within Section III that takes an area larger than $\frac{pq}{2n}$. Note that the area calculated assumed that $n > 2$ in order to take area from $V^\circ(w_{n-2})$. Since Black was unsuccessful in Section III with the larger area that $n > 2$ allowed, they would also be unsuccessful with $n = 2$.

Now we choose b_1 in Section IV, which has general form $V^+(b_1)$ as shown in Figure 4.5b. This has vertices, clockwise from bottom left, $(\frac{x+y}{2}, -\frac{q}{2})$, $(\frac{x+y}{2}, y)$, $(\frac{x-y}{2}, 0)$, $(\frac{x-y}{2}, \frac{q}{2})$, $(\frac{p}{2n} + \frac{x+y}{2}, \frac{q}{2})$, $(\frac{p}{2n} + \frac{x+y}{2}, 0)$, $(\frac{p}{2n} + \frac{x-y}{2}, y)$, and $(\frac{p}{2n} + \frac{x-y}{2}, -\frac{q}{2})$ which give an area of

$$Area(V^+(b_1)) = q \times (\frac{p}{2n} + \frac{x+y}{2} - \frac{x-y}{2}) + 2 \times \frac{q}{2} \times (\frac{x-y}{2} - \frac{x+y}{2}) - y^2 = \frac{pq}{2n} - y^2 \leq \frac{pq}{2n}\,.$$

Therefore no winning solution lies within Section IV either.

Thus, if $\frac{p}{q} \geq n$, White has a winning strategy in choosing to locate their points in a regular $1 \times n$ orthogonal row. Otherwise Black can always win. □

Theorem 4.2.1 is the pinnacle of this chapter, solving the open question as to who wins the One-Round Voronoi Game played out on a rectangular arena. From this we have learnt, vitally, that if challenged to a game on a board wider than its height by more than a factor of the number of points being played then it is better to feign gallantry and allow the challenger to play first.

Chapter 5

The Stackelberg Game: keeping regular

Following the solution to the One-Round Voronoi Game we naturally may want to consider similar games based upon the competitive locating of points and subsequent dividing of territories. In order to appease White's tears after they have potentially been tricked into going first in a game of point-placement, an alternative game (or rather, an extension of the previous game) is the Stackelberg game where all is not lost if Black gains over half of the contested area.

The set-up is identical to that of the Voronoi game. We consider the Voronoi game as before with two players, White and Black, who take turns to place a total of n points into the playing arena (without the ability to place atop or move an existing point) before it is partitioned into the Voronoi diagram of these points. Each player gains a score equal to the area of the Voronoi cells generated by their points W and B respectively and each player's objective is to maximise this score not to be more than their competitor's score, but to have the largest score. That is, White and Black wish to maximise their respective scores

$$\mathcal{W} = \sum_{w \in W} Area(V(w))$$
$$\mathcal{B} = \sum_{b \in B} Area(V(b))$$

where, as before, we have the notation scheme:

$$\mathcal{VD}(W) = \{V^{\circ}(x) : x \in W\}$$
$$\mathcal{VD}(W \cup b) = \{V^{+}(x) : x \in W \cup b\}$$
$$\mathcal{VD}(W \cup B) = \{V(x) : x \in W \cup B\}.$$

This is subtly different to the Voronoi game wherein each player cared solely about controlling more than the other player (or over half of the playing arena) and so did not present an arrangement in such cases where they could not win over half of the playing area. Because of this, the Stackelberg game is the obvious extension to the Voronoi game.

Stackelberg games (generally defined to be a game in which a leader and a follower compete for certain quantities) present themselves in a wide range of applications so, perhaps unsurprisingly, there is substantial literature on a diverse range of interpretations. For a full classification of these competitive facility location problems and their many variations see the survey Plastria (2001), and the detailed Eiselt and Laporte (1997) for a study focused upon the more sequential problems.

Many bi-level Stackelberg location models make use of an attractiveness measure for each facility, the most popular of which is the gravity-based model proposed by Reilly (1931) wherein the patronage of each customer is decided (deterministically or randomly) based upon a function proportional to the attractiveness score of the facility and inversely proportional to the distance between the facility and customer. Both the location and attractiveness of new facilities is

allowed to be optimised in Küçükaydın, Aras, and Kuban Altınel (2012) where the leader locates new facilities within a market containing the follower's existing facilities in order to maximise captured demand, before the follower is allowed the opportunity to adjust their facilities.

Given one existing facility and a number of demand points, Drezner (1982) located a new facility in order to maximise its attracted buying power both in the situation where the existing facility is fixed, and where the follower is allowed to open a new facility. A centroid model is proposed in the presence of continuous demand in Bhadury, Eiselt, and Jaramillo (2003) which gives the follower the opportunity to respond to the leader's facility placement with placements of their own.

Serra and Revelle (1994) introduced a model wherein both players locate the same number of facilities in a network with customers patronising only the closest facility, and two accompanying heuristic algorithms are presented therein. However, in a cruel twist the objective of each player is to minimise the score of the other player. Nevertheless this may not be a surprising sentiment of each player since, as Moore and Bard (1990) indicated, the players' objectives almost always conflict with one another in the Stackelberg game.

In the hope of some level of benevolence between warring players White and Black, again we shall focus on the One-Round Stackelberg Game over a rectangular playing arena $\mathcal{P}$ with length p and height q. Just as in the Voronoi game, this is impossible to write in a closed form since the objectives rely entirely on the relative locations of the other points and so we approach the problem from a geometrical standpoint.

Firstly we shall note that the winning arrangement found for White for the Voronoi game carries over to this game since, if $\frac{p}{q} \geq n$, it was shown that deviating from this arrangement in any way would give Black more than $\frac{pq}{2n}$ and so decrease White's score. We also found the optimal strategy for Black in response to this arrangement given that the condition $\frac{p}{q} \geq n$ held in the proof of Theorem 4.2.1. The supremum of all areas of $V^+(b_1)$ in Sections III and IV was found to be $\frac{pq}{2n}$, achieved when b_1 lay atop one of White's existing points. Therefore Black's optimal strategy would be that described in Lemma 4.1.1, placing each separate point as close as possible to one of White's points and thereby securing a score of $\frac{(1-\varepsilon)pq}{2}$.

What remains to be explored for the Stackelberg game is how best White can mitigate the damage of Black's placements when $\frac{1}{n} < \frac{p}{q} < n$. [Note that since we will not enforce that $p \geq q$ within this chapter we must ensure that $\frac{p}{q} < n$ holds upon reflection in $y = x$ (i.e. for p and q swapped giving $\frac{q}{p} < n$), thus providing the $\frac{1}{n} < \frac{p}{q}$ condition.]

Since the Lemmas 4.1.2, 4.1.3, 4.2.2, and 4.2.3 outlined significant weaknesses in certain arrangements, we shall first consider arrangements that still satisfy these results and explore how Black can best exploit these positions. This investigation begins in Section 5.1 wherein an early result shows that White must play a certain grid arrangement. From there we consider Black's possible responses, exploring their best positions for stealing area from White and then their best overall strategy for when White plays a row (in Sections 5.2 and 5.3) or a grid (in Sections 5.4 and 5.5).

5.1 White's optimal strategy: a grid

It was proven in Chapter 4 that any winning arrangement of White's points in the Voronoi game must have cells $V^\circ(w)$ of equal area (Lemma 4.1.2), each with every horizontal and vertical half of the cell equal (Lemma 4.1.3), and that if any arm does not touch the boundary of $\mathcal{P}$ then the opposite arm is not shorter than the perpendicular arms (Lemma 4.2.2) and these perpendicular arms are of equal length (Lemma 4.2.3). It is natural to wonder what forms an arrangement can take if it adheres to all of these results, and this is summarised in Lemma 5.1.1.

Firstly, let us define a regular orthogonal grid. A set of n points is a *regular orthogonal* $a \times b$ *grid* within $\mathcal{P}$ ($n = ab$ and $a, b \geq 1$) if, without loss of generality locating the origin at the bottom left vertex of $\mathcal{P}$, for every point $w \in W$ there exists $i, j \in \mathbb{Z}$, $0 \leq i < a$ and $0 \leq j < b$, such that $w = (\frac{p}{2a} + \frac{p}{a}i, \frac{q}{2b} + \frac{q}{b}j)$. Additionally, a regular orthogonal $a \times b$ grid is a *square regular orthogonal* $a \times b$ *grid* if $\frac{p}{a} = \frac{q}{b}$. From this point onwards, unless explicitly stated otherwise, we shall simply use the term *grid* to mean a regular orthogonal grid, and *square grid* to mean a square regular orthogonal grid.

The following result establishes the properties of an arrangement which satisfies Lemmas 4.1.2, 4.1.3, 4.2.2, and 4.2.3 (Byrne et al., 2021).

Lemma 5.1.1. *For any arrangement W satisfying Lemmas 4.1.2, 4.1.3, 4.2.2, and 4.2.3, if $\frac{p}{q} \geq n$ then W is a $1 \times n$ grid; otherwise, W is a square grid or no such arrangement exists.*

Proof. Firstly let us clarify that, from Theorem 4.2.1, if $\frac{p}{q} \geq n$ then the only winning strategy for White in the Voronoi game is a $1 \times n$ row. This, however, does not provide us with our required result here since we no longer restrict W to being a winning arrangement.

If $\frac{p}{q} \geq n$ then, by Lemmas 4.1.2 and 4.1.3, the area of every half cell of $\mathcal{VD}(W)$ is $\frac{pq}{2n} = \frac{p}{q} \times \frac{q^2}{2n} \geq \frac{q^2}{2}$. In order to achieve this area, since the height of every cell is bounded above by q, the left and right arms of every cell must be at least $\frac{q}{2}$. If any cell were not to touch opposite sides of $\mathcal{P}$ then, by Corollary 4.2.1, its arms must be of equal length and so would be of length no less than $\frac{q}{2}$ which would make it touch the horizontal sides of $\mathcal{P}$. Therefore every cell touches opposite sides of $\mathcal{P}$. If a cell were to touch both vertical sides of $\mathcal{P}$ then, by Lemma 4.2.2, at least one of the vertical arms would have to be longer than the horizontal arms, the minimum length therefore being $\frac{p}{2}$. If this vertical arm did not touch the boundary of $\mathcal{P}$ then the same logic would apply to the other vertical arm, forcing it to have length at least $\frac{p}{2}$, which would create two vertical arms with lengths summing to p ($> q$). However, if this arm did touch the boundary of $\mathcal{P}$ then the half cell containing the arm, split along the horizontal arms, would have area $p \times \frac{p}{2} = \frac{p^2}{2} > \frac{pq}{2n}$. Thus every cell must touch each horizontal edge of $\mathcal{P}$.

By Lemma 4.2.3 the vertical arms of every cell are therefore $\frac{q}{2}$, i.e. every point of W is placed on the horizontal centre line of $\mathcal{P}$. Noting that all bisectors are now vertical lines, the only way to distribute these across $\mathcal{P}$ in order to divide $\mathcal{P}$ into equal areas (of $\frac{pq}{n}$) satisfying Lemma 4.1.2 is to place them at intervals of $\frac{p}{n}$. This corresponds to the $1 \times n$ grid.

For the $\frac{p}{q} < n$ case, let us consider the point w whose cell $V^\circ(w)$ contains the bottom left corner of $\mathcal{P}$. If $V^\circ(w)$ were to touch both horizontal edges of $\mathcal{P}$ then by Lemma 4.2.2 its left arm would be of length no less than $\frac{q}{2}$, causing the left half of $V^\circ(w)$ to have area at least $\frac{q^2}{2} > \frac{p}{qn} \times \frac{q^2}{2} = \frac{pq}{2n}$. $V^\circ(w)$ also cannot touch both vertical sides of $\mathcal{P}$ by the same argument presented in the $\frac{p}{q} \geq n$ case. Therefore we can apply the result from Corollary 4.2.1 and all arms of the cell are of equal length, d say.

Since the bottom left vertex of $\mathcal{P}$ is contained in $V^\circ(w)$ there are no $\mathcal{CC}^4(w)$, $\mathcal{CC}^5(w)$, $\mathcal{CC}^6(w)$, or $\mathcal{CC}^7(w)$ bisectors, so the entire third quadrant of w contained in $\mathcal{P}$ is also contained in $V^\circ(w)$. Therefore the bottom left quadrant of $V^\circ(w)$ is a square of area d^2. By Lemmas 4.1.2 and 4.1.3, the top right quadrant of $V^\circ(w)$ must also have area d^2, and with arms $u = r = d$ this top right quadrant must also be a square.

Considering the bisector which contributes the vertical segment bounding the top right quadrant of $V^\circ(w)$, the other point, $w' = (x, y)$, in this bisector must lie on the line $y = x - 2d$ for $0 \leq y \leq d$ (as shown in Figure 5.1) and no other point may lie between w and this line. Since $B(w, w')$ is a bound on the advancement of $V^\circ(w')$ and no other point can be closer than w or w' to the lower breakpoint of $B(w, w')$ (else this would contradict the shape of the top right quadrant of $V^\circ(w)$), the left arm of w' must also be of length d.

We can easily show that $V^\circ(w')$ cannot touch opposite sides of $\mathcal{P}$ since w is blocking it from touching both vertical sides of $\mathcal{P}$ and to touch both horizontal sides of $\mathcal{P}$ would mean, by Lemma 4.2.3, that its upper and lower arms are equal and so $\frac{q}{2}$, contradicting $0 \leq y \leq d$. Therefore, utilising Corollary 4.2.1, all arms of $V^\circ(w')$ have length d. This places $w' = (3d, d)$, on the same horizontal as w, so the bisector $B(w, w')$ is vertical, and the bottom right quadrant of $V^\circ(w)$ is also square. This forces the top left quadrant to also be square in order to have area d^2.

Analogously this argument can be applied to the right-hand boundary of $V^\circ(w')$ (since the bottom left quadrant of $V^\circ(w')$ is now seen to be a $d \times d$ square) to establish that its unique neighbour w'' has arms of length d and is situated at $(5d, d)$, and can be continued to give a row of points $w^{(i)} = ((2i + 1)d, d)$ for $i \in \mathbb{Z}^+$, giving $2d \times 2d$ square Voronoi cells up until the right-hand boundary of $\mathcal{P}$. By symmetry the argument is identical for the points above this row (starting from w we get a column of $2d \times 2d$ square Voronoi cells, and then identically upwards from w', and w'' and so on).

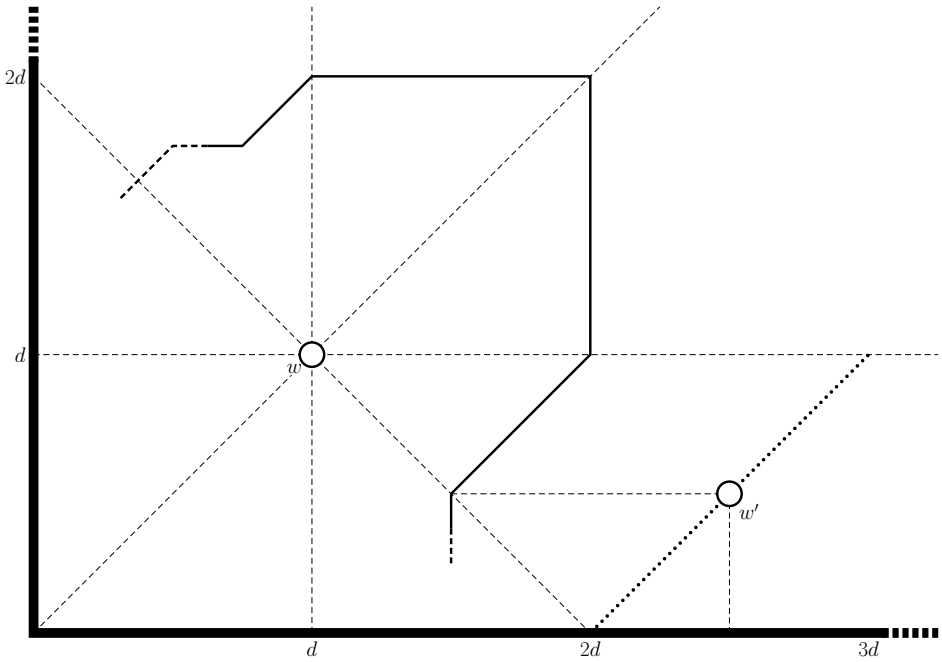

Figure 5.1: $V^\circ(w)$ and a neighbouring point w'.

The iterative use of this argument gives a square grid arrangement. We should be careful to note, however, that in order for this to work we require that the dimensions of $\mathcal{P}$ allow n squares of length $2d$ to fit within it. That is, there exists $a, b \in \mathbb{N}$ such that $a = \frac{p}{2d}$ and $b = \frac{q}{2d}$ where $a \times b = n$ for some $d \in \mathbb{R}^+$ (alternatively, $4d^2 = \frac{pq}{n}$ gives $2d = \sqrt{\frac{pq}{n}}$ so our conditions are $a = \sqrt{\frac{pn}{q}} \in \mathbb{N}$ and $b = \sqrt{\frac{qn}{p}} \in \mathbb{N}$). □

Since adherence to Lemmas 4.1.2, 4.1.3, 4.2.2, and 4.2.3 lends an obvious advantage to White in the Voronoi game, it may also be considered sensible to implement the strategies suggested by these results in the Stackelberg game. Therefore we shall explore such arrangements in the Stackelberg setting. Though Lemma 5.1.1 provided constraints on the aspect ratio of $\mathcal{P}$, we shall explore the $a \times b$ grid where $a, b > 1$, and $1 \times n$ row strategies (even relaxing the square grid constraint) for any aspect ratio to test the relationship between the games and outline how best White's positions can be exploited by Black.

5.2 White plays a $1 \times n$ row

Firstly we shall explore the placement of Black's point b_1 assuming that White plays their points in a row. Without loss of generality let this be horizontally (a rotation of $\mathcal{P}$ can easily fix this – note that, whichever rotation we choose, we are only required to explore $\frac{p}{n} < q$) and label the vertices of W running from left to right as w_1 through to w_n. Since White's arrangement is repetitive and has such symmetry, our search for Black's optimal location is greatly simplified as we need only consider the placement of b_1 within a small selection of areas of $\mathcal{P}$.

We want to investigate the possible Voronoi diagrams $\mathcal{VD}(W \cup b_1)$ (in order to find the placement of b_1 so as to maximise $Area(V^+(b_1))$ which should give us an idea of how Black should play all of their points). To do this we aim to partition the arena into subsets within which the Voronoi diagram is structurally identical; that is, the vertices and line segments of the Voronoi diagram have the same algebraic representation in terms of the coordinates of b_1. We require this so that, once the algebraic representation of the area of $V^+(b_1)$ is found, we can maximise this over the partition to find the optimal placement of b_1 within that partition, thereby reducing Black's problem into many smaller, more manageable subproblems. Since $\mathcal{P}$

is rectangular and all of White's bisectors are vertical then, from Averbakh et al. (2015), the partitioning lines are simply the configuration lines of each of White's points.

The partition of the top right quadrant of a Voronoi cell of a general point $w_i \in W$ is shown in Figure 5.2. Ignoring the bounding above and below of $\mathcal{P}$ (taking q to be sufficiently large), notice that this partition is made up of configuration lines $\mathcal{CL}^1(w_j)$ for every $j \leq i$ and $\mathcal{CL}^3(w_k)$ for every $k > i$, creating exactly $n + 1$ partition cells, irrespective of the value of i. For ease of computation we shall say $w_i = (0, 0)$ and $b_1 = (x, y)$.

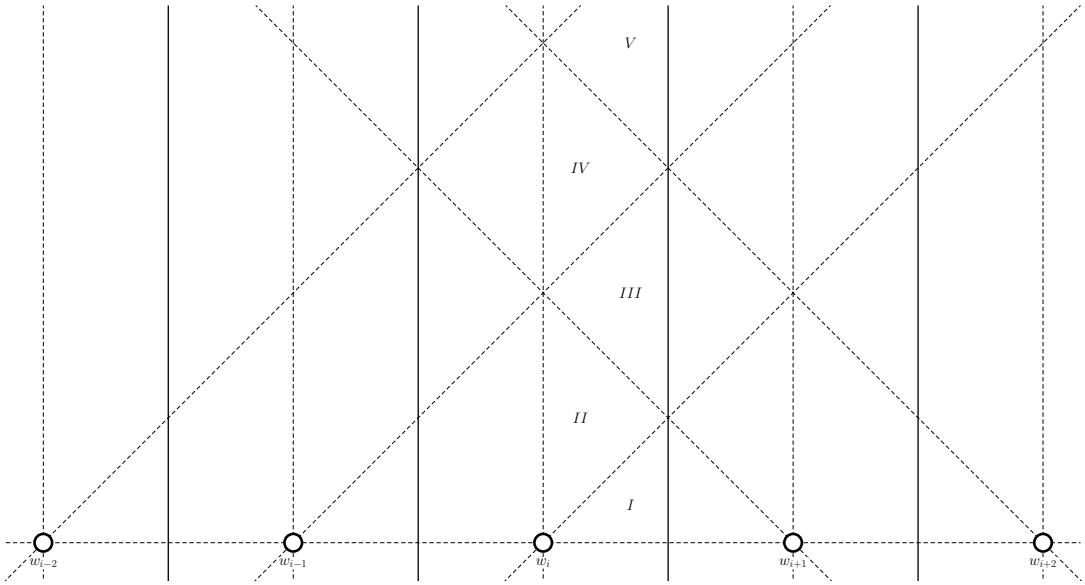

Figure 5.2: The partition of w_i in $\mathcal{P}$ in a boundless $\mathcal{P}$ of fixed width.

Observing the cell structures of $V^+(b_1)$ for b_1 in the first few sections, as shown in Figure 5.3, we can see the repetitive nature of these structures as each configuration line is crossed.

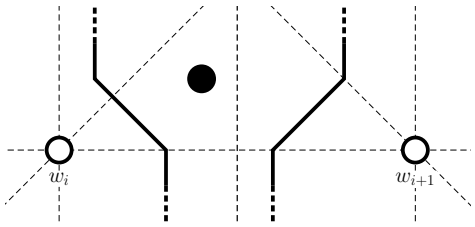

(a) Voronoi cell $V^+(b_1)$ for b_1 in Section I.

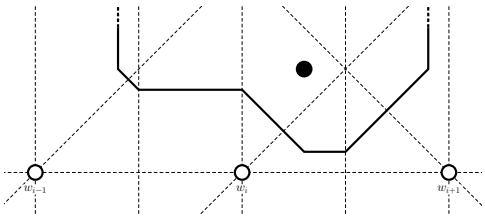

(b) Voronoi cell $V^+(b_1)$ for b_1 in Section II.

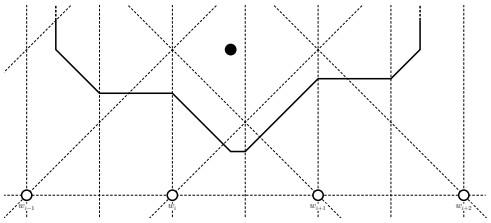

(c) Voronoi cell $V^+(b_1)$ for b_1 in Section III.

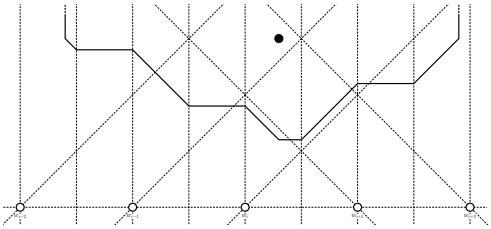

(d) Voronoi cell $V^+(b_1)$ for b_1 in Section IV.

Figure 5.3: Voronoi cells $V^+(b_1)$ for b_1 in respective sections according to Figure 5.2.

Let us first observe $V^+(b_1)$ when b_1 is in Section I of Figure 5.2. Assuming $i < n$, $V^+(b_1)$ has vertices $(\frac{x-y}{2}, \frac{q}{2})$, $(\frac{x-y}{2}, y)$, $(\frac{x+y}{2}, 0)$, $(\frac{x+y}{2}, -\frac{q}{2})$, $(\frac{p}{2n} + \frac{x-y}{2}, -\frac{q}{2})$, $(\frac{p}{2n} + \frac{x-y}{2}, 0)$, $(\frac{x+y}{2} + \frac{p}{2n}, y)$, and $(\frac{x+y}{2} + \frac{p}{2n}, \frac{q}{2})$ and so an area

$$\begin{aligned} Area(V^+(b_1)) &= (\frac{p}{2n} + \frac{x-y}{2} - \frac{x+y}{2}) \times q + 2 \times (y \times \frac{q}{2} - \frac{1}{2}y^2) \\ &= \frac{pq}{2n} - y^2 \end{aligned}$$

which is simply maximised at $(0, 0)$. If $i = n$ then this instance of $V^+(b_1)$ will be maximised by also playing as close to w_n as possible, stealing a total area bounded above by $\frac{pq}{2n}$.

5.2.1 The encroachment of $V^+(b_1)$ into $V^\circ(w_j)$

It may now seem a daunting task to work out the area of $V^+(b_1)$ for every possible placement of b_1. Instead, one more appealing approach would be to calculate the area that b_1 can steal from each Voronoi cell in $\mathcal{VD}(W)$, obtaining a formula based on the generator's location in relation to w_i and to b_1. With this information we may be able to piece such areas together in order to obtain a general formula for the area of $V^+(b_1)$.

Theft from $V^\circ(w_i)$ Firstly, the area stolen from $V^\circ(w_i)$ takes two different forms depending on whether $b_1 \in \mathcal{CC}^1(w_i)$ or $b_1 \in \mathcal{CC}^2(w_i)$. If $b_1 \in \mathcal{CC}^1(w_i)$ then the area can only take the form that we have already explored in Section I so we need not continue further along this avenue. The area stolen from $V^\circ(w_i)$ if $b_1 \in \mathcal{CC}^2(w_i)$ has vertices $(-\frac{p}{2n}, \frac{x+y}{2})$, $(0, \frac{x+y}{2})$, $(x, \frac{y-x}{2})$, $(\frac{p}{2n}, \frac{y-x}{2})$, $(\frac{p}{2n}, \frac{q}{2})$, and $(-\frac{p}{2n}, \frac{q}{2})$ and totals

$$\begin{aligned} Area(V^+(b_1) \cap V^\circ(w_i)) &= \frac{p}{n} \times (\frac{q}{2} - \frac{x+y}{2}) + \frac{p}{2n} \times x - \frac{1}{2}x^2 \\ &= -\frac{x^2}{2} - \frac{p}{2n}y + \frac{pq}{2n}\,. \end{aligned}$$

Theft from $V^\circ(w_j)$ for $j < i$ Next let us investigate what occurs when $b_1 \in \mathcal{CC}^1(w_j)$ for $j < i$. If there exists a j such that $b_1 \in \mathcal{CC}^1(w_j) \setminus \mathcal{CC}^1(w_{j+1})$ then $V^+(b_1)$ enters $V^\circ(w_j)$. Therefore, writing w_j as $(\frac{(j-i)p}{n}, 0)$, the area stolen from $V^\circ(w_j)$ if $b_1 \in \mathcal{CC}^1(w_j) \setminus \mathcal{CC}^1(w_{j+1})$ has vertices $(\frac{x-y}{2} + \frac{(j-i)p}{2n}, y)$, $(\frac{(2(j-i)+1)p}{2n}, \frac{x+y}{2} - \frac{(j-i+1)p}{2n})$, $(\frac{(2(j-i)+1)p}{2n}, \frac{q}{2})$, and $(\frac{x-y}{2} + \frac{(j-i)p}{2n}, \frac{q}{2})$ and totals

$$\begin{aligned} Area(V^+(b_1) \cap V^\circ(w_j)) &= \frac{1}{2} \times (\frac{(2(j-i)+1)p}{2n} - (\frac{x-y}{2} + \frac{(j-i)p}{2n})) \\ &\quad \times (\frac{q}{2} - y + \frac{q}{2} - (\frac{x+y}{2} - \frac{(j-i+1)p}{2n})) \\ &= \frac{1}{2} \times (\frac{(j-i+1)p}{2n} - \frac{x-y}{2}) \times (\frac{(j-i+1)p}{2n} + q - \frac{x+3y}{2}) \\ &= \frac{1}{2} \times ((\frac{(j-i+1)p}{2n})^2 + \frac{(j-i+1)p}{2n}(q - \frac{x+3y}{2} - \frac{x-y}{2}) \\ &\quad - \frac{x-y}{2}(q - \frac{x+3y}{2})) \\ &= \frac{x^2}{8} - \frac{3y^2}{8} + \frac{xy}{4} + (\frac{(i-j-1)p}{4n} - \frac{q}{4})x + (\frac{(i-j-1)p}{4n} + \frac{q}{4})y \\ &\quad - \frac{(i-j-1)pq}{4n} + \frac{(i-j-1)^2p^2}{8n^2}\,. \end{aligned}$$

If $b_1 \in \mathcal{CC}^2(w_j)$ then $V^+(b_1)$ always steals from $V^\circ(w_j)$. This area stolen has vertices $(\frac{(2(j-i)-1)p}{2n}, \frac{x+y}{2} - \frac{(j-i)p}{2n})$, $(\frac{(j-i)p}{n}, \frac{x+y}{2} - \frac{(j-i)p}{2n})$, $(\frac{(2(j-i)+1)p}{2n}, \frac{x+y}{2} - \frac{(j-i+1)p}{2n})$, $(\frac{(2(j-i)+1)p}{2n}, \frac{q}{2})$, and $(\frac{(2(j-i)-1)p}{2n}, \frac{q}{2})$ and totals

$$\begin{aligned} Area(V^+(b_1) \cap V^\circ(w_j)) &= \frac{p}{n} \times (\frac{q}{2} - (\frac{x+y}{2} - \frac{(j-i)p}{2n})) + \frac{1}{2}(\frac{p}{2n})^2 \\ &= -\frac{p}{2n}x - \frac{p}{2n}y + \frac{pq}{2n} - \frac{(4(i-j)-1)p^2}{8n^2}\,. \end{aligned}$$

Theft from $V^\circ(w_k)$ for $k > i$ Now moving our focus over to the Voronoi cells of w_k for $k > i$, we have the analogous situations explored above. If there exists a k such that $b_1 \in \mathcal{CC}^4(w_k) \setminus \mathcal{CC}^4(w_{k-1})$ then $V^+(b_1)$ enters $V^\circ(w_k)$. Therefore, writing w_k as $(\frac{(k-i)p}{n}, 0)$, the area stolen from $V^\circ(w_k)$ if $b_1 \in \mathcal{CC}^4(w_k) \setminus \mathcal{CC}^4(w_{k-1})$ has vertices $(\frac{(2(k-i)-1)p}{2n}, \frac{y-x}{2} + \frac{(k-i-1)p}{2n})$, $(\frac{x+y}{2} + \frac{(k-i)p}{2n}, y)$, $(\frac{x+y}{2} + \frac{(k-i)p}{2n}, \frac{q}{2})$, and $(\frac{(2(k-i)-1)p}{2n}, \frac{q}{2})$ and totals

$$\begin{aligned} Area(V^+(b_1) \cap V^\circ(w_k)) &= \frac{1}{2} \times (\frac{x+y}{2} + \frac{(k-i)p}{2n} - \frac{(2(k-i)-1)p}{2n}) \\ &\quad \times (\frac{q}{2} - (\frac{y-x}{2} + \frac{(k-i-1)p}{2n}) + \frac{q}{2} - y) \\ &= \frac{1}{2} \times (\frac{x+y}{2} - \frac{(k-i-1)p}{2n}) \times (\frac{x-3y}{2} - \frac{(k-i-1)p}{2n} + q) \\ &= \frac{x^2}{8} - \frac{3y^2}{8} - \frac{xy}{4} + (\frac{q}{4} - \frac{(k-i-1)p}{4n})x + (\frac{(k-i-1)p}{4n} + \frac{q}{4})y \\ &\quad - \frac{(k-i-1)pq}{4n} + \frac{(k-i-1)^2p^2}{8n^2}\,. \end{aligned}$$

We are comforted to see that this area is in fact identical, up to a reflection, to that for $b_1 \in \mathcal{CC}^2(w_j)$ where the axes have been reflecting in the y-axis (i.e. x becomes $-x$ and $i-j$ becomes $k-i$).

And as before, if $b_1 \in \mathcal{CC}^3(w_k)$ then $V^+(b_1)$ always steals from $V^\circ(w_k)$. This area stolen has vertices $(\frac{(2(k-i)-1)p}{2n}, \frac{y-x}{2} + \frac{(k-i-1)p}{2n})$, $(\frac{(k-i)p}{n}, \frac{y-x}{2} + \frac{(k-i)p}{2n})$, $(\frac{(2(k-i)+1)p}{2n}, \frac{y-x}{2} + \frac{(k-i)p}{2n})$, $(\frac{(2(k-i)+1)p}{2n}, \frac{q}{2})$, and $(\frac{(2(k-i)-1)p}{2n}, \frac{q}{2})$ and totals

$$\begin{aligned} Area(V^+(b_1) \cap V^\circ(w_k)) &= \frac{p}{n} \times (\frac{q}{2} - (\frac{y-x}{2} + \frac{(k-i)p}{2n})) + \frac{1}{2}(\frac{p}{2n})^2 \\ &= \frac{p}{2n}x - \frac{p}{2n}y + \frac{pq}{2n} - \frac{(4(k-i)-1)p^2}{8n^2}\,. \end{aligned}$$

This is again identical to the area found for $b_1 \in \mathcal{CC}^2(w_j)$ after the reflection described previously.

We have now found all formulae for the area of $V^+(b_1)$ contained in each Voronoi cell of $\mathcal{VD}(W)$ when White plays a row. From these we can derive the area for a general cell $V^+(b_1)$ where $b_1 \in V^\circ(w_i)$ for some i, and find the optimal solution within each of the partition cells that produce such a structure of $V^+(b_1)$. Figure 5.4 will depict all optimal locations of b_1 within each section under the certain circumstances we will discuss below unless optima have location $(0,0)$, a placement already described in Lemma 4.1.1; Section IV and Section III are depicted as the poster children for the general Section $2l$ and Section $2l+1$ results respectively, and for clarity these respective sections will be shaded in each figure.

5.2.2 $V^+(b_1)$ not touching the vertical edges of $\mathcal{P}$

Since we have already explored Section I, we will look only at $b_1 \in \mathcal{CC}^2(w_i)$. Firstly, ignoring intersections with the vertical boundaries of $\mathcal{P}$, we can see from Figure 5.3 that the left and right ends of $V^+(b_1)$ always have the same structure. This is because there is always a j such that $b_1 \in \mathcal{CC}^1(w_j) \setminus \mathcal{CC}^1(w_{j+1})$ and similarly always a k such that $b_1 \in \mathcal{CC}^4(w_k) \setminus \mathcal{CC}^4(w_{k-1})$. Furthermore, viewing j and k as points l away from i we can write each partition cell in Figure 5.2 as either $(\mathcal{CC}^1(w_{i-l}) \setminus \mathcal{CC}^1(w_{i-l+1})) \cap (\mathcal{CC}^4(w_{i+l}) \setminus \mathcal{CC}^4(w_{i+l-1}))$ or $(\mathcal{CC}^1(w_{i-l}) \setminus \mathcal{CC}^1(w_{i-l+1})) \cap (\mathcal{CC}^4(w_{i+l+1}) \setminus \mathcal{CC}^4(w_{i+l}))$ (exploring the top right quadrant of $V^\circ(w_i)$ means we may interact with w_j either for all $j = i-l, \ldots, i+l$ or for all $j = i-l, \ldots, i+l+1$).

Section $2l$ Therefore we have one of two area formulae, the first being for $b_1 \in (\mathcal{CC}^1(w_{i-l}) \setminus \mathcal{CC}^1(w_{i-l+1})) \cap (\mathcal{CC}^4(w_{i+l}) \setminus \mathcal{CC}^4(w_{i+l-1})) = \mathcal{CC}^1(w_{i-l}) \bigcap_{j=i-l+1}^{i} \mathcal{CC}^2(w_j) \bigcap_{j=i+1}^{i+l-1} \mathcal{CC}^3(w_j) \cap \mathcal{CC}^4(w_{i+l})$ for $l \in \mathbb{N}$ (this would be Section $2l$ in Figure 5.2) with

$$
\begin{aligned}
Area(V^+(b_1)) &= Area(V^+(b_1) \cap V^\circ(w_{i-l})) + \sum_{j=i-l+1}^{i-1} Area(V^+(b_1) \cap V^\circ(w_j)) \\
&\quad + Area(V^+(b_1) \cap V^\circ(w_i)) + \sum_{j=i+1}^{i+l-1} Area(V^+(b_1) \cap V^\circ(w_j)) \\
&\quad + Area(V^+(b_1) \cap V^\circ(w_{i+l})) \\
&= \frac{x^2}{8} - \frac{3y^2}{8} + \frac{xy}{4} + (\frac{(i-(i-l)-1)p}{4n} - \frac{q}{4})x + (\frac{(i-(i-l)-1)p}{4n} + \frac{q}{4})y \\
&\quad - \frac{(i-(i-l)-1)pq}{4n} + \frac{(i-(i-l)-1)^2p^2}{8n^2} \\
&\quad + \sum_{j=i-l+1}^{i-1} (-\frac{p}{2n}x - \frac{p}{2n}y + \frac{pq}{2n} - \frac{(4(i-j)-1)p^2}{8n^2}) - \frac{x^2}{2} - \frac{p}{2n}y + \frac{pq}{2n} \\
&\quad + \sum_{j=i+1}^{i+l-1} (\frac{p}{2n}x - \frac{p}{2n}y + \frac{pq}{2n} - \frac{(4(j-i)-1)p^2}{8n^2}) + \frac{x^2}{8} - \frac{xy}{4} - \frac{3y^2}{8} \\
&\quad + (\frac{q}{4} - \frac{((i+l)-i-1)p}{4n})x + (\frac{((i+l)-i-1)p}{4n} + \frac{q}{4})y \\
&\quad - \frac{((i+l)-i-1)pq}{4n} + \frac{((i+l)-i-1)^2p^2}{8n^2} \\
&= -\frac{x^2}{4} - \frac{3y^2}{4} + (\frac{(l-2)p}{2n} + \frac{q}{2})y - \frac{(l-2)pq}{2n} + \frac{(l-1)^2p^2}{4n^2} \\
&\quad + (-\frac{p}{2n}x - \frac{p}{2n}y + \frac{pq}{2n} + \frac{p^2}{8n^2}) \times ((i-1) - (i-l+1-1)) - \sum_{j=i-l+1}^{i-1} (\frac{4(i-j)p^2}{8n^2}) \\
&\quad + (\frac{p}{2n}x - \frac{p}{2n}y + \frac{pq}{2n} + \frac{p^2}{8n^2}) \times ((i+l-1) - (i+1-1)) - \sum_{j=i+1}^{i+l-1} (\frac{4(j-i)p^2}{8n^2}) \\
&= -\frac{x^2}{4} - \frac{3y^2}{4} + (\frac{(l-2)p}{2n} + \frac{q}{2})y - \frac{(l-2)pq}{2n} + \frac{(l-1)^2p^2}{4n^2} \\
&\quad + (l-1)(-\frac{p}{n}y + \frac{pq}{n} + \frac{p^2}{4n^2}) - \frac{p^2}{2n^2}(\sum_{i-j=1}^{l-1} (i-j) + \sum_{j-i=1}^{l-1} (j-i)) \\
&= -\frac{x^2}{4} - \frac{3y^2}{4} + (-\frac{lp}{2n} + \frac{q}{2})y + \frac{lpq}{2n} - \frac{(l-1)lp^2}{4n^2}\,.
\end{aligned}
$$

This area has partial derivatives

$$
\begin{aligned}
\frac{\delta A}{\delta x} &= -\frac{x}{2} \\
\frac{\delta A}{\delta y} &= -\frac{3y}{2} - \frac{lp}{2n} + \frac{q}{2}
\end{aligned}
$$

giving the optimal value $b_1^* = (0, \frac{q}{3} - \frac{lp}{3n})$ with $Area(V^+(b_1^*)) = \frac{lpq}{3n} + \frac{(3-2l)lp^2}{12n^2} + \frac{q^2}{12}$. This is depicted in Figure 5.4b for $l = 2$. For b_1^* to lie within Section $2l$ we must have $x^* + (l-1)\frac{p}{n} \leq y^* \leq l\frac{p}{n} - x^*$ so it must be the case that $\frac{(4l-3)p}{n} \leq q \leq \frac{4lp}{n}$.

If $\frac{4lp}{n} \leq q$ then the optimum must lie at the intersection of $x = 0$ and $y = l\frac{p}{n} - x$ (since $\frac{\delta A}{\delta x} = -\frac{x}{2}$, the area will always increase as x moves towards 0 and since $\frac{4lp}{n} \leq q$ the global optimum lies above Section $2l$). Therefore the optimum in this section is $b_1^* = (0, l\frac{p}{n})$ achieving $Area(V^+(b_1)) = \frac{lpq}{n} + \frac{(1-6l)lp^2}{4n^2}$. This is depicted in Figure 5.4a.

Alternatively, if $\frac{(4l-3)p}{n} \geq q$ then the optimum must lie at the intersection of $x = 0$ and $y = x + (l-1)\frac{p}{n}$ (since $\frac{\delta A}{\delta x} = -\frac{x}{2}$, the area will always increase as x moves towards 0 and since $\frac{(4l-3)p}{n} \geq q$ the global optimum lies below Section $2l$). Therefore the optimum in this section is $b_1^* = (0, (l-1)\frac{p}{n})$ achieving $Area(V^+(b_1)) = \frac{(2l-1)pq}{2n} - \frac{3(2l-1)(l-1)p^2}{4n^2}$. This is depicted in Figure 5.4c.

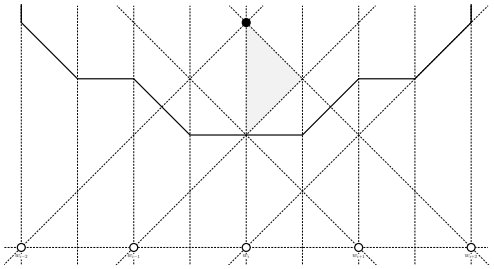

(a) $b_1 = (0, l\frac{p}{n})$ only if $\frac{4lp}{n} \leq q$.

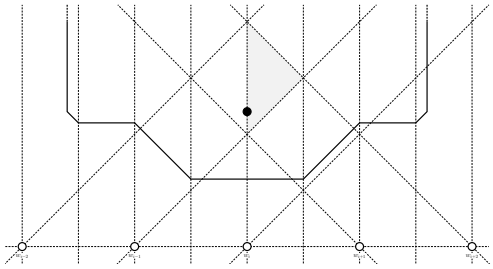

(b) $b_1 = (0, \frac{q}{3} - \frac{lp}{3n})$ only if $\frac{(4l-3)p}{n} \leq q \leq \frac{4lp}{n}$.

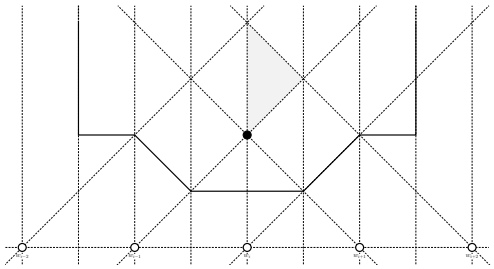

(c) $b_1 = (0, (l-1)\frac{p}{n})$ only if $\frac{(4l-3)p}{n} \geq q$.

Figure 5.4: Maximal area Voronoi cells $V^+(b_1)$ for b_1 within Section $2l$ not touching the vertical edges of $\mathcal{P}$.

Section $2l+1$ The other area formula for $b_1 \in (\mathcal{CC}^1(w_{i-l}) \setminus \mathcal{CC}^1(w_{i-l+1})) \cap (\mathcal{CC}^4(w_{i+l+1}) \setminus \mathcal{CC}^4(w_{i+l})) = \mathcal{CC}^1(w_{i-l}) \bigcap_{j=i-l+1}^{i} \mathcal{CC}^2(w_j) \bigcap_{j=i+1}^{i+l} \mathcal{CC}^3(w_j) \cap \mathcal{CC}^4(w_{i+l+1})$ for $l \in \mathbb{N}$ (this would be Section $2l+1$ in Figure 5.2) is, adapting from the formula found for Section $2l$,

$$
\begin{aligned}
Area(V^+(b_1)) = {} & Area(V^+(b_1) \cap V^\circ(w_{i-l})) + \sum_{j=i-l+1}^{i-1} Area(V^+(b_1) \cap V^\circ(w_j)) \\
& + Area(V^+(b_1) \cap V^\circ(w_i)) + \sum_{j=i+1}^{i+l} Area(V^+(b_1) \cap V^\circ(w_j)) \\
& + Area(V^+(b_1) \cap V^\circ(w_{i+l+1})) \\
= {} & -\frac{x^2}{4} - \frac{3y^2}{4} + (-\frac{lp}{2n} + \frac{q}{2})y + \frac{lpq}{2n} - \frac{(l-1)lp^2}{4n^2} - \Big(\frac{x^2}{8} - \frac{3y^2}{8} - \frac{xy}{4} \\
& + (\frac{q}{4} - \frac{((i+l)-i-1)p}{4n})x + (\frac{((i+l)-i-1)p}{4n} + \frac{q}{4})y - \frac{((i+l)-i-1)pq}{4n} \\
& + \frac{((i+l)-i-1)^2p^2}{8n^2}\Big) + \frac{p}{2n}x - \frac{p}{2n}y + \frac{pq}{2n} - \frac{(4((i+l)-i)-1)p^2}{8n^2} \\
& + \frac{x^2}{8} - \frac{3y^2}{8} - \frac{xy}{4} + (\frac{q}{4} - \frac{((i+l+1)-i-1)p}{4n})x + (\frac{((i+l+1)-i-1)p}{4n} + \frac{q}{4})y \\
& - \frac{((i+l+1)-i-1)pq}{4n} + \frac{((i+l+1)-i-1)^2p^2}{8n^2}
\end{aligned}
$$

$$
\begin{aligned}
&= -\frac{x^2}{4} - \frac{3y^2}{4} + (-\frac{lp}{2n} + \frac{q}{2})y + \frac{lpq}{2n} - \frac{(l-1)lp^2}{4n^2} \\
&\quad - \left(\frac{p}{4n}x - \frac{p}{4n}y + \frac{pq}{4n} + \frac{(-2l+1)p^2}{8n^2}\right) + \frac{p}{2n}x - \frac{p}{2n}y + \frac{pq}{2n} - \frac{(4l-1)p^2}{8n^2} \\
&= -\frac{x^2}{4} - \frac{3y^2}{4} + \frac{p}{4n}x + (-\frac{(2l+1)p}{4n} + \frac{q}{2})y + \frac{(2l+1)pq}{4n} - \frac{l(l+1)p^2}{4n^2}\,.
\end{aligned}
$$

This area has partial derivatives

$$
\begin{aligned}
\frac{\delta A}{\delta x} &= -\frac{x}{2} + \frac{p}{4n} \\
\frac{\delta A}{\delta y} &= -\frac{3y}{2} - \frac{(2l+1)p}{4n} + \frac{q}{2}
\end{aligned}
$$

giving the optimal value $b_1^* = (\frac{p}{2n}, \frac{q}{3} - \frac{(2l+1)p}{6n})$ and $Area(V^+((\frac{p}{2n}, \frac{q}{3} - \frac{(2l+1)p}{6n}))) = \frac{(2l+1)pq}{6n} - \frac{(2l^2+2l-1)p^2}{12n^2} + \frac{q^2}{12}$. For b_1^* to lie within Section $2l$ we must have $l\frac{p}{n} - x^* \leq y^* \leq x^* + l\frac{p}{n}$ so it must be the case that $\frac{(4l-1)p}{n} \leq q \leq \frac{(4l+2)p}{n}$. This is depicted in Figure 5.4e.

If $\frac{(4l+2)p}{n} \leq q$ then the optimum must lie at the intersection of $x = \frac{p}{2n}$ and $y = x + l\frac{p}{n}$ (since $x^* = \frac{p}{2n}$ does not restrict the values of y over Section $2l+1$ and since $\frac{(4l-1)p}{n} \geq q$ the global optimum lies above Section $2l+1$). Therefore the optimum in this section is $b_1^* = (\frac{p}{2n}, \frac{(2l+1)p}{2n})$ achieving $Area(V^+(b_1)) = \frac{(2l+1)pq}{2n} - \frac{(6l^2+6l+1)p^2}{4n^2}$. This is depicted in Figure 5.4d.

Alternatively, if $\frac{(4l-1)p}{n} \geq q$ then the optimum must lie at the intersection of $x = \frac{p}{2n}$ and $y = l\frac{p}{n} - x$ (since $x^* = \frac{p}{2n}$ does not restrict the values of y over Section $2l+1$ and since $\frac{(4l-1)p}{n} \geq q$ the global optimum lies below Section $2l+1$). Therefore the optimum in this section is $b_1^* = (\frac{p}{2n}, \frac{(2l-1)p}{2n})$ achieving $Area(V^+(b_1)) = \frac{lpq}{n} - \frac{(3l-1)lp^2}{2n^2}$. This is depicted in Figure 5.4f.

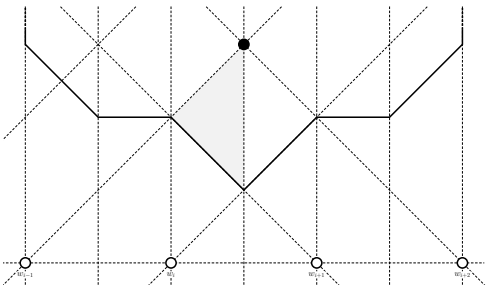

(d) $b_1 = (\frac{p}{2n}, \frac{(2l+1)p}{2n})$ only if $\frac{(4l+2)p}{n} \leq q$.

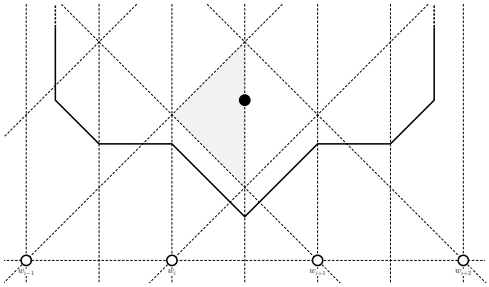

(e) $b_1 = (\frac{p}{2n}, \frac{q}{3} - \frac{(2l+1)p}{6n})$ only if $\frac{(4l-1)p}{n} \leq q \leq \frac{(4l+2)p}{n}$.

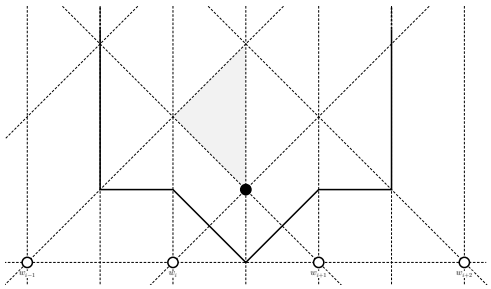

(f) $b_1 = (\frac{p}{2n}, \frac{(2l-1)p}{2n})$ only if $\frac{(4l-1)p}{n} \geq q$.

Figure 5.4: Maximal area Voronoi cells $V^+(b_1)$ for b_1 within Section $2l+1$ not touching the vertical edges of $\mathcal{P}$.

5.2.3 $V^+(b_1)$ touching only the leftmost vertical edge of $\mathcal{P}$

Now the only areas not yet calculated are those that intersect the vertical boundaries of $\mathcal{P}$. Since placing b_1 in Section $2l$ will cause $V^+(b_1)$ to steal from $V^\circ(w_j)$ for $j = i-l, ..., i+l$ and placing b_1 in Section $2l+1$ will cause $V^+(b_1)$ to steal from $V^\circ(w_j)$ for $j = i-l, ..., i+l+1$, $V^+(b_1)$ intersects a vertical boundary of $\mathcal{P}$ if b_1 is in Section $2l$ and $i-l \leq 0$ or $i+l > n$, or if b_1 is in Section $2l+1$ and $i-l \leq 0$ or $i+l+1 > n$. That is, $V^+(b_1)$ will intersect the leftmost boundary of $\mathcal{P}$ if b_1 is placed in Section $2i$ or above, and the rightmost boundary of $\mathcal{P}$ if placed in Section $2(n-i)+1$ or above.

Section $2l$ If $i \leq \frac{n}{2}$ then it can be the case that $V^+(b_1)$ intersects only the leftmost boundary (and not the rightmost boundary) of $\mathcal{P}$. For this, b_1 will have to be contained in Sections $2i$ to $2(n-i)$. In order to compute the area of $V^+(b_1)$ for b_1 within these sections, we can take the area calculated previously for b_1 in Section $2l$ where $V^+(b_1)$ does not touch either vertical edge of $\mathcal{P}$ and remove the extra areas included in the previous calculation which do not exist in the set-up studied here (i.e. the areas entering $V^\circ(w_j)$ for $j < 1$); in calculations presented henceforth, whenever we use a previously formulated area expression and wish to remove an area from the original calculation, we shall display the foreign (or phantom) area A being removed within quotation marks: "A". Thus, if b_1 is in Section $2l$ for $l = i, ..., n-i$ then, for $i > 1$,

$$
\begin{aligned}
Area(V^+(b_1)) &= \sum_{j=1}^{i-1} Area(V^+(b_1) \cap V^\circ(w_j)) + Area(V^+(b_1) \cap V^\circ(w_i)) \\
&\quad + \sum_{j=i+1}^{i+l-1} Area(V^+(b_1) \cap V^\circ(w_j)) + Area(V^+(b_1) \cap V^\circ(w_{i+l})) \\
&= -\frac{x^2}{4} - \frac{3y^2}{4} + (-\frac{lp}{2n} + \frac{q}{2})y + \frac{lpq}{2n} - \frac{(l-1)lp^2}{4n^2} - \text{“}Area(V^+(b_1) \cap V^\circ(w_{i-l}))\text{”} \\
&\quad - \sum_{j=i-l+1}^{0} \text{“}Area(V^+(b_1) \cap V^\circ(w_j))\text{”} \\
&= -\frac{x^2}{4} - \frac{3y^2}{4} + (-\frac{lp}{2n} + \frac{q}{2})y + \frac{lpq}{2n} - \frac{(l-1)lp^2}{4n^2} - \Big(\frac{x^2}{8} - \frac{3y^2}{8} + \frac{xy}{4} \\
&\quad + (\frac{(i-(i-l)-1)p}{4n} - \frac{q}{4})x + (\frac{(i-(i-l)-1)p}{4n} + \frac{q}{4})y \\
&\quad - \frac{(i-(i-l)-1)pq}{4n} + \frac{(i-(i-l)-1)^2p^2}{8n^2}\Big) \\
&\quad - \sum_{j=i-l+1}^{0} (-\frac{p}{2n}x - \frac{p}{2n}y + \frac{pq}{2n} - \frac{(4(i-j)-1)p^2}{8n^2}) \\
&= -\frac{3x^2}{8} - \frac{3y^2}{8} - \frac{xy}{4} - (\frac{(l-1)p}{4n} - \frac{q}{4})x + (-\frac{(3l-1)p}{4n} + \frac{q}{4})y + \frac{(3l-1)pq}{4n} \\
&\quad - \frac{(l-1)(3l-1)p^2}{8n^2} - (-\frac{p}{2n}x - \frac{p}{2n}y + \frac{pq}{2n} + \frac{p^2}{8n^2}) \times (0 - (i-l+1-1)) \\
&\quad + \frac{p^2}{2n^2} \sum_{j=i-l+1}^{0} (i-j) \\
&= -\frac{3x^2}{8} - \frac{3y^2}{8} - \frac{xy}{4} + (\frac{(l-2i+1)p}{4n} + \frac{q}{4})x + (-\frac{(l+2i-1)p}{4n} + \frac{q}{4})y \\
&\quad + \frac{(l+2i-1)pq}{4n} - \frac{(3l^2-3l-i+1)p^2}{8n^2} + \frac{p^2}{2n^2}\frac{(l-1+i)(l-1-(i-1))}{2} \\
&= -\frac{3x^2}{8} - \frac{3y^2}{8} - \frac{xy}{4} + (\frac{(l-2i+1)p}{4n} + \frac{q}{4})x + (-\frac{(l+2i-1)p}{4n} + \frac{q}{4})y \\
&\quad + \frac{(l+2i-1)pq}{4n} - \frac{(l^2-l+1-3i+2i^2)p^2}{8n^2}
\end{aligned}
$$

or, for $i = 1$,

$$\begin{aligned}
Area(V^+(b_1)) &= Area(V^+(b_1) \cap V^\circ(w_1)) + \sum_{j=2}^{l} Area(V^+(b_1) \cap V^\circ(w_j)) + Area(V^+(b_1) \cap V^\circ(w_{l+1})) \\
&= -\frac{x^2}{2} - \frac{p}{2n}y + \frac{pq}{2n} + \sum_{j=2}^{l}(\frac{p}{2n}x - \frac{p}{2n}y + \frac{pq}{2n} - \frac{(4(j-1)-1)p^2}{8n^2}) \\
&\quad + \frac{x^2}{8} - \frac{3y^2}{8} - \frac{xy}{4} + (\frac{q}{4} - \frac{(l-1)p}{4n})x + (\frac{(l-1)p}{4n} + \frac{q}{4})y \\
&\quad - \frac{(l-1)pq}{4n} + \frac{(l-1)^2p^2}{8n^2} \\
&= -\frac{3x^2}{8} - \frac{3y^2}{8} - \frac{xy}{4} + (\frac{q}{4} - \frac{(l-1)p}{4n})x + (\frac{(l-3)p}{4n} + \frac{q}{4})y - \frac{(l-3)pq}{4n} \\
&\quad + \frac{(l-1)^2p^2}{8n^2} + (l-1)(\frac{p}{2n}x - \frac{p}{2n}y + \frac{pq}{2n} + \frac{5p^2}{8n^2}) - \frac{p^2}{2n^2}\sum_{j=2}^{l}(j) \\
&= -\frac{3x^2}{8} - \frac{3y^2}{8} - \frac{xy}{4} + (\frac{q}{4} + \frac{(l-1)p}{4n})x + (-\frac{(l+1)p}{4n} + \frac{q}{4})y + \frac{(l+1)pq}{4n} \\
&\quad - \frac{l(l-1)p^2}{8n^2}
\end{aligned}$$

(identical to the previous area upon a substitution of $i = 1$, so we need only use this former representation).

This area has partial derivatives

$$\begin{aligned}
\frac{\delta A}{\delta x} &= -\frac{3x}{4} - \frac{y}{4} + \frac{(l-2i+1))p}{4n} + \frac{q}{4} \\
\frac{\delta A}{\delta y} &= -\frac{3y}{4} - \frac{x}{4} - \frac{(l+2i-1))p}{4n} + \frac{q}{4} \\
&\Rightarrow -2x^* + \frac{(2l-2i+1)p}{2n} + \frac{q}{2} = 0 \Rightarrow x^* = \frac{(2(l-i)+1)p}{4n} + \frac{q}{4} \\
\text{and } &\Rightarrow 2y^* + \frac{(2l+2i-1)p}{2n} - \frac{q}{2} = 0 \Rightarrow y^* = -\frac{(2(l+i)-1)p}{4n} + \frac{q}{4}
\end{aligned}$$

but $x^* > \frac{p}{2n}$ (since $\frac{p}{4n} < \frac{q}{4}$) so we are required to investigate when b_1 is placed on the boundary of Section $2l$. Note that since the global optimum lies to the right of Section $2l$ we will not find the optimum on the boundary $x = 0$ outside its endpoints.

- Upon boundary $y = x + (l-1)\frac{p}{n}$ we have $Area(V^+((x, x + \frac{(l-1)p}{n}))) = -x^2 + (-\frac{(2(l+i)-3)p}{2n} + \frac{q}{2})x + \frac{(l+i-1)pq}{2n} - \frac{(6l^2+4il+2i^2-11l-7i+6)p^2}{8n^2}$, maximised by $x^* = -\frac{(2(l+i)-3)p}{4n} + \frac{q}{4}$ giving $Area(V^+((-\frac{(2(l+i)-3)p}{4n} + \frac{q}{4}, \frac{(2(l-i)-1)p}{4n} + \frac{q}{4}))) = \frac{(2(l+i)-1)pq}{8n} - \frac{(8l^2-10l-2i+3)p^2}{16n^2} + \frac{q^2}{16}$. However, for $0 \leq -\frac{(2(l+i)-3)p}{4n} + \frac{q}{4} \leq \frac{p}{2n}$ to be true we require $\frac{(2(l+i)-3)p}{n} \leq q \leq \frac{(2(l+i)-1)p}{n}$. If $\frac{(2(l+i)-3)p}{n} \geq q$ then the optimum lies on the endpoint $(0, \frac{(l-1)p}{n})$ giving $Area(V^+((0, \frac{(l-1)p}{n})))$ $= \frac{(l+i-1)pq}{2n} - \frac{(6l^2+4il+2i^2-11l-7i+6)p^2}{8n^2}$, and if $\frac{(2(l+i)-1)p}{n} \leq q$ then the optimum lies on the endpoint $(\frac{p}{2n}, \frac{(2l-1)p}{2n})$ giving $Area(V^+((\frac{p}{2n}, \frac{(2l-1)p}{2n}))) = \frac{(2(l+i)-1)pq}{4n} - \frac{(6l^2+2i^2+4il-7l-3i+2)p^2}{8n^2}$.

- Upon boundary $y = l\frac{p}{n} - x$ we have $Area(V^+((x, \frac{lp}{n} - x))) = -\frac{x^2}{2} + \frac{lp}{n}x + \frac{(2(l+i)-1)pq}{4n} - \frac{(6l^2+2i^2+4il-3l-3i+1)p^2}{8n^2}$, maximised by $x^* = \frac{lp}{2n}$ which is only in Section $2l$ for $l = 1$. So if $l > 1$ the optimum on this boundary will lie on the endpoint $(\frac{p}{2n}, \frac{(2l-1)p}{2n})$ giving $Area(V^+((\frac{p}{2n}, \frac{(2l-1)p}{2n}))) = \frac{(2(l+i)-1)pq}{4n} - \frac{(6l^2+2i^2+4il-7l-3i+2)p^2}{8n^2}$.

Since the optimum over boundary $y = l\frac{p}{n} - x$ is found at the endpoint of the boundary $y = x + (l-1)\frac{p}{n}$, we need only take the results from the latter for the optimal placement over all of Section $2l$. This means that our optimal areas are: if $\frac{(2(l+i)-1)p}{n} \leq q$ then

$Area(V^+((\frac{p}{2n},\frac{(2l-1)p}{2n}))) = \frac{(2(l+i)-1)pq}{4n} - \frac{(6l^2+2i^2+4il-7l-3i+2)p^2}{8n^2}$; if $\frac{(2(l+i)-3)p}{n} \leq q \leq \frac{(2(l+i)-1)p}{n}$ then $Area(V^+((-\frac{(2(l+i)-3)p}{4n}+\frac{q}{4},\frac{(2(l-i)-1)p}{4n}+\frac{q}{4}))) = \frac{(2(l+i)-1)pq}{8n} - \frac{(8l^2-10l-2i+3)p^2}{16n^2} + \frac{q^2}{16}$; and if $\frac{(2(l+i)-3)p}{n} \geq q$ then $Area(V^+((0,\frac{(l-1)p}{n}))) = \frac{(l+i-1)pq}{2n} - \frac{(6l^2+4li+2i^2-11l-7i+6)p^2}{8n^2}$.

Section $2l+1$ Alternatively, if $V^+(b_1)$ hits the leftmost, and not the rightmost, boundary (so $i < \frac{n}{2}$) and b_1 is in Section $2l+1$ for $l = i, ..., n-i-1$ then, for $i > 1$,

$$\begin{aligned}
Area(V^+(b_1)) &= \sum_{j=1}^{i-1} Area(V^+(b_1)\cap V^\circ(w_j)) + Area(V^+(b_1)\cap V^\circ(w_i)) \\
&\quad + \sum_{j=i+1}^{i+l} Area(V^+(b_1)\cap V^\circ(w_j)) + Area(V^+(b_1)\cap V^\circ(w_{i+l+1})) \\
&= -\frac{3x^2}{8} - \frac{3y^2}{8} - \frac{xy}{4} + (\frac{(l-2i+1))p}{4n} + \frac{q}{4})x + (-\frac{(l+2i-1))p}{4n} + \frac{q}{4})y \\
&\quad + \frac{(l+2i-1)pq}{4n} - \frac{(l^2-l+1-3i+2i^2)p^2}{8n^2} - \Big(\frac{x^2}{8} - \frac{3y^2}{8} - \frac{xy}{4} \\
&\quad + (\frac{q}{4} - \frac{((i+l)-i-1)p}{4n})x + (\frac{((i+l)-i-1)p}{4n} + \frac{q}{4})y - \frac{((i+l)-i-1)pq}{4n} \\
&\quad + \frac{((i+l)-i-1)^2p^2}{8n^2}\Big) + \frac{p}{2n}x - \frac{p}{2n}y + \frac{pq}{2n} - \frac{(4((i+l)-i)-1)p^2}{8n^2} \\
&\quad + \frac{x^2}{8} - \frac{3y^2}{8} - \frac{xy}{4} + (\frac{q}{4} - \frac{((i+l+1)-i-1)p}{4n})x + (\frac{((i+l+1)-i-1)p}{4n} + \frac{q}{4})y \\
&\quad - \frac{((i+l+1)-i-1)pq}{4n} + \frac{((i+l+1)-i-1)^2p^2}{8n^2} \\
&= -\frac{3x^2}{8} - \frac{3y^2}{8} - \frac{xy}{4} + (\frac{(l-2i+1))p}{4n} + \frac{q}{4})x + (-\frac{(l+2i-1))p}{4n} + \frac{q}{4})y \\
&\quad + \frac{(l+2i-1)pq}{4n} - \frac{(l^2-l+1-3i+2i^2)p^2}{8n^2} - \frac{(l-1)^2p^2}{8n^2} + \frac{l^2p^2}{8n^2} \\
&\quad + \frac{p}{4n}x - \frac{p}{4n}y + \frac{pq}{4n} - \frac{(4l-1)p^2}{8n^2} \\
&= -\frac{3x^2}{8} - \frac{3y^2}{8} - \frac{xy}{4} + (\frac{(l-2i+2)p}{4n} + \frac{q}{4})x + (-\frac{(l+2i)p}{4n} + \frac{q}{4})y \\
&\quad + \frac{(l+2i)pq}{4n} - \frac{(l^2+l+2i^2-3i+1)p^2}{8n^2}
\end{aligned}$$

or, for $i = 1$,

$$\begin{aligned}
Area(V^+(b_1)) &= Area(V^+(b_1)\cap V^\circ(w_i)) + \sum_{j=2}^{l+1} Area(V^+(b_1)\cap V^\circ(w_j)) + Area(V^+(b_1)\cap V^\circ(w_{l+2})) \\
&= -\frac{3x^2}{8} - \frac{3y^2}{8} - \frac{xy}{4} + (\frac{q}{4} + \frac{(l-1)p}{4n})x + (-\frac{(l+1)p}{4n} + \frac{q}{4})y + \frac{(l+1)pq}{4n} \\
&\quad - \frac{l(l-1)p^2}{8n^2} + (\frac{p}{2n}x - \frac{p}{2n}y + \frac{pq}{2n} - \frac{(4l-1)p^2}{8n^2}) \\
&\quad + \frac{x^2}{8} - \frac{3y^2}{8} - \frac{xy}{4} + (\frac{q}{4} - \frac{lp}{4n})x + (\frac{lp}{4n} + \frac{q}{4})y - \frac{lpq}{4n} + \frac{l^2p^2}{8n^2} \\
&\quad - (\frac{x^2}{8} - \frac{3y^2}{8} - \frac{xy}{4} + (\frac{q}{4} - \frac{(l-1)p}{4n})x + (\frac{(l-1)p}{4n} + \frac{q}{4})y - \frac{(l-1)pq}{4n} + \frac{(l-1)^2p^2}{8n^2}) \\
&= -\frac{3x^2}{8} - \frac{3y^2}{8} - \frac{xy}{4} + (\frac{lp}{4n} + \frac{q}{4})x + (-\frac{(l+2)p}{4n} + \frac{q}{4})y + \frac{(l+2)pq}{4n} \\
&\quad - \frac{l(l+1)p^2}{8n^2}
\end{aligned}$$

(which, again, we check is identical to the representation found for $i > 1$ so we shall proceed to use the former formulation).

This area has partial derivatives

$$\begin{aligned}
\frac{\delta A}{\delta x} &= -\frac{3x}{4} - \frac{y}{4} + \frac{(l-2i+2)p}{4n} + \frac{q}{4} \\
\frac{\delta A}{\delta y} &= -\frac{3y}{4} - \frac{x}{4} - \frac{(l+2i)p}{4n} + \frac{q}{4} \\
&\Rightarrow -2x^* + \frac{(2(l-i)+3)p}{2n} + \frac{q}{2} = 0 \Rightarrow x^* = \frac{(2(l-i)+3)p}{4n} + \frac{q}{4} \\
\textit{and} \Rightarrow -2y^* &- \frac{(2l+2i+1)p}{2n} + \frac{q}{2} = 0 \Rightarrow y^* = -\frac{(2(l+i)+1)p}{4n} + \frac{q}{4}\,.
\end{aligned}$$

Using identical logic to that in Section $2l$, $x^* > \frac{p}{2n}$ so we explore the boundaries (all boundaries this time).

- Upon boundary $x = \frac{p}{2n}$ we have $Area(V^+((\frac{p}{2n}, y))) = -\frac{3y^2}{8} + (-\frac{(2l+4i+1)p}{8n} + \frac{q}{4})y + \frac{(2l+4i+1)pq}{8n} - \frac{(4l^2+8i^2-4i-1)p^2}{32n^2}$, maximised by $y^* = -\frac{(2l+4i+1)p}{6n} + \frac{q}{3}$ giving $Area(V^+((\frac{p}{2n}, -\frac{(2l+4i+1)p}{6n} + \frac{q}{3}))) = \frac{(2l+4i+1)pq}{12n} + \frac{(-2l^2-2i^2+4il+l+5i+1)p^2}{24n^2} + \frac{q^2}{24}$. However, for $\frac{(2l-1)p}{2n} \leq y^* \leq \frac{(2l+1)p}{2n}$ we require $\frac{(4(l+i)-5)p}{2n} \leq q \leq \frac{(8l+4i+7)p}{2n}$. If $\frac{(4(l+i)-5)p}{2n} \geq q$ then the optimum lies on the endpoint $(\frac{p}{2n}, \frac{(2l-1)p}{2n})$ giving $Area(V^+((\frac{p}{2n}, \frac{(2l-1)p}{2n}))) = \frac{(l+i)pq}{2n} - \frac{(6l^2+2i^2+4il-3l-3i)p^2}{8n^2}$, and if $\frac{(8l+4i+7)p}{2n} \leq q$ then the optimum lies on the endpoint $(\frac{p}{2n}, \frac{(2l+1)p}{2n})$ giving $Area(V^+((\frac{p}{2n}, \frac{(2l+1)p}{2n}))) = \frac{(2(l+i)+1)pq}{4n} - \frac{(6l^2+2i^2+4il+5l+i+1)p^2}{8n^2}$.

- Upon boundary $y = \frac{lp}{n} - x$ we have $Area(V^+((x, \frac{lp}{n} - x))) = -\frac{x^2}{2} + \frac{(2l+1)p}{2n}x + \frac{(l+i)pq}{2n} - \frac{(6l^2+2i^2+4il-3i+l+1)p^2}{8n^2}$, maximised by $x^* = \frac{(2l+1)p}{2n} > \frac{p}{2n}$, so the optimum is achieved at $x = \frac{p}{2n}$, the value of which has been found above.

- Upon boundary $y = x + \frac{lp}{n}$ we have $Area(V^+((x, x + \frac{lp}{n}))) = -x^2 + (-\frac{(2(l+i)-1)p}{2n} + \frac{q}{2})x + \frac{(l+i)pq}{2n} - \frac{(6l^2+2i^2+4il+l-3i+1)p^2}{8n^2}$, maximised by $x^* = -\frac{(2(l+i)-1)p}{4n} + \frac{q}{4}$ giving $Area(V^+((-\frac{(2(l+i)-1)p}{4n} + \frac{q}{4}, \frac{(2(l-i)+1)p}{4n} + \frac{q}{4}))) = \frac{(2l+2i+1)pq}{8n} - \frac{(8l^2+6l-2i+1))p^2}{16n^2} + \frac{q^2}{16}$. However, for $0 \leq x^* \leq \frac{p}{2n}$ we require $\frac{(2(l+i)-1)p}{n} \leq q \leq \frac{(2(l+i)+1)p}{n}$. If $\frac{(2(l+i)-1)p}{n} \geq q$ then the optimum lies on the endpoint $(0, \frac{lp}{n})$: this lies on the boundary $y = \frac{lp}{n} - x$ upon which it was found never to be optimal. Alternatively, if $\frac{(2(l+i)+1)p}{n} \leq q$ then the optimum lies on the endpoint $(\frac{p}{2n}, \frac{(2l+1)p}{2n})$ upon the boundary $x = \frac{p}{2n}$ for which all optimal values have been found.

Following this it is clear that, from the exploration of the boundaries $y = x + \frac{lp}{n}$ and $y = \frac{lp}{n} - x$, if $\frac{(2(l+i)+1)p}{n} \leq q$ or $\frac{(2(l+i)-1)p}{n} \geq q$ then the optimum lies on the boundary $x = \frac{p}{2n}$. What remains to be seen is whether it is optimal to place on the boundary $y = x + \frac{lp}{n}$ or $x = \frac{p}{2n}$ when $\frac{(2(l+i)-1)p}{n} \leq q \leq \frac{(2(l+i)+1)p}{n}$, so we are required to compare the optimal values found within boundaries $x = \frac{p}{2n}$ and $y = x + \frac{lp}{n}$ (so not the endpoints). Firstly, if $\frac{(2(l+i)-1)p}{n} \leq q \leq \frac{(2(l+i)+1)p}{n}$ then

$$\begin{aligned}
\frac{(4(l+i)-5)p}{2n} &= \frac{(2(l+i)-2.5)p}{n} \\
&< \frac{(2(l+i)-1)p}{n} \leq q \leq \frac{(2(l+i)+1)p}{n} \\
&< \frac{(2(l+i)+2l+3.5)p}{n} = \frac{(8l+4i+7)p}{2n}
\end{aligned}$$

so the optimum upon $x = \frac{p}{2n}$ for these values of p and q is within the boundary (not an endpoint).

Therefore we must check

$$\begin{aligned}
&\frac{(2l+4i+1)pq}{12n} + \frac{(-2l^2-2i^2+4il+l+5i+1)p^2}{24n^2} + \frac{q^2}{24} \\
&\qquad - \left(\frac{(2l+2i+1)pq}{8n} - \frac{(8l^2+6l-2i+1))p^2}{16n^2} + \frac{q^2}{16} \right) \\
&= \frac{(-2l+2i-1)pq}{24n} + \frac{(20l^2-4i^2+8il+20l+4i+5)p^2}{48n^2} - \frac{q^2}{48} \\
&= \frac{1}{48} \left(\frac{(20l^2-4i^2+8il+20l+4i+5)p^2}{n^2} - \frac{(4(l-i)+2)pq}{n} - q^2 \right) \\
&\geq \frac{p^2}{48n^2}((20l^2-4i^2+8il+20l+4i+5) - (4(l-i)+2)(2(l+i)+1) - (2(l+i)+1)^2) \\
&= \frac{p^2}{48n^2}(8l^2+8l+2) > 0\,.
\end{aligned}$$

This settles all concerns and proves that the optimum is always located on the boundary $x = \frac{p}{2n}$. This means that our optimal areas are: if $\frac{(8l+4i+7)p}{2n} \leq q$ then $Area(V^+((\frac{p}{2n}, \frac{(2l+1)p}{2n}))) = \frac{(2(l+i)+1)pq}{4n} - \frac{(6l^2+2i^2+4il+5l+i+1)p^2}{8n^2}$ as depicted in Figure 5.4g; if $\frac{(4(l+i)-5)p}{2n} \leq q \leq \frac{(8l+4i+7)p}{2n}$ then $Area(V^+((\frac{p}{2n}, -\frac{(2l+4i+1)p}{6n} + \frac{q}{3}))) = \frac{(2l+4i+1)pq}{12n} + \frac{(-2l^2-2i^2+4il+l+5i+1)p^2}{24n^2} + \frac{q^2}{24}$ as depicted in Figure 5.4h; and if $\frac{(4(l+i)-5)p}{2n} \geq q$ then $Area(V^+((\frac{p}{2n}, \frac{(2l-1)p}{2n}))) = \frac{(l+i)pq}{2n} - \frac{(6l^2+2i^2+4il-3l-3i)p^2}{8n^2}$ as depicted in Figure 5.4i.

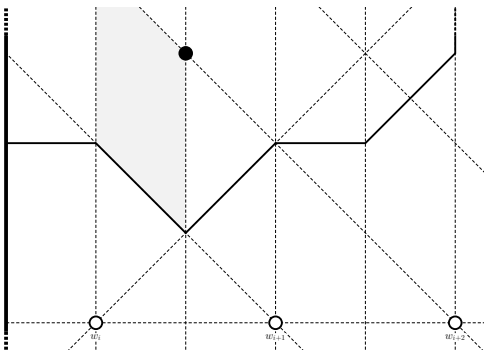

(g) $b_1 = (\frac{p}{2n}, \frac{(2l+1)p}{2n})$ only if $\frac{(8l+4i+7)p}{2n} \leq q$.

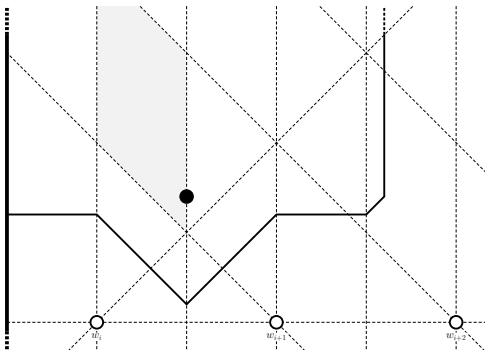

(h) $b_1 = (\frac{p}{2n}, -\frac{(2l+4i+1)p}{6n} + \frac{q}{3})$ only if $\frac{(4(l+i)-5)p}{2n} \leq q \leq \frac{(8l+4i+7)p}{2n}$.

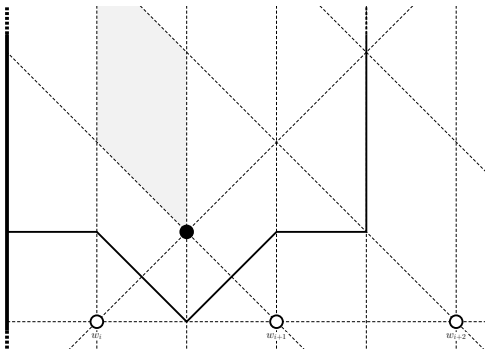

(i) $b_1 = (\frac{p}{2n}, \frac{(2l-1)p}{2n})$ only if $\frac{(4(l+i)-5)p}{2n} \geq q$.

Figure 5.4: Maximal area Voronoi cells $V^+(b_1)$ for b_1 within Section $2l+1$ touching the leftmost vertical edge of $\mathcal{P}$.

It is interesting to note that the structures of $V^+(b_1)$ for b_1 in Section $2l+1$ and $2(l+1)$ are identical, owing to the fact that the partitioning line $\mathcal{CC}^1(w_{i-l})$ which would normally divide the two does not exist, simply because w_{i-l} does not exist for $l \geq i$ (which our values of l satisfy).

We can verify that the areas already found are in fact identical for these two sections. We will use this idea to greatly simplify our work in the following subsection.

However, before we do, let us compare the optimal locations of b_1 found in Section $2l+1$ and Section $2(l+1)$. In both of our calculations, the optimum was never found to be within the sections themselves so the boundary cases had to be explored. The optimum over Section $2(l+1)$ was found to be on the boundary $y = x + \frac{lp}{n}$, which is shared with Section $2l+1$, whilst the optimum over Section $2l+1$ was found to be on the boundary $x = \frac{p}{2n}$. Therefore the optimum over Section $2l+1$ and $2(l+1)$ is found on the $x = \frac{p}{2n}$ boundary, as described in the Section $2l+1$ workings.

It is important to note that this comparison is between Sections $2l+1$ and $2(l+1)$ for $l = i, ..., n-i-1$, so for Section $2l$ where $l = i$ (the lowest possible value of l) there does not exist a Section $2l-1$ within which the Voronoi cell $V^+(b_1)$ touches the leftmost boundary of $\mathcal{P}$, so we must remember to use the Section $2l$ results for Section $2i$, as depicted in Figures 5.4j, 5.4k, and 5.4l.

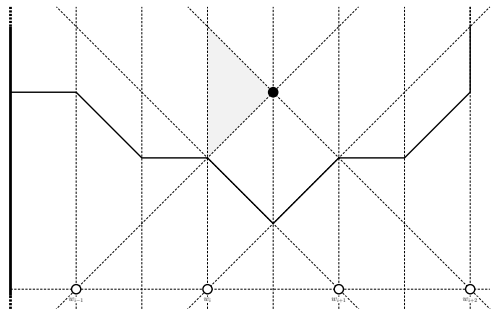

(j) $b_1 = (\frac{p}{2n}, \frac{(2i-1)p}{2n})$ only if $\frac{(2(i+i)-1)p}{n} \leq q$.

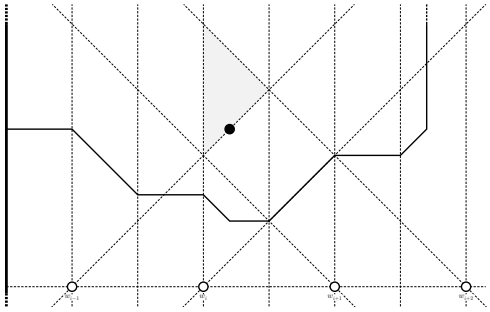

(k) $b_1 = (-\frac{(4i-3)p}{4n} + \frac{q}{4}, -\frac{p}{4n} + \frac{q}{4})$ only if $\frac{(4i-3)p}{n} \leq q \leq \frac{(4i-1)p}{n}$.

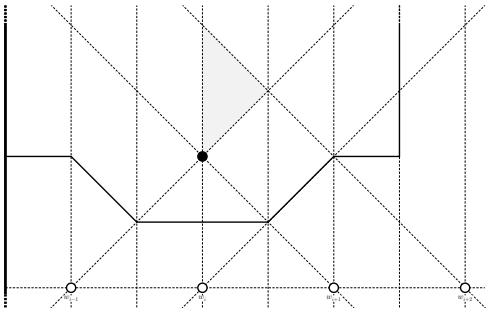

(l) $b_1 = (0, \frac{(i-1)p}{n})$ only if $\frac{(4i-3)p}{n} \geq q$.

Figure 5.4: Maximal area Voronoi cells $V^+(b_1)$ for b_1 within Section $2i$ touching the leftmost vertical edge of $\mathcal{P}$.

5.2.4 $V^+(b_1)$ touching only the rightmost vertical edge of $\mathcal{P}$

Naturally the next avenue to explore is that of points b_1 which intersect the rightmost and not the leftmost boundary of $\mathcal{P}$. If $i > \frac{n}{2}$ then it can be the case that $V^+(b_1)$ intersects only the rightmost boundary (and not the leftmost boundary) of $\mathcal{P}$. For this, b_1 will have to be contained in Sections $2(n-i)+1$ to $2i-1$ (for $n-i > 0$ and note that if b_1 is in an even section then we require $i > \frac{n}{2}$, otherwise we require $i \geq \frac{n}{2}$). For these sections, as described above for the case on intersecting the leftmost vertical edge of $\mathcal{P}$, the partitioning lines between Sections $2l$ and $2l+1$ no longer exist; they would be $\mathcal{CC}^3(w_{i+l})$ but w_{i+l} does not exist. Therefore $V^+(b_1)$ takes the same form for b_1 in Sections $2l$ and $2l+1$ and we can explore them together. However, we must still check the first section (Section $2(n-i)+1$), for which (as described for Section $2i$ for $V^+(b_1)$ touching the leftmost vertical edge of $\mathcal{P}$) there is no Section $2l$ with which it can be paired.

If b_1 is in Section $2(n-i)+1$ (so $2l+1$ where $l=n-i$) or in Section $2l$ or Section $2l+1$ for $l=n-i+1,...,i-1$ then, making use of our calculations for $V^+(b_1)$ not touching either vertical boundary of $\mathcal{P}$, for $i<n$,

$$\begin{aligned}
Area(V^+(b_1)) &= Area(V^+(b_1)\cap V^\circ(w_{i-l})) + \sum_{j=i-l+1}^{i-1} Area(V^+(b_1)\cap V^\circ(w_j)) \\
&\quad + Area(V^+(b_1)\cap V^\circ(w_i)) + \sum_{j=i+1}^{n} Area(V^+(b_1)\cap V^\circ(w_j)) + Area(V^+(b_1)\cap V^\circ(w_{i+l})) \\
&= -\frac{x^2}{4} - \frac{3y^2}{4} + (-\frac{lp}{2n}+\frac{q}{2})y + \frac{lpq}{2n} - \frac{(l-1)lp^2}{4n^2} - \sum_{j=n+1}^{i+l-1} \text{“}Area(V^+(b_1)\cap V^\circ(w_j))\text{”} \\
&\quad - \text{“}Area(V^+(b_1)\cap V^\circ(w_{i+l}))\text{”} \\
&= -\frac{x^2}{4} - \frac{3y^2}{4} + (-\frac{lp}{2n}+\frac{q}{2})y + \frac{lpq}{2n} - \frac{(l-1)lp^2}{4n^2} - \sum_{j=n+1}^{i+l-1} (\frac{p}{2n}x - \frac{p}{2n}y + \frac{pq}{2n} - \frac{(4(j-i)-1)p^2}{8n^2}) \\
&\quad - (\frac{x^2}{8} - \frac{3y^2}{8} - \frac{xy}{4} + (\frac{q}{4} - \frac{((i+l)-i-1)p}{4n})x + (\frac{((i+l)-i-1)p}{4n} + \frac{q}{4})y \\
&\quad - \frac{((i+l)-i-1)pq}{4n} + \frac{((i+l)-i-1)^2p^2}{8n^2}) \\
&= -\frac{3x^2}{8} - \frac{3y^2}{8} + \frac{xy}{4} + (\frac{(l-1)p}{4n} - \frac{q}{4})x + (-\frac{(3l-1)p}{4n} + \frac{q}{4})y \\
&\quad + \frac{(3l-1)pq}{4n} - \frac{(3l-1)(l-1)p^2}{8n^2} - (i+l-1-n)(\frac{p}{2n}x - \frac{p}{2n}y + \frac{pq}{2n} + \frac{p^2}{8n^2}) \\
&\quad + \frac{p^2}{2n^2}\sum_{j=n+1}^{i+l-1}(j-i) \\
&= -\frac{3x^2}{8} - \frac{3y^2}{8} + \frac{xy}{4} - (\frac{(l-2n+2i-1)p}{4n} + \frac{q}{4})x + (-\frac{(l+2n-2i+1)p}{4n} + \frac{q}{4})y \\
&\quad + \frac{(l+2n-2i+1)pq}{4n} - \frac{(l^2-l+2n^2+n-4in+2i^2-i)p^2}{8n^2}
\end{aligned}$$

or, for $i=n$,

$$\begin{aligned}
Area(V^+(b_1)) &= Area(V^+(b_1)\cap V^\circ(w_{n-l})) + \sum_{j=n-l+1}^{n-1} Area(V^+(b_1)\cap V^\circ(w_j)) \\
&\quad + Area(V^+(b_1)\cap V^\circ(w_n)) \\
&= \frac{x^2}{8} - \frac{3y^2}{8} + \frac{xy}{4} + (\frac{(n-(n-l)-1)p}{4n} - \frac{q}{4})x + (\frac{(n-(n-l)-1)p}{4n} + \frac{q}{4})y \\
&\quad - \frac{(n-(n-l)-1)pq}{4n} + \frac{(n-(n-l)-1)^2p^2}{8n^2} \\
&\quad + \sum_{j=n-l+1}^{n-1}(-\frac{p}{2n}x - \frac{p}{2n}y + \frac{pq}{2n} - \frac{(4(n-j)-1)p^2}{8n^2}) - \frac{x^2}{2} - \frac{p}{2n}y + \frac{pq}{2n} \\
&= -\frac{3x^2}{8} - \frac{3y^2}{8} + \frac{xy}{4} + (\frac{(l-1)p}{4n} - \frac{q}{4})x + (\frac{(l-3)p}{4n} + \frac{q}{4})y - \frac{(l-3)pq}{4n} + \frac{(l-1)^2p^2}{8n^2} \\
&\quad + (n-1-(n-l))(-\frac{p}{2n}x - \frac{p}{2n}y + \frac{pq}{2n} + \frac{p^2}{8n^2}) - \frac{p^2}{2n^2}\sum_{j=n-l+1}^{n-1}(n-j) \\
&= -\frac{3x^2}{8} - \frac{3y^2}{8} + \frac{xy}{4} - (\frac{(l-1)p}{4n} + \frac{q}{4})x + (-\frac{(l+1)p}{4n} + \frac{q}{4})y + \frac{(l+1)pq}{4n} - \frac{(l-1)lp^2}{8n^2}\,.
\end{aligned}$$

As before, this is identical to the representation found by substituting $i=n$ into the previous area formula, so it is this former formula that we use for our studies.

The area has partial derivatives

$$\frac{\delta A}{\delta x} = -\frac{3x}{4} + \frac{y}{4} - \frac{(l-2n+2i-1)p}{4n} - \frac{q}{4}$$
$$\frac{\delta A}{\delta y} = -\frac{3y}{4} + \frac{x}{4} - \frac{(l+2n-2i+1)p}{4n} + \frac{q}{4}$$
$$\Rightarrow -2x^* - \frac{(2l-2n+2i-1)p}{2n} - \frac{q}{2} = 0 \Rightarrow x^* = -\frac{(2l-2(n-i)-1)p}{4n} - \frac{q}{4}$$
$$\text{and } \Rightarrow -2y^* - \frac{(2l+2n-2i+1)p}{2n} + \frac{q}{2} = 0 \Rightarrow y^* = -\frac{(2l+2(n-i)+1)p}{4n} + \frac{q}{4}$$

but $x^* = \frac{(2(n-i-l)+1)p}{4n} - \frac{q}{4} \leq \frac{1}{4}(\frac{p}{n} - q) < 0$ so we are required to investigate when b_1 is placed on the boundaries of its respective section – noting that the optimum will never lie on a non-endpoint of $x = \frac{p}{2n}$ because $x^* < 0$.

Within Section $2(n-i)+1$, for which $Area(V^+(b_1)) = -\frac{3x^2}{8} - \frac{3y^2}{8} + \frac{xy}{4} + (\frac{(n-i+1)p}{4n} - \frac{q}{4})x + (-\frac{(3(n-i)+1)p}{4n} + \frac{q}{4})y + \frac{(3(n-i)+1)pq}{4n} - \frac{3(n-i)^2p^2}{8n^2}$, we produce the following calculations.

- Upon boundary $y = \frac{(n-i)p}{n} - x$ we have $Area(V^+((x, \frac{(n-i)p}{n} - x))) = -x^2 + (\frac{(4(n-i)+1)p}{2n} - \frac{q}{2})x + \frac{(4(n-i)+1)pq}{4n} - \frac{(6(n-i)^2+(n-i))p^2}{4n^2}$, maximised by $x^* = \frac{(4(n-i)+1)p}{4n} - \frac{q}{4}$ giving $Area(V^+(\frac{(4(n-i)+1)p}{4n} - \frac{q}{4}, -\frac{p}{4n} + \frac{q}{4}))) = \frac{(4(n-i)+1)pq}{8n} - \frac{(8(n-i)^2-4(n-i)-1)p^2}{16n^2} + \frac{q^2}{16}$. However, for $0 \leq \frac{(4(n-i)+1)p}{4n} - \frac{q}{4} \leq \frac{p}{2n}$ to be true we require $\frac{(4(n-i)-1)p}{n} \leq q \leq \frac{(4(n-i)+1)p}{n}$. If $q \leq \frac{(4(n-i)-1)p}{n}$ then the optimum lies on the endpoint $(\frac{p}{2n}, \frac{(2(n-i)-1)p}{2n})$ giving $Area(V^+((\frac{p}{2n}, \frac{(2(n-i)-1)p}{2n})))$ $= \frac{(n-i)pq}{n} - \frac{(6(n-i)^2-3(n-i))p^2}{4n^2}$. If $\frac{(4(n-i)+1)p}{n} \leq q$ then the optimum lies on the endpoint $(0, \frac{(n-i)p}{n})$ giving $Area(V^+((0, \frac{(n-i)p}{n}))) = \frac{(4(n-i)+1)pq}{4n} - \frac{(6(n-i)^2+(n-i))p^2}{4n^2}$.
- Upon boundary $y = x + \frac{(n-i)p}{n}$ we have $Area(V^+((x, x + \frac{(n-i)p}{n}))) = -\frac{x^2}{2} - \frac{(n-i)p}{n}x + \frac{(4(n-i)+1)pq}{4n} - \frac{(6(n-i)^2+n-i)p^2}{4n^2}$, maximised by $x^* = -\frac{(n-i)p}{n} < 0$ so the optimum is achieved at $x = 0$, the value of which has been found above.

Thus the optimum lies on the boundary $y = \frac{(n-i)p}{n} - x$ with maximal areas $Area(V^+((0, \frac{(n-i)p}{n}))) = \frac{(4(n-i)+1)pq}{4n} - \frac{(6(n-i)^2+(n-i))p^2}{4n^2}$ if $\frac{(4(n-i)+1)p}{n} \leq q$ as depicted in Figure 5.4m, $Area(V^+((\frac{(4(n-i)+1)p}{4n} - \frac{q}{4}, -\frac{p}{4n} + \frac{q}{4}))) = \frac{(4(n-i)+1)pq}{8n} - \frac{(8(n-i)^2-4(n-i)-1)p^2}{16n^2} + \frac{q^2}{16}$ if $\frac{(4(n-i)-1)p}{n} \leq q \leq \frac{(4(n-i)+1)p}{n}$ as depicted in Figure 5.4n, and $Area(V^+((\frac{p}{2n}, \frac{(2(n-i)-1)p}{2n}))) = \frac{(n-i)pq}{n} - \frac{(6(n-i)^2-3(n-i))p^2}{4n^2}$ if $q \leq \frac{(4(n-i)-1)p}{n}$ as depicted in Figure 5.4o.

Alternatively, consider placing on the boundary of Section $2l$ and Section $2l+1$ (i.e. upon the boundaries $x = 0$, $y = x + \frac{(l-1)p}{n}$, $x = \frac{p}{2n}$, and $y = x + \frac{lp}{n}$).

- Upon boundary $x = 0$ we have $Area(V^+((0, y))) = -\frac{3y^2}{8} + (-\frac{(l+2n-2i+1)p}{4n} + \frac{q}{4})y + \frac{(l+2n-2i+1)pq}{4n} - \frac{(l^2-l+2n^2+n-4in+2i^2-i)p^2}{8n^2}$, maximised by $y^* = -\frac{(l+2n-2i+1)p}{3n} + \frac{q}{3}$ giving $Area(V^+(0, -\frac{(l+2n-2i+1)p}{3n} + \frac{q}{3})) = \frac{(l+2n-2i+1)pq}{6n} - \frac{(2(l-(n-i))^2-5l-(n-i)-1)p^2}{24n^2} + \frac{q^2}{24}$. However, for $\frac{(l-1)p}{n} \leq -\frac{(l+2n-2i+1)p}{3n} + \frac{q}{3} \leq \frac{lp}{n}$ to be true we require $\frac{(4l+2(n-i)-2)p}{n} \leq q \leq \frac{(4l+2(n-i)+1)p}{n}$. If $\frac{(4l+2(n-i)-2)p}{n} \geq q$ then the optimum lies on the endpoint $(0, \frac{(l-1)p}{n})$ giving $Area(V^+((0, \frac{(l-1)p}{n}))) = \frac{(l+n-i)pq}{2n} - \frac{(6l^2+4l(n-i)+2(n-i)^2-7l-3(n-i)+1)p^2}{4n^2}$, and if $\frac{(4l+2(n-i)+1)p}{n} \leq q$ then $Area(V^+((0, \frac{lp}{n}))) = \frac{(2l+2(n-i)+1)pq}{4n} - \frac{(6l^2+4l(n-i)+2(n-i)^2+l+(n-i))p^2}{8n^2}$.
- Upon boundary $y = x + (l-1)\frac{p}{n}$ we have $Area(V^+((x, x + \frac{(l-1)p}{n}))) = -\frac{x^2}{2} - \frac{(2l-1)p}{2n}x + \frac{(l+n-i)pq}{2n} - \frac{(6l^2+4l(n-i)+2(n-i)^2-7l-3(n-i)+1)p^2}{8n^2}$, maximised by $x^* = -\frac{(2l-1)p}{2n} < 0$ so the optimum is achieved at $x = 0$, the value of which has been found above.
- Upon boundary $y = x + l\frac{p}{n}$ we have $Area(V^+((x, x + \frac{lp}{n}))) = -\frac{x^2}{2} - \frac{lp}{n}x + \frac{(2l+2(n-i)+1)pq}{4n} - \frac{(6l^2+4l(n-i)+2(n-i)^2+l+n-i)p^2}{8n^2}$, maximised by $x^* = -\frac{lp}{n} < 0$ so the optimum is achieved at $x = 0$, the value of which has been found above.

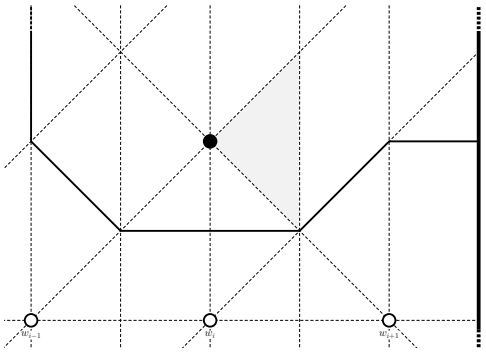

(m) $b_1 = (0, \frac{(n-i)p}{n})$ only if $\frac{(4(n-i)+1)p}{n} \leq q$.

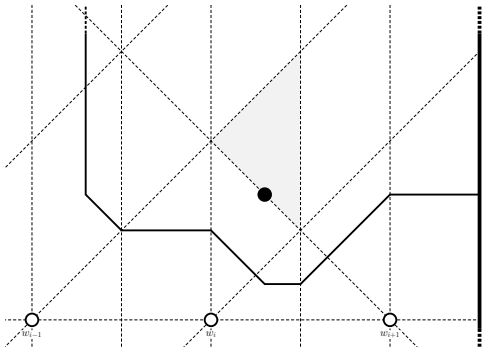

(n) $b_1 = (\frac{(4(n-i)+1)p}{4n} - \frac{q}{4}, -\frac{p}{4n} + \frac{q}{4})$ only if $\frac{(4(n-i)-1)p}{n} \leq q \leq \frac{(4(n-i)+1)p}{n}$.

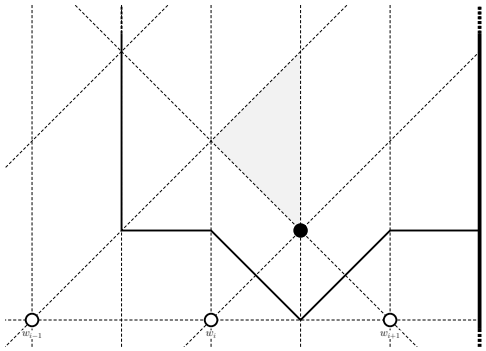

(o) $b_1 = (\frac{p}{2n}, \frac{(2(n-i)-1)p}{2n})$ only if $\frac{(4(n-i)-1)p}{n} \geq q$.

Figure 5.4: Maximal area Voronoi cells $V^+(b_1)$ for b_1 within Section $2(n-i)+1$ touching the rightmost vertical edge of $\mathcal{P}$.

Thus the optimum lies on the boundary $x = 0$, with maximal areas $Area(V^+((0, \frac{lp}{n}))) = \frac{(2l+2(n-i)+1)pq}{4n} - \frac{(6l^2+4l(n-i)+2(n-i)^2+l+(n-i))p^2}{8n^2}$ if $\frac{(4l+2(n-i)+1)p}{n} \leq q$ as depicted in Figure 5.4p, $Area(V^+(0, -\frac{(l+2n-2i+1)p}{3n}+\frac{q}{3})) = \frac{(l+2n-2i+1)pq}{6n} - \frac{(2(l-(n-i))^2-5l-(n-i)-1)p^2}{24n^2}+\frac{q^2}{24}$ if $\frac{(4l+2(n-i)-2)p}{n} \leq q \leq \frac{(4l+2(n-i)+1)p}{n}$ as depicted in Figure 5.4q, and $Area(V^+((0, \frac{(l-1)p}{n}))) = \frac{(l+n-i)pq}{2n} - \frac{(6l^2+4l(n-i)+2(n-i)^2-7l-3(n-i)+1)p^2}{4n^2}$ if $\frac{(4l+2(n-i)-2)p}{n} \geq q$ as depicted in Figure 5.4r.

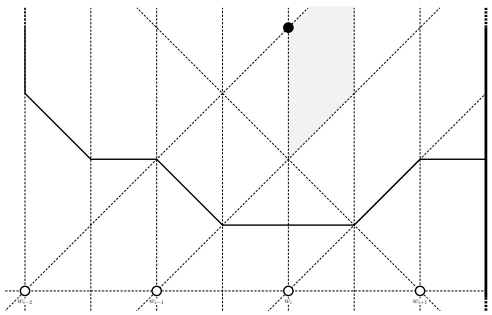

(p) $b_1 = (0, \frac{lp}{n})$ only if $\frac{(4l+2(n-i)+1)p}{n} \leq q$.

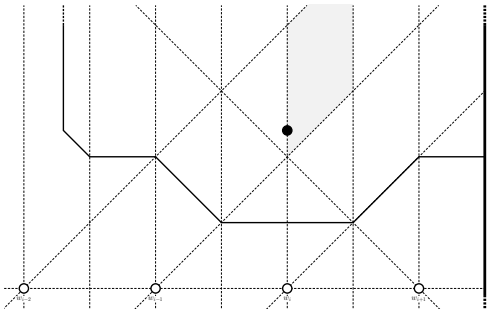

(q) $b_1 = (0, -\frac{(l+2n-2i+1)p}{3n} + \frac{q}{3})$ only if $\frac{(4l+2(n-i)-2)p}{n} \leq q \leq \frac{(4l+2(n-i)+1)p}{n}$.

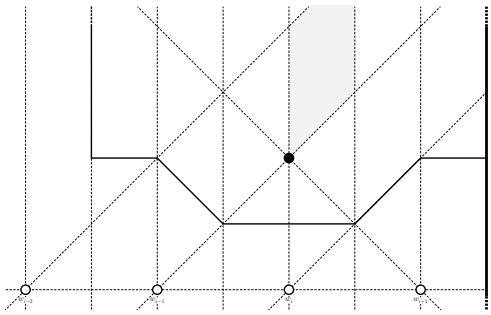

(r) $b_1 = (0, \frac{(l-1)p}{n})$ only if $\frac{(4l+2(n-i)-2)p}{n} \geq q$.

Figure 5.4: Maximal area Voronoi cells $V^+(b_1)$ for b_1 within Section $2l$ touching the rightmost vertical edge of $\mathcal{P}$.

We should note here that Section I also applies in this case of intersecting the right boundary and not the left boundary of $\mathcal{P}$, though it is plain to see that the optimum for this scenario will lie as close as possible to $(0, 0)$ and give an area up to (but not achieving) $\frac{pq}{2n}$.

5.2.5 $V^+(b_1)$ touching both vertical edges of $\mathcal{P}$

Finally we shall investigate the points b_1 whose cells $V^+(b_1)$ touch both vertical boundaries of $\mathcal{P}$. These cells are produced for b_1 in Section $2i$ and above if $i > \frac{n}{2}$ or Section $2(n-i)+1$ and above if $i \leq \frac{n}{2}$. Importantly, within these sections the structure of $V^+(b_1)$ is identical no matter the section, even or odd. This is because, in actuality, there are no sections beyond Section $\max[2i, 2(n-i)+1]$ as it is defined by the edges $x = 0$, $x = \frac{p}{2n}$, $\mathcal{CC}^1(w_1)$, and $\mathcal{CC}^3(w_n)$.

Therefore the area for b_1 in this region is, for $1 < i < n$,

$$
\begin{aligned}
Area(V^+(b_1)) &= \sum_{j=1}^{i-1} Area(V^+(b_1) \cap V^\circ(w_j)) + Area(V^+(b_1) \cap V^\circ(w_i)) \\
&\quad + \sum_{j=i+1}^{n} Area(V^+(b_1) \cap V^\circ(w_j)) \\
&= \sum_{j=1}^{i-1} (-\frac{p}{2n}x - \frac{p}{2n}y + \frac{pq}{2n} - \frac{(4(i-j)-1)p^2}{8n^2}) - \frac{x^2}{2} - \frac{p}{2n}y + \frac{pq}{2n} \\
&\quad + \sum_{j=i+1}^{n} (\frac{p}{2n}x - \frac{p}{2n}y + \frac{pq}{2n} - \frac{(4(j-i)-1)p^2}{8n^2}) \\
&= (i-1)(-\frac{p}{2n}x - \frac{p}{2n}y + \frac{pq}{2n} + \frac{p^2}{8n^2}) - \frac{p^2}{2n^2}\sum_{j=1}^{i-1}(i-j) - \frac{x^2}{2} - \frac{p}{2n}y + \frac{pq}{2n} \\
&\quad + (n-i)(\frac{p}{2n}x - \frac{p}{2n}y + \frac{pq}{2n} + \frac{p^2}{8n^2}) - \frac{p^2}{2n^2}\sum_{j=i+1}^{n}(j-i) \\
&= -\frac{x^2}{2} + (n-2i+1)\frac{p}{2n}x - \frac{p}{2}y + \frac{pq}{2} + (n-1)\frac{p^2}{8n^2} - \frac{p^2}{2n^2}\frac{(i-1)i}{2} \\
&\quad - \frac{p^2}{2n^2}\frac{(n-i)(n-i+1)}{2} \\
&= -\frac{x^2}{2} + \frac{(n-2i+1)p}{2n}x - \frac{p}{2}y + \frac{pq}{2} - \frac{(2n^2+4i^2-4in+n-4i+1)p^2}{8n^2}
\end{aligned}
$$

or, for $i = 1$,

$$\begin{aligned}
Area(V^+(b_1)) &= Area(V^+(b_1) \cap V^\circ(w_1)) + \sum_{j=2}^{n} Area(V^+(b_1) \cap V^\circ(w_j)) \\
&= -\frac{x^2}{2} - \frac{p}{2n}y + \frac{pq}{2n} + \sum_{j=2}^{n}(\frac{p}{2n}x - \frac{p}{2n}y + \frac{pq}{2n} - \frac{(4(j-1)-1)p^2}{8n^2}) \\
&= -\frac{x^2}{2} - \frac{p}{2n}y + \frac{pq}{2n} + (n-1)(\frac{p}{2n}x - \frac{p}{2n}y + \frac{pq}{2n} + \frac{5p^2}{8n^2}) - \frac{p^2}{2n^2}\sum_{j=2}^{n} j \\
&= -\frac{x^2}{2} + \frac{(n-1)p}{2n}x - \frac{p}{2}y + \frac{pq}{2} - \frac{(2n^2-3n+1)p^2}{8n^2}
\end{aligned}$$

or, for $i = n$,

$$\begin{aligned}
Area(V^+(b_1)) &= \sum_{j=1}^{n-1} Area(V^+(b_1) \cap V^\circ(w_j)) + Area(V^+(b_1) \cap V^\circ(w_n)) \\
&= \sum_{j=1}^{n-1}(-\frac{p}{2n}x - \frac{p}{2n}y + \frac{pq}{2n} - \frac{(4(n-j)-1)p^2}{8n^2}) - \frac{x^2}{2} - \frac{p}{2n}y + \frac{pq}{2n} \\
&= (n-1)(-\frac{p}{2n}x - \frac{p}{2n}y + \frac{pq}{2n} - \frac{(4n-1)p^2}{8n^2}) + \frac{p^2}{2n^2}\sum_{j=1}^{n-1} j - \frac{x^2}{2} - \frac{p}{2n}y + \frac{pq}{2n} \\
&= -\frac{x^2}{2} - \frac{(n-1)p}{2n}x - \frac{p}{2}y + \frac{pq}{2} - \frac{(2n^2-3n+1)p^2}{8n^2}\,.
\end{aligned}$$

All of these areas have partial derivative $\frac{\delta A}{\delta y} = -\frac{p}{2}$ providing, as expected, justification that the area increases as y decreases within the region.

If $1 < i < n$ then

$$\frac{\delta A}{\delta x} = -x + \frac{(n-2i+1)p}{2n}$$

giving $x^* = \frac{(n-2i+1)p}{2n}$. We have $x^* \geq 0 \Leftrightarrow n-2i+1 \geq 0 \Leftrightarrow \frac{n+1}{2} \geq i$ and $x^* \leq \frac{p}{2n} \Leftrightarrow n-2i+1 \leq 1 \Leftrightarrow \frac{n}{2} \leq i$ so this maximum is only achieved for $i = \lceil \frac{n}{2} \rceil$. In this case, if n is even then the maximum within Section $n+1$ of $w_{\frac{n}{2}}$ is found at $x^* = \frac{p}{2n}$, and if n is odd then the maximum within Section $n+1$ of $w_{\frac{n+1}{2}}$ is found at $x^* = 0$. Before explicitly stating the coordinates of b_1^* for these sections we will explore those values of i which did not satisfy these constraints.

For $1 < i < n$ where $i \neq \lceil \frac{n}{2} \rceil$, x^* is never within this region. Therefore we must explore the boundary of the region; by $\frac{\delta A}{\delta y}$ we need only explore the lower boundary.

Since $x^* < 0$ when $i > \frac{n+1}{2}$, for these i the region we are exploring is Section $2i$ and the bottommost point on the lower boundary (satisfying $\frac{\delta A}{\delta y}$) is also the leftmost point (satisfying $\frac{\delta A}{\delta x}$) so this point, $(0, \frac{(i-1)p}{n})$, is our optimum, as well as being the optimum for $i = \frac{n+1}{2}$ when n is odd as found above. This gives $Area(V^+((0, \frac{(i-1)p}{n}))) = \frac{pq}{2} - \frac{(2n^2+4i^2-3n-4i+1)p^2}{8n^2}$ as depicted in Figure 5.4s.

Since $x^* > \frac{p}{2n}$ when $i < \frac{n}{2}$, for these i the region we are exploring is Section $2(n-i)+1$ and the bottommost point on the lower boundary (satisfying $\frac{\delta A}{\delta y}$) is also the rightmost point (satisfying $\frac{\delta A}{\delta x}$), so this point, $(\frac{p}{2n}, \frac{(2(n-i)-1)p}{2n})$, is our optimum, as well as being the optimum for $i = \frac{n}{2}$ when n is even as found above. This gives $Area(V^+((\frac{p}{2n}, \frac{(2(n-i)-1)p}{2n}))) = \frac{pq}{2} - \frac{(6n^2+4i^2-8in-3n)p^2}{8n^2}$ as depicted in Figure 5.4t.

If $i = 1$ then

$$\frac{\delta A}{\delta x} = -x + \frac{(n-1)p}{2n}$$

giving $x^* = \frac{(n-1)p}{2n} \geq \frac{p}{2n}$. As before, since $i < \frac{n}{2}$ the region is $2(n-1)+1$ so our optimum lies at the bottom rightmost point of Section $2n-1$, $(\frac{p}{2n}, \frac{(2n-3)p}{2n})$, giving $Area(V^+((\frac{p}{2n}, \frac{(2n-3)p}{2n}))) =$

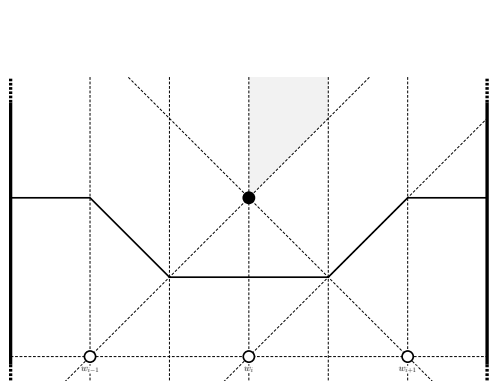

(s) $b_1 = (0, \frac{(i-1)p}{n})$ only if $i > \frac{n}{2}$.

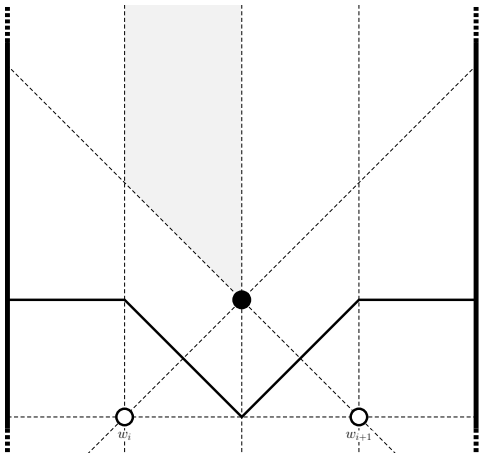

(t) $b_1 = (\frac{p}{2n}, \frac{(2(n-i)-1)p}{2n})$ only if $i \leq \frac{n}{2}$.

Figure 5.4: Maximal area Voronoi cells $V^+(b_1)$ for b_1 within Section $n+1$, touching both vertical edges of $\mathcal{P}$.

$\frac{pq}{2} - \frac{(6n^2-11n+4)p^2}{8n^2}$ (identical to the above calculation for $i < \frac{n}{2}$ after substituting $i = 1$).

Finally, if $i = n$ then

$$\frac{\delta A}{\delta x} = -x - \frac{(n-1)p}{2n}$$

giving $x^* = -\frac{(n-1)p}{2n} < 0$. As before, since $i > \frac{n}{2}$ the region is $2n$ so our optimum lies at the bottom leftmost point of Section $2n$, $(0, \frac{(n-1)p}{n})$, giving $Area(V^+((0, \frac{(n-1)p}{n}))) = \frac{pq}{2} - \frac{(6n^2-7n+1)p^2}{8n^2}$ (identical to the above calculation for $i \geq \frac{n}{2}$ after substituting $i = n$).

This concludes our search for the optimisation of each structure of $V^+(b_1)$ which touches both vertical boundaries of $\mathcal{P}$, and with it our search for the optimisation of every structure of $V^+(b_1)$ given that White plays a $1 \times n$ row.

5.3 Black's optimal strategy: White plays a $1 \times n$ row

At this stage we have calculated the optimal locations of b_1 within every possible partition cell of $\mathcal{P}$ when White plays a $1 \times n$ row. To recap, Figure 5.4 shows all optimal locations of b_1 within each section under the certain circumstances discussed above (not depicting the optimum found in Section I since this had location $(0, 0)$).

5.3.1 Black's best point

An obvious question of interest is which point b_1 is the best point – as in, which position of b_1 gives the largest area of $V^+(b_1)$? The availability of each section in which to place b_1, and the areas of the Voronoi cells $V^+(b_1)$, depend entirely on the relationship between $\frac{p}{n}$ and q so this is not a straightforward question to answer. Nevertheless we shall determine what position $b^* = (x^*, y^*)$ of b_1 claims the largest area of $V^+(b_1)$ for which ratios of $\frac{p}{n}$ and q.

Let us begin by fixing the bottom right corner of $\mathcal{P}$ at $(0, -\frac{q}{2})$ so that $w_i = (\frac{(2i-1)p}{2n}, 0)$ for $i = 1, ..., n$. Firstly it is clear to see from Figure 5.4 that Black's best point b^* will have x-coordinate $\frac{kp}{2n}$ for some $k \in \mathbb{N}$. Furthermore, it is never advantageous when seeking to maximise the area of $V^+(b_1)$ to have $V^+(b_1)$ bounded on one side by a vertical edge of $\mathcal{P}$ since this blocks $V^+(b_1)$ from gaining territory on the other side of the boundary of $\mathcal{P}$, which it might be able to do if b_1 were moved a horizontal distance of $\frac{p}{n}$ away from this edge. For this reason we can easily claim that the best point b^* has x-coordinate $x^* \in \{\frac{p}{2} - \frac{p}{2n}, \frac{p}{2}, \frac{p}{2} + \frac{p}{2n}\}$. By the symmetry of $\mathcal{P}$ and W, not only does $x^* = \frac{p}{2}$ produce a Voronoi cell symmetrical about $x = \frac{p}{2}$, but the values $x^* = \frac{p}{2} - \frac{p}{2n}$ and $x^* = \frac{p}{2} + \frac{p}{2n}$ will produce identical Voronoi cells (after reflection in $x^* = \frac{p}{2}$).

Therefore we need only consider the location of b^* within the top right quadrant of $V^\circ(w_i)$ for $i = \lceil \frac{n}{2} \rceil$, though requiring different investigations depending on whether n is even or odd.

Before we delve into the details with respect to the parity of n, let us recapitulate the results depicted in Figure 5.4 in Table 5.1.

Section	Optimum	Area	Condition
$2l$	$\left(\frac{(2i-1)p}{2n}, (l-1)\frac{p}{n}\right)$	$\frac{(2l-1)pq}{2n} - \frac{3(2l-1)(l-1)p^2}{4n^2}$	$q \leq \frac{(4l-3)p}{n}$
	$\left(\frac{(2i-1)p}{2n}, \frac{q}{3} - \frac{lp}{3n}\right)$	$\frac{lpq}{3n} + \frac{(3-2l)lp^2}{12n^2} + \frac{q^2}{12}$	$\frac{(4l-3)p}{n} \leq q \leq \frac{4lp}{n}$
	$\left(\frac{(2i-1)p}{2n}, l\frac{p}{n}\right)$	$\frac{lpq}{n} + \frac{(1-6l)lp^2}{4n^2}$	$\frac{4lp}{n} \leq q$
$2l+1$	$\left(\frac{ip}{n}, \frac{(2l-1)p}{2n}\right)$	$\frac{lpq}{n} - \frac{(3l-1)lp^2}{2n^2}$	$q \leq \frac{(4l-1)p}{n}$
	$\left(\frac{ip}{n}, \frac{q}{3} - \frac{(2l+1)p}{6n}\right)$	$\frac{(2l+1)pq}{6n} - \frac{(2l^2+2l-1)p^2}{12n^2} + \frac{q^2}{12}$	$\frac{(4l-1)p}{n} \leq q \leq \frac{(4l+2)p}{n}$
	$\left(\frac{ip}{n}, \frac{(2l+1)p}{2n}\right)$	$\frac{(2l+1)pq}{2n} - \frac{(6l^2+6l+1)p^2}{4n^2}$	$\frac{(4l+2)p}{n} \leq q$

Table 5.1: Optima contained in each section of $V^\circ(w_i)$ assuming that Black's Voronoi cell does not touch either vertical edge of $\mathcal{P}$.

We shall refer to these optima as the *bottom*, *middle*, and *top* optima within each section, listed in the order that they appear in Table 5.1 with examples depicted in Figures 5.4c and 5.4f, Figures 5.4b and 5.4e, and Figures 5.4a and 5.4d respectively.

We know the optimal positions b_1^* within each of these sections, but we must ask how these optima compare to one another across sections. It is important to realise that some optima within different sections lie on the same point, while capturing different areas (for example the equivalent optima in Figure 5.4c for Section VI would lie on the same point as shown in Figure 5.4a). This is due to the fact that many of these positions represent the convergence of b_1 to a point, yet these different results are obtained from converging via different paths (i.e. via different sections), choosing different bisectors upon degenerate configuration lines. These are the easiest comparisons to make and can be done by simply referring to graphs of the points as shown, by way of an example, in Figure 5.5.

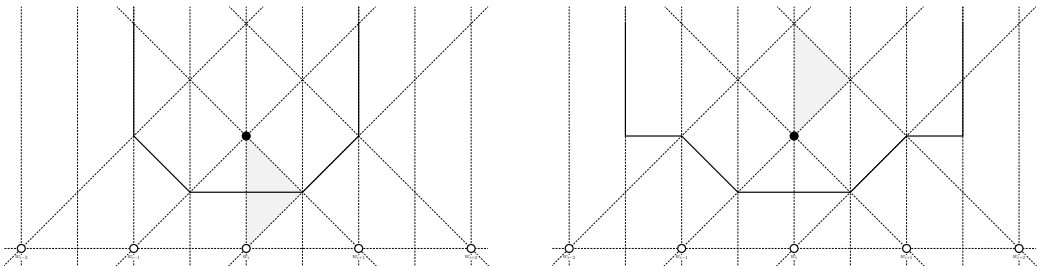

(a) $V^+((\frac{(2i-1)p}{2n}, \frac{p}{n}))$ for $(\frac{(2i-1)p}{2n}, \frac{p}{n})$ in Section II. (b) $V^+((\frac{(2i-1)p}{2n}, \frac{p}{n}))$ for $(\frac{(2i-1)p}{2n}, \frac{p}{n})$ in Section IV.

Figure 5.5: Comparison of identical optimal positions within different sections (shaded).

From Figure 5.5 it is clear to see that if an optimal point we are comparing is located on the boundary of two sections, the upper section will always outperform the lower section. Therefore the remaining optima to consider are the middle and the bottom optima, as well as the optima for $V^+(b_1)$ touching the appropriate vertical boundaries of $\mathcal{P}$.

Now we ask when, if ever, it is better to locate in Section k as opposed to Section $k+2$ for $k > 0$, assuming that the resulting Voronoi cell of Black does not touch either vertical boundary of $\mathcal{P}$.

For even Sections $2l$, we know that the bottom optimum of Section $2(l+1)$ is the optimum over Section $2(l+1)$ if $\frac{(4(l+1)-3)p}{n} = \frac{(4l+1)p}{n} \geq q$, whereas the middle optimum of Section $2l$ is the optimum over Section $2l$ if $\frac{(4l-3)p}{n} \leq q \leq \frac{4lp}{n}$ so we must compare the area that the bottom optimum of Section $2(l+1)$ captures compared to that of the middle optimum of $2l$ when $\frac{(4l-3)p}{n} \leq q \leq \frac{4lp}{n}$:

$$\begin{aligned}
&\left(\frac{(2(l+1)-1)pq}{2n} - \frac{3(2(l+1)-1)((l+1)-1)p^2}{4n^2}\right) - \left(\frac{lpq}{3n} + \frac{(3-2l)lp^2}{12n^2} + \frac{q^2}{12}\right) \\
&\quad = \frac{(2l+1)pq}{2n} - \frac{3(2l+1)lp^2}{4n^2} - \frac{lpq}{3n} + \frac{(2l-3)lp^2}{12n^2} - \frac{q^2}{12} \\
&\quad = \frac{(4l+3)pq}{6n} - \frac{(4l+3)lp^2}{3n^2} - \frac{q^2}{12} \geq 0 \\
&\quad \Leftrightarrow q^2 - \frac{2(4l+3)p}{n}q + \frac{4(4l+3)lp^2}{n^2} \leq 0\,.
\end{aligned}$$

Now it is the case that

$$\begin{aligned}
q^2 - \frac{2(4l+3)p}{n}q + \frac{4(4l+3)lp^2}{n^2} &= (q - \frac{(4l+3)p}{n})^2 + \frac{4(4l+3)lp^2}{n^2} - (\frac{(4l+3)p}{n})^2 \\
&= (q - \frac{(4l+3)p}{n})^2 - \frac{3(4l+3)p^2}{n^2} \leq 0 \\
&\Leftrightarrow \frac{(4l+3)p}{n} - \frac{\sqrt{3(4l+3)}p}{n} \leq q \leq \frac{(4l+3)p}{n} + \frac{\sqrt{3(4l+3)}p}{n}\,.
\end{aligned}$$

Now it remains to find the intersection of $[\frac{(4l-3)p}{n}, \frac{4lp}{n}]$ (the values of q for which the middle optimum is the optimum over Section $2l$) and $[\frac{(4l+3-\sqrt{3(4l+3)})p}{n}, \frac{(4l+3+\sqrt{3(4l+3)})p}{n}]$ (the values of q for which the bottom optimum of Section $2(l+1)$ is better than the middle optimum of Section $2l$). It is clear that $\frac{4lp}{n} < \frac{(4l+3+\sqrt{3(4l+3)})p}{n}$. More involved is the following calculation:

$$\begin{aligned}
\frac{(4l-3)p}{n} - \frac{(4l+3-\sqrt{3(4l+3)})p}{n} &= \frac{(\sqrt{3(4l+3)}-6)p}{n} \geq 0 \\
&\Leftrightarrow \sqrt{3(4l+3)} - 6 \geq 0 \\
&\Leftrightarrow 3(4l+3) \geq 36 \\
&\Leftrightarrow l \geq \frac{9}{4}\,.
\end{aligned}$$

Therefore if $l \leq 2$ then the bottom optimum of Section $2(l+1)$ is better than the middle optimum of Section $2l$ for $\frac{(4l+3-\sqrt{3(4l+3)})p}{n} \leq q$. Otherwise, if $l \geq 3$, the bottom optimum of Section $2(l+1)$ will always be better than the middle optimum of Section $2l$, and so we must compare the bottom optima of both sections when $\frac{(4l-3)p}{n} \geq q$:

$$\begin{aligned}
&\left(\frac{(2(l+1)-1)pq}{2n} - \frac{3(2(l+1)-1)((l+1)-1)p^2}{4n^2}\right) - \left(\frac{(2l-1)pq}{2n} - \frac{3(2l-1)(l-1)p^2}{4n^2}\right) \\
&\quad = \frac{(2l+1)pq}{2n} - \frac{3(2l+1)lp^2}{4n^2} - \frac{(2l-1)pq}{2n} + \frac{3(2l-1)(l-1)p^2}{4n^2} \\
&\quad = \frac{pq}{n} - \frac{3(4l-1)p^2}{4n^2} \geq 0 \\
&\quad \Leftrightarrow \frac{3(4l-1)p}{4n} \leq q\,.
\end{aligned}$$

Now

$$\frac{3(4l-1)p}{4n} \leq \frac{(4l-3)p}{n} \Leftrightarrow 3(4l-1) \leq 4(4l-3) \Leftrightarrow l \geq \frac{9}{4}$$

so if $l \geq 3$ (the condition which requires us to compare these two local optima) then the bottom optimum of Section $2(l+1)$ is better than the bottom optimum of Section $2l$ for $\frac{3(4l-1)p}{4n} \leq q$.

Let us digest our findings, for which it may be more intuitive to describe the efficacy of each section's optima from Section II upwards. These results are summarised in the following table.

Now we must analogously explore the odd sections $2l+1$. The bottom optimum of Section

Section	Optimum	Area	Condition
II	$(x^*, 0)$	$\frac{pq}{2n}$	$q \leq \frac{p}{n}$
	$(x^*, \frac{q}{3} - \frac{p}{3n})$	$\frac{pq}{3n} + \frac{p^2}{12n^2} + \frac{q^2}{12}$	$\frac{p}{n} \leq q \leq \frac{(7-\sqrt{21})p}{n}$
IV	$(x^*, \frac{p}{n})$	$\frac{3pq}{2n} - \frac{9p^2}{4n^2}$	$\frac{(7-\sqrt{21})p}{n} \leq q \leq \frac{5p}{n}$
	$(x^*, \frac{q}{3} - \frac{2p}{3n})$	$\frac{2pq}{3n} - \frac{p^2}{6n^2} + \frac{q^2}{12}$	$\frac{5p}{n} \leq q \leq \frac{(11-\sqrt{33})p}{n}$
VI	$(x^*, \frac{2p}{n})$	$\frac{5pq}{2n} - \frac{15p^2}{2n^2}$	$\frac{(11-\sqrt{33})p}{n} \leq q \leq \frac{33p}{4n}$
$2l$	$(x^*, (l-1)\frac{p}{n})$	$\frac{(2l-1)pq}{2n} - \frac{3(2l-1)(l-1)p^2}{4n^2}$	$\frac{3(4l-5)p}{4n} \leq q \leq \frac{3(4l-1)p}{4n}$

Table 5.2: Optima contained in even sections at $x^* = \frac{(2i-1)p}{2n}$ assuming that Black's Voronoi cell does not touch either vertical edge of $\mathcal{P}$.

$2(l+1)+1$ is the optimum of Section $2(l+1)+1$ if $q \leq \frac{(4(l+1)-1)p}{n} = \frac{(4l+3)p}{n}$ whereas the middle optimum of Section $2l+1$ is the optimum over Section $2l+1$ if $\frac{(4l-1)p}{n} \leq q \leq \frac{(4l+2)p}{n}$, so we must compare the area that the bottom optimum of Section $2(l+1)+1$ captures compared to that of the middle optimum of $2l+1$ when $\frac{(4l-1)p}{n} \leq q \leq \frac{(4l+2)p}{n}$:

$$\begin{aligned}
&\left(\frac{(l+1)pq}{n} - \frac{(3(l+1)-1)(l+1)p^2}{2n^2}\right) - \left(\frac{(2l+1)pq}{6n} - \frac{(2l^2+2l-1)p^2}{12n^2} + \frac{q^2}{12}\right) \\
&\quad = \frac{(l+1)pq}{n} - \frac{(3l+2)(l+1)p^2}{2n^2} - \frac{(2l+1)pq}{6n} + \frac{(2l^2+2l-1)p^2}{12n^2} - \frac{q^2}{12} \\
&\quad = \frac{(4l+5)pq}{6n} - \frac{(16l^2+28l+13)p^2}{12n^2} - \frac{q^2}{12} \geq 0 \\
&\quad \Leftrightarrow q^2 - \frac{2(4l+5)pq}{n} + \frac{(16l^2+28l+13)p^2}{n^2} \leq 0\,.
\end{aligned}$$

Now it is the case that

$$\begin{aligned}
q^2 - \frac{2(4l+5)pq}{n} + \frac{(16l^2+28l+13)p^2}{n^2} &= \left(q - \frac{(4l+5)p}{n}\right)^2 + \frac{(16l^2+28l+13)p^2}{n^2} - \left(\frac{(4l+5)p}{n}\right)^2 \\
&= \left(q - \frac{(4l+5)p}{n}\right)^2 - \frac{12(l+1)p^2}{n^2} \leq 0 \\
&\Leftrightarrow \frac{(4l+5)p}{n} - \frac{2\sqrt{3(l+1)}p}{n} \leq q \leq \frac{(4l+5)p}{n} + \frac{2\sqrt{3(l+1)}p}{n}\,.
\end{aligned}$$

Now it remains to find the intersection of $\left[\frac{(4l-1)p}{n}, \frac{(4l+2)p}{n}\right]$ (the values of q for which the middle optimum is the optimum over Section $2l+1$) and $\left[\frac{(4l+5-2\sqrt{3(l+1)})p}{n}, \frac{(4l+5+2\sqrt{3(l+1)})p}{n}\right]$ (the values of q for which the bottom optimum of Section $2(l+1)+1$ is better than the middle optimum of Section $2l+1$). It is clear that $\frac{(4l+2)p}{n} < \frac{(4l+5+2\sqrt{3(l+1)})p}{n}$. More involved is the following calculation:

$$\begin{aligned}
\frac{(4l-1)p}{n} - \frac{(4l+5-2\sqrt{3(l+1)})p}{n} = \frac{(2\sqrt{3(l+1)}-6)p}{n} &\geq 0 \\
&\Leftrightarrow 2\sqrt{3(l+1)} - 6 \geq 0 \\
&\Leftrightarrow 3(l+1) \geq 9 \\
&\Leftrightarrow l \geq 2\,.
\end{aligned}$$

Therefore if $l = 1$ then the bottom optimum of Section $2(l+1)+1$ is better than the middle optimum of Section $2l+1$ for $\frac{(4l+5-2\sqrt{3(l+1)})p}{n} \leq q$. Otherwise, if $l \geq 2$, the bottom optimum of Section $2(l+1)+1$ will always be better than the middle optimum of Section $2l+1$, and so we must compare the bottom optima of both sections when $\frac{(4l-1)p}{n} \geq q$:

$$\begin{aligned}\left(\frac{(l+1)pq}{n} - \frac{(3(l+1)-1)(l+1)p^2}{2n^2}\right) - \left(\frac{lpq}{n} - \frac{(3l-1)lp^2}{2n^2}\right)\\ = \frac{(l+1)pq}{n} - \frac{(3l+2)(l+1)p^2}{2n^2} - \frac{lpq}{n} + \frac{(3l-1)lp^2}{2n^2}\\ = \frac{pq}{n} - \frac{(3l+1)p^2}{n^2} \geq 0\\ \Leftrightarrow \frac{(3l+1)p}{n} \leq q\,.\end{aligned}$$

Now

$$\frac{(3l+1)p}{n} \leq \frac{(4l-1)p}{n} \Leftrightarrow (3l+1) \leq (4l-1) \Leftrightarrow l \geq 2$$

so if $l \geq 2$ (the condition which requires us to compare these two local optima) then the bottom optimum of Section $2(l+1)+1$ is better than the bottom optimum of Section $2l+1$ for $\frac{(3l+1)p}{n} \leq q$.

In contrast to our analysis of the optima in even sections, we must compare Section III with the outlier Section I in order to discern when it is more fruitful to settle with the poor-quality Section I optimum. We can do this simply by comparing the area from the bottom optimum in Section III with the maximum area possible achieved in Section I:

$$\left(\frac{pq}{n} - \frac{p^2}{n^2}\right) - \frac{pq}{2n} = \frac{pq}{2n} - \frac{p^2}{n^2} \geq 0 \Leftrightarrow q \geq \frac{2p}{n}\,.$$

Thus, within odd sections we can only do better than $\frac{pq}{2n}$ if $\frac{2p}{n} \leq q$, otherwise it is preferable to locate in Section I.

Let us again digest our findings, summarised in Table 5.3.

Section	Optimum	Area	Condition
I	$(*, 0)$	$\frac{pq}{2n}$	$q \leq \frac{2p}{n}$
III	$(x^*, \frac{p}{2n})$	$\frac{pq}{n} - \frac{p^2}{n^2}$	$\frac{2p}{n} \leq q \leq \frac{3p}{n}$
	$(x^*, \frac{q}{3} - \frac{p}{2n})$	$\frac{pq}{2n} - \frac{p^2}{4n^2} + \frac{q^2}{12}$	$\frac{3p}{n} \leq q \leq \frac{(9-2\sqrt{6})p}{n}$
V	$(x^*, \frac{3p}{2n})$	$\frac{2pq}{n} - \frac{5p^2}{n^2}$	$\frac{(9-2\sqrt{6})p}{n} \leq q \leq \frac{7p}{n}$
$2l+1$	$(x^*, \frac{(2l-1)p}{2n})$	$\frac{lpq}{n} - \frac{(3l-1)lp^2}{2n^2}$	$\frac{(3l-2)p}{n} \leq q \leq \frac{(3l+1)p}{n}$

Table 5.3: Optima contained in even sections at $x^* = \frac{ip}{n}$ assuming that Black's Voronoi cell does not touch either vertical edge of $\mathcal{P}$.

Having found the optimal locations within the set of even sections and the set of odd sections dependent on the ratio between $\frac{p}{n}$ and q, it remains to compare Table 5.2 and Table 5.3. We shall explore the global optima as q increases, starting from the top of the tables and working our way down comparing areas across the tables each time q increases so as to enter a new condition.

Beginning with $q \leq \frac{p}{n}$, both tables give the same maximal area of $\frac{pq}{2n}$ no matter whether locating in Section I and II. However, this area can be improved if $\frac{p}{n} \leq q$ by playing the middle optimum of Section II so it is no longer optimal to locate in Section I. The next condition occurs when $\frac{2p}{n} \leq q$ so we must compare the middle optimum of Section II with the bottom optimum of Section III:

$$\left(\frac{pq}{n}-\frac{p^2}{n^2}\right)-\left(\frac{pq}{3n}+\frac{p^2}{12n^2}+\frac{q^2}{12}\right)=\frac{pq}{n}-\frac{p^2}{n^2}-\frac{pq}{3n}-\frac{p^2}{12n^2}-\frac{q^2}{12}$$
$$=\frac{2pq}{3n}-\frac{13p^2}{12n^2}-\frac{q^2}{12}\geq 0$$
$$\Leftrightarrow q^2-\frac{8pq}{n}+\frac{13p^2}{n^2}\leq 0$$
$$\Leftrightarrow \left(q-\frac{4p}{n}\right)^2-\frac{3p^2}{n^2}\leq 0$$
$$\Leftrightarrow \frac{4p}{n}-\frac{\sqrt{3}p}{n}\leq q\leq \frac{4p}{n}+\frac{\sqrt{3}p}{n}\,.$$

Since $\frac{2p}{n}<\frac{(4-\sqrt{3})p}{n}<\frac{(7-\sqrt{21})p}{n}<\frac{(4+\sqrt{3})p}{n}$, the bottom optimum of Section III is better than the middle optimum of Section II for $\frac{(4-\sqrt{3})p}{n}\leq q$ as long as the middle optimum of Section II is the optimal location within even sections.

The subsequent condition to be met as q increases is when $\frac{(7-\sqrt{21})p}{n}\leq q$ and we must compare the bottom optimum of Section IV to the bottom optimum of Section III:

$$\left(\frac{3pq}{2n}-\frac{9p^2}{4n^2}\right)-\left(\frac{pq}{n}-\frac{p^2}{n^2}\right)=\frac{3pq}{2n}-\frac{9p^2}{4n^2}-\frac{pq}{n}+\frac{p^2}{n^2}$$
$$=\frac{pq}{2n}-\frac{5p^2}{4n^2}\geq 0$$
$$\Leftrightarrow q\geq\frac{5p}{2n}\,.$$

The bottom optimum of Section IV is better than the bottom optimum of Section III for $\frac{5p}{2n}\leq q$ and since $\frac{(7-\sqrt{21})p}{n}<\frac{5p}{2n}<\frac{3p}{n}$ it is the global optimum at least until $q=\frac{3p}{n}$.

Subsequently, for $\frac{3p}{n}\leq q\leq\frac{(9-2\sqrt{6})p}{n}$ the optimum in odd sections becomes the middle optimum of Section III so we must compare this to the bottom optimum of Section IV:

$$\left(\frac{pq}{2n}-\frac{p^2}{4n^2}+\frac{q^2}{12}\right)-\left(\frac{3pq}{2n}-\frac{9p^2}{4n^2}\right)=\frac{pq}{2n}-\frac{p^2}{4n^2}+\frac{q^2}{12}-\frac{3pq}{2n}+\frac{9p^2}{4n^2}$$
$$=\frac{q^2}{12}-\frac{pq}{n}+\frac{2p^2}{n^2}\geq 0$$
$$\Leftrightarrow q^2-\frac{12pq}{n}+\frac{24p^2}{n^2}\geq 0$$
$$\Leftrightarrow \left(q-\frac{6p}{n}\right)^2-\frac{12p^2}{n^2}\geq 0$$
$$\Leftrightarrow q\leq\frac{6p}{n}-\frac{2\sqrt{3}p}{n}\text{ or }q\geq\frac{6p}{n}+\frac{2\sqrt{3}p}{n}\,.$$

Since $\frac{(6-2\sqrt{3})p}{n}<\frac{3p}{n}<\frac{(9-2\sqrt{6})p}{n}<\frac{(6+2\sqrt{3})p}{n}$ the middle optimum of Section III never beats the bottom optimum of Section IV. Given this fact, we know also that the middle optimum of Section IV (which beats the bottom optimum of Section IV at $\frac{5p}{n}\leq q$) beats the middle optimum of Section III.

This, when $\frac{(9-2\sqrt{6})p}{n}\leq q$, brings us to the comparison of the bottom optimum of Section V and the middle optimum of Section IV:

$$\left(\frac{2pq}{n}-\frac{5p^2}{n^2}\right)-\left(\frac{2pq}{3n}-\frac{p^2}{6n^2}+\frac{q^2}{12}\right)=\frac{2pq}{n}-\frac{5p^2}{n^2}-\frac{2pq}{3n}+\frac{p^2}{6n^2}-\frac{q^2}{12}$$
$$=\frac{4pq}{3n}-\frac{29p^2}{6n^2}-\frac{q^2}{12}\geq 0$$
$$\Leftrightarrow q^2-\frac{16pq}{n}+\frac{58p^2}{n^2}\leq 0$$
$$\Leftrightarrow \left(q-\frac{8p}{n}\right)^2-\frac{6p^2}{n^2}\leq 0$$
$$\Leftrightarrow \frac{8p}{n}-\frac{\sqrt{6}p}{n}\leq q\leq \frac{8p}{n}+\frac{\sqrt{6}p}{n}\,.$$

Since $\frac{(11-\sqrt{33})p}{n}$, the value of q at which the middle optimum of Section IV is no longer optimal for even sections, is less than $\frac{(8-\sqrt{6})p}{n}$, the middle optimum of Section IV is the global optimum for its whole range, and for $\frac{(11-\sqrt{33})p}{n}\leq q$ the bottom optimum of VI (the subsequent optimum in even sections) is the next global optimum. We must therefore compare the bottom optimum of Section V to the bottom optimum of Section VI:

$$\left(\frac{2pq}{n}-\frac{5p^2}{n^2}\right)-\left(\frac{5pq}{2n}-\frac{15p^2}{2n^2}\right)=\frac{2pq}{n}-\frac{5p^2}{n^2}-\frac{5pq}{2n}+\frac{15p^2}{2n^2}$$
$$=\frac{5p^2}{2n^2}-\frac{pq}{2n}\geq 0$$
$$\Leftrightarrow q\leq \frac{5p}{n}\,.$$

Since $\frac{5p}{n}<\frac{(11-\sqrt{33})p}{n}\leq q$, the bottom optimum of Section V is never better than the bottom optimum of Section VI.

At this point, since the condition values are now our general $\frac{3(4l-5)p}{4n}$ and $\frac{(3l-2)p}{n}$ values (for even and odd sections respectively), we have compared all of the necessary initial areas and can compare the general bottom optima of Section $2l$ and Section $2l+1$ (and of Section $2l+1$ and Section $2(l+1)$) for $l\geq 3$.

At $\frac{(3l-2)p}{n}\leq q$ we must compare the bottom optima of Section $2l+1$ with that of Section $2l$:

$$\left(\frac{lpq}{n}-\frac{(3l-1)lp^2}{2n^2}\right)-\left(\frac{(2l-1)pq}{2n}-\frac{3(2l-1)(l-1)p^2}{4n^2}\right)$$
$$=\frac{lpq}{n}-\frac{(3l-1)lp^2}{2n^2}-\frac{(2l-1)pq}{2n}+\frac{3(2l-1)(l-1)p^2}{4n^2}$$
$$=\frac{pq}{2n}-\frac{(7l-3)p^2}{4n^2}\geq 0$$
$$\Leftrightarrow \frac{(7l-3)p}{2n}\leq q\,.$$

Since $\frac{3(4l-1)p}{4n}$, the value of q at which the bottom optimum of Section $2l$ is bested by the bottom optimum of Section $2(l+1)$, is less than $\frac{(7l-3)p}{2n}$ (because $3(4l-1)\geq 2(7l-3)\Leftrightarrow l\leq\frac{3}{2}$), the bottom optimum of Section $2l+1$ never beats the bottom optimum of Section $2l$ while this is the global optimum, and we must compare the bottom optimum of Section $2l+1$ with the bottom optimum of Section $2(l+1)$ when $\frac{3(4l-1)p}{4n}\leq q$:

$$\left(\frac{lpq}{n} - \frac{(3l-1)lp^2}{2n^2}\right) - \left(\frac{(2(l+1)-1)pq}{2n} - \frac{3(2(l+1)-1)((l+1)-1)p^2}{4n^2}\right)$$
$$= \frac{lpq}{n} - \frac{(3l-1)lp^2}{2n^2} - \frac{(2l+1)pq}{2n} + \frac{3(2l+1)lp^2}{4n^2}$$
$$= -\frac{pq}{2n} + \frac{5lp^2}{4n^2} \geq 0$$
$$\Leftrightarrow q \leq \frac{5lp}{2n}\,.$$

However, $\frac{5lp}{2n} < \frac{3(4l-1)p}{4n}$ (because $\frac{5l}{2} \geq \frac{3(4l-1)}{4} \Leftrightarrow l \leq \frac{3}{2}$ so the bottom optimum of Section $2l+1$ is never better than the bottom optimum of Section $2(l+1)$).

Thus we have determined, for every possible proportion of p and q, all of the optimal locations of Black's point given that Black's Voronoi cell does not touch either vertical edge of $\mathcal{P}$. These are shown in Table 5.4.

Section	Optimum	Area	Condition
I	$(*, 0)$	$\frac{pq}{2n}$	$q \leq \frac{p}{n}$
II	$(x^*, \frac{q}{3} - \frac{p}{3n})$	$\frac{pq}{3n} + \frac{p^2}{12n^2} + \frac{q^2}{12}$	$\frac{p}{n} \leq q \leq \frac{(4-\sqrt{3})p}{n}$
III	$(x^* + \frac{p}{2n}, \frac{p}{2n})$	$\frac{pq}{n} - \frac{p^2}{n^2}$	$\frac{(4-\sqrt{3})p}{n} \leq q \leq \frac{5p}{2n}$
IV	$(x^*, \frac{p}{n})$	$\frac{3pq}{2n} - \frac{9p^2}{4n^2}$	$\frac{5p}{2n} \leq q \leq \frac{5p}{n}$
IV	$(x^*, \frac{q}{3} - \frac{2p}{3n})$	$\frac{2pq}{3n} - \frac{p^2}{6n^2} + \frac{q^2}{12}$	$\frac{5p}{n} \leq q \leq \frac{(11-\sqrt{33})p}{n}$
VI	$(x^*, \frac{2p}{n})$	$\frac{5pq}{2n} - \frac{15p^2}{2n^2}$	$\frac{(11-\sqrt{33})p}{n} \leq q \leq \frac{33p}{4n}$
$2l$	$(x^*, (l-1)\frac{p}{n})$	$\frac{(2l-1)pq}{2n} - \frac{3(2l-1)(l-1)p^2}{4n^2}$	$\frac{3(4l-5)p}{4n} \leq q \leq \frac{3(4l-1)p}{4n}$

Table 5.4: Optima within one quarter cell of $V^\circ(w_i)$ at $x^* = \frac{ip}{2n}$ assuming that Black's Voronoi cell does not touch either vertical edge of $\mathcal{P}$.

Finally we must determine Black's best point in the case that Black's Voronoi cell may touch a vertical edge of $\mathcal{P}$, and for this we will explore the cases of the parity of n separately.

n even If n is even then we are investigating the top right quadrant of $V^\circ(w_{\frac{n}{2}})$ and so concern ourselves with $x^* = \frac{(n-1)p}{2n}$ upon which the optima of (all but one) even sections lie, and with $x^* = \frac{p}{2}$ upon which the optima of odd sections lie, and with $y = x - \frac{p}{2n}$ upon which the optima of Section $\frac{n}{2}$ lie (for reference, these are the optima depicted in Figures 5.4j to 5.4l).

On $x^* = \frac{(n-1)p}{2n}$, the Voronoi cells of points in Sections II to $n-2$ will not touch either vertical boundary of $\mathcal{P}$ and Section n will touch the leftmost boundary of $\mathcal{P}$. On $x^* = \frac{p}{2}$, Sections I to $n-1$ will not touch either vertical boundary of $\mathcal{P}$ and Section $n+1$ is the final section, touching both vertical edges of $\mathcal{P}$.

Therefore we need to compare the optima over Section n (shown in Table 5.5) and Section $n+1$ (the optimum $(\frac{p}{2n}, \frac{(n-1)p}{2n})$ achieves $\frac{pq}{2} - \frac{3(n-1)np^2}{8n^2}$) with appropriate optima in Table 5.4.

Section	Optimum	Area	Condition
n	$(\frac{(n-1)p}{2n}, \frac{(n-2)p}{2n})$	$\frac{(n-1)pq}{2n} - \frac{(3n^2-9n+6)p^2}{8n^2}$	$q \leq \frac{(2n-3)p}{n}$
	$(\frac{p}{4n} + \frac{q}{4}, \frac{q}{4} - \frac{p}{4n})$	$\frac{(2n-1)pq}{8n} - \frac{(2n^2-6n+3)p^2}{16n^2} + \frac{q^2}{16}$	$\frac{(2n-3)p}{n} \leq q \leq \frac{(2n-1)p}{n}$
	$(\frac{p}{2}, \frac{(n-1)p}{2n})$	$\frac{(2n-1)pq}{4n} - \frac{(3n^2-5n+2)p^2}{8n^2}$	$\frac{(2n-1)p}{n} \leq q$

Table 5.5: Optima within Section n of the top right quadrant of $V^\circ(w_{\frac{n}{2}})$.

Within the calculations for general Sections $2l$ and $2l+1$ leading to Table 5.4, we compared the bottom optima of Section $2l$ to $2l+1$ and of Section $2l+1$ to $2(l+1)$. It is useful to note that while the Voronoi cell of the 'bottom' optimum of Section n does share a border with the leftmost boundary of $\mathcal{P}$, this bordering does not remove any area since the boundary of

$\mathcal{P}$ is incident on the perimeter of the Voronoi cell (i.e. the point captures the same area as the equivalent point in Section n which does not touch the leftmost boundary of $\mathcal{P}$). Since the 'bottom' optimum of Section n acts as if it does not touch either vertical boundary of $\mathcal{P}$, we can use all of the results from Table 5.4 and check the optima in Section n against that of Section $n+1$ (along with some checks for small n).

Firstly comparing the optima of Section n and Section $n+1$, by an identical argument to the one shown in Figure 5.5, the 'top' optimum of Section n is beaten by the optimum in Section $n+1$ (simply because they lie in the same location with Section $n+1$ lying on a more preferential side of $\mathcal{CC}^3(w_n)$). We should, however, compare the optimum of Section $n+1$ with the 'middle' optimum of Section n:

$$\begin{aligned}
&\left(\frac{pq}{2} - \frac{3(n-1)np^2}{8n^2}\right) - \left(\frac{(2n-1)pq}{8n} - \frac{(2n^2-6n+3)p^2}{16n^2} + \frac{q^2}{16}\right) \\
&\qquad = \frac{pq}{2} - \frac{3(n-1)np^2}{8n^2} - \frac{(2n-1)pq}{8n} + \frac{(2n^2-6n+3)p^2}{16n^2} - \frac{q^2}{16} \\
&\qquad = \frac{(2n+1)pq}{8n} - \frac{(4n^2-3)p^2}{16n^2} - \frac{q^2}{16} \geq 0 \\
&\qquad \Leftrightarrow q^2 - \frac{2(2n+1)pq}{n} + \frac{(4n^2-3)p^2}{n^2} \leq 0 \\
&\qquad \Leftrightarrow \left(q - \frac{(2n+1)p}{n}\right)^2 - \frac{4(n+1)p^2}{n^2} \leq 0 \\
&\qquad \Leftrightarrow \frac{(2n+1)p}{n} - \frac{2\sqrt{(n+1)}p}{n} \leq q \leq \frac{(2n+1)p}{n} + \frac{2\sqrt{(n+1)}p}{n}\,.
\end{aligned}$$

Now

$$\frac{(2n-3)p}{n} < \frac{(2n+1-2\sqrt{(n+1)})p}{n} \Leftrightarrow 2\sqrt{(n+1)} < 4 \Leftrightarrow n < 3$$

so if $n = 2$ then the 'middle' optimum of Section n is better than the optimum over Section $n+1$ if $q \leq \frac{(2n+1-2\sqrt{(n+1)})p}{n}$. In this case, the remaining comparisons are very straightforward as the only sections existing when $n = 2$ are Sections I, II, and III so we can record the optima straightforwardly, as displayed in Table 5.6.

Section	b^*	Area	Condition
I	$(*, 0)$	$\frac{pq}{2n}$	$q \leq \frac{p}{2}$
II	$(\frac{p}{8} + \frac{q}{4}, \frac{q}{4} - \frac{p}{8})$	$\frac{3pq}{16} + \frac{p^2}{64} + \frac{q^2}{16}$	$\frac{p}{2} \leq q \leq \frac{(5-2\sqrt{3})p}{2}$
III	$(\frac{p}{2}, \frac{p}{4})$	$\frac{pq}{2} - \frac{3p^2}{16}$	$\frac{(5-2\sqrt{3})p}{2} \leq q$

Table 5.6: The best point b^* for $n = 2$.

If $n \neq 2$ then the optimum in Section $n+1$ is always better than the 'middle' optimum of Section n. This leads us to the comparison of the 'bottom' optimum of Section n and the optimum of Section $n+1$:

$$\begin{aligned}
&\left(\frac{pq}{2} - \frac{3(n-1)np^2}{8n^2}\right) - \left(\frac{(n-1)pq}{2n} - \frac{(3n^2-9n+6)p^2}{8n^2}\right) \\
&\qquad = \frac{pq}{2} - \frac{3(n-1)np^2}{8n^2} - \frac{(n-1)pq}{2n} + \frac{(3n^2-9n+6)p^2}{8n^2} \\
&\qquad = \frac{pq}{2n} - \frac{3(n-1)p^2}{4n^2} \geq 0 \\
&\qquad \Leftrightarrow \frac{3(n-1)p}{2n} \leq q
\end{aligned}$$

and, for a sanity check, the comparison of the 'bottom' optimum of Section n and the bottom optimum of Section $n-2$ (note that Section $n-2$ may not always exist and we shall discuss these finer details shortly):

$$\left(\frac{(n-1)pq}{2n} - \frac{(3n^2-9n+6)p^2}{8n^2}\right) - \left(\frac{((n-2)-1)pq}{2n} - \frac{3((n-2)-1)((\frac{n-2}{2})-1)p^2}{4n^2}\right)$$
$$= \frac{(n-1)pq}{2n} - \frac{(3n^2-9n+6)p^2}{8n^2} - \frac{(n-3)pq}{2n} + \frac{3(n-3)(n-4)p^2}{8n^2}$$
$$= \frac{pq}{n} - \frac{3(2n-5)p^2}{4n^2} \geq 0$$
$$\Leftrightarrow \frac{3(2n-5)p}{4n} \leq q$$

(the identical condition for Section $2l$ and $2(l+1)$ where Section $2(l+1)$ does not touch either vertical boundaries of $\mathcal{P}$ as expected). Finally, checking that $\frac{3(2n-5)p}{4n} < \frac{3(n-1)p}{2n}$ confirms that the optimum in Section $n+1$ is better than the 'bottom' optimum in Section n when this optimum is better than the bottom optimum of Section $n-2$, so we need not compare the optima of Section $n+1$ and $n-2$.

Now, for $l > 1$, the bottom optimum in Section $2l$ was always found to be optimal within some range of q in Table 5.4 as, since the 'bottom' optimum in Section n is identical to the general bottom optimum in Section $2l$, it is simply true that we can use all of the results summarised in Table 5.4 until Section n at which point we use the results we have most recently found. Hence the best points b^* for every even $n \neq 2$ are recorded in Table 5.7.

Section	Optimum	Area	Condition
I	$(*, 0)$	$\frac{pq}{2n}$	$q \leq \frac{p}{n}$
II	$(\frac{(n-1)p}{2n}, \frac{q}{3} - \frac{p}{3n})$	$\frac{pq}{3n} + \frac{p^2}{12n^2} + \frac{q^2}{12}$	$\frac{p}{n} \leq q \leq \frac{(4-\sqrt{3})p}{n}$
III	$(\frac{p}{2}, \frac{p}{2n})$	$\frac{pq}{n} - \frac{p^2}{n^2}$	$\frac{(4-\sqrt{3})p}{n} \leq q \leq \frac{5p}{2n}$
IV	$(\frac{(n-1)p}{2n}, \frac{p}{n})$	$\frac{3pq}{2n} - \frac{9p^2}{4n^2}$	$\frac{5p}{2n} \leq q \leq \frac{5p}{n}$
IV	$(\frac{(n-1)p}{2n}, \frac{q}{3} - \frac{2p}{3n})$	$\frac{2pq}{3n} - \frac{p^2}{6n^2} + \frac{q^2}{12}$	$\frac{5p}{n} \leq q \leq \frac{(11-\sqrt{33})p}{n}$
VI	$(\frac{(n-1)p}{2n}, \frac{2p}{n})$	$\frac{5pq}{2n} - \frac{15p^2}{2n^2}$	$\frac{(11-\sqrt{33})p}{n} \leq q \leq \frac{33p}{4n}$
$2l$	$(\frac{(n-1)p}{2n}, (l-1)\frac{p}{n})$	$\frac{(2l-1)pq}{2n} - \frac{3(2l-1)(l-1)p^2}{4n^2}$	$\frac{3(4l-5)p}{4n} \leq q \leq \frac{3(4l-1)p}{4n}$
n	$(\frac{(n-1)p}{2n}, \frac{(n-2)p}{2n})$	$\frac{(n-1)pq}{2n} - \frac{(3n^2-9n+6)p^2}{8n^2}$	$\frac{3(2n-5)p}{4n} \leq q \leq \frac{3(n-1)p}{2n}$
$n+1$	$(\frac{p}{2n}, \frac{(n-1)p}{2n})$	$\frac{pq}{2} - \frac{3(n-1)np^2}{8n^2}$	$\frac{3(n-1)p}{2n} \leq q$

Table 5.7: The best point b^* for even $n \neq 2$.

n odd If n is odd then we are investigating the top right quadrant of $V^\circ(w_{\frac{n+1}{2}})$ and so concern ourselves with $x^* = \frac{p}{2}$ upon which the optima of all even sections lie, and with $x^* = \frac{(n+1)p}{2n}$ upon which the optima of (all but one) odd sections lie, and with $y = \frac{(n-i)p}{n} - x$ upon which the optima of Section i lie (for reference, these are the optima depicted in Figures 5.4m to 5.4o).

On $x^* = \frac{p}{2}$, the Voronoi cells of points in Sections II to $n-1$ will not touch either vertical boundaries of $\mathcal{P}$, and Section $n+1$ is the final section, touching both vertical edges of $\mathcal{P}$. On $x^* = \frac{(n+1)p}{2n}$, the Voronoi cells of points in Sections I to $n-2$ will not touch either vertical boundaries of $\mathcal{P}$ and Section n will touch the rightmost boundary of $\mathcal{P}$.

Therefore, as before, we need to compare the optima over Section n (shown in Table 5.8) and Section $n+1$ (the optimum $(\frac{p}{2}, \frac{(n-1)p}{2n})$ achieves $\frac{pq}{2} - \frac{3(n-1)np^2}{8n^2}$) with appropriate optima in Table 5.4.

Now the only optimum within an odd section (ignoring Section I) to be a global optimal point for Voronoi cells not touching either vertical boundary of $\mathcal{P}$ is the bottom optimum of Section III. Since the areas achieved by the optima in Section n for Voronoi cells touching the rightmost vertical boundary of $\mathcal{P}$ are no greater than the areas achieved by the optima of Section n for Voronoi cells that touch neither vertical boundary of $\mathcal{P}$ and the latter are not global optima unless $n = 3$, the optima of our Section n will never be global optima unless $n = 3$. Therefore we only need consider the optima in Section n if $n = 3$, and by the argument

Section	Optimum	Area	Condition
n	$(\frac{(n+1)p}{2n}, \frac{(n-2)p}{2n})$	$\frac{(n-1)pq}{2n} - \frac{3(n-2)(n-1)p^2}{8n^2}$	$q \leq \frac{(2n-3)p}{n}$
	$(\frac{(4n-1)p}{4n} - \frac{q}{4}, -\frac{p}{4n} + \frac{q}{4})$	$\frac{(2n-1)pq}{8n} - \frac{(2n^2-6n+3)p^2}{16n^2} + \frac{q^2}{16}$	$\frac{(2n-3)p}{n} \leq q \leq \frac{(2n-1)p}{n}$
	$(\frac{p}{2}, \frac{(n-1)p}{2n})$	$\frac{(2n-1)pq}{4n} - \frac{(3n-2)(n-1)p^2}{8n^2}$	$\frac{(2n-1)p}{n} \leq q$

Table 5.8: Optima within Section n of the top right quadrant of $V^\circ(w_{\frac{n+1}{2}})$.

from Figure 5.5 we need never consider the 'top' optima of Section n. Moreover, we can avoid all further calculations by noting that the bottom optimum of Section III and of Section IV in Table 5.4 (two consecutive global optima) are, respectively, exactly the same location and achieve exactly the same area as the 'bottom' optimum of Section III in the case that the Voronoi cells touch the rightmost boundary of $\mathcal{P}$, and the optimum of Section IV in the case that the Voronoi cells touch both vertical boundaries of $\mathcal{P}$. Therefore we already know our global optima and these are displayed in Table 5.9.

Section	Optimum	Area	Condition
I	$(*, 0)$	$\frac{pq}{2n}$	$q \leq \frac{p}{n}$
II	$(\frac{p}{2}, \frac{q}{3} - \frac{p}{3n})$	$\frac{pq}{3n} + \frac{p^2}{12n^2} + \frac{q^2}{12}$	$\frac{p}{n} \leq q \leq \frac{(4-\sqrt{3})p}{n}$
III	$(\frac{(n+1)p}{2n}, \frac{p}{2n})$	$\frac{pq}{n} - \frac{p^2}{n^2}$	$\frac{(4-\sqrt{3})p}{n} \leq q \leq \frac{5p}{2n}$
IV	$(\frac{p}{2}, \frac{p}{3})$	$\frac{pq}{2} - \frac{p^2}{4}$	$\frac{5p}{2n} \leq q$

Table 5.9: The best point b^* for $n = 3$.

The ideas here can also be transferred to the $n \neq 3$ case. All that remains is to compare the optima found in Table 5.4 to the optimum of Section $n+1$, yet once we realise that the optimum of Section $n+1$ touching both vertical boundaries of $\mathcal{P}$ is identical in location and area to the bottom optimum of Section $n+1$, touching neither vertical boundary of $\mathcal{P}$ which is the global optimum for cells not touching either vertical boundary, we know that we have already found the hierarchy of optima and we can simply copy the results from Table 5.4 (and these also hold true for $n = 3$). Hence the best points b^* for every odd n are recorded in Table 5.10.

Section	Optimum	Area	Condition
I	$(*, 0)$	$\frac{pq}{2n}$	$q \leq \frac{p}{n}$
II	$(\frac{p}{2}, \frac{q}{3} - \frac{p}{3n})$	$\frac{pq}{3n} + \frac{p^2}{12n^2} + \frac{q^2}{12}$	$\frac{p}{n} \leq q \leq \frac{(4-\sqrt{3})p}{n}$
III	$(\frac{(n+1)p}{2n}, \frac{p}{2n})$	$\frac{pq}{n} - \frac{p^2}{n^2}$	$\frac{(4-\sqrt{3})p}{n} \leq q \leq \frac{5p}{2n}$
IV	$(\frac{p}{2}, \frac{p}{n})$	$\frac{3pq}{2n} - \frac{9p^2}{4n^2}$	$\frac{5p}{2n} \leq q \leq \frac{5p}{n}$
IV	$(\frac{p}{2}, \frac{q}{3} - \frac{2p}{3n})$	$\frac{2pq}{3n} - \frac{p^2}{6n^2} + \frac{q^2}{12}$	$\frac{5p}{n} \leq q \leq \frac{(11-\sqrt{33})p}{n}$
VI	$(\frac{p}{2}, \frac{2p}{n})$	$\frac{5pq}{2n} - \frac{15p^2}{2n^2}$	$\frac{(11-\sqrt{33})p}{n} \leq q \leq \frac{33p}{4n}$
$2l$	$(\frac{p}{2}, (l-1)\frac{p}{n})$	$\frac{(2l-1)pq}{2n} - \frac{3(2l-1)(l-1)p^2}{4n^2}$	$\frac{3(4l-5)p}{4n} \leq q \leq \frac{3(4l-1)p}{4n}$
$n+1$	$(\frac{p}{2}, \frac{(n-1)p}{2n})$	$\frac{pq}{2} - \frac{3(n-1)np^2}{8n^2}$	$\frac{3(2n-3)p}{4n} \leq q$

Table 5.10: The best point b^* for odd n.

And thus we have found all of the best points b^* in $\mathcal{P}$ for every combination of p, q, and n.

5.3.2 Black's best arrangement

As interesting as Black's best point may be, Black must also consider the placement of their other $n-1$ points, and the best single point may actually be a poor placement when considering where to place Black's remaining points.

On top of the relationship between $\frac{p}{n}$ and q restricting what sections are available within which to place Black's points, the idea of modelling the interaction between different black points and consideration of where a black cell would steal from another black cell, thereby reducing the effectiveness of their placement, fills the writer with fear. However, we can learn something

from the optimisation of b_1 within every possible partition of $\mathcal{P}$, as depicted in Figure 5.4 and the tables of Black's best single points.

Making use of the work summarised in Table 5.4 we can achieve crude upper bounds on the area that Black can steal with the naïve suggestion that Black manages to steal the area of their best point for each point. This supposition is not so crazy for low values of q; it is clear that Black can steal a maximum of $\frac{pq}{2}$ if $\frac{p}{n} \geq q$ by placing their points b_i as close as possible to w_i. However, for $\frac{p}{n} \leq q \leq \frac{(4-\sqrt{3})p}{n}$ for which the middle optimum of Section II is the best point, one can easily see that it is not possible to locate n of these points such that no two of Black's Voronoi cells overlap.

Observe from Figure 5.3 that every point $b_1 = (x, y)$ placed in Section III and above steals from at least four quarter cells in $\mathcal{VD}(W)$ all of the area from y upwards (or placed in Section IV and above if b_1 is placed within a quarter cell sharing a vertical boundary with $\mathcal{P}$). Naturally it would be wasteful if Black were to steal such a portion of a single quarter cell more than once (i.e. by two separate placements b_1 and b_2). Since there are a total of $4n$ quarter cells to steal from and n Black points to be positioned in order to steal from these quarter cells, an effective position for $b \in B$ would steal as much area as possible from a particular four quarter cells. This suggests that a utilisation of a row of points as depicted in Figure 5.4f equally spaced with a horizontal separation of $\frac{2p}{n}$ above and below the white row would work rather effectively. Let us formally describe such an arrangement.

With white points being ordered w_1 to w_n left to right where $w_i = (\frac{(2i-1)p}{2n}, 0)$, this arrangement for Black as described would be $b_i^u = (\frac{ip}{n}, \frac{p}{2n})$ and $b_i^d = (\frac{ip}{n}, -\frac{p}{2n})$ for $i = 1, ..., \lfloor \frac{n}{2} \rfloor$ (being the points played above and below White's row respectively). Of course, if n is odd then we have one remaining point b_n to place, and one Voronoi cell $V^\circ(w_n)$ which remains unchallenged by any of Black's points $b_i^{\{u,d\}}$ so it makes most sense to place b_n as close as possible to w_n in order to steal the most $(\frac{pq}{2n})$ from $V^\circ(w_n)$. These arrangements (for n even and odd) are always possible (i.e. the points b_i^u and b_i^d exist) and are pictured in Figure 5.6.

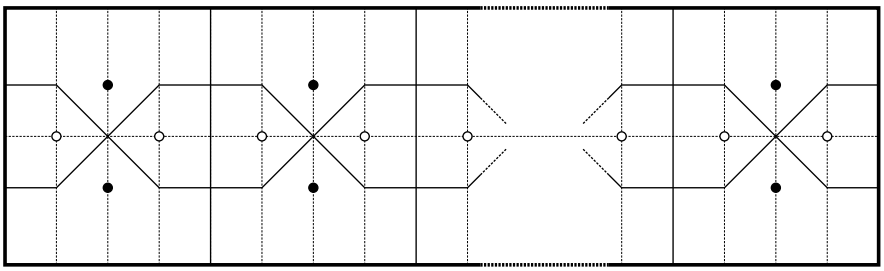

(a) n even.

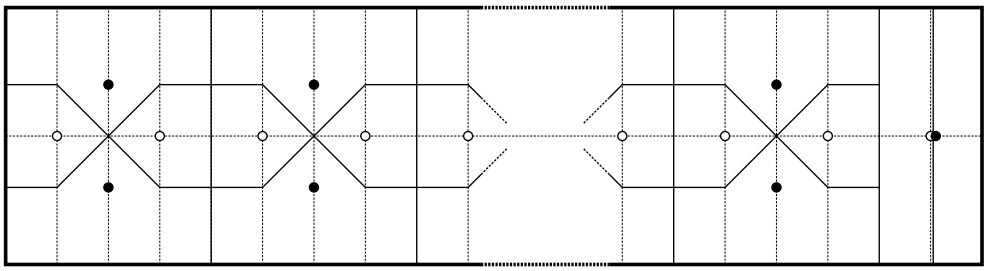

(b) n odd.

Figure 5.6: Arrangements exploiting the efficacy of the best point in Section III.

If n is even then this arrangement scores an area of $pq - 3n \times \frac{p^2}{4n^2} = pq - \frac{3p^2}{4n}$, capturing all of $\mathcal{P}$ outside $-\frac{p}{2n} < y < \frac{p}{2n}$. We know that this arrangement is optimal for $\frac{(4-\sqrt{3})p}{n} \leq q \leq \frac{5p}{2n}$ since it is under this condition that the best point b^* is the lower optimum of Section III and so this arrangement is composed entirely of non-overlapping best points b^*.

Furthermore, we hold that this arrangement is optimal for even n even when $\frac{5p}{2n} \leq q$. This is due to the fact that increasing q merely increases the area controlled by Black's points without

altering White's area. If $\{b_i^u, b_i^d\}_{i\in[1,\dots,n]}$ is not the optimal arrangement for Black then there must be another arrangement which controls more area within $-\frac{p}{2n} < y < \frac{p}{2n}$ of $\mathcal{P}$. However, no arrangement containing a point with a y-coordinate of absolute value greater than $\frac{5p}{2n}$ can steal more area within $-\frac{p}{2n} < y < \frac{p}{2n}$ of $\mathcal{P}$. Therefore this better arrangement must also exist for $\frac{5p}{2n} \geq q$ and so be the optimal arrangement for some range of $\frac{(4-\sqrt{3})p}{n} \leq q \leq \frac{5p}{2n}$, providing an obvious contradiction.

Thus we have found Black's optimal play for even n and $\frac{(4-\sqrt{3})p}{n} \leq q$ in response to White playing a row. Results for odd n and $\frac{(4-\sqrt{3})p}{n} \geq q$ are less obvious, though we suspect that the best point within Section III will be prevalent in optimal arrangements, not least effective arrangements.

5.4 White plays an $a \times b$ grid

Next we shall explore the placement of Black's point b_1 within grids with depth greater than one. We assume that the points are positioned in an $a \times b$ grid and without loss of generality let us assume $\frac{p}{a} \geq \frac{q}{b}$. Since White's arrangement is repetitive and has such symmetry, our search for Black's optimal location is greatly simplified as we need only consider the placement of b_1 within a small selection of areas of $\mathcal{P}$.

Again we shall investigate the possible Voronoi diagrams $\mathcal{VD}(W \cup b_1)$ (in order to find the placement of b_1 so as to maximise $Area(V^+(b_1))$) by partitioning the arena into subsets within which the Voronoi diagram is structurally identical. Since $\mathcal{P}$ is rectangular and all of White's bisectors are vertical and horizontal then, from Averbakh et al. (2015), the partitioning lines are simply the configuration lines of each of White's points.

In any $a \times b$ grid of points W in $\mathcal{P}$ with $a, b \geq 2$, there exists a 2×2 subgrid within the arrangement. An example of such a subgrid is shown in Figure 5.7 along with its partition of the space into regions within which the cell $V^+(b_1)$ is structurally identical. This subgrid can be found by choosing any point $w_0 \in W$ and orienting $\mathcal{P}$ so that w_0 is the bottom left vertex of a 2×2 subgrid. Having done this we will label the adjacent point to the right of w_0 by w_{0_R} and then label every pair of left and right points directly above w_0 and w_{0_R} by w_{i_L} and w_{i_R} respectively and every pair of left and right points directly below w_0 and w_{0_R} by w_{-i_L} and w_{-i_R} respectively, where i marcates these pairs as being the ith pairs away from w_0 and w_{0_R} in their given directions. That is, taking $w_0 = (0, 0)$, we have the following expressions: $w_{i_L} = \left(0, \frac{iq}{b}\right)$ and $w_{i_R} = \left(\frac{p}{a}, \frac{iq}{b}\right)$ for $i \in \mathbb{Z}$ (where $w_{0_L} = w_0$). Similarly define $w_{i_{LL}} = \left(-\frac{p}{a}, \frac{iq}{b}\right)$ for $i \in \mathbb{Z}$ to be the set of points adjacent to the left of w_{i_L}. Note that w_{i_L} and w_{i_R} may not exist for $i \in \mathbb{Z} \setminus \{0, 1\}$, nor may $w_{i_{LL}}$ for any $i \in \mathbb{Z}$, so these are not depicted in Figure 5.7.

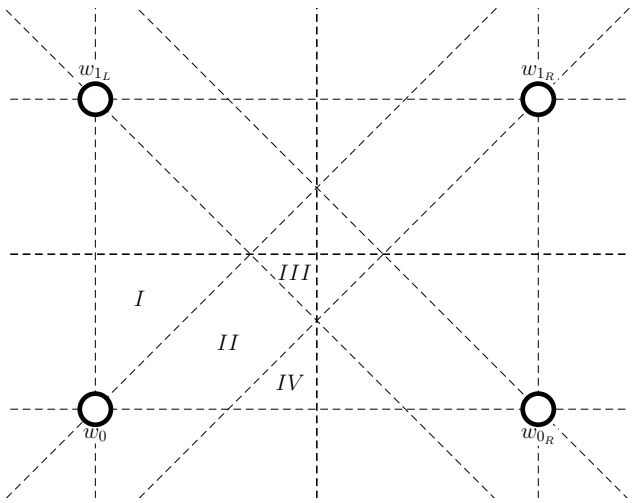

Figure 5.7: The partition of $\mathcal{P}$ for an example 2×2 subgrid of W.

Without loss of generality let us choose to place b_1 within the first quadrant of $V^\circ(w_0)$. By the symmetry of this 2×2 subgrid, every possible cell type of $V^+(b_1)$ can be grown from this placement, adjusting the number of white points with which to generate a bisector outside the 2×2 subgrid in whichever direction we choose (as will be shown). Note that it is only the points w_{i_L}, w_{i_R}, and $w_{0_{LL}}$ and $w_{1_{LL}}$ that can contribute a bisector part to the perimeter of $V^+(b_1)$ since $\frac{p}{a} \geq \frac{q}{b}$. We can also use this quadrant to investigate the structures that $V^+(b_1)$ can take when placed outside a 2×2 subgrid (i.e. placed in a quadrant of $V^\circ(w)$ for some w which borders the perimeter of $\mathcal{P}$) by introducing boundaries along the borders of $V^\circ(w_0)$ as required (as will also be shown).

The observant reader may realise that there should perhaps be at least another configuration line contributing to the partition in Figure 5.7: the potential configuration line $\mathcal{CL}^4(w_{-1_R})$, for example. While indeed b_1 will interact with w_{-1_R} (if existing) if $b_1 \in \mathcal{CC}^1(w_0)$, this interaction will be identical no matter whether $b_1 \in \mathcal{CC}^3(w_{-1_R})$ or $b_1 \in \mathcal{CC}^4(w_{-1_R})$. This is because the only bisector part present in $B(b_1, w_{-1_R})$ is the diagonal part, identical in its representation for both $\mathcal{CC}^3(w_{-1_R})$ and $\mathcal{CC}^4(w_{-1_R})$ bisectors. In order to present a horizontal or vertical bisector part, one of the quadrant lines of b_1 must enter the cell $V^\circ(w_{-1_R})$. Therefore the only configuration lines required are from those points in W lying on the quadrant lines through w_1. For that reason we may also ignore the configuration lines $\mathcal{CC}^3(w_{-i_R})$, $\mathcal{CC}^5(w_{i_R})$, and $\mathcal{CC}^7(w_{1_{LL}})$ for all $i \in \mathbb{N}$. Moreover, since $\frac{p}{a} \geq \frac{q}{b}$, the configuration lines of w_{0_R} and $w_{0_{LL}}$ do not enter the first quadrant of $V^\circ(w_0)$, so the only lines contributing to our partition are $\mathcal{CC}^7(w_{i_L})$ and $\mathcal{CC}^1(w_{-i_L})$ for $i \in \mathbb{N}$.

As $\frac{p}{2a}$ increases in relation to $\frac{q}{2b}$ from the proportions shown in Figure 5.7, the partitioning lines $\mathcal{CC}^7(w_{i_L})$ and then $\mathcal{CC}^1(w_{-i_L})$ for $i \in \mathbb{N}$ will begin to contribute to the partition of $\mathcal{P}$. In this way, momentously, the partition confined to the top right quadrant of $V^\circ(w_0)$ is identical to the partition studied for White's row arrangement (shown in Figure 5.2) but reflected in $y = x$ and with the width $\frac{p}{2n}$ and height $\frac{q}{2}$ of the quadrant being explored replaced by $\frac{q}{2b}$ and $\frac{p}{2a}$ respectively (truncated, instead, by the bisector $B(w_0, w_{0_R})$). In this way we have the partition cells as in Figure 5.2 which are Section I ($\mathcal{CC}^2(w_0)$), Section $2l$ ($\mathcal{CC}^1(w_{1-l_L}) \setminus \mathcal{CC}^8(w_{l_L})$) for $0 \leq \frac{(l-1)q}{b} \leq \frac{p}{2a}$, and Section $2l+1$ ($\mathcal{CC}^8(w_{l_L}) \setminus \mathcal{CC}^1(w_{-l_L})$) for $\frac{q}{2b} \leq \frac{(2l-1)q}{2b} \leq \frac{p}{2a}$, as shown in Figure 5.8. Note that, since b is finite, Sections $2l$ and $2l+1$ do not always exist. If w_0 is on the ith row of White points (counting from the bottom of the $a \times b$ grid) then the last possible partition section will be bounded by either $\mathcal{CL}^2(w_{1-i_L})$ (so would be Section $2i$) or by $\mathcal{CL}^8(w_{b-i_L})$ (so would be Section $2(b-i)+1$) depending on whether $-(1-i) \geq b-i \Leftrightarrow i \geq \frac{b+1}{2}$ or not, respectively.

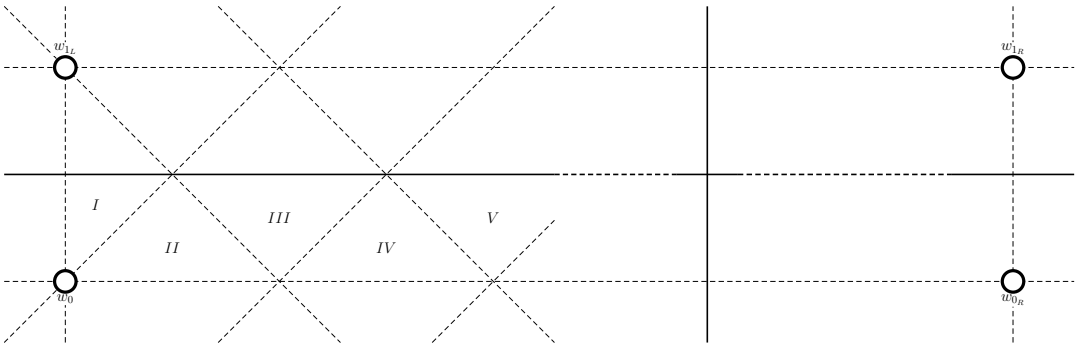

Figure 5.8: The partition of $\mathcal{P}$ for a general 2×2 subgrid of W.

In order to obtain a feel for how $V^+(b_1)$ can appear under White's grid arrangements, in Figure 5.9 we shall draw the first three unique structures that $V^+(b_1)$ can take from the partition displayed in Figure 5.7 (combining II and IV into what we refer to as Section II). Whilst they are shown to extend to the furthest that a grid arrangement would allow, one can easily imagine how the cells are truncated if they hit the boundary of $\mathcal{P}$ before closing (for example, if $w_{0_{LL}}$ and $w_{1_{LL}}$ do not exist then $V^+(b_1)$ in Figure 5.9a will be prevented from expanding any further left than the boundary of $\mathcal{P}$ at $x = -\frac{p}{2a}$).

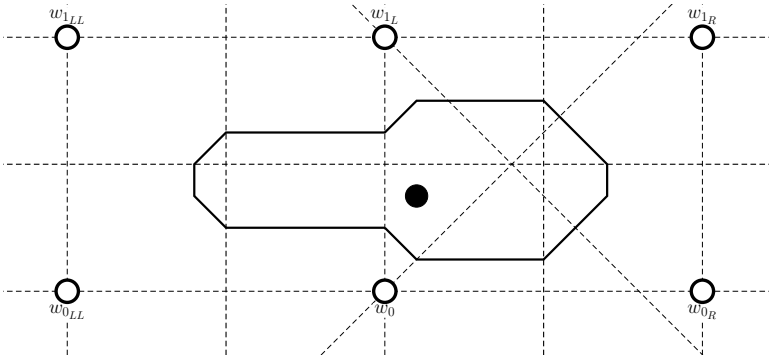

(a) Voronoi cell $V^+(b_1)$ for b_1 in Section I.

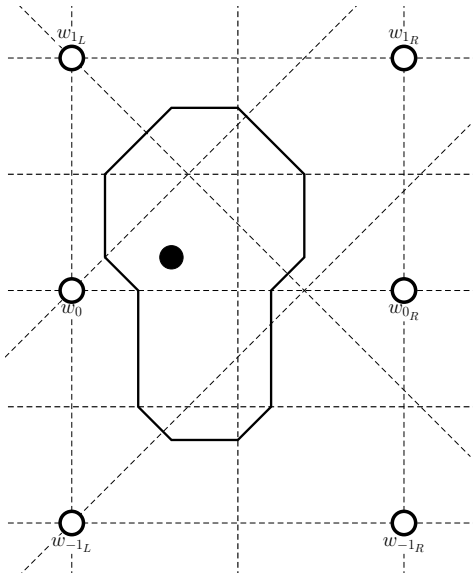

(b) Voronoi cell $V^+(b_1)$ for b_1 in Section II.

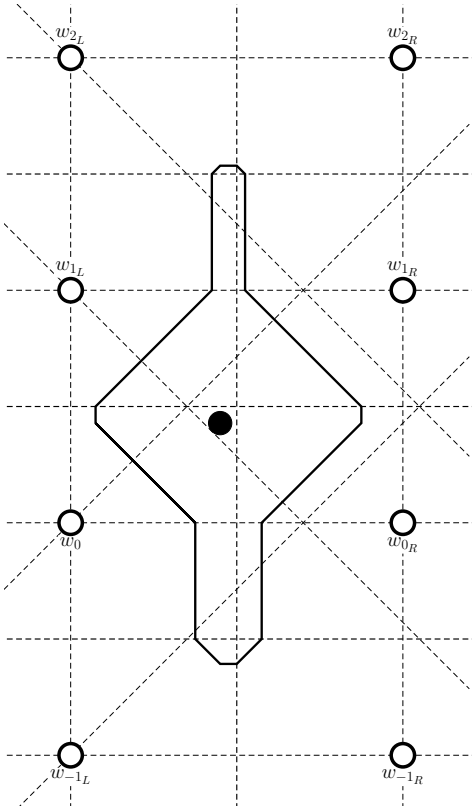

(c) Voronoi cell $V^+(b_1)$ for b_1 in Section III.

Figure 5.9: Voronoi cells $V^+(b_1)$ for b_1 in respective sections according to Figure 5.8.

From these figures we can see that our situation is very similar to the situation we faced in Section 5.2. Yet again, if b_1 is placed within Section I then $V^+(b_1)$ exhibits a particularly unique structure, whilst Section $2l$ and $2l+1$ Voronoi cells resemble one another fairly closely, with $V^+(b_1)$ entering $V^\circ(w_{l+1_L}) \cup V^\circ(w_{l+1_R})$ as b_1 ventures from Section $2l$ to $2l+1$ and enters into $V^\circ(w_{-(l+1)_L}) \cup V^\circ(w_{-(l+1)_R})$ as b_1 ventures from Section $2l+1$ to $2(l+1)$. Therefore, as before, it will prove useful to analyse the area of $V^+(b_1)$ stolen from each constituent block $V^\circ(w_{i_L}) \cup V^\circ(w_{i_R})$ for $i \in \mathbb{Z}$ in the case that $b_1 = (x, y)$ is not in Section I.

Theft from $V^\circ(w_{0_L}) \cup V^\circ(w_{0_R})$ Firstly we will look at the area of $V^+(b_1)$ intersected with $V^\circ(w_{0_L}) \cup V^\circ(w_{0_R})$. Since $b_1 \in \mathcal{CC}^1(w_{0_L}) \cap \mathcal{CC}^4(w_{0_R})$ (as we are not considering b_1 in Section I) this area always exists, has vertices $(\frac{x-y}{2}, \frac{q}{2b})$, $(\frac{x-y}{2}, y)$, $(\frac{x+y}{2}, 0)$, $(\frac{x+y}{2}, -\frac{q}{2b})$, $(\frac{p}{2a} + \frac{x-y}{2}, -\frac{q}{2b})$, $(\frac{p}{2a} + \frac{x-y}{2}, 0)$, $(\frac{p}{2a} + \frac{x+y}{2}, y)$, and $(\frac{p}{2a} + \frac{x+y}{2}, \frac{q}{2b})$, and totals

$$\begin{aligned} Area(V^+(b_1) \cap (V^\circ(w_{0_L}) \cup V^\circ(w_{0_R}))) &= (\frac{p}{2a} + \frac{x+y}{2} - \frac{x+y}{2}) \times \frac{q}{b} - y^2 \\ &= \frac{pq}{2ab} - y^2 \,. \end{aligned}$$

It is clear that this area is maximised by $y = 0$ and is invariant in the value of x.

Theft from $V^\circ(w_{i_L}) \cup V^\circ(w_{i_R})$ for $b_1 \in \mathcal{CC}^8(w_{i_L})$ or $b_1 \in \mathcal{CC}^1(w_{-i_L})$ Now we shall determine the areas of $V^+(b_1)$ intersected with $V^\circ(w_{i_L}) \cup V^\circ(w_{i_R})$ in which $V^+(b_1)$ steals area at every y value of $V^\circ(w_{i_L}) \cup V^\circ(w_{i_R})$. That is, if $i > 0$, that $V^+(b_1)$ also enters $V^\circ(w_{i+1_L}) \cup V^\circ(w_{i+1_R})$ (if existing) so $b_1 \in \mathcal{CC}^8(w_{i_L})$ (which restricts b_1 to also lie within $\mathcal{CC}^5(w_{i_R})$) and, if $i < 0$, that $V^+(b_1)$ also enters $V^\circ(w_{i-1_L}) \cup V^\circ(w_{i-1_R})$ (if existing) so $b_1 \in \mathcal{CC}^1(w_{i_L})$ (which restricts b_1 to also lie within $\mathcal{CC}^4(w_{i_R})$). This restricts b_1 to lie within Sections $2i+1$ and beyond if $i > 0$ or Sections $2(-i+1)$ and beyond if $i < 0$. By symmetry these areas (for $i > 0$ and $i < 0$) have the same structure and, since these structures rely only on the distance between b_1 and the generators of the Voronoi cells in question, the representations are nigh identical.

For $i > 0$ the area has vertices $(\frac{iq}{2b} + \frac{x-y}{2}, \frac{(2i+1)q}{2b})$, $(\frac{iq}{2b} + \frac{x-y}{2}, \frac{iq}{b})$, $(\frac{(i-1)q}{2b} + \frac{x-y}{2}, \frac{(2i-1)q}{2b})$, $(\frac{p}{2a} - \frac{(i-1)q}{2b} + \frac{x+y}{2}, \frac{(2i-1)q}{2b})$, $(\frac{p}{2a} - \frac{iq}{2b} + \frac{x+y}{2}, \frac{iq}{b})$, and $(\frac{p}{2a} - \frac{iq}{2b} + \frac{x+y}{2}, \frac{(2i+1)q}{2b})$ and totals

$$\begin{aligned} Area(V^+(b_1) \cap (V^\circ(w_{i_L}) \cup V^\circ(w_{i_R}))) &= (\frac{p}{2a} - \frac{iq}{2b} + \frac{x+y}{2} - (\frac{iq}{2b} + \frac{x-y}{2})) \times \frac{q}{b} + \left(\frac{q}{2b}\right)^2 \\ &= (\frac{p}{2a} - \frac{iq}{b} + y) \times \frac{q}{b} + \frac{q^2}{4b^2} \\ &= \frac{q}{b}y + \frac{pq}{2ab} - \frac{(4i-1)q^2}{4b^2} \,. \end{aligned}$$

For $i < 0$ the area has vertices $(\frac{x+y}{2} - \frac{(i+1)q}{2b}, \frac{(2i+1)q}{2b})$, $(\frac{x+y}{2} - \frac{iq}{2b}, \frac{iq}{b})$, $(\frac{x+y}{2} - \frac{iq}{2b}, \frac{(2i-1)q}{2b})$, $(\frac{p}{2a} + \frac{iq}{2b} + \frac{x-y}{2}, \frac{(2i-1)q}{2b})$, $(\frac{p}{2a} + \frac{iq}{2b} + \frac{x-y}{2}, \frac{iq}{b})$, and $(\frac{p}{2a} + \frac{(i+1)q}{2b} + \frac{x-y}{2}, \frac{(2i+1)q}{2b})$ and totals

$$\begin{aligned} Area(V^+(b_1) \cap (V^\circ(w_{i_L}) \cup V^\circ(w_{i_R}))) &= (\frac{p}{2a} + \frac{iq}{2b} + \frac{x-y}{2} - (\frac{x+y}{2} - \frac{iq}{2b})) \times \frac{q}{b} + \left(\frac{q}{2b}\right)^2 \\ &= (\frac{p}{2a} + \frac{iq}{b} - y) \times \frac{q}{b} + \frac{q^2}{4b^2} \\ &= -\frac{q}{b}y + \frac{pq}{2ab} + \frac{(4i+1)q^2}{4b^2} \,. \end{aligned}$$

Again, neither area depends on the value of x; however, the area is maximised if $i > 0$ by $y = \frac{p}{2a}$ and if $i < 0$ by $y = 0$.

Theft from $V^\circ(w_{i_L}) \cup V^\circ(w_{i_R})$ for $b_1 \in \mathcal{CC}^7(w_{i_L})$ or $b_1 \in \mathcal{CC}^2(w_{-i_L})$ Finally we shall determine the areas of $V^+(b_1)$ intersected with $V^\circ(w_{i_L}) \cup V^\circ(w_{i_R})$ in which $V^+(b_1)$ steals only at certain values of y in $V^\circ(w_{i_L}) \cup V^\circ(w_{i_R})$. That is, if $i > 0$, that $V^+(b_1)$ does not enter $V^\circ(w_{i+1_L}) \cup V^\circ(w_{i+1_R})$ (if existing) so $b_1 \in \mathcal{CC}^7(w_{i_L})$ (which restricts b_1 to also lie within $\mathcal{CC}^6(w_{i_R})$) and, if $i < 0$, that $V^+(b_1)$ does not enter $V^\circ(w_{i-1_L}) \cup V^\circ(w_{i-1_R})$ (if existing) so $b_1 \in \mathcal{CC}^2(w_{i_L})$ (which restricts b_1 to also lie within $\mathcal{CC}^3(w_{i_R})$). This restricts b_1 to lie within Sections $2i-1$ and $2i$ if $i > 0$ (note that this area only holds for b_1 within Section II if $i = 1$) or Sections $2(-i)$ and $2(-i)+1$ if $i < 0$. Analogously to above, both of these areas are the same structures with only subtly different representations.

For $i > 0$ the area has vertices $(\frac{p}{2a}, \frac{iq}{2b} + \frac{x+y}{2})$, $(x, \frac{iq}{2b} + \frac{x+y}{2})$, $(\frac{(i-1)q}{2b} + \frac{x-y}{2}, \frac{(2i-1)q}{2b})$, and $(\frac{p}{2a} - \frac{(i-1)q}{2b} + \frac{x+y}{2}, \frac{(2i-1)q}{2b})$ and totals

$$\begin{aligned}
Area(V^+(b_1) \cap (V^\circ(w_{i_L}) \cup V^\circ(w_{i_R}))) &= \left(\frac{p}{2a} - \left(\frac{(i-1)q}{2b} + \frac{x-y}{2}\right)\right) \times \left(\frac{iq}{2b} + \frac{x+y}{2} - \frac{(2i-1)q}{2b}\right) \\
&= \left(\frac{p}{2a} - \frac{(i-1)q}{2b} - \frac{x-y}{2}\right) \times \left(-\frac{(i-1)q}{2b} + \frac{x+y}{2}\right) \\
&= -\frac{x^2}{4} + \frac{y^2}{4} + \frac{p}{4a}x + \left(\frac{p}{4a} - \frac{(i-1)q}{2b}\right) y \\
&\quad - \frac{(i-1)pq}{4ab} + \frac{(i-1)^2q^2}{4b^2}\,.
\end{aligned}$$

For $i < 0$ the area has vertices $(-\frac{(i+1)q}{2b} + \frac{x+y}{2}, \frac{(2i+1)q}{2b})$, $(x, \frac{iq}{2b} - \frac{x-y}{2})$, $(\frac{p}{2a}, \frac{iq}{2b} - \frac{x-y}{2})$, and $(\frac{p}{2a} + \frac{(i+1)q}{2b} + \frac{x-y}{2}, \frac{(2i+1)q}{2b})$ and totals

$$\begin{aligned}
Area(V^+(b_1) \cap (V^\circ(w_{i_L}) \cup V^\circ(w_{i_R}))) &= \left(\frac{p}{2a} - \left(-\frac{(i+1)q}{2b} + \frac{x+y}{2}\right)\right) \times \left(\frac{(2i+1)q}{2b} - \left(\frac{iq}{2b} - \frac{x-y}{2}\right)\right) \\
&= \left(\frac{p}{2a} + \frac{(i+1)q}{2b} - \frac{x+y}{2}\right) \times \left(\frac{(i+1)q}{2b} + \frac{x-y}{2}\right) \\
&= -\frac{x^2}{4} + \frac{y^2}{4} + \frac{p}{4a}x - \left(\frac{p}{4a} + \frac{(i+1)q}{2b}\right) y \\
&\quad + \frac{(i+1)pq}{4ab} + \frac{(i+1)^2q^2}{4b^2}\,.
\end{aligned}$$

Now both areas are maximised by $x = \frac{p}{2a}$ to give, if $i > 0$,

$$Area(V^+(b_1) \cap (V^\circ(w_{i_L}) \cup V^\circ(w_{i_R}))) = \frac{y^2}{4} + \left(\frac{p}{4a} - \frac{(i-1)q}{2b}\right) y - \frac{(i-1)pq}{4ab} + \frac{p^2}{16a^2} + \frac{(i-1)^2q^2}{4b^2}$$

and, if $i < 0$,

$$Area(V^+(b_1) \cap (V^\circ(w_{i_L}) \cup V^\circ(w_{i_R}))) = \frac{y^2}{4} - \left(\frac{p}{4a} + \frac{(i+1)q}{2b}\right) y + \frac{(i+1)pq}{4ab} + \frac{p^2}{16a^2} + \frac{(i+1)^2q^2}{4b^2}$$

(and if this optimum is not achievable then, fixing y, the area increases as x moves closer to $\frac{p}{2a}$). If $i > 0$ then the maximiser is

$$\begin{aligned}
y &= \frac{(i-1)q}{b} - \frac{p}{2a} \\
&= \frac{(2i-3)q}{2b} - \frac{p}{2a} + \frac{q}{2b} \\
&\leq \frac{q}{2b}
\end{aligned}$$

relying on the fact that, since Section $2i-1$ must exist in some form (for $i \neq 1$) for this area to be formed, it must be the case that $\frac{(2i-3)q}{2b} \leq \frac{p}{2a}$. On the other hand, if $i < 0$ then the maximiser is

$$\begin{aligned}
y &= \frac{p}{2a} + \frac{(i+1)q}{b} \\
&\geq 0
\end{aligned}$$

relying on the fact that, since Section $2(-i)$ must exist in some form for this area to be formed, it must be the case that $\frac{(-i-1)q}{b} \leq \frac{p}{2a}$.

Not only are these calculations useful for formulating the representation of the different areas of $V^+(b_1)$ for b_1 contained in different sections within the first quadrant of $V^\circ(w_0)$, but they provide a very strong clue to where we will find the optimum to maximise $Area(V^+(b_1))$.

Recall from Section 5.3 (in particular the discussion surrounding Figure 5.5) that Black will always improve upon their area, when locating upon the boundary of two sections, by choosing to locate in the higher section – or in our case, the rightmost section. Additionally we have found that the x-coordinate of b_1 does not affect the area of $V^+(b_1)$ within most Voronoi cells in $\mathcal{VD}(W)$ and, when the value of x does contribute to the representation of $Area(V^+(b_1))$, the optimal direction of movement is rightwards within the first quadrant of $V^\circ(w_0)$. Combining these two properties, we can say that the optimum b_1 within Section II and beyond lies on the line $x^* = \frac{p}{2a}$; for any fixed y, $Area(V^+(b_1))$ increases as x increases within a section, and will increase upon crossing a configuration line into a section of greater value (increasing x) so the best point for fixed y lies at $x = \frac{p}{2a}$.

This remains true no matter whether $V^+(b_1)$ intersects the top or bottom perimeter of $\mathcal{P}$. Therefore, since our interest is Black's best point, in contrast to Section 5.2 we need not calculate the areas of every possible $V^+(b_1)$ structure and optimise this area over the partition within which this structure is maintained. Now we need only explore Section I and the line $x^* = \frac{p}{2a}$, taking care to remember to check for special cases if $V^+(b_1)$ interacts with the boundary of $\mathcal{P}$.

5.5 Black's optimal strategy: White plays an $a \times b$ grid

5.5.1 Black's best point

Many ideas from our discussion in Section 5.3 carry over to the case where White plays a grid. We will limit our exploration of Black's best point b^* to *core quadrants*. We will call the first quadrant of $V^\circ(w_0)$ a *core* quadrant if it borders only other Voronoi cells (and not the boundary of $\mathcal{P}$); that is, if w_{0_R} and w_{1_L} both exist. It is only these quadrants that we are interested in because, as explained in Section 5.3, Black's best point will never be contained in a quadrant bordering $\mathcal{P}$ as long as core quadrants exist. As before, Black's best point will never be located next to the boundary of $\mathcal{P}$. This is simply because, if $V^+(b_1)$ touches one boundary of $\mathcal{P}$, translating the point a distance $\frac{p}{a}$ or $\frac{q}{b}$ perpendicularly away from a vertical or horizontal boundary of $\mathcal{P}$ respectively will allow $V^+(b_1)$ to enter a new uncharted pair of Voronoi cells $V^\circ(w_{i_L}) \cup V^\circ(w_{i_R})$ (up to orientation), and if $V^+(b_1)$ touches opposite boundaries of $\mathcal{P}$ then, since b_1 is more effective at stealing area from Voronoi cells closest to b_1, b_1 does better when equally distant from both boundaries. This will be explained in greater detail later within this section.

As in Section 5.3, Figure 5.10 will depict all optimal locations of b_1 within each required section under the particular circumstances we will discuss below; again, Section IV and Section III are depicted as the poster children for the general Section $2l$ and Section $2l+1$ results respectively and for clarity these respective sections will be shaded in each figure.

As described above there are two areas of interest within these core quadrants: Section I, and the line $x^* = \frac{p}{2a}$.

Section I First we explore $V^+(b_1)$ for b_1 in Section I. It has vertices, tracing the perimeter clockwise, $(0, \frac{x+y}{2})$, $(x, \frac{y-x}{2})$, $(\frac{p}{2a}, \frac{y-x}{2})$, $(\frac{p}{2a}+\frac{x+y}{2}, y)$, $(\frac{p}{2a}+\frac{x+y}{2}, \frac{q}{2b})$, $(\frac{p}{2a}, \frac{q}{2b}+\frac{x+y}{2})$, $(x, \frac{q}{2b}+\frac{x+y}{2})$, $(0, \frac{q}{2b}+\frac{y-x}{2})$, $(-\frac{p}{2a}, \frac{q}{2b}+\frac{y-x}{2})$, $(-\frac{p}{2a}-\frac{y-x}{2}, \frac{q}{2b})$, $(-\frac{p}{2a}-\frac{y-x}{2}, y)$, and $(-\frac{p}{2a}, \frac{x+y}{2})$, giving an area

$$\begin{aligned} Area(V^+(b_1)) &= (\frac{p}{2a}+\frac{x+y}{2}) \times (\frac{q}{2b}+\frac{x+y}{2}-\frac{y-x}{2}) - x^2 - (\frac{x+y}{2})^2 \\ &\quad + (\frac{p}{2a}+\frac{y-x}{2}) \times (\frac{q}{2b}+\frac{y-x}{2}-\frac{x+y}{2}) - (\frac{y-x}{2})^2 \\ &= \frac{q}{2b}(\frac{p}{a}+y) + x(x) - \frac{3x^2+y^2}{2} \\ &= -\frac{x^2}{2} - \frac{y^2}{2} + \frac{q}{2b}y + \frac{pq}{2ab} \end{aligned}$$

or, if points $w_{0_{LL}}$ and $w_{1_{LL}}$ do not exist (i.e. $V^\circ(w_0)$ borders the perimeter of $\mathcal{P}$),

$$
\begin{aligned}
Area(V^+(b_1)) &= (\frac{p}{2a} + \frac{x+y}{2}) \times (\frac{q}{2b} + \frac{x+y}{2} - \frac{y-x}{2}) - x^2 - (\frac{x+y}{2})^2 \\
&\quad + \frac{p}{2a} \times (\frac{q}{2b} + \frac{y-x}{2} - \frac{x+y}{2}) \\
&= \frac{q}{2b}(\frac{p}{a} + \frac{x+y}{2}) + x(\frac{x+y}{2}) - \frac{5x^2+2xy+y^2}{4} \\
&= -\frac{3x^2}{4} - \frac{y^2}{4} + \frac{q}{4b}x + \frac{q}{4b}y + \frac{pq}{2ab}\,.
\end{aligned}
$$

Assuming that points $w_{0_{LL}}$ and $w_{1_{LL}}$ do exist, to find the maximum of this over Section I we first use gradient methods

$$
\begin{aligned}
\frac{\delta A}{\delta x} &= -x \\
\frac{\delta A}{\delta y} &= -y + \frac{q}{2b}
\end{aligned}
$$

to ascertain that the maximum of $Area(V^+(b_1))$ is found at $b_1^* = (0, \frac{q}{2b})$ (still contained in Section I), giving $Area(V^+(b_1^*)) = \frac{pq}{2ab} + \frac{q^2}{8b^2}$. This is depicted in Figure 5.10a.

Alternatively, if the points $w_{0_{LL}}$ and $w_{1_{LL}}$ do not exist, we have gradients

$$
\begin{aligned}
\frac{\delta A}{\delta x} &= -\frac{3x}{2} + \frac{q}{4b} \\
\frac{\delta A}{\delta y} &= -\frac{y}{2} + \frac{q}{4b}
\end{aligned}
$$

so the area reaches its maximum at $b_1^* = (\frac{q}{6b}, \frac{q}{2b})$ (still contained in Section I), giving $Area(V^+(b_1^*)) = \frac{pq}{2ab} + \frac{q^2}{12b^2}$. This is depicted in Figure 5.10b.

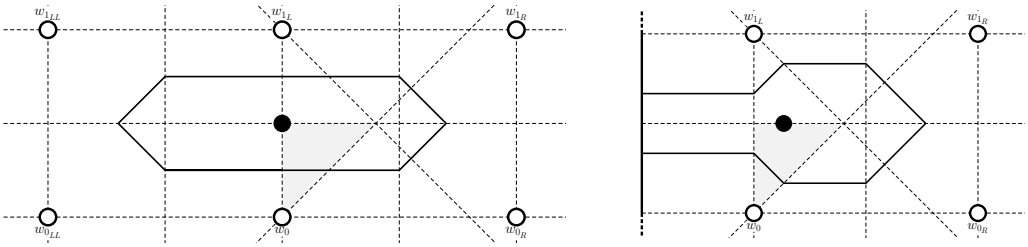

(a) $b_1 = (0, \frac{q}{2b})$. (b) $b_1 = (\frac{q}{6b}, \frac{q}{2b})$.

Figure 5.10: Maximal area Voronoi cells $V^+(b_1)$ for b_1 within Section I.

Section $2l$ upon $x^* = \frac{p}{2a}$ Within the first quadrant of $V^\circ(w_0)$, the line $x^* = \frac{p}{2a}$ can be in an even section, an odd section, or both (entering into Section $2l+1$ from Section $2l$ as y increases from 0). Therefore we must explore the area formulae for b_1 in each section separately. Beginning with the placement of b_1 inside the even Section $2l$ (where $\frac{(l-1)q}{b} \leq \frac{p}{2a} \leq \frac{lq}{b} \Rightarrow l = \lceil \frac{pb}{2qa} \rceil$), $V^+(b_1)$ will extend into Voronoi cells $V^\circ(w_{i_L}) \cup V^\circ(w_{i_R})$ for $i \in \{-l, \ldots, l\}$ (if existing).

Now the effect caused by the non-existence of these faraway Voronoi cells (i.e. the area that the boundary of $\mathcal{P}$ cuts off) can greatly diminish the suitability of the placement of b_1 if we are in search of Black's best point. It is clear that, if w_{l_L} does not exist while w_{-l-1_L} does, simply choosing w_0 to be the point directly below it (w_{-1_L}) will be beneficial to increasing the maximum area that $V^+(b_1)$ can take when locating within the first quadrant of $V^\circ(w_0)$, simply because this translation of our point of reference $\frac{q}{b}$ lower will allow $V^+(b_1)$ not only to keep exactly the same area as before but also to enter another previously untapped Voronoi cell of White's. The same is clearly true for the analogous case where it is w_{-l_L} that does not exist

while w_{l+1_L} does, and these alterations of w_0 can of course be repeated until all Voronoi cells $V^\circ(w_{i_L}) \cup V^\circ(w_{i_R})$ for $i \in \{-l, \dots, l\}$ exist (in which case $b > 2l$ and $V^+(b_1)$ does not interact with $\mathcal{P}$, and we may not necessarily have a unique best point of reference for w_0), or until both w_{l_L} and w_{-l-1_L} or w_{-l_L} and w_{l+1_L} do not exist.

If both w_{l_L} and w_{-l-1_L} or w_{-l_L} and w_{l+1_L} do not exist while w_{i_L} does for $i \in \{-l, \dots, l-1\}$ or for $i \in \{-l+1, \dots, l\}$ respectively then it is the case that $b = 2l$ and $V^+(b_1)$ touches only one bounding edge of $\mathcal{P}$. In this scenario we must decide which area we would prefer: that stolen from $V^\circ(w_{l_L}) \cup V^\circ(w_{l_R})$ or from $V^\circ(w_{-l_L}) \cup V^\circ(w_{-l_R})$. Since b_1 is being located in the first quadrant of $V^\circ(w_0)$, lying closer to w_{l_L} than w_{-l_L}, it can steal a larger area from $V^\circ(w_{l_L}) \cup V^\circ(w_{l_R})$ than it could from $V^\circ(w_{-l_L}) \cup V^\circ(w_{-l_R})$, so it is favourable for w_0 to be chosen to be on the lth row of points in W (counting from the bottom of the grid) so that $V^+(b_1)$ consists of areas stolen from $V^\circ(w_{i_L}) \cup V^\circ(w_{i_R})$ for all $i \in \{-l+1, \dots, l\}$ (as opposed to for all $i \in \{-l, \dots, l-1\}$).

This idea also applies to areas $V^+(b_1)$ that touch both horizontal bounding edges of $\mathcal{P}$ (so both w_{l_L} and w_{-l_L} do not exist, meaning that $b < 2l$) since, for $i \in \mathbb{Z}^+$, the area stolen from $V^\circ(w_{\pm i_L}) \cup V^\circ(w_{\pm i_R})$ will always be greater than that stolen from $V^\circ(w_{\pm(i+1)_L}) \cup V^\circ(w_{\pm(i+1)_R})$, and also the area stolen from $V^\circ(w_{i_L}) \cup V^\circ(w_{i_R})$ will always be greater than or equal to the area stolen from $V^\circ(w_{-i_L}) \cup V^\circ(w_{-i_R})$. Therefore it is still optimal to choose w_0 to be on the $\lceil \frac{b}{2} \rceil$th row of points in W in order to steal from $V^\circ(w_{i_L}) \cup V^\circ(w_{i_R})$ for all $i \in \{-\lceil \frac{b}{2} \rceil + 1, \dots, \lfloor \frac{b}{2} \rfloor\}$. Note though that, as described in the work preceding Figure 5.8, the final section possible in the top right quadrant of $V^\circ(w_0)$, where w_0 is on the $\lceil \frac{b}{2} \rceil$th row of points in W, is Section $b+1$, no matter whether b is even or odd. Therefore there is only one section within which $V^\circ(w_0)$ touches both horizontal edges of $\mathcal{P}$ and this is Section $b+1$. We will explore this section separately to this investigation, after the Section $2l+1$ material is presented. Thus we shall only consider $b \geq 2l$ here.

Now that we have chosen the optimal w_0 and recorded which Voronoi cells $V^\circ(w_{i_L}) \cup V^\circ(w_{i_R})$ will be entered, we can calculate the areas of the Voronoi cell $V^+(b_1)$ for different values of b and optimise the location of b_1 upon $x^* = \frac{p}{2a}$ within Section $2l$. If $b > 2l$ $\left(= 2\lceil \frac{pb}{2qa} \rceil\right)$ then

$$
\begin{aligned}
Area(V^+(b_1)) &= Area(V^+(b_1) \cap (V^\circ(w_{-l_L}) \cup V^\circ(w_{-l_R}))) \\
&\quad + \sum_{i=-(l-1)}^{-1} Area(V^+(b_1) \cap (V^\circ(w_{i_L}) \cup V^\circ(w_{i_R}))) \\
&\quad + Area(V^+(b_1) \cap (V^\circ(w_{0_L}) \cup V^\circ(w_{0_R}))) \\
&\quad + \sum_{i=1}^{l-1} Area(V^+(b_1) \cap (V^\circ(w_{i_L}) \cup V^\circ(w_{i_R}))) \\
&\quad + Area(V^+(b_1) \cap (V^\circ(w_{l_L}) \cup V^\circ(w_{l_R}))) \\
&= \frac{y^2}{4} - \left(\frac{p}{4a} + \frac{(-l+1)q}{2b}\right) y + \frac{(-l+1)pq}{4ab} + \frac{p^2}{16a^2} + \frac{(-l+1)^2q^2}{4b^2} \\
&\quad + \sum_{i=-l+1}^{-1} \left(-\frac{q}{b}y + \frac{pq}{2ab} + \frac{(4i+1)q^2}{4b^2}\right) \\
&\quad + \frac{pq}{2ab} - y^2 \\
&\quad + \sum_{i=1}^{l-1} \left(\frac{q}{b}y + \frac{pq}{2ab} - \frac{(4i-1)q^2}{4b^2}\right) \\
&\quad + \frac{y^2}{4} + (\frac{p}{4a} - \frac{(l-1)q}{2b})y - \frac{(l-1)pq}{4ab} + \frac{p^2}{16a^2} + \frac{(l-1)^2q^2}{4b^2} \\
&= -\frac{y^2}{2} - \frac{(l-2)pq}{2ab} + \frac{p^2}{8a^2} + \frac{(l-1)^2q^2}{2b^2} + 2\sum_{i=1}^{l-1} \left(\frac{pq}{2ab} - \frac{(4i-1)q^2}{4b^2}\right) \\
&= -\frac{y^2}{2} + \frac{lpq}{2ab} + \frac{p^2}{8a^2} - \frac{(l-1)lq^2}{2b^2}
\end{aligned}
$$

and if $b = 2l$ then, adapting this formula,

$$\begin{aligned}
Area(V^+(b_1)) &= -\frac{y^2}{2} + \frac{lpq}{2ab} + \frac{p^2}{8a^2} - \frac{(l-1)lq^2}{2b^2} \\
&\quad - \text{“}Area(V^+(b_1) \cap (V^\circ(w_{-l_L}) \cup V^\circ(w_{-l_R}))\text{”} \\
&= -\frac{y^2}{2} + \frac{lpq}{2ab} + \frac{p^2}{8a^2} - \frac{(l-1)lq^2}{2b^2} \\
&\quad - \left(\frac{y^2}{4} - \left(\frac{p}{4a} - \frac{(l-1)q}{2b}\right)y - \frac{(l-1)pq}{4ab} + \frac{p^2}{16a^2} + \frac{(l-1)^2q^2}{4b^2}\right) \\
&= -\frac{3y^2}{4} + \left(\frac{p}{4a} - \frac{(l-1)q}{2b}\right)y + \frac{(3l-1)pq}{4ab} + \frac{p^2}{16a^2} - \frac{(l-1)(3l-1)q^2}{4b^2}
\end{aligned}$$

It is straightforward to see that $(\frac{p}{2a}, 0)$ is the optimum if $b > 2l$ giving $Area(V^+((\frac{p}{2a}, 0))) = \frac{lpq}{2ab} + \frac{p^2}{8a^2} - \frac{(l-1)lq^2}{2b^2}$. This is depicted in Figure 5.10c.

For $b = 2l$ we have derivative

$$\frac{\delta A}{\delta y} = -\frac{3y}{2} + \frac{p}{4a} - \frac{(l-1)q}{2b}$$

which gives our optimum to be at $y^* = \frac{p}{6a} - \frac{(l-1)q}{3b} = \frac{p}{6a} - \frac{(b-2)q}{6b}$. However, in order for $b_1 = \left(\frac{p}{2a}, \frac{p}{6a} - \frac{(b-2)q}{6b}\right)$ to lie within Section b it must be the case that, if $\frac{(b-2)q}{2b} \leq \frac{p}{2a} \leq \frac{(b-1)q}{2b}$, b_1 lies below $\mathcal{CL}^2(w_{-\frac{b-2}{2}_L})$ and, if $\frac{(b-1)q}{2b} \leq \frac{p}{2a} \leq \frac{q}{2}$, b_1 lies below $\mathcal{CL}^8(w_{\frac{b}{2}_L})$.

Therefore if $\frac{(b-2)q}{2b} \leq \frac{p}{2a} \leq \frac{(b-1)q}{2b}$ then it must be the case that $y \leq x - \frac{(b-2)q}{2b}$ so we require

$$\frac{p}{6a} - \frac{(b-2)q}{6b} \leq \frac{p}{2a} - \frac{(b-2)q}{2b} \Leftrightarrow \frac{(b-2)q}{3b} \leq \frac{2p}{3a} \Leftrightarrow \frac{(b-2)q}{4b} \leq \frac{p}{2a}\,.$$

Hence b_1 is the optimum in Section b for all values $\frac{(b-2)q}{2b} \leq \frac{p}{2a} \leq \frac{(b-1)q}{2b}$.

Otherwise, if $\frac{(b-1)q}{2b} \leq \frac{p}{2a} \leq \frac{q}{2}$ then it must be the case that $y \leq \frac{q}{2} - x$ so we require

$$\frac{p}{6a} - \frac{(b-2)q}{6b} \leq \frac{q}{2} - \frac{p}{2a} \Leftrightarrow \frac{2p}{3a} \leq \frac{(2b-1)q}{3b} \Leftrightarrow \frac{p}{2a} \leq \frac{(2b-1)q}{4b}\,.$$

Therefore if $\frac{(b-1)q}{2b} \leq \frac{p}{2a} \leq \frac{(2b-1)q}{4b}$ then b_1 is the optimum in Section b. Otherwise, if $\frac{(2b-1)q}{4b} \leq \frac{p}{2a} \leq \frac{q}{2}$ then b_1 will lie above Section b. If this is the case then the optimum over Section b must lie on the boundary between Section b and $b+1$. However, as we saw when exploring Black's best point when White plays a row (see Figure 5.5 for example), any point lying in Section b on the boundary with Section $b+1$ will be dominated by the identical point within Section $b+1$. Therefore Black's best point will not lie in Section b if $\frac{(2b-1)q}{4b} \leq \frac{p}{2a}$.

To summarise, if b is even then: if $\frac{(b-2)q}{2b} \leq \frac{p}{2a} \leq \frac{(2b-1)q}{4b}$ then the optimum in Section b is $(\frac{p}{2a}, \frac{p}{6a} - \frac{(b-2)q}{6b})$ giving $Area(V^+((\frac{p}{2a}, \frac{p}{6a} - \frac{(b-2)q}{6b}))) = \frac{(2b-1)pq}{6ab} + \frac{p^2}{12a^2} - \frac{(b-2)(4b-1)q^2}{12b^2}$ (depicted in Figure 5.10d), otherwise if $\frac{(2b-1)q}{4b} \leq \frac{p}{2a} \leq \frac{q}{2}$ then the optimum lies on the boundary with Section $b+1$ and is not Black's best point (and so is not drawn).

Section $2l+1$ upon $x^* = \frac{p}{2a}$ We now consider the placement of b_1 on $x^* = \frac{p}{2a}$ inside the odd Section $2l+1$ (where $\frac{(2l-1)q}{2b} \leq \frac{p}{2a} \leq \frac{(2l+1)q}{2b} \Rightarrow l = \lceil \frac{pb-qa}{2qa} \rceil$) where $V^+(b_1)$ will extend into Voronoi cells $V^\circ(w_{i_L}) \cup V^\circ(w_{i_R})$ for $i \in \{-l, \ldots, l+1\}$ (if existing).

Now, as before, we will explore the effect caused by the non-existence of these faraway Voronoi cells (i.e. what area the boundary of $\mathcal{P}$ cuts off). We can use identical processes to those described in Section $2l$ in order to find the best point in W to assign to be w_0. If $b > 2l+1$ then we can choose w_0 such that all Voronoi cells $V^\circ(w_{i_L}) \cup V^\circ(w_{i_R})$ for $i \in \{-l, \ldots, l+1\}$ exist and $V^+(b_1)$ does not interact with $\mathcal{P}$ (again we will not have a unique best point of reference for w_0 if $b \neq 2l+2$).

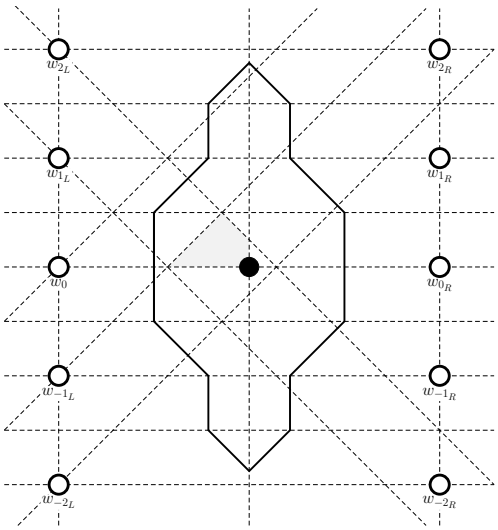

(c) $b_1 = (\frac{p}{2a}, 0)$.

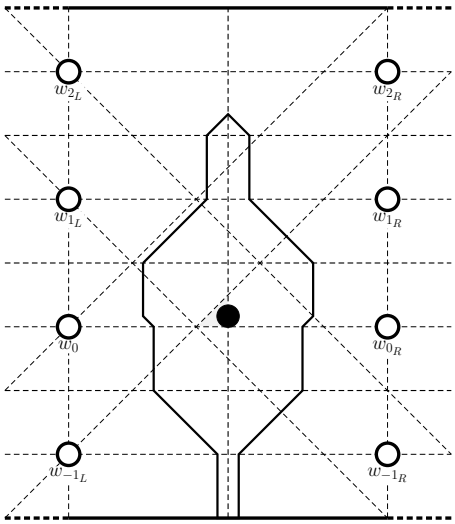

(d) $b_1 = (\frac{p}{2a}, \frac{p}{6a} - \frac{(b-2)q}{6b})$ only if $\frac{(b-2)q}{2b} \leq \frac{p}{2a} \leq \frac{(2b-1)q}{4b}$ and $b = 2l$.

Figure 5.10: Maximal area Voronoi cells $V^+(b_1)$ for b_1 within Section $2l$ upon $x^* = \frac{p}{2a}$.

If both w_{l+1_L} and w_{-l-1_L} or w_{-l_L} and w_{l+2_L} do not exist while w_{i_L} does for $i \in \{-l, \ldots, l\}$ or for $i \in \{-l+1, \ldots, l+1\}$ respectively then it is the case that $b = 2l+1$ and $V^+(b_1)$ touches only one bounding edge of $\mathcal{P}$. In this scenario we must again decide which area we would prefer: that stolen from $V^\circ(w_{l+1_L}) \cup V^\circ(w_{l+1_R})$ or from $V^\circ(w_{-l_L}) \cup V^\circ(w_{-l_R})$. Since b_1 is being located in the first quadrant of $V^\circ(w_0)$, lying closer to w_{-l_L} than w_{l+1_L}, it can steal a larger area from $V^\circ(w_{-l_L}) \cup V^\circ(w_{-l_R})$ than it could from $V^\circ(w_{l+1_L}) \cup V^\circ(w_{l+1_R})$, so it is favourable for w_0 to be chosen to be on the $l+1$th row of points in W (counting from the bottom of the grid) so that $V^+(b_1)$ consists of areas stolen from $V^\circ(w_{i_L}) \cup V^\circ(w_{i_R})$ for all $i \in \{-l, \ldots, l\}$ (as opposed to for all $i \in \{-l+1, \ldots, l+1\}$).

Using an identical argument to that for even sections, for areas $V^+(b_1)$ that touch both horizontal bounding edges of $\mathcal{P}$ (so both w_{l+1_L} and w_{-l_L} do not exist, meaning that $b < 2l+1$) it is still optimal to choose w_0 to be on the $\lceil \frac{b}{2} \rceil$th row of points in W in order to steal from $V^\circ(w_{i_L}) \cup V^\circ(w_{i_R})$ for all $i \in \{-\lceil \frac{b}{2} \rceil + 1, \ldots, \lfloor \frac{b-1}{2} \rfloor\}$. As justified in our analysis of Sections $2l$ it is only within this final Section $b+1$ that both horizontal edges of $\mathcal{P}$ are touched, and we shall explore this section after finishing a full investigation of Sections $2l+1$ for $b \geq 2l+1$.

Now that we have chosen the optimal w_0 and recorded which Voronoi cells $V^\circ(w_{i_L}) \cup V^\circ(w_{i_R})$ will be entered, we can calculate the areas of the Voronoi cell $V^+(b_1)$ for different values of b and optimise the location of b_1 upon $x^* = \frac{p}{2a}$ within Section $2l+1$. We calculate these areas by taking the area found in Section $2l$ and adapting it for Section $2l+1$ (noting that a move from Section $2l$ to $2l+1$ means that $V^+(b_1)$ enters $V^\circ(w_{l+1_L}) \cup V^\circ(w_{l+1_R})$ for the first time). If $b > 2l+1 \left(= 2\lceil \frac{pb-qa}{2qa} \rceil + 1\right)$ then

$$\begin{aligned} Area(V^+(b_1)) = &-\frac{y^2}{2} + \frac{lpq}{2ab} + \frac{p^2}{8a^2} - \frac{(l-1)lq^2}{2b^2} \\ &- \text{“}Area(V^+(b_1) \cap (V^\circ(w_{l_L}) \cup V^\circ(w_{l_R})))\text{”} \\ &+ Area(V^+(b_1) \cap (V^\circ(w_{l_L}) \cup V^\circ(w_{l_R}))) \\ &+ Area(V^+(b_1) \cap (V^\circ(w_{l+1_L}) \cup V^\circ(w_{l+1_R}))) \end{aligned}$$

$$
\begin{aligned}
&= -\frac{y^2}{2} + \frac{lpq}{2ab} + \frac{p^2}{8a^2} - \frac{(l-1)lq^2}{2b^2} \\
&\quad - \left(\frac{y^2}{4} + (\frac{p}{4a} - \frac{(l-1)q}{2b})y - \frac{(l-1)pq}{4ab} + \frac{p^2}{16a^2} + \frac{(l-1)^2q^2}{4b^2} \right) \\
&\quad + \frac{q}{b}y + \frac{pq}{2ab} - \frac{(4l-1)q^2}{4b^2} \\
&\quad + \frac{y^2}{4} + \left(\frac{p}{4a} - \frac{((l+1)-1)q}{2b} \right) y - \frac{((l+1)-1)pq}{4ab} + \frac{p^2}{16a^2} + \frac{((l+1)-1)^2q^2}{4b^2} \\
&= -\frac{y^2}{2} + \frac{q}{2b}y + \frac{(l+1)pq}{4ab} + \frac{p^2}{8a^2} - \frac{l^2q^2}{2b^2}
\end{aligned}
$$

and if $b = 2l+1$ then, adapting this formula,

$$
\begin{aligned}
Area(V^+(b_1)) &= -\frac{y^2}{2} + \frac{q}{2b}y + \frac{(l+1)pq}{4ab} + \frac{p^2}{8a^2} - \frac{l^2q^2}{2b^2} \\
&\quad - \text{“}Area(V^+(b_1) \cap (V^\circ(w_{l+1_L}) \cup V^\circ(w_{l+1_R}))\text{”} \\
&= -\frac{y^2}{2} + \frac{q}{2b}y + \frac{(l+1)pq}{4ab} + \frac{p^2}{8a^2} - \frac{l^2q^2}{2b^2} \\
&\quad - \left(\frac{y^2}{4} + \left(\frac{p}{4a} - \frac{lq}{2b} \right) y - \frac{lpq}{4ab} + \frac{p^2}{16a^2} + \frac{l^2q^2}{4b^2} \right) \\
&= -\frac{3y^2}{4} - \left(\frac{p}{4a} - \frac{(l+1)q}{2b} \right) y + \frac{(2l+1)pq}{4ab} + \frac{p^2}{16a^2} - \frac{3l^2q^2}{4b^2}\,.
\end{aligned}
$$

Clearly $(\frac{p}{2a}, \frac{q}{2b})$ is the optimum if $b > 2l+1$ giving $Area(V^+((\frac{p}{2a}, \frac{q}{2b}))) = \frac{(4l-1)pq}{4ab} + \frac{p^2}{8a^2} - \frac{(4l^2-1)q^2}{8b^2}$ as depicted in Figure 5.10e.

For $b = 2l+1$ we have derivative

$$
\frac{\delta A}{\delta y} = -\frac{3y}{2} - \frac{p}{4a} + \frac{(l+1)q}{2b}
$$

which gives our optimum to be at $y^* = -\frac{p}{6a} + \frac{(l+1)q}{3b} = -\frac{p}{6a} + \frac{(b+1)q}{6b}$. However, in order for $b_1 = (\frac{p}{2a}, \frac{(b+1)q}{6b} - \frac{p}{6a})$ to lie within Section $b+1$ it must be the case that, if $\frac{(b-2)q}{2b} \leq \frac{p}{2a} \leq \frac{(b-1)q}{2b}$, b_1 lies above $\mathcal{CL}^8(w_{\frac{b-1}{2}_L})$ and, if $\frac{(b-1)q}{2b} \leq \frac{p}{2a} \leq \frac{q}{2}$, b_1 lies above $\mathcal{CL}^2(w_{-\frac{b-1}{2}_L})$.

Therefore, if $\frac{(b-2)q}{2b} \leq \frac{p}{2a} \leq \frac{(b-1)q}{2b}$ then it must be the case that $\frac{(b-1)q}{2b} - x \leq y$ so we require

$$
\frac{(b-1)q}{2b} - \frac{p}{2a} \leq \frac{(b+1)q}{6b} - \frac{p}{6a} \Leftrightarrow \frac{(b-2)q}{3b} \leq \frac{p}{3a} \Leftrightarrow \frac{(b-2)q}{2b} \leq \frac{p}{2a}\,.
$$

Hence b_1 is the optimum in Section b for all values $\frac{(b-2)q}{2b} \leq \frac{p}{2a} \leq \frac{(b-1)q}{2b}$.

Otherwise, if $\frac{(b-1)q}{2b} \leq \frac{p}{2a} \leq \frac{q}{2}$ then it must be the case that $x - \frac{(b-1)q}{2b} \leq y$ so we require

$$
\frac{p}{2a} - \frac{(b-1)q}{2b} \leq \frac{(b+1)q}{6b} - \frac{p}{6a} \Leftrightarrow \frac{2p}{3a} \leq \frac{(2b-1)q}{3b} \Leftrightarrow \frac{p}{2a} \leq \frac{(2b-1)q}{4b}\,.
$$

Therefore, if $\frac{(b-1)q}{2b} \leq \frac{p}{2a} \leq \frac{(2b-1)q}{4b}$ then b_1 is the optimum in Section b. Otherwise, if $\frac{(2b-1)q}{4b} \leq \frac{p}{2a} \leq \frac{q}{2}$ then b_1 will lie below Section b. If this is the case then, following identical working as that for even b, the optimum over Section b must lie on the boundary between Section b and $b+1$ whereupon it will be dominated by the identical point within Section $b+1$. Therefore Black's best point will not lie in Section b if $\frac{(2b-1)q}{4b} \leq \frac{p}{2a}$.

To summarise, if b is odd then: if $\frac{(b-2)q}{2b} \leq \frac{p}{2a} \leq \frac{(2b-1)q}{4b}$ then the optimum in Section b is $(\frac{p}{2a}, \frac{(b+1)q}{6b} - \frac{p}{6a})$ giving $Area(V^+((\frac{p}{2a}, \frac{(b+1)q}{6b} - \frac{p}{6a}))) = \frac{(5b-1)pq}{24ab} + \frac{p^2}{12a^2} - \frac{(b-2)(2b-1)q^2}{12b^2}$ (depicted in Figure 5.10f), otherwise if $\frac{(2b-1)q}{4b} \leq \frac{p}{2a} \leq \frac{q}{2}$ then the optimum lies on the boundary with Section $b+1$ and is not Black's best point (and so is not drawn).

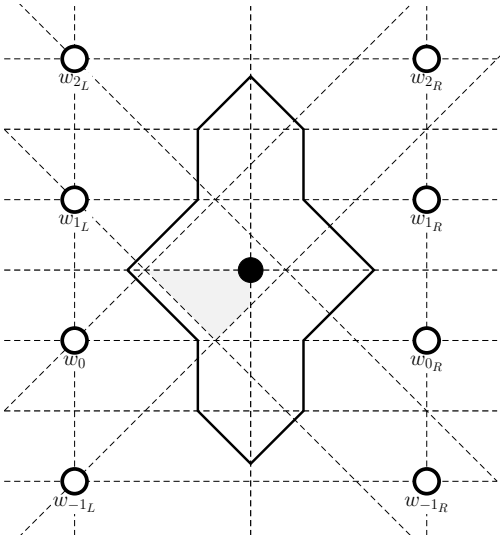

(e) $b_1 = (\frac{p}{2a}, \frac{q}{2b})$.

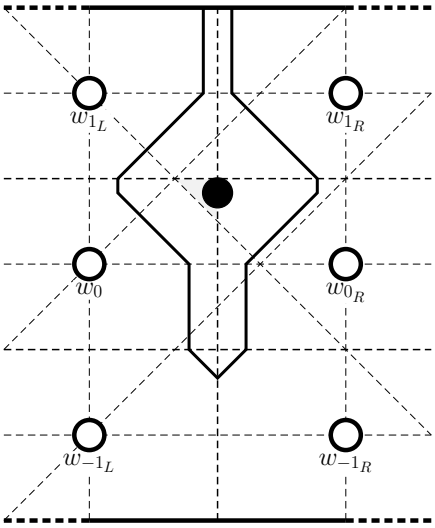

(f) $b_1 = (\frac{p}{2a}, \frac{(b+1)q}{6b} - \frac{p}{6a})$ only if $\frac{(b-2)q}{2b} \leq \frac{p}{2a} \leq \frac{(2b-1)q}{4b}$ and $b = 2l+1$.

Figure 5.10: Maximal area Voronoi cells $V^+(b_1)$ for b_1 within Section $2l+1$ upon $x^* = \frac{p}{2a}$.

Section $b+1$ upon $x^* = \frac{p}{2a}$ Finally we explore Section $b+1$, the last possible section, where w_0 is chosen to be on the $\lceil \frac{b}{2} \rceil$th row. If b_1 is placed within this section then $V^+(b_1)$ touches both horizontal boundaries of $\mathcal{P}$. This simply has the areas, if b is even,

$$\begin{aligned}
Area(V^+(b_1)) = &\sum_{i=-\frac{b-2}{2}}^{-1} Area(V^+(b_1) \cap (V^\circ(w_{i_L}) \cup V^\circ(w_{i_R}))) \\
&+ Area(V^+(b_1) \cap (V^\circ(w_{0_L}) \cup V^\circ(w_{0_R}))) \\
&+ \sum_{i=1}^{\frac{b}{2}} Area(V^+(b_1) \cap (V^\circ(w_{i_L}) \cup V^\circ(w_{i_R}))) \\
= &\sum_{i=-\frac{b-2}{2}}^{-1} \left(-\frac{q}{b}y + \frac{pq}{2ab} + \frac{(4i+1)q^2}{4b^2} \right) + \frac{pq}{2ab} - y^2 \\
&+ \sum_{i=1}^{\frac{b}{2}} \left(\frac{q}{b}y + \frac{pq}{2ab} - \frac{(4i-1)q^2}{4b^2} \right) \\
= &-y^2 + \frac{q}{b}y + \frac{pq}{2a} - \frac{(b^2-b+1)q^2}{4b^2}
\end{aligned}$$

and, if b is odd,

$$\begin{aligned}
Area(V^+(b_1)) = &\sum_{i=-\frac{b-1}{2}}^{-1} Area(V^+(b_1) \cap (V^\circ(w_{i_L}) \cup V^\circ(w_{i_R}))) \\
&+ Area(V^+(b_1) \cap (V^\circ(w_{0_L}) \cup V^\circ(w_{0_R}))) \\
&+ \sum_{i=1}^{\frac{b-1}{2}} Area(V^+(b_1) \cap (V^\circ(w_{i_L}) \cup V^\circ(w_{i_R})))
\end{aligned}$$

$$= \sum_{i=-\frac{b-1}{2}}^{-1} \left(-\frac{q}{b}y + \frac{pq}{2ab} + \frac{(4i+1)q^2}{4b^2} \right) + \frac{pq}{2ab} - y^2$$
$$+ \sum_{i=1}^{\frac{b-1}{2}} \left(\frac{q}{b}y + \frac{pq}{2ab} - \frac{(4i-1)q^2}{4b^2} \right)$$
$$= -y^2 + \frac{pq}{2a} - \frac{(b-1)q^2}{4b}.$$

It is clear that $(\frac{p}{2a}, \frac{q}{2b})$ and $(\frac{p}{2a}, 0)$ are the optima for b is even and b is odd, and these are both in Section $b+1$ for b even and odd respectively. We are certainly pleased to see this result since, as we might expect, both of these points lie on the horizontal line of symmetry of $\mathcal{P}$ and can be considered to be the centre of $\mathcal{P}$ which we would presume to be an effective placement. This gives us areas $Area(V^+((\frac{p}{2a}, \frac{q}{2b}))) = \frac{pq}{2a} - \frac{(b-1)q^2}{4b}$ and $Area(V^+((\frac{p}{2a}, 0))) = \frac{pq}{2a} - \frac{(b-1)q^2}{4b}$ (interestingly, identical to each other) as depicted in Figures 5.10g and 5.10h respectively.

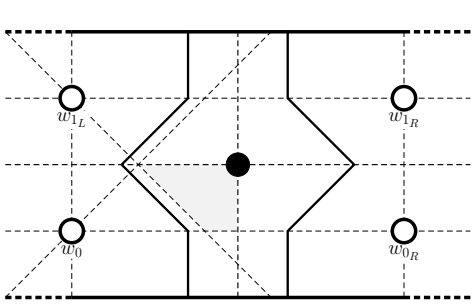

(g) $b_1 = (\frac{p}{2a}, \frac{q}{2b})$.

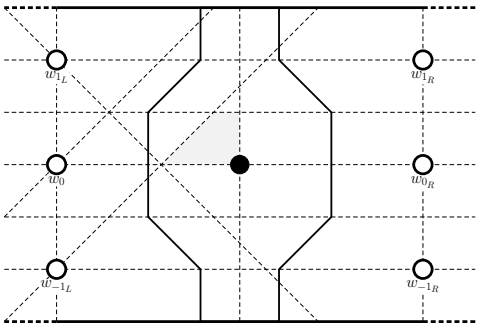

(h) $b_1 = (\frac{p}{2a}, 0)$.

Figure 5.10: Maximal area Voronoi cells $V^+(b_1)$ for b_1 within Section $b+1$ upon $x^* = \frac{p}{2a}$.

And thus we have found every optimal location within every possible partition of $\mathcal{P}$ that is a candidate for Black's best point b^*. To recap, Figure 5.10 shows all of the potential candidates for b^* within each appropriate section. Following our discussion of the choice of w_0 (and the fact that the best choice of w_0 for b_1 in Section I only requires that the first quadrant of $V^+(b_1)$ is a core quadrant and, if possible, that w_{-1_L} exists) we can say with confidence that, without loss of generality, the best point b^* lies in the first quadrant of the $(\lceil \frac{a}{2} \rceil, \lceil \frac{b}{2} \rceil)$th point in W (where the (i,j)th point in W is the point $w \in W$ which is in the ith column (counting from the left) and jth row (counting from the bottom)). This quadrant is the unique (or one of two or four identical) most central quadrant in $\mathcal{P}$, thus furthest from the boundaries of $\mathcal{P}$. Hence the best point b^* will lie in this quadrant and in Section I or on the line $x^* = \frac{p}{2a}$ and we must determine which optimum within which of these areas gives the best point depending on the relationship between p, q, a, and b.

Fortunately the nature of our investigation into $x^* = \frac{p}{2a}$ allows us to fairly easily compare optima upon this line where we have relatively restrictive conditions on which sections contain $x^* = \frac{p}{2a}$. For $\frac{(2l-1)q}{2b} \leq \frac{p}{2a} \leq \frac{lq}{b}$ and assuming that $2l+1 < b$ (we will assess $2l+1 \geq b$ later), $x^* = \frac{p}{2a}$ enters Sections $2l$ and $2l+1$ so we shall compare the optima within these sections for this condition. In Section $2l$, $Area(V^+((\frac{p}{2a}, 0))) = \frac{lpq}{2ab} + \frac{p^2}{8a^2} - \frac{(l-1)lq^2}{2b^2}$ and in Section $2l+1$, $Area(V^+((\frac{p}{2a}, \frac{q}{2b}))) = \frac{(4l-1)pq}{4ab} + \frac{p^2}{8a^2} - \frac{(4l^2-1)q^2}{8b^2}$. The optimum in Section $2l+1$ is better than that in Section $2l$ if

$$\left(\frac{(4l-1)pq}{4ab}+\frac{p^2}{8a^2}-\frac{(4l^2-1)q^2}{8b^2}\right)-\left(\frac{lpq}{2ab}+\frac{p^2}{8a^2}-\frac{(l-1)lq^2}{2b^2}\right)$$
$$=\frac{(4l-1)pq}{4ab}+\frac{p^2}{8a^2}-\frac{(4l^2-1)q^2}{8b^2}-\frac{lpq}{2ab}-\frac{p^2}{8a^2}+\frac{(l-1)lq^2}{2b^2}$$
$$=\frac{(2l-1)pq}{4ab}-\frac{(4l-1)q^2}{8b^2}\geq 0$$
$$\Leftrightarrow \frac{p}{2a}\geq\frac{(4l-1)q}{4(2l-1)b}.$$

Now
$$\frac{(2l-1)q}{2b}\leq\frac{(4l-1)q}{4(2l-1)b}\Leftrightarrow 8l^2-12l+3\leq 0\Leftrightarrow\frac{3-\sqrt{3}}{4}\leq l\leq\frac{3+\sqrt{3}}{4}$$
so if $l>1$ then the optimum in Section $2l+1$ is always better than the optimum in Section $2l$. Otherwise, if $l=1$ then Section $2l$ (II) is better than Section $2l+1$ (III) for $\left(\frac{q}{2b}=\right)\frac{(2l-1)q}{2b}\leq\frac{p}{2a}\leq\frac{(4l-1)q}{4(2l-1)b}\left(=\frac{3q}{4b}\right)$.

For $\frac{lq}{b}\leq\frac{p}{2a}\leq\frac{(2l+1)q}{2b}$ and assuming that $2(l+1)<b$ (we will assess $2(l+1)\geq b$ soon), $x^*=\frac{p}{2a}$ enters Sections $2l+1$ and $2(l+1)$ (note that $x^*=\frac{p}{2a}$ will never enter Section I because $\frac{p}{2a}\geq\frac{q}{2b}$). In Section $2l+1$, $Area(V^+((\frac{p}{2a},\frac{q}{2b})))=\frac{(4l-1)pq}{4ab}+\frac{p^2}{8a^2}-\frac{(4l^2-1)q^2}{8b^2}$ and in Section $2(l+1)$, $Area(V^+((\frac{p}{2a},0)))=\frac{(l+1)pq}{2ab}+\frac{p^2}{8a^2}-\frac{(l+1)lq^2}{2b^2}$ so the optimum in Section $2(l+1)$ is better than that in Section $2l+1$ if
$$\left(\frac{(l+1)pq}{2ab}+\frac{p^2}{8a^2}-\frac{(l+1)lq^2}{2b^2}\right)-\left(\frac{(4l-1)pq}{4ab}+\frac{p^2}{8a^2}-\frac{(4l^2-1)q^2}{8b^2}\right)$$
$$=-\frac{(2l-3)pq}{4ab}-\frac{(4l+1)q^2}{8b^2}\geq 0$$
$$\Leftrightarrow\frac{(3-2l)p}{2a}\geq\frac{(4l+1)q}{4b}.$$

Now if $(3-2l)\leq 0$ (i.e. $l\geq\frac{3}{2}$) then $0\geq\frac{(3-2l)p}{2a}\geq\frac{(4l+1)q}{4b}$ so the optimum in Section $2(l+1)$ is never better than the optimum in Section $2l+1$. Otherwise if $l=1$ then $\frac{p}{2a}\geq\frac{(4l+1)q}{4(3-2l)b}=\frac{5q}{4b}>\frac{q}{b}=\frac{lq}{b}$, so the optimum in Section $2(l+1)$ (IV) is better than the optimum in Section $2l+1$ (III) for $\frac{5q}{4b}\leq\frac{p}{2a}\leq\frac{3q}{2b}=\frac{(2l+1)q}{2b}$.

Upon $x^*=\frac{p}{2a}$ we have the possibility of two special cases with regard to the area of $V^+(b_1)$ to which we must give careful consideration: Section b (within which b_1 produces a Voronoi cell touching exactly one horizontal boundary of $\mathcal{P}$) and Section $b+1$ (within which b_1 produces a Voronoi cell touching both horizontal boundaries). Therefore we must compare the areas of Section $b-1$ with Section b as well as the areas of Section b with Section $b+1$.

Firstly, suppose b is even. For $\frac{(b-2)q}{2b}\leq\frac{p}{2a}\leq\frac{(b-1)q}{2b}$ and assuming $b>2$ (since $\frac{p}{2a}\geq\frac{q}{2b}$), $x^*=\frac{p}{2a}$ enters Sections $b-1$ and b whose maximal areas are $Area(V^+((\frac{p}{2a},\frac{q}{2b})))=\frac{(2b-5)pq}{4ab}+\frac{p^2}{8a^2}-\frac{(b^2-4b+3)q^2}{8b^2}$ and $Area(V^+((\frac{p}{2a},\frac{p}{6a}-\frac{(b-2)q}{6b})))=\frac{(2b-1)pq}{6ab}+\frac{p^2}{12a^2}-\frac{(b-2)(4b-1)q^2}{12b^2}$ respectively. The optimum in Section b is better than the optimum in Section $b-1$ if
$$\left(\frac{(2b-1)pq}{6ab}+\frac{p^2}{12a^2}-\frac{(b-2)(4b-1)q^2}{12b^2}\right)-\left(\frac{(2b-5)pq}{4ab}+\frac{p^2}{8a^2}-\frac{(b^2-4b+3)q^2}{8b^2}\right)$$
$$=-\frac{(2b-13)pq}{12ab}-\frac{p^2}{24a^2}-\frac{(5b^2-6b-5)q^2}{24b^2}\geq 0$$
$$\Leftrightarrow\frac{p^2}{a^2}+\frac{2(2b-13)pq}{ab}+\frac{(5b^2-6b-5)q^2}{b^2}\leq 0$$

$$\Leftrightarrow \left(\frac{p}{a}+\frac{(2b-13)q}{b}\right)^2+\frac{(b^2+46b-174)q^2}{b^2}\leq 0$$
$$\Leftrightarrow \frac{(13-2b-\sqrt{-(b^2+46b-174)})q}{2b}\leq\frac{p}{2a}\leq\frac{(13-2b+\sqrt{-(b^2+46b-174)})q}{2b}\,.$$

Now this condition only holds if $b^2+46b-174\leq 0\Leftrightarrow -23-\sqrt{703}\leq b\leq -23+\sqrt{703}\approx 3.5$ so b must be either 2 or 3, and since b is even it must be the case that $b=2$ which contradicts our assumption. So the optimum in Section $b-1$ is better than the optimum in Section b for all $b\neq 2$. This result is actually as expected: the optimum in Section $2(l+1)$ is dominated by the optimum in Section $2l+1$ and the structure in Section b has a lesser area than the structure in a general Section $2(l+1)$ would have for a value of $l=\frac{b-2}{2}$; and this paragraph simply serves as a sanity check.

For $\frac{(b-1)q}{2b}\leq\frac{p}{2a}\leq\frac{q}{2}$, $x^*=\frac{p}{2a}$ enters Sections b and $b+1$ whose maximal areas are $Area(V^+((\frac{p}{2a},\frac{p}{6a}-\frac{(b-2)q}{6b})))=\frac{(2b-1)pq}{6ab}+\frac{p^2}{12a^2}-\frac{(b-2)(4b-1)q^2}{12b^2}$ (only for $\frac{(b-2)q}{2b}\leq\frac{p}{2a}\leq\frac{(2b-1)q}{4b}$ so we now only consider the interval $\frac{(b-1)q}{2b}\leq\frac{p}{2a}\leq\frac{(2b-1)q}{4b}$) and $Area(V^+((\frac{p}{2a},\frac{q}{2b})))=\frac{pq}{2a}-\frac{(b-1)q^2}{4b}$ respectively. The optimum in Section $b+1$ is better than the optimum in Section b if

$$\begin{aligned}&\left(\frac{pq}{2a}-\frac{(b-1)q^2}{4b}\right)-\left(\frac{(2b-1)pq}{6ab}+\frac{p^2}{12a^2}-\frac{(b-2)(4b-1)q^2}{12b^2}\right)\\&=\frac{(b+1)pq}{6ab}-\frac{p^2}{12a^2}+\frac{(b^2-6b+2)q^2}{12b^2}\geq 0\\&\Leftrightarrow\frac{p^2}{a^2}-\frac{2(b+1)pq}{ab}-\frac{(b^2-6b+2)q^2}{b^2}\leq 0\\&\Leftrightarrow\left(\frac{p}{a}-\frac{(b+1)q}{b}\right)^2-\frac{(2b^2-4b+3)q^2}{b^2}\leq 0\\&\Leftrightarrow\frac{(b+1-\sqrt{2b^2-4b+3})q}{2b}\leq\frac{p}{2a}\leq\frac{(b+1+\sqrt{2b^2-4b+3})q}{2b}\,.\end{aligned}$$

Now $2b^2-4b+3=2(b-1)^2+1>0$ so the condition holds for all b. Comparing the limits of both conditions,

$$\begin{aligned}\frac{(b-1)q}{2b}-\frac{(b+1-\sqrt{2b^2-4b+3})q}{2b}&=\frac{(-2+\sqrt{2(b-1)^2+1})q}{2b}\geq 0\\&\Leftrightarrow\sqrt{2(b-1)^2+1}\geq 2\\&\Leftrightarrow 2(b-1)^2\geq 3\\&\Leftrightarrow b\leq\frac{2-\sqrt{6}}{2}\text{ or }b\geq\frac{2+\sqrt{6}}{2}\end{aligned}$$

and

$$\frac{(b+1+\sqrt{2b^2-4b+3})q}{2b}-\frac{(2b-1)q}{4b}=\frac{(3+2\sqrt{2(b-1)^2+1})q}{4b}\geq 0\,.$$

Hence the optimum in Section $b+1$ is better than the optimum in Section b unless $b=2$ (since $b\geq\frac{2+\sqrt{6}}{2}$) in which case the optimum in Section b (II) is better than the optimum in Section $b+1$ (III) for $\left(\frac{(b-1)q}{2b}=\right)\frac{q}{4}\leq\frac{p}{2a}\leq\frac{(3+\sqrt{3})q}{4}\left(=\frac{(b+1+\sqrt{2b^2-4b+3})q}{2b}\right)$.

Finally, suppose instead that b is odd. For $\frac{(b-2)q}{2b}\leq\frac{p}{2a}\leq\frac{(b-1)q}{2b}$, $x^*=\frac{p}{2a}$ enters Sections $b-1$ and b whose maximal areas are $Area(V^+((\frac{p}{2a},0)))=\frac{(b-1)pq}{4ab}+\frac{p^2}{8a^2}-\frac{(b-3)(b-1)q^2}{8b^2}$ and $Area(V^+((\frac{p}{2a},\frac{(b+1)q}{6b}-\frac{p}{6a})))=\frac{(5b-1)pq}{24ab}+\frac{p^2}{12a^2}-\frac{(b-2)(2b-1)q^2}{12b^2}$ respectively. The optimum in Section b is better than the optimum in Section $b-1$ if

$$\begin{aligned}&\left(\frac{(5b-1)pq}{24ab}+\frac{p^2}{12a^2}-\frac{(b-2)(2b-1)q^2}{12b^2}\right)-\left(\frac{(b-1)pq}{4ab}+\frac{p^2}{8a^2}-\frac{(b-3)(b-1)q^2}{8b^2}\right)\\&=-\frac{(b-5)pq}{24ab}-\frac{p^2}{24a^2}-\frac{(b^2+2b-5)q^2}{24b^2}\geq 0\end{aligned}$$

$$= \frac{p^2}{a^2} + \frac{(b-5)pq}{ab} + \frac{(b^2+2b-5)q^2}{b^2} \leq 0$$
$$= \left(\frac{p}{a} + \frac{(b-5)q}{2b}\right)^2 + \frac{(3b^2+18b-45)q^2}{4b^2} \leq 0$$
$$= \frac{(b-5-\sqrt{-3(b^2+6b-15)})q}{4b} \leq \frac{p}{2a} \leq \frac{(b-5+\sqrt{-3(b^2+6b-15)})q}{4b}\,.$$

Now this condition only holds if $b^2+6b-15 = (b+3)^2-24 \leq 0 \Leftrightarrow -3-\sqrt{24} \leq b \leq -3+2\sqrt{6} \approx 1.9$ so it holds for no value of b. Hence the optimum in Section $b-1$ is better than the optimum in Section b.

For $\frac{(b-1)q}{2b} \leq \frac{p}{2a} \leq \frac{q}{2}$, $x^* = \frac{p}{2a}$ enters Sections b and $b+1$ whose maximal areas are $Area(V^+((\frac{p}{2a}, \frac{(b+1)q}{6b} - \frac{p}{6a}))) = \frac{(5b-1)pq}{24ab} + \frac{p^2}{12a^2} - \frac{(b-2)(2b-1)q^2}{12b^2}$ (only for $\frac{(b-2)q}{2b} \leq \frac{p}{2a} \leq \frac{(2b-1)q}{4b}$ so we now only consider the interval $\frac{(b-1)q}{2b} \leq \frac{p}{2a} \leq \frac{(2b-1)q}{4b}$ as before) and $Area(V^+((\frac{p}{2a}, 0))) = \frac{pq}{2a} - \frac{(b-1)q^2}{4b}$ respectively. The optimum in Section $b+1$ is better than the optimum in Section b if

$$\left(\frac{pq}{2a} - \frac{(b-1)q^2}{4b}\right) - \left(\frac{(5b-1)pq}{24ab} + \frac{p^2}{12a^2} - \frac{(b-2)(2b-1)q^2}{12b^2}\right)$$
$$= \frac{(7b+1)pq}{24ab} - \frac{p^2}{12a^2} - \frac{(b^2+2b-2)q^2}{12b^2} \geq 0$$
$$\Leftrightarrow \frac{p^2}{a^2} - \frac{(7b+1)pq}{2ab} + \frac{(b^2+2b-2)q^2}{b^2} \leq 0$$
$$\Leftrightarrow \left(\frac{p}{a} - \frac{(7b+1)q}{4b}\right)^2 - \frac{(33b^2-18b+33)q^2}{16b^2} \leq 0$$
$$\Leftrightarrow \frac{(7b+1-\sqrt{3(11b^2-6b+11)})q}{8b} \leq \frac{p}{2a} \leq \frac{(7b+1+\sqrt{3(11b^2-6b+11)})q}{8b}\,.$$

Comparing the limits of both conditions,

$$\frac{(7b+1-\sqrt{3(11b^2-6b+11)})q}{8b} - \frac{(b-1)q}{2b} = \frac{(3b+5-\sqrt{3(11b^2-6b+11)})q}{8b} \geq 0$$
$$\Leftrightarrow 3b+5 \geq \sqrt{3(11b^2-6b+11)}$$
$$\Leftrightarrow 24b^2-48b+8 = 8(3b^2-6b+1) \leq 0$$
$$\Leftrightarrow \frac{3-\sqrt{6}}{3} \leq b \leq \frac{3+\sqrt{6}}{3} \approx 1.8$$

and

$$\frac{(7b+1+\sqrt{3(11b^2-6b+11)})q}{8b} - \frac{(2b-1)q}{4b} = \frac{(3b+3+\sqrt{3(11(b-\frac{3}{11})^2+\frac{112}{11})}))q}{8b} \geq 0\,.$$

Hence the optimum in Section $b+1$ is better than the optimum in Section b.

Thus we have analysed all possible solutions upon $x^* = \frac{p}{2a}$ and discerned the best possible location on $x^* = \frac{p}{2a}$ for every combination of p, q, a, and b. These are summarised in Table 5.11.

Now all that remains is to compare the optima upon $x^* = \frac{p}{2a}$ with the optima in Section I according to the conditions in Table 5.11 as well as the existence of $w_{0_{LL}}$. Since we have chosen w_0 to be the $(\lceil\frac{a}{2}\rceil, \lceil\frac{b}{2}\rceil)$th point in W, the condition that $w_{0_{LL}}$ does not exist amounts to $a = 2$ (importantly, this condition has no effect upon the optima upon $x^* = \frac{p}{2a}$).

Recalling our earlier results, the maximal area in Section I is $Area(V^+((0, \frac{q}{2b}))) = \frac{pq}{2ab} + \frac{q^2}{8b^2}$ unless $a = 2$ in which case the maximal area is $Area(V^+((\frac{q}{6b}, \frac{q}{2b}))) = \frac{pq}{2ab} + \frac{q^2}{12b^2}$. Studying the areas claimed by the optima within Table 5.11 we can see that, if all other variables are fixed, the value of every optimal area increases with p at a rate of at least $\frac{q}{2ab}$ (which is the rate of increase of the optimal values for Section I). Moreover, the value of the optimum upon $x^* = \frac{p}{2a}$ further increases with $\frac{p}{2a}$ whenever the optimal solution is replaced by the next (better) solution.

Section	Optimum	Area	Condition
II	$(\frac{p}{2a}, 0)$	$\frac{pq}{2ab} + \frac{p^2}{8a^2}$	$\frac{q}{2b} \leq \frac{p}{2a} \leq \frac{3q}{4b}$
III	$(\frac{p}{2a}, \frac{q}{2b})$	$\frac{3pq}{4ab} + \frac{p^2}{8a^2} - \frac{3q^2}{8b^2}$	$\frac{3q}{4b} \leq \frac{p}{2a} \leq \frac{5q}{4b}$
IV	$(\frac{p}{2a}, 0)$	$\frac{pq}{ab} + \frac{p^2}{8a^2} - \frac{q^2}{b^2}$	$\frac{5q}{4b} \leq \frac{p}{2a} \leq \frac{3q}{2b}$
$2l+1$	$(\frac{p}{2a}, \frac{q}{2b})$	$\frac{(4l-1)pq}{4ab} + \frac{p^2}{8a^2} - \frac{(4l^2-1)q^2}{8b^2}$	$\frac{(2l-1)q}{2b} \leq \frac{p}{2a} \leq \frac{(2l+1)q}{2b}$
$b=2$	$(\frac{p}{2a}, \frac{p}{6a})$	$\frac{pq}{4a} + \frac{p^2}{12a^2}$	$\frac{q}{4} \leq \frac{p}{2a} \leq \frac{(3+\sqrt{3})q}{4}$
$b+1=3$	$(\frac{p}{2a}, \frac{q}{4})$	$\frac{pq}{2a} - \frac{q^2}{8}$	$\frac{(3+\sqrt{3})q}{4} \leq \frac{p}{2a}$
$b-1$ even	$(\frac{p}{2a}, 0)$	$\frac{(b-1)pq}{4ab} + \frac{p^2}{8a^2} - \frac{(b-3)(b-1)q^2}{8b^2}$	$\frac{(b-2)q}{2b} \leq \frac{p}{2a} \leq \frac{(b-1)q}{2b}$
$b+1$ even	$(\frac{p}{2a}, 0)$	$\frac{pq}{2a} - \frac{(b-1)q^2}{4b}$	$\frac{(b-1)q}{2b} \leq \frac{p}{2a}$
$b+1$ odd	$(\frac{p}{2a}, \frac{q}{2b})$	$\frac{pq}{2a} - \frac{(b-1)q^2}{4b}$	$\frac{(b-1)q}{2b} \leq \frac{p}{2a}$

Table 5.11: Optima upon $x^* = \frac{p}{2a}$.

Therefore, for $b \neq 2$, if the optimum in Section I is better than the optimum upon $x^* = \frac{p}{2a}$ at $\frac{p}{2a} = X$ then the optimum in Section I is better than the optimum upon $x^* = \frac{p}{2a}$ for all $\frac{p}{2a} \leq X$, and similarly if the optimum upon $x^* = \frac{p}{2a}$ is better than the optimum in Section I at $\frac{p}{2a} = X$ then the optimum upon $x^* = \frac{p}{2a}$ is better than the optimum in Section I for all $\frac{p}{2a} \geq X$. Hence there exists a value X of $\frac{p}{2a}$ at which point the values of the optima in Section I and upon $x^* = \frac{p}{2a}$ are equal, and this determines our best point b^*. Additionally, since the value of the optimum in Section I is reduced if $a = 2$, the value X for $a > 2$ will be more than the analogous value X' for $a = 2$.

If $a > 2$ and $b > 2$ then we can simply compare the area within Section I with the smallest possible maximal area upon $x^* = \frac{p}{2a}$ (Section II):

$$\left(\frac{pq}{2ab} + \frac{q^2}{8b^2}\right) - \left(\frac{pq}{2ab} + \frac{p^2}{8a^2}\right) = \frac{q^2}{8b^2} - \frac{p^2}{8a^2} \geq 0 \Leftrightarrow \frac{q}{b} \geq \frac{p}{a}$$

but $\frac{p}{a} \geq \frac{q}{b}$ so if $a > 2$ and $b > 2$ then the optimum lies upon $x^* = \frac{p}{2a}$. The same is indeed true for $a = 2$ as described above. Therefore we have the best points b^* as outlined in Table 5.12.

Section	Optimum	Area	Condition
II	$(\frac{p}{2a}, 0)$	$\frac{pq}{2ab} + \frac{p^2}{8a^2}$	$\frac{q}{2b} \leq \frac{p}{2a} \leq \frac{3q}{4b}$
III	$(\frac{p}{2a}, \frac{q}{2b})$	$\frac{3pq}{4ab} + \frac{p^2}{8a^2} - \frac{3q^2}{8b^2}$	$\frac{3q}{4b} \leq \frac{p}{2a} \leq \frac{5q}{4b}$
IV	$(\frac{p}{2a}, 0)$	$\frac{pq}{ab} + \frac{p^2}{8a^2} - \frac{q^2}{b^2}$	$\frac{5q}{4b} \leq \frac{p}{2a} \leq \frac{3q}{2b}$
$2l+1$	$(\frac{p}{2a}, \frac{q}{2b})$	$\frac{(4l-1)pq}{4ab} + \frac{p^2}{8a^2} - \frac{(4l^2-1)q^2}{8b^2}$	$\frac{(2l-1)q}{2b} \leq \frac{p}{2a} \leq \frac{(2l+1)q}{2b}$
$b-1$ even	$(\frac{p}{2a}, 0)$	$\frac{(b-1)pq}{4ab} + \frac{p^2}{8a^2} - \frac{(b-3)(b-1)q^2}{8b^2}$	$\frac{(b-2)q}{2b} \leq \frac{p}{2a} \leq \frac{(b-1)q}{2b}$
$b+1$ even	$(\frac{p}{2a}, 0)$	$\frac{pq}{2a} - \frac{(b-1)q^2}{4b}$	$\frac{(b-1)q}{2b} \leq \frac{p}{2a}$
$b+1$ odd	$(\frac{p}{2a}, \frac{q}{2b})$	$\frac{pq}{2a} - \frac{(b-1)q^2}{4b}$	$\frac{(b-1)q}{2b} \leq \frac{p}{2a}$

Table 5.12: The best point b^* for $b \neq 2$.

Alternatively, if $a > 2$ and $b = 2$ then we must compare the maximal areas within Section I and Section b:

$$\left(\frac{pq}{4a} + \frac{q^2}{32}\right) - \left(\frac{pq}{4a} + \frac{p^2}{12a^2}\right) = \frac{q^2}{32} - \frac{p^2}{12a^2} \geq 0 \Leftrightarrow \frac{p}{2a} \leq \frac{\sqrt{6}q}{8}\,.$$

The optimum in Section b is valid for $\frac{q}{4} \leq \frac{p}{2a} \leq \frac{(3+\sqrt{3})q}{4}$ so the optimum within Section I is b^* for $\frac{q}{4} \leq \frac{p}{2a} \leq \frac{\sqrt{6}q}{8}$ but we need not compare the maximal area in Section I any further. This gives the best points b^* as displayed in Table 5.13.

Section	Optimum	Area	Condition
I	$(0, \frac{q}{2b})$	$\frac{pq}{4a} + \frac{q^2}{32}$	$\frac{q}{4} \leq \frac{p}{2a} \leq \frac{\sqrt{6}q}{8}$
b	$(\frac{p}{2a}, \frac{p}{6a})$	$\frac{pq}{4a} + \frac{p^2}{12a^2}$	$\frac{\sqrt{6}q}{8} \leq \frac{p}{2a} \leq \frac{(3+\sqrt{3})q}{4}$
$b+1$	$(\frac{p}{2a}, \frac{q}{4})$	$\frac{pq}{2a} - \frac{q^2}{8}$	$\frac{(3+\sqrt{3})q}{4} \leq \frac{p}{2a}$

Table 5.13: The best point b^* for $b = 2$ and $a \neq 2$.

Finally if $a = 2$ and $b = 2$ then, comparing the maximal areas within Section I and Section b,

$$\left(\frac{pq}{8} + \frac{q^2}{48}\right) - \left(\frac{pq}{8} + \frac{p^2}{48}\right) = \frac{q^2}{48} - \frac{p^2}{48} \geq 0 \Leftrightarrow \frac{q}{b} \geq \frac{p}{a}\,.$$

Therefore, since $\frac{p}{a} \geq \frac{q}{b}$, the optimum in Section b is always better than the optimum in Section I. This gives the best points b^* as displayed in Table 5.14.

Section	Optimum	Area	Condition
b	$(\frac{p}{2a}, \frac{p}{6a})$	$\frac{pq}{4a} + \frac{p^2}{12a^2}$	$\frac{q}{4} \leq \frac{p}{2a} \leq \frac{(3+\sqrt{3})q}{4}$
$b+1$	$(\frac{p}{2a}, \frac{q}{4})$	$\frac{pq}{2a} - \frac{q^2}{8}$	$\frac{(3+\sqrt{3})q}{4} \leq \frac{p}{2a}$

Table 5.14: The best point b^* for $b = 2$ and $a = 2$.

And thus, we have found the best points b^* in response to White playing an $a \times b$ grid.

5.5.2 Black's best arrangement

We have found Black's best point b^* but, as we have seen in Section 5.3, these are often not useful points to play when considering a whole arrangement. As we saw towards the end of Section 5.3, a good point for Black to play within an arrangement steals the best proportion of two halves of White's cells in $\mathcal{VD}(W)$. However, as Black's points venture further away from w_0 they steal less and less from the the two Voronoi cells they steal the most from, sacrificing this area in order to steal more area from a greater number of White's Voronoi cells. Therefore it may be useful to explore how Black performs playing closer to White's points, and we shall investigate Black's possible placements within Sections I, II, and III.

Core quadrants

We have already investigated the core quadrants in our search for Black's best point so there is little extra work we need do within these quadrants.

Section I was given a full exploration in our search for b^* so we will simply refer the reader to the results summarised in Figures 5.10a and 5.10b. On the other hand, only the areas upon $x^* = \frac{p}{2a}$ were optimised within Sections II and III. It requires little effort, however, to extend the results already investigated to cases where $x^* = \frac{p}{2a}$ does not lie within the section in question.

Each constituent area component $V^+(b_1) \cap (V^\circ(w_{i_L}) \cup V^\circ(w_{i_R}))$ calculated in Section 5.4 was found to be either independent of the value of x, or maximised by choosing x as close as possible to $\frac{p}{2a}$ (which leads us to the result that b^* must lie on $x^* = \frac{p}{2a}$ or Section I). In Sections II and IV, these maximum values of x are $\frac{q}{b}$ and $\frac{3q}{2b}$ (at $y = 0$ and $y = \frac{q}{2b}$), so we must consider the optimal solutions within these sections if $\frac{p}{2a} > \frac{q}{b}$ and $\frac{p}{2a} > \frac{3q}{2b}$ respectively. Therefore, in order to confirm that the maximisation of y in our previous work does not conflict with this maximisation of x that we must now consider, we need only to check that the optima obtained through our previous discoveries are $\left(\frac{q}{b}, 0\right)$ and $\left(\frac{3q}{2b}, \frac{q}{2b}\right)$ respectively (i.e. x is maximal at $\frac{p}{2a} = \frac{q}{b}$ and $\frac{p}{2a} = \frac{3q}{2b}$).

Section II For Section II, assuming $V^+(b_1)$ does not touch the boundary of $\mathcal{P}$, the maximal area when $\frac{p}{2a} \leq \frac{q}{b}$ is $Area(V^+((\frac{p}{2a}, 0))) = \frac{pq}{2ab} + \frac{p^2}{8a^2}$ as depicted in Figure 5.11a. If $\frac{p}{2a} > \frac{q}{b}$ then, since the optimum at $\frac{p}{2a} = \frac{q}{b}$ is $(\frac{q}{b}, 0)$ as required, our previous results give that the optimum is at $b_1 = \left(\frac{q}{b}, 0\right)$ with

$$\begin{aligned}
Area(V^+(b_1)) &= Area(V^+(b_1) \cap (V^\circ(w_{1_L}) \cup V^\circ(w_{1_R}))) \\
&\quad + Area(V^+(b_1) \cap (V^\circ(w_{0_L}) \cup V^\circ(w_{0_R}))) \\
&\quad + Area(V^+(b_1) \cap (V^\circ(w_{-1_L}) \cup V^\circ(w_{-1_R}))) \\
&= \left(-\frac{1}{4}\left(\frac{q}{b}\right)^2 + \frac{0^2}{4} + \frac{p}{4a}\frac{q}{b} + \left(\frac{p}{4a} - \frac{(1-1)q}{2b}\right) \times 0 - \frac{(1-1)pq}{4ab} + \frac{(1-1)^2q^2}{4b^2}\right) \\
&\quad + \left(\frac{pq}{2ab} - 0^2\right) + \left(-\frac{1}{4}\left(\frac{q}{b}\right)^2 + \frac{0^2}{4} + \frac{p}{4a}\frac{q}{b} - \left(\frac{p}{4a} + \frac{(-1+1)q}{2b}\right) \times 0\right. \\
&\quad \left. + \frac{(-1+1)pq}{4ab} + \frac{(-1+1)^2q^2}{4b^2}\right) \\
&= \frac{pq}{ab} - \frac{q^2}{2b^2}
\end{aligned}$$

as depicted in Figure 5.11b.

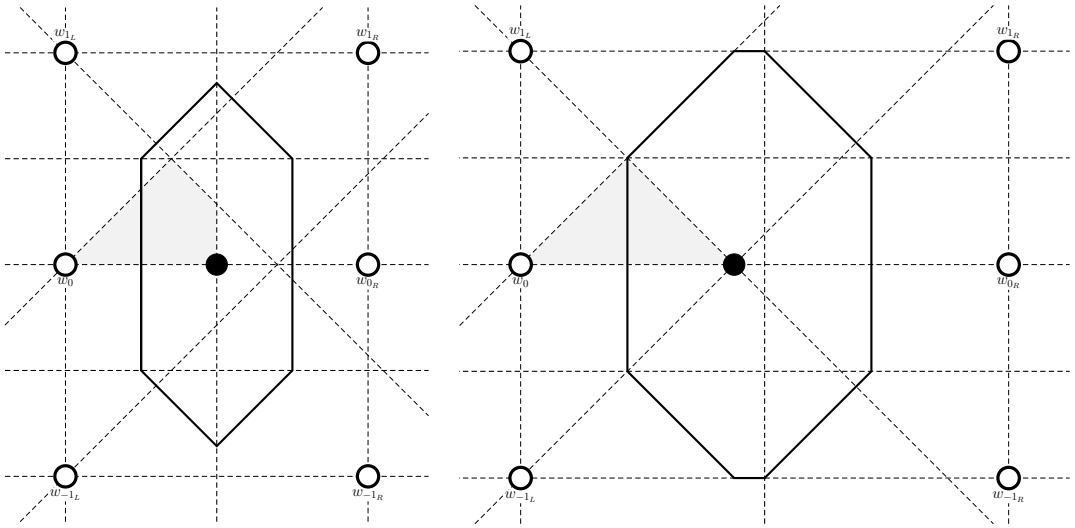

(a) $b_1 = (\frac{p}{2a}, 0)$ only if $\frac{p}{2a} \leq \frac{q}{b}$. (b) $b_1 = (\frac{q}{b}, 0)$ only if $\frac{p}{2a} \geq \frac{q}{b}$.

Figure 5.11: Maximal area Voronoi cells $V^+(b_1)$ for b_1 within Section II not touching the horizontal edges of $\mathcal{P}$.

Otherwise if w_{-1_L} does not exist then, using the results of Section b from above: if $\frac{p}{2a} \leq \frac{3q}{4b}$ then the maximal area is $Area(V^+((\frac{p}{2a}, \frac{p}{6a}))) = \frac{pq}{2ab} + \frac{p^2}{12a^2}$ as depicted in Figure 5.12a; if $\frac{3q}{4b} \leq \frac{p}{2a} \leq \frac{q}{b}$ then the optimum is $(\frac{p}{2a}, \frac{q}{b} - \frac{p}{2a})$ (upon the boundary between Section II and Section III) giving

$$\begin{aligned}
Area(V^+(b_1)) &= -\frac{3}{4}\left(\frac{q}{b} - \frac{p}{2a}\right)^2 + \left(\frac{p}{4a} - \frac{(1-1)q}{2b}\right)\left(\frac{q}{b} - \frac{p}{2a}\right) \\
&\quad + \frac{(3(1)-1)pq}{4ab} + \frac{p^2}{16a^2} - \frac{(1-1)(3(1)-1)q^2}{4b^2} \\
&= \frac{3pq}{2ab} - \frac{p^2}{4a^2} - \frac{3q^2}{4b^2}
\end{aligned}$$

as depicted in Figure 5.12b; and if $\frac{p}{2a} \geq \frac{q}{b}$, since the optimum at $\frac{p}{2a} = \frac{q}{b}$ is $(\frac{q}{b}, 0)$, our previous

results give that the optimum is at $b_1 = (\frac{q}{b}, 0)$ with

$$\begin{aligned} Area(V^+(b_1)) &= Area(V^+(b_1) \cap (V^\circ(w_{1_L}) \cup V^\circ(w_{1_R}))) \\ &\quad + Area(V^+(b_1) \cap (V^\circ(w_{0_L}) \cup V^\circ(w_{0_R}))) \\ &= -\frac{1}{4}\left(\frac{q}{b}\right)^2 + \frac{0^2}{4} + \frac{p}{4a}\frac{q}{b} + \left(\frac{p}{4a} - \frac{(1-1)q}{2b}\right) \times 0 - \frac{(1-1)pq}{4ab} + \frac{(1-1)^2q^2}{4b^2} \\ &\quad + \frac{pq}{2ab} - 0^2 \\ &= \frac{3pq}{4ab} - \frac{q^2}{4b^2} \end{aligned}$$

as depicted in Figure 5.12c.

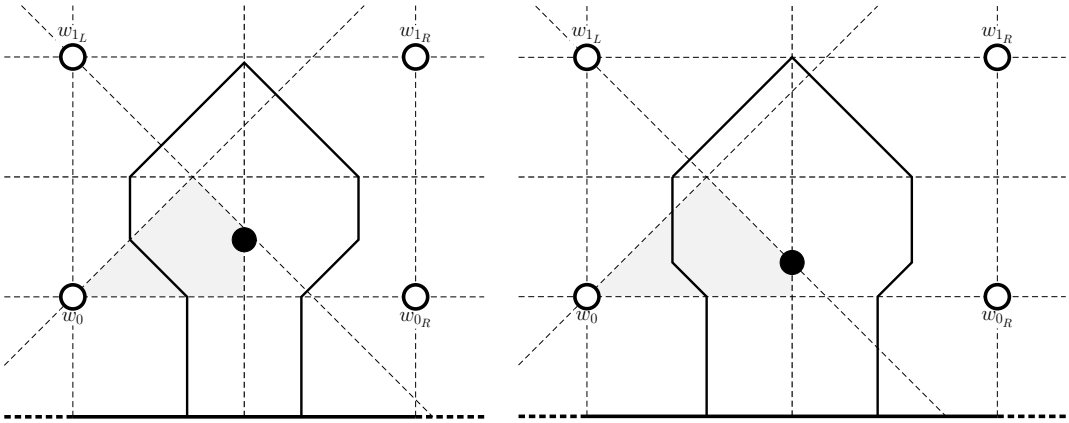

(a) $b_1 = (\frac{p}{2a}, \frac{p}{6a})$ only if $\frac{p}{2a} \leq \frac{3q}{4b}$.

(b) $b_1 = (\frac{p}{2a}, \frac{q}{b} - \frac{p}{2a})$ only if $\frac{3q}{4b} \leq \frac{p}{2a} \leq \frac{q}{b}$.

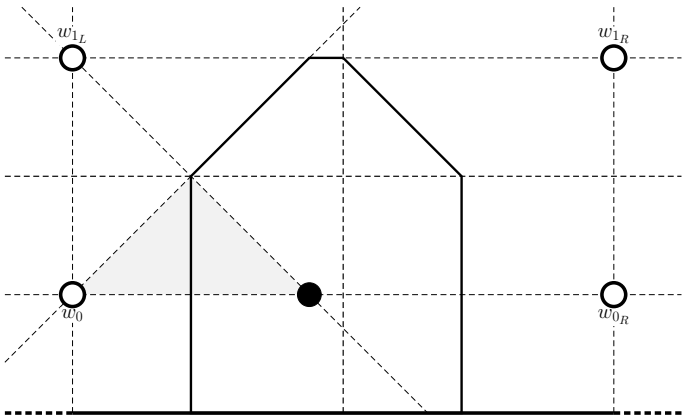

(c) $b_1 = (\frac{q}{b}, 0)$ only if $\frac{p}{2a} \geq \frac{q}{b}$.

Figure 5.12: Maximal area Voronoi cells $V^+(b_1)$ for b_1 within Section II touching the bottommost horizontal edge of $\mathcal{P}$.

Section III For Section III, assuming $V^+(b_1)$ does not touch the boundary of $\mathcal{P}$, the maximal area when $\frac{p}{2a} \leq \frac{3q}{2b}$ is $Area(V^+((\frac{p}{2a}, \frac{q}{2b}))) = \frac{3pq}{4ab} + \frac{p^2}{8a^2} - \frac{3q^2}{8b^2}$ as depicted in Figure 5.12d. If $\frac{p}{2a} \geq \frac{3q}{2b}$ then, since the optimum at $\frac{p}{2a} = \frac{3q}{2b}$ is $\left(\frac{3q}{2b}, \frac{q}{2b}\right)$ as required, our previous results give that the optimum is at $b_1 = \left(\frac{3q}{2b}, \frac{q}{2b}\right)$ with

$$
\begin{aligned}
Area(V^+(b_1)) &= Area(V^+(b_1) \cap (V^\circ(w_{2_L}) \cup V^\circ(w_{2_R})) \\
&\quad + Area(V^+(b_1) \cap (V^\circ(w_{1_L}) \cup V^\circ(w_{1_R})) \\
&\quad + Area(V^+(b_1) \cap (V^\circ(w_{0_L}) \cup V^\circ(w_{0_R})) \\
&\quad + Area(V^+(b_1) \cap (V^\circ(w_{-1_L}) \cup V^\circ(w_{-1_R})) \\
&= \left(-\frac{1}{4}\left(\frac{3q}{2b}\right)^2 + \frac{1}{4}\left(\frac{q}{2b}\right)^2 + \frac{p}{4a}\frac{3q}{2b} + \left(\frac{p}{4a} - \frac{(2-1)q}{2b}\right)\frac{q}{2b} - \frac{(2-1)pq}{4ab} + \frac{(2-1)^2q^2}{4b^2}\right) \\
&\quad + \left(\frac{q}{b}\frac{q}{2b} + \frac{pq}{2ab} - \frac{(4(1)-1)q^2}{4b^2}\right) + \left(\frac{pq}{2ab} - \left(\frac{q}{2b}\right)^2\right) + \left(-\frac{1}{4}\left(\frac{3q}{2b}\right)^2 + \frac{1}{4}\left(\frac{q}{2b}\right)^2\right. \\
&\quad \left. + \frac{p}{4a}\frac{3q}{2b} - \left(\frac{p}{4a} + \frac{(-1+1)q}{2b}\right)\frac{q}{2b} + \frac{(-1+1)pq}{4ab} + \frac{(-1+1)^2q^2}{4b^2}\right) \\
&= \frac{3pq}{2ab} - \frac{3q^2}{2b^2}
\end{aligned}
$$

as depicted in Figure 5.12e.

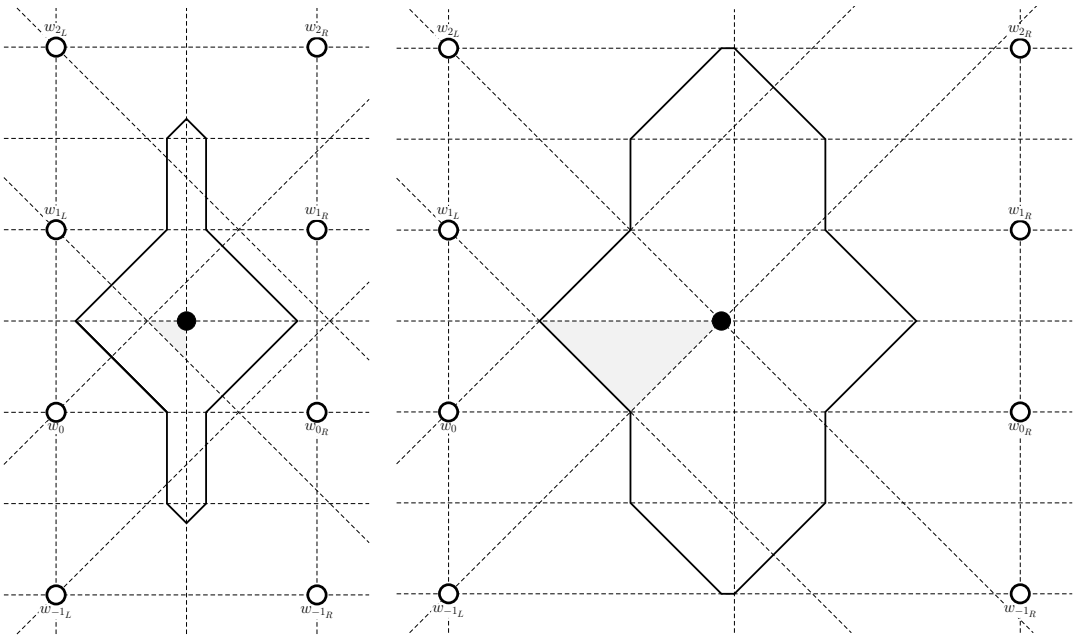

(d) $b_1 = (\frac{p}{2a}, \frac{q}{2b})$ only if $\frac{p}{2a} \leq \frac{3q}{2b}$.

(e) $b_1 = (\frac{3q}{2b}, \frac{q}{2b})$ only if $\frac{p}{2a} \geq \frac{3q}{2b}$.

Figure 5.12: Maximal area Voronoi cells $V^+(b_1)$ for b_1 within Section III not touching the horizontal edges of $\mathcal{P}$.

Otherwise, if w_{-1_L} does not exist (a situation previously not necessary to study) then

$$
\begin{aligned}
Area(V^+(b_1)) &= Area(V^+(b_1) \cap (V^\circ(w_{2_L}) \cup V^\circ(w_{2_R})) \\
&\quad + Area(V^+(b_1) \cap (V^\circ(w_{1_L}) \cup V^\circ(w_{1_R})) \\
&\quad + Area(V^+(b_1) \cap (V^\circ(w_{0_L}) \cup V^\circ(w_{0_R})) \\
&= \left(-\frac{x^2}{4} + \frac{y^2}{4} + \frac{p}{4a}x + \left(\frac{p}{4a} - \frac{(2-1)q}{2b}\right)y - \frac{(2-1)pq}{4ab} + \frac{(2-1)^2q^2}{4b^2}\right) \\
&\quad + \left(\frac{q}{b}y + \frac{pq}{2ab} - \frac{(4(1)-1)q^2}{4b^2}\right) + \left(\frac{pq}{2ab} - y^2\right)
\end{aligned}
$$

$$= -\frac{x^2}{4} - \frac{3y^2}{4} + \frac{p}{4a}x + \left(\frac{p}{4a} + \frac{q}{2b}\right)y + \frac{3pq}{4ab} - \frac{q^2}{2b^2}$$

gives partial derivatives

$$\frac{\delta A}{\delta x} = -\frac{x}{2} + \frac{p}{4a}$$
$$\frac{\delta A}{\delta y} = -\frac{3y}{2} + \frac{p}{4a} + \frac{q}{2b}$$

which gives optimal $y^* = \frac{p}{6a} + \frac{q}{3b} \geq \frac{q}{6b} + \frac{q}{3b} = \frac{q}{2b}$. Therefore, since the area is maximised by choosing x as close as possible to $\frac{p}{2a}$ and choosing y as close as possible to $y^* \geq \frac{q}{2b}$, the maximal areas within Section III are, for $\frac{p}{2a} \leq \frac{3q}{2b}$, $Area(V^+((\frac{p}{2a}, \frac{q}{2b}))) = \frac{7pq}{8ab} + \frac{p^2}{16a^2} - \frac{7q^2}{16b^2}$ as depicted in Figure 5.12f and, for $\frac{p}{2a} \geq \frac{3q}{2b}$, $Area(V^+(((\frac{3q}{2b}, \frac{q}{2b}))) = \frac{5pq}{4ab} - \frac{q^2}{b^2}$ as depicted in Figure 5.12g.

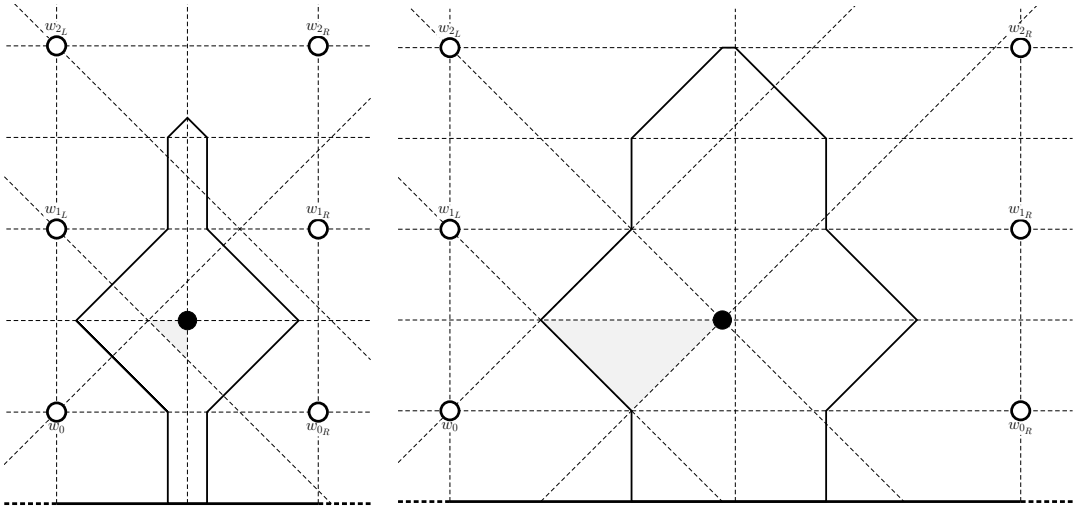

(f) $b_1 = (\frac{p}{2a}, \frac{q}{2b})$ only if $\frac{p}{2a} \leq \frac{3q}{2b}$.

(g) $b_1 = (\frac{3q}{2b}, \frac{q}{2b})$ only if $\frac{p}{2a} \geq \frac{3q}{2b}$.

Figure 5.12: Maximal area Voronoi cells $V^+(b_1)$ for b_1 within Section III touching the bottom-most horizontal edge of $\mathcal{P}$.

Otherwise, if w_{2_L} does not exist then, using the results of Section b from above: if $\frac{p}{2a} \leq \frac{5q}{4b}$ then the maximal area is $Area(V^+((\frac{p}{2a}, \frac{2q}{3b} - \frac{p}{6a}))) = \frac{7pq}{12ab} + \frac{p^2}{12a^2} - \frac{5q^2}{12b^2}$ as depicted in Figure 5.12h; if $\frac{5q}{4b} \leq \frac{p}{2a} \leq \frac{3q}{2b}$ then the optimum is $(\frac{p}{2a}, \frac{p}{2a} - \frac{q}{b})$ (upon the boundary between Section III and Section IV) giving

$$\begin{aligned} Area(V^+(b_1)) &= -\frac{3}{4}\left(\frac{p}{2a} - \frac{q}{b}\right)^2 - \left(\frac{p}{4a} - \frac{(1+1)q}{2b}\right)\left(\frac{p}{2a} - \frac{q}{b}\right) \\ &\quad + \frac{(2(1)+1)pq}{4ab} + \frac{p^2}{16a^2} - \frac{3(1)^2q^2}{4b^2} \\ &= \frac{9pq}{4ab} - \frac{p^2}{4a^2} - \frac{5q^2}{2b^2} \end{aligned}$$

as depicted in Figure 5.12i; and if $\frac{p}{2a} \geq \frac{3q}{2b}$, since the optimum at $\frac{p}{2a} = \frac{3q}{2b}$ is $(\frac{3q}{2b}, \frac{q}{2b})$, our previous results give that the optimum is at $b_1 = (\frac{3q}{2b}, \frac{q}{2b})$ with

$$
\begin{aligned}
Area(V^+(b_1)) &= Area(V^+(b_1) \cap (V^\circ(w_{1_L}) \cup V^\circ(w_{1_R}))) + Area(V^+(b_1) \cap (V^\circ(w_{0_L}) \cup V^\circ(w_{0_R}))) \\
&\quad + Area(V^+(b_1) \cap (V^\circ(w_{-1_L}) \cup V^\circ(w_{-1_R}))) \\
&= \left(\frac{q}{b}\frac{q}{2b} + \frac{pq}{2ab} - \frac{(4(1)-1)q^2}{4b^2}\right) + \left(\frac{pq}{2ab} - \left(\frac{q}{2b}\right)^2\right) + \left(-\frac{1}{4}\left(\frac{3q}{2b}\right)^2 + \frac{1}{4}\left(\frac{q}{2b}\right)^2\right. \\
&\quad \left. + \frac{p}{4a}\frac{3q}{2b} - \left(\frac{p}{4a} + \frac{(-1+1)q}{2b}\right)\frac{q}{2b} + \frac{(-1+1)pq}{4ab} + \frac{(-1+1)^2q^2}{4b^2}\right) \\
&= \frac{5pq}{4ab} - \frac{q^2}{b^2}
\end{aligned}
$$

as depicted in Figure 5.12j.

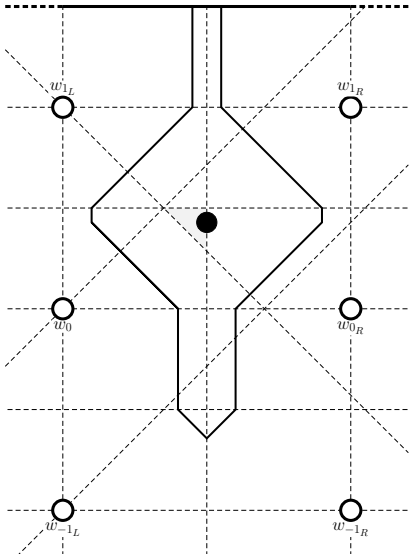

(h) $b_1 = (\frac{p}{2a}, \frac{2q}{3b} - \frac{p}{6a})$ only if $\frac{p}{2a} \leq \frac{5q}{4b}$.

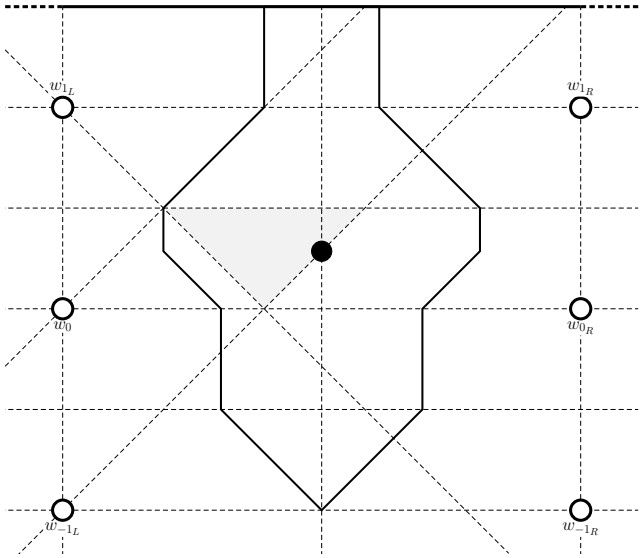

(i) $b_1 = (\frac{p}{2a}, \frac{p}{2a} - \frac{q}{b})$ only if $\frac{5q}{4b} \leq \frac{p}{2a} \leq \frac{3q}{2b}$.

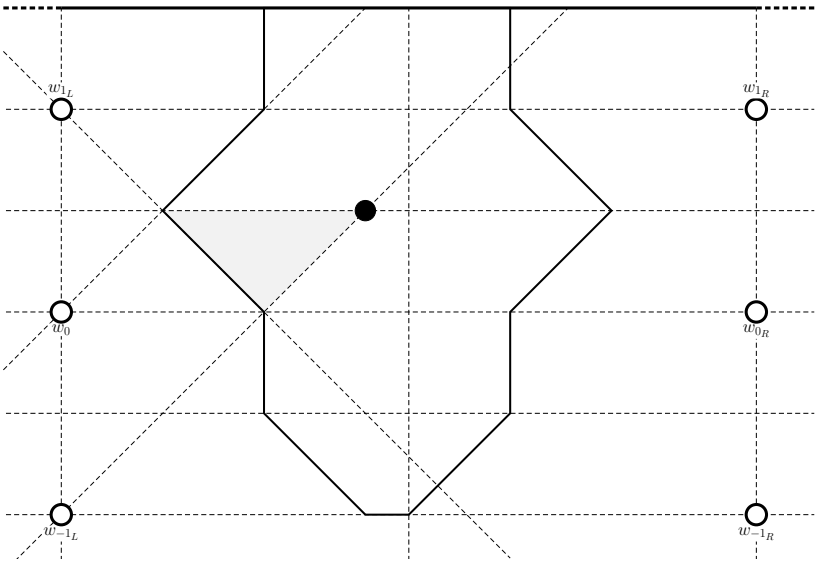

(j) $b_1 = (\frac{3q}{2b}, \frac{q}{2b})$ only if $\frac{p}{2a} \geq \frac{3q}{2b}$.

Figure 5.12: Maximal area Voronoi cells $V^+(b_1)$ for b_1 within Section III touching the topmost horizontal edge of $\mathcal{P}$.

Finally, if neither w_{-1_L} nor w_{2_L} exists then

$$\begin{aligned}
Area(V^+(b_1)) &= Area(V^+(b_1) \cap (V^\circ(w_{1_L}) \cup V^\circ(w_{1_R}))) \\
&\quad + Area(V^+(b_1) \cap (V^\circ(w_{0_L}) \cup V^\circ(w_{0_R}))) \\
&= -\frac{x^2}{4} - \frac{3y^2}{4} + \frac{p}{4a}x + (-\frac{p}{4a} + \frac{q}{b})y + \frac{pq}{ab} - \frac{3q^2}{4b^2} - (\frac{p}{2a} - \frac{x+y}{2}) \times \frac{x-y}{2} \\
&= -y^2 + \frac{q}{b}y + \frac{pq}{ab} - \frac{3q^2}{4b^2}
\end{aligned}$$

is maximised by $y = \frac{q}{2b}$, irrespective of the value of x. Therefore the optimum is $(x, \frac{q}{2b})$ as depicted in Figure 5.12k.

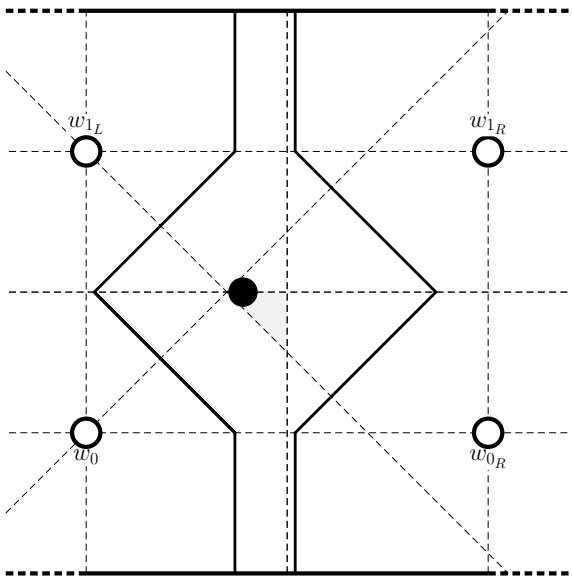

(k) $b_1 = (x, \frac{q}{2b})$.

Figure 5.12: Maximal area Voronoi cells $V^+(b_1)$ for b_1 within Section III touching both horizontal edges of $\mathcal{P}$.

Edge quadrants

Now, to consider the placement of b_1 in a quadrant of $V^\circ(w)$ which borders the perimeter of $\mathcal{P}$, we shall use the structures explored above and determine all possible cells $V^\circ(b_1)$ in the presence of one boundary of $\mathcal{P}$.

Firstly let us imagine that the quadrant of the cell containing b_1 touches $\mathcal{P}$ but does not contain a corner of $\mathcal{P}$ – i.e. it borders exactly one of the edges of $\mathcal{P}$, so exactly one of w_{1_L} or w_{0_R} does not exist. We shall refer to this type of quadrant as an *edge quadrant*. In Figure 5.9 this would amount to discarding all area either above $y = \frac{q}{2b}$ or to the right of $x = \frac{p}{2a}$ and we must consider both cuts. However, before we dive into our calculations, let us notice that a vertical cut at $x = \frac{p}{2a}$ would produce Voronoi cells $V^+(b_1)$ for b_1 in Section II and beyond exactly resembling those studied in Section 5.2, reflected in $y = x$. It should be a great relief to spot this as it saves us having to repeat our calculations since we can simply take our results from Section 5.2, remembering to exchange $\frac{p}{n}$ and q with $\frac{q}{b}$ and $\frac{p}{a}$ respectively.

Therefore we need only explore Section I with the vertical cut, and then all sections with the horizontal cut. Another important point to note is that, with a horizontal cut, the partitioning lines donated by points w_{i_L} for $i > 0$ no longer exist (since the points w_{i_L} no longer exist). This means that there is no distinction between Voronoi cells of points in Section $2l$ and Section $2l + 1$, so we can explore these together.

But, despite the fear of holding the reader back from diving into the analysis, we can (and will) say still more. The structures from Section I with a vertical cut and Section II (and III) with a horizontal cut are identical up to the reflection in $x = y$ as already described. Therefore we need only investigate Section I and transfer the representation symmetrically to Section II (and III).

Section I Finding the area of the cell obtained through a horizontal cut according to the Section I structure (with vertices $(0, \frac{x+y}{2})$, $(x, \frac{y-x}{2})$, $(\frac{p}{2a}, \frac{y-x}{2})$, $(\frac{p}{2a} + \frac{x+y}{2}, y)$, $(\frac{p}{2a} + \frac{x+y}{2}, \frac{q}{2b})$, $(-\frac{p}{2a} - \frac{y-x}{2}, \frac{q}{2b})$, $(-\frac{p}{2a} - \frac{y-x}{2}, y)$, and $(-\frac{p}{2a}, \frac{x+y}{2})$) to be

$$\begin{aligned} Area(V^+(b_1)) &= (\frac{p}{2a} + \frac{x+y}{2}) \times (\frac{q}{2b} - \frac{y-x}{2}) - \frac{1}{2}x^2 - \frac{1}{2}(\frac{x+y}{2})^2 \\ &\quad + (\frac{p}{2a} + \frac{y-x}{2}) \times (\frac{q}{2b} - \frac{x+y}{2}) - \frac{1}{2}(\frac{y-x}{2})^2 \\ &= -\frac{x^2}{4} - \frac{3y^2}{4} + (-\frac{p}{2a} + \frac{q}{2b})y + \frac{pq}{2ab}\,, \end{aligned}$$

or, if $w_{0_{LL}}$ does not exist (i.e. $V^\circ(w_0)$ also touches the perimeter of $\mathcal{P}$ on its left edge),

$$\begin{aligned} Area(V^+(b_1)) &= (\frac{p}{2a} + \frac{x+y}{2}) \times (\frac{q}{2b} - \frac{y-x}{2}) - \frac{1}{2}x^2 - \frac{1}{2}(\frac{x+y}{2})^2 + (\frac{p}{2a}) \times (\frac{q}{2b} - \frac{x+y}{2}) \\ &= -\frac{3x^2}{8} - \frac{3y^2}{8} - \frac{xy}{4} + \frac{q}{4b}x + (-\frac{p}{2a} + \frac{q}{4b})y + \frac{pq}{2ab} \end{aligned}$$

gives partial derivatives

$$\begin{aligned} \frac{\delta A}{\delta x} &= -\frac{x}{2} \\ \frac{\delta A}{\delta y} &= -\frac{3y}{2} - \frac{p}{2a} + \frac{q}{2b} \end{aligned}$$

enforcing $y^* = -\frac{p}{3a} + \frac{q}{3b} \not> 0$, or, if $w_{0_{LL}}$ does not exist, gives partial derivatives

$$\begin{aligned} \frac{\delta A}{\delta x} &= -\frac{3x}{4} - \frac{y}{4} + \frac{q}{4b} \\ \frac{\delta A}{\delta y} &= -\frac{3y}{4} - \frac{x}{4} - \frac{p}{2a} + \frac{q}{4b} \\ &\Rightarrow 2x^* - \frac{p}{2a} - \frac{q}{2b} = 0 \Rightarrow x^* = \frac{p}{4a} + \frac{q}{4b}, y^* = -\frac{3p}{4a} + \frac{q}{4b} \end{aligned}$$

where $y^* = -\frac{3p}{4a} + \frac{q}{4b} \not> 0$ since $\frac{p}{a} \geq \frac{q}{b}$. Therefore for both instances we must explore the boundary of Section I for an optimal location of b_1.

- Upon boundary $x = 0$ we have $Area(V^+((0, y))) = -\frac{3y^2}{4} + (-\frac{p}{2a} + \frac{q}{2b})y + \frac{pq}{2ab}$, maximised by $y^* = -\frac{p}{3a} + \frac{q}{3b} \not> 0$. Therefore the maximum will be at $b_1^* = (0, 0)$ where $Area(V^+(b_1^*)) = \frac{pq}{2ab}$. Alternatively, if $(-\frac{p}{a}, 0)$ does not exist then $Area(V^+((0, y))) = -\frac{3y^2}{8} + (-\frac{p}{2a} + \frac{q}{4b})y + \frac{pq}{2ab}$, maximised by $y^* = -\frac{2p}{3a} + \frac{q}{3b} \not> 0$. Therefore the maximum will also be at $b_1^* = (0, 0)$ where $Area(V^+(b_1^*)) = \frac{pq}{2ab}$.

- Upon boundary $x = y$ we have $Area(V^+((x, x))) = -x^2 + (-\frac{p}{2a} + \frac{q}{2b})x + \frac{pq}{2ab}$ which is maximised by $x^* = -\frac{p}{4a} + \frac{q}{4b} \not> 0$, so again the maximum is found at $b_1^* = (0, 0)$. Alternatively, if $(-\frac{p}{a}, 0)$ does not exist then $Area(V^+((x, x))) = -x^2 + (-\frac{p}{2a} + \frac{q}{2b})x + \frac{pq}{2ab}$ is maximised by $x^* = -\frac{p}{4a} + \frac{q}{4b} \not> 0$ so again the maximum lies at $b_1^* = (0, 0)$.

- Upon boundary $y = \frac{q}{2b}$, since its endpoints are shared with endpoints of the other two boundaries which were found not to be optimal over those boundaries, any area will be less than the maximised area already found, and thus the optimum will not exist on this boundary.

Therefore the optimal location of b_1 in Section I of an edge quadrant for a horizontal edge is to place as close as possible to White's point, and since this technique is summarised in Lemma 4.1.1 we do not depict this in Figure 5.10.

Now, the cell obtained through a vertical cut according to the Section I structure has vertices $(0, \frac{x+y}{2})$, $(x, \frac{y-x}{2})$, $(\frac{p}{2a}, \frac{y-x}{2})$, $(\frac{p}{2a}, \frac{q}{2b} + \frac{x+y}{2})$, $(x, \frac{q}{2b} + \frac{x+y}{2})$, $(0, \frac{q}{2b} + \frac{y-x}{2})$, $(-\frac{p}{2a}, \frac{q}{2b} + \frac{y-x}{2})$, $(-\frac{p}{2a} - \frac{y-x}{2}, \frac{q}{2b})$, $(-\frac{p}{2a} - \frac{y-x}{2}, y)$, and $(-\frac{p}{2a}, \frac{x+y}{2})$ and area

$$\begin{aligned} Area(V^+(b_1)) &= -\frac{x^2}{2} - \frac{y^2}{2} + \frac{q}{2b}y + \frac{pq}{2ab} - (\frac{x+y}{2} \times (\frac{q}{2b} - y) + (\frac{x+y}{2})^2) \\ &= -\frac{3x^2}{4} - \frac{y^2}{4} - \frac{q}{4b}x + \frac{q}{4b}y + \frac{pq}{2ab}\,. \end{aligned}$$

Note that since $a > 1$, the points $w_{0_{LL}}$ and $w_{1_{LL}}$ always exist. The partial derivatives

$$\begin{aligned} \frac{\delta A}{\delta x} &= -\frac{3x}{2} - \frac{q}{4b} \\ \frac{\delta A}{\delta y} &= -\frac{y}{2} + \frac{q}{4b} \end{aligned}$$

give $b_1^* = (-\frac{q}{6b}, \frac{q}{2b})$ which is not contained in Section I so again we must explore the boundary of Section I.

- Upon boundary $x = 0$ we have $Area(V^+((0, y))) = -\frac{y^2}{4} + \frac{q}{4b}y + \frac{pq}{2ab}$ which is maximised by $y^* = \frac{q}{2b}$ to give $Area(V^+((0, \frac{q}{2b})) = \frac{pq}{2ab} + \frac{q^2}{16b^2}$.
- Upon boundary $x = y$ we have $Area(V^+((x, x))) = -x^2 + \frac{pq}{2ab}$ which is maximised by $x^* = 0$ to give $Area(V^+((0, 0))) = \frac{pq}{2ab}$.
- Upon boundary $y = \frac{q}{2b}$, since its endpoints are shared with endpoints of the other two boundaries which were found not to be optimal over those boundaries, any area will be less than the maximised area already found, and thus the optimum will not exist on this boundary.

Therefore, for the vertical cut, the optimal location in Section I is $b_1^* = (0, \frac{q}{2b})$ giving $Area(V^+((0, \frac{q}{2b})) = \frac{pq}{2ab} + \frac{q^2}{16b^2}$. This is depicted in Figure 5.12l.

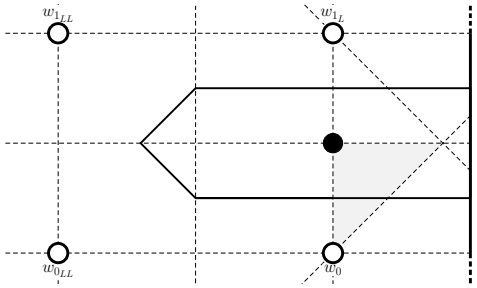

(l) $Area(V^+((0, \frac{q}{2b}))) = \frac{pq}{2ab} + \frac{q^2}{16b^2}$.

Figure 5.12: Maximal area Voronoi cell $V^+(b_1)$ touching a vertical boundary for b_1 within Section I.

Section II (and III) So what does this tell us about Section II and Section III?

For the horizontal edge situation in Sections II and III, the results can be transformed directly from the vertical edge situation studied for Section I since this work did not rely on any relationship between the sizes of $\frac{p}{a}$ and $\frac{q}{b}$. Therefore, retracing our steps, the area

$$Area(V^+(b_1)) = -\frac{x^2}{4} - \frac{3y^2}{4} + \frac{p}{4a}x - \frac{p}{4a}y + \frac{pq}{2ab}$$

has partial derivatives

$$\frac{\delta A}{\delta x} = -\frac{x}{2} + \frac{p}{4a}$$
$$\frac{\delta A}{\delta y} = -\frac{3y}{2} - \frac{p}{4a}$$

which give an optimum $b_1^* = (\frac{p}{2a}, -\frac{p}{6a})$ which is obviously not within Section II or Section III. Therefore the optimum will lie upon either one of the boundaries $y = 0$ or $y = x - \frac{q}{b}$ of Section II and Section III:

- Upon the boundary $y = 0$, the optimum will clearly lie at $(\frac{p}{2a}, 0)$ giving $Area(V^+((\frac{p}{2a}, 0))) = \frac{pq}{2ab} + \frac{p^2}{16a^2}$. However, if $\frac{p}{2a} \geq \frac{q}{b}$ then this point will not lie within Section II or III so the optimum will instead be $(\frac{q}{b}, 0)$, giving $Area(V^+((\frac{q}{b}, 0))) = \frac{3pq}{4ab} - \frac{q^2}{4b^2}$.
- Upon the boundary $y = x - \frac{q}{b}$ we have $Area(V^+(x, x - \frac{q}{b})) = -x^2 + \frac{3q}{2b}x + \frac{3pq}{4ab} - \frac{3q^2}{4b^2}$ which is maximised by $x^* = \frac{3q}{4b}$. Since this is not within Section II or III the optimum must lie at the closest endpoint, the intersection of $y = 0$ and $y = x - \frac{q}{b}$ already studied.

Hence $b_1 = (\frac{p}{2a}, 0)$ gives the largest possible $Area(V^+((\frac{p}{2a}, 0))) = \frac{pq}{2ab} + \frac{p^2}{16a^2}$ as depicted in Figure 5.12m, unless $\frac{p}{2a} > \frac{q}{b}$ in which case $b_1 = (\frac{q}{b}, 0)$ gives the largest possible $Area(V^+((\frac{q}{b}, 0))) = \frac{3pq}{4ab} - \frac{q^2}{4b^2}$ as depicted in Figure 5.12n.

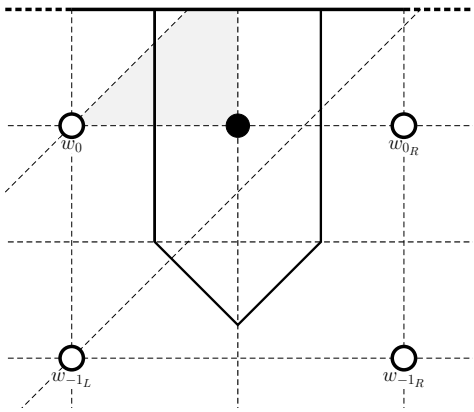

(m) $b_1 = (\frac{p}{2a}, 0)$ only if $\frac{p}{2a} \leq \frac{q}{b}$.

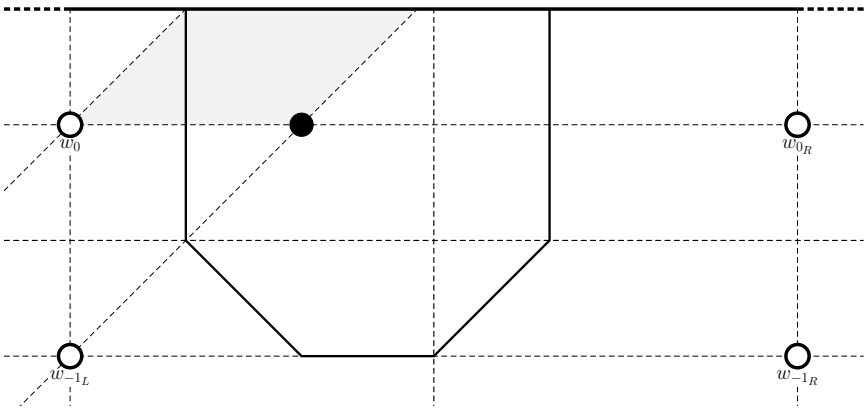

(n) $b_1 = (\frac{q}{b}, 0)$ only if $\frac{p}{2a} > \frac{q}{b}$.

Figure 5.12: Maximal area Voronoi cells $V^+(b_1)$ touching a horizontal boundary for b_1 within Sections II and III.

Corner quadrants

Now let us imagine that the quadrant of the cell containing b_1 contains a corner of $\mathcal{P}$ – i.e. both outside boundaries of this quadrant are on the perimeter of $\mathcal{P}$ (neither w_{1_L} nor w_{0_R} exists). We shall refer to this type of quadrant as a *corner quadrant*. In Figure 5.9 this would amount to discarding all areas above $y = \frac{q}{2b}$ and to the right of $x = \frac{p}{2a}$. Fortuitously, as with many cases for edge quadrants, Section II and beyond in corner quadrants have already been covered in Section 5.2 since the areas are identical after a reflection in $y = x$ and suitable rescaling of p and q. To our delight, the same is also true for areas within Section I, even without the described reflection, since these cells would only require bisectors from one row of points in W. Therefore with one fell swoop we can discard having to explore any corner quadrants as the results are contained in the work in Section 5.2.

Having found all local optima within the sections closest to each w_i we can experiment with different combinations of these points in order to form reasonable arrangements for Black. However, while we were able to make use of the best point b^* within the first sections when White plays a row, we find that the points drawn in Figure 5.12 make pretty lousy team players. This is due to the fact that without any existing black points the placement of b_1 within any section, with the exception of Section I, is always improved by locating closer to the line $x = \frac{p}{2a}$ in order to make the most of the alluring area left to capture from the Voronoi cells $V^\circ(w_{i_R})$. In this way $V^+(b_1)$ steals a mediocre amount from a large number of Voronoi cells, instead of a large amount from a few cells which we were hoping for (points which steal efficiently from fewer cells provide less risk of overlapping with other black points and so will work well within an arrangement).

It is for this reason that it is probably a more fruitful approach to consider the best points from Black's row strategy for candidates within an arrangement for the grid scenario. Since, when White plays a row, $\mathcal{P}$ provides a physical cap bounding the area available to capture in the opposite direction of the generator of the cell within which Black is locating, the optimal locations better reflect the attempt to steal as much as possible from fewer cells (at least for smaller sections). One such effective arrangement is the grid adaptation of the optimal row arrangement found in Section 5.3 (see Figure 5.6 for a reminder) whereby, at least for the preferable even b scenario, each column w_{i_X} of white points for $i = 1, \ldots, a$ can be sandwiched between points of Black to create a columns of the arrangement in Figure 5.6a, rotated by 90°, where $n = b$. Similarly for a row arrangement W, this response from Black does seem, at least for certain values of $\frac{p}{a}$ and $\frac{q}{b}$, to be a good arrangement. However, if the challenges in proving the optimality of an arrangement presented in Section 5.3 left us hiding behind our cushions then we should certainly avert our eyes from the problem of finding optimal arrangements in response to a grid, since the supreme difficulties exhibited here far overshadow what we have already seen. This is in part due to the fact that a point which steals from $V^\circ(w_0)$ will encroach on the thefts from cells below, and above, and to the left or right of $V^\circ(w_0)$ – a whole new direction to consider in contrast to the two-dimensional reasoning exploited in Section 5.3.

For this reason we should feel content at having found the best points in response to both a general row and a general grid arrangement, as well as an optimal black arrangement for the row case, and reward ourselves with a forage among the bounties that the non-grid world may furnish.

Chapter 6

The Stackelberg Game: going off-grid

Since we have discerned that White can perform quite poorly for certain $\mathcal{P}$ when playing a grid, we are also interested in the non-grid arrangements of W. We shall still enforce that they are balanced; the Voronoi cells $V^\circ(w)$ must be fair (of equal area) and locally optimal (area-symmetrical). Our primary focus in this section is to find white arrangements that satisfy these restrictions, and only then shall we concern ourselves with determining Black's best response to such an arrangement.

It is at this point that we must discuss degenerate bisectors between White's points and how to share the area contained within the quarterplanes. In our discussion for degenerate bisectors between White and Black we argued that the rule we decide upon does not matter since either Black's strategy is obvious (in the case that customers are curious and Black controls both quarterplanes) or degenerate bisectors are never optimal and so not of interest for Black (in the case that the areas are shared or remain under White's control). Moreover, since locating on a diagonal configuration line often corresponded to the supremum of the area of Black's Voronoi cell if b_1 was restricted to a certain partition cell, we concluded that the best treatment of Black's placements upon a diagonal configuration line through one of White's points was to allow (or force) Black to choose one quarterplane to claim.

However, contemplating the appropriate decision for degenerate bisectors among White's points requires subtly different considerations, owing to the fact that at this point in the game White is not contesting area. White will not lose out on capturing area (yet) since Black is still to play. The problem White sees is one of dividing up the area of $\mathcal{P}$ between their points so the concepts of loyal, or curious, demand is a confusing one. However, the allocation of these quarterplanes is important if White is to be balanced.

Again we shall highlight three possible allocation schemes for the quarterplanes. The area within the quarterplanes of degenerate bisectors between White's points can be shared equally between the points. This most effectively reflects an independent customer base who decide on their patronage depending purely upon which point is closest, choosing between multiple points without bias if these points are equidistant from the customer's location. There is an interesting interaction that can occur if this method is chosen, whereby different sections of one union of quarterplanes are divided in different proportions between different points (see Figure 6.14 for an example of a situation where this apparent unequal division would exist). We shall call this scheme the *share* rule.

Alternatively, White could choose which quarterplane is allocated to which point as if they were choosing the bisector orientation as Black has done in previous investigations. In some scenarios the players White and Black may be able to assert some control over the demand if this demand is equidistant between two of their points (i.e. if capturing area in which their agents work, or targeting this area for marketing) which this approach more suitably models.

Finally, the computational geometry approach, which takes the view of Voronoi cells as being the set of all points which are strictly closer to the generator than any other point, would suggest that these quarterplanes ought not to be assigned to any point, and are in fact lost space – a no man's land of squandered demand. We shall call this scheme the *discard* rule.

There is no obvious best method and so we shall consider any one of these rules that might be of interest in particular instances. For ease in the optimisation of non-degenerate bisectors we shall choose to apply the second option (whereupon White chooses between two appropriate non-degenerate bisectors) and these bisectors will not be referred to as explicitly degenerate when representing the supremum of non-degenerate bisectors. However, whenever degenerate bisectors are purposefully explored we must state which of the alternative schemes we are applying.

For these calculations the following result is of use, for which let us define a *degenerate* arrangement W to be an arrangement W that contains a degenerate bisector within its Voronoi diagram $\mathcal{VD}(W)$.

Lemma 6.0.1. *Assuming there are no collinear points within W, any balanced degenerate arrangement W under the share (or discard) rule is also balanced under the discard (or share) rule if and only if, for every degenerate bisector in $\mathcal{VD}(W)$, each quarterplane segment has equal area.*

Proof. ($\Rightarrow$) If any such arrangement W is balanced no matter the chosen rule, then choose two points, w_i and w_j, in W whose bisector $B(w_i, w_j)$ is degenerate and contributes to $\mathcal{VD}(W)$. Without loss of generality let us orientate $\mathcal{P}$ such that w_j lies on $\mathcal{CL}^2(w_i)$. In this case the top left and bottom right quadrants of $V^\circ(w_i)$ and $V^\circ(w_j)$ contain the quarterplane segments of $B(w_i, w_j)$ (note that these quarterplane segments may not be present in $\mathcal{VD}(W)$ in which case we shall give them an area of 0). Moreover, the quarterplane segments in these quadrants of $V^\circ(w_i)$ contain only this quarterplane segment from $B(w_i, w_j)$, since in order for $V^\circ(w_i)$ to have another quarterplane segment within its top left quadrant, say, there must be another point lying on $CL^1(w_i) \cup CL^5(w_i)$, which would require collinear points. The same is clearly true for the quarterplane segments of $V^\circ(w_j)$.

Given that W is balanced, these quadrants must be of equal size within each Voronoi cell under the share rule and the discard rule. Therefore the areas of the quarterplanes in the top left quadrants must equal the area of the quarterplanes in the bottom right quadrants in each Voronoi cell.

($\Leftarrow$) If a degenerate arrangement W is such that, for any degenerate bisector $B(w_i, w_j)$, the quarterplane segments present in $\mathcal{VD}(W)$ are of equal area then, if this arrangement is balanced under the share (discard) rule, excluding (including) the quarterplanes for the discard (share) rule would remove (add) identical areas to opposite quadrants of each cell, still remaining balanced. □

Additionally, returning to the discussion in Section 2.4 concerning how to deal with the prospect of degenerate bisectors between white and black points, while the curious case (both quarterplanes are gifted to Black) makes the Voronoi game trivial since Black can easily win (by simply placing each point close enough to each White point upon a diagonal configuration line in order to steal at least $75(1-\varepsilon)\%$ of $\mathcal{P}$), in the Stackelberg game this does not satisfy us in our quest for the best strategy. If quarterplanes were curious then Black could position their points so as to steal at least $75(1-\varepsilon)\%$ of each $V^\circ(w)$ for $w \in W$. Moreover, Black would increase their score if they were to place on the diagonal through w opposite to the smallest quadrant of $V^\circ(w)$ since all other three quadrants of $V^\circ(w)$ would be claimed. For this reason it makes sense for White to aim for configurations in which each quadrant is the same area (by Lemma 4.1.4 this is one step beyond a balanced configuration). Sensible deduction then seems to suggest that each player's optimal strategy is thus: White attempts to find a 'super-balanced' arrangement W such that every quadrant has the same area (e.g. any grid, or see Figure 6.21 for a non-grid example), while Black places each of their points as close as possible to White's points on the diagonal opposite to the smallest quadrant of each of White's Voronoi cells.

6.1 The $n = 2$ case

We will begin our exploration of non-grid arrangements with the basic $n = 2$ case, assuming non-degeneracy in our bisector. We have the set-up for $n = 2$ as shown in Figure 6.1 where, from Lemma 4.2.1, $x_1 = \frac{p}{4}$ and $x_2 = \frac{3p}{4}$, and owing to this symmetry it must be the case that $y_2 = q - y_1$ (relatively straightforward to see by dividing $\mathcal{P}$ down $x = \frac{p}{2}$ and using area arguments).

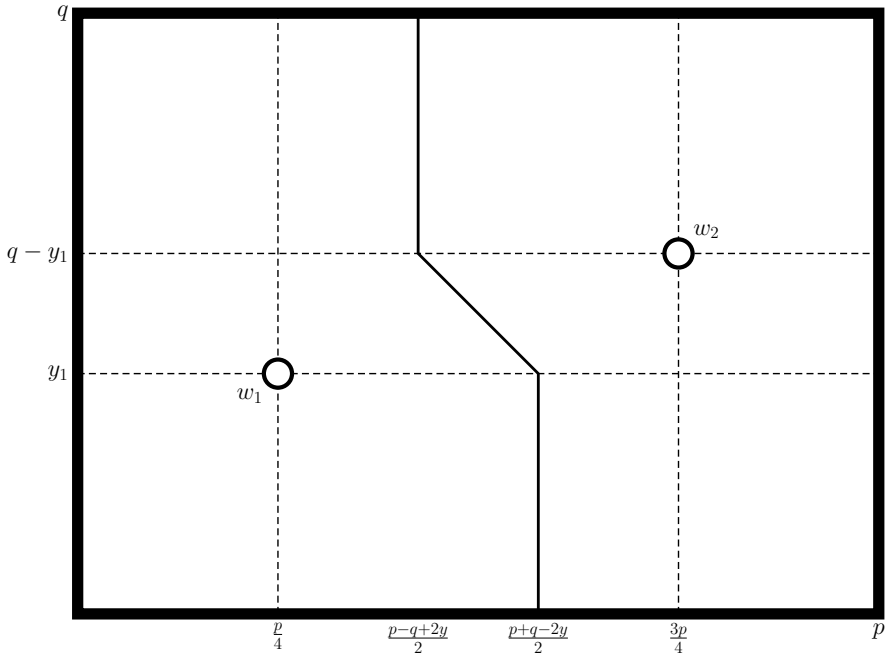

Figure 6.1: White's possible strategies for $n = 2$.

Using the fact that the area within $V^\circ(w_1)$ below the horizontal of w_1 must equal $\frac{pq}{4}$, we have

$$y_1 \times \frac{p+q-2y_1}{2} = \frac{pq}{4} \Rightarrow y_1^2 - (\frac{p}{2} + \frac{q}{2})y_1 + \frac{pq}{4} = 0 \Rightarrow (y_1 - \frac{p}{2})(y_1 - \frac{q}{2}) = 0$$
$$\Rightarrow y_1 = \frac{q}{2} \ \textit{or} \ \ y_1 = \frac{p}{2}\,.$$

The first solution is the regular orthogonal grid we explored in the previous sections, but the second gives a balanced non-grid arrangement $w_1 = (\frac{p}{4}, \frac{p}{2})$, $w_2 = (\frac{3p}{4}, q - \frac{p}{2})$ (as well as its reflection $w_1 = (\frac{p}{4}, q - \frac{p}{2})$, $w_2 = (\frac{3p}{4}, \frac{p}{2})$) depicted in Figure 6.2. Note that this arrangement works only when $\frac{p}{2} \leq \frac{q}{2}$ (i.e. $p \leq q$), otherwise the arena can be rotated (thereby swapping p and q). Moreover, in order for this bisector to exist as it does (i.e. vertically), it must be the case that $q - \frac{p}{2} - \frac{3p}{4} \leq \frac{p}{2} - \frac{p}{4} \Rightarrow q \leq \frac{3p}{2}$ (otherwise the bisector becomes a horizontal type and we swap the roles of p and q). Therefore this arrangement exists for $p \leq q \leq \frac{3p}{2}$.

Alas, before White can start celebrating, this arrangement may be easily thwarted. We will explore Black placing a point $b_1 = (x, y)$ within $\mathcal{CC}^2(w_1) \cap \mathcal{CC}^5(w_2)$ as shown in Figure 6.3. $V^+(b_1)$ has vertices, anticlockwise from bottom left, $(0, \frac{4x+4y+p}{8})$, $(\frac{p}{4}, \frac{4x+4y+p}{8})$, $(x, \frac{4y-4x+3p}{8})$, $(\frac{4x-4y+p+4q}{8}, \frac{4y-4x+3p}{8})$, $(\frac{4x-4y+p+4q}{8}, y)$, $(\frac{4x+4y+5p-4q}{8}, q-\frac{p}{2})$, $(\frac{4x+4y+5p-4q}{8}, q)$, and $(0, q)$ giving an area

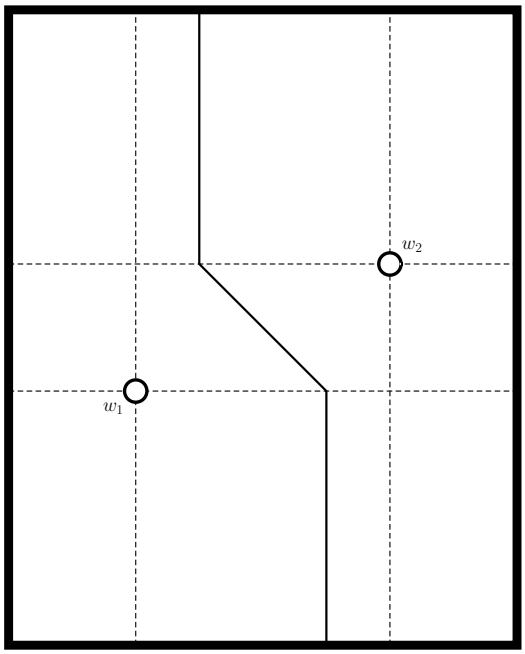

Figure 6.2: White's balanced arrangement $w_1 = (\frac{p}{4}, \frac{p}{2})$ and $w_2 = (\frac{3p}{4}, q - \frac{p}{2})$ for $p \leq q \leq \frac{3p}{2}$.

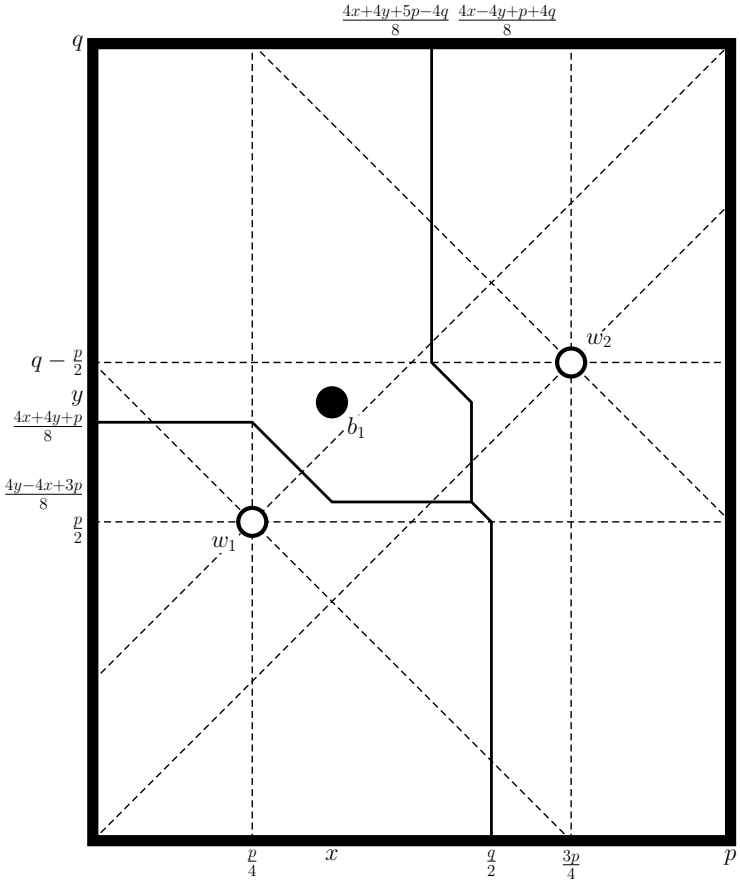

Figure 6.3: $\mathcal{VD}^+$ for $b_1 \in \mathcal{CC}^2(w_1) \cap \mathcal{CC}^5(w_2)$ for $n = 2$.

$$
\begin{aligned}
Area(V^+(b_1)) &= \left(q - \frac{4x+4y+p}{8}\right)\left(\frac{4x+4y+5p-4q}{8}\right) + \frac{1}{2}\left(\frac{4x-4y+p+4q}{4} - x - \frac{p}{4}\right)\left(x - \frac{p}{4}\right) \\
&\quad + \frac{1}{2}\left(q - \frac{p}{2} + y - \frac{4x+4y+p}{4}\right)\left(q - \frac{p}{2} - y\right) \\
&= \frac{-16x^2 - 16y^2 - 32xy - 8px + 48qx + 8py + 16qy + 7p^2 - 4pq}{64} \\
&= -\frac{(x+y)^2}{4} + \frac{-p+6q}{8}x + \frac{p+2q}{8}y + \frac{7p^2-4pq}{64}\,.
\end{aligned}
$$

The use of gradient methods produces

$$
\begin{aligned}
\frac{\delta A}{\delta x} &= -\frac{x+y}{2} + \frac{-p+6q}{8} \\
\frac{\delta A}{\delta y} &= -\frac{x+y}{2} + \frac{p+2q}{8}
\end{aligned}
$$

which shows that there is no maximum (otherwise $\frac{-p+6q}{8} = \frac{p+2q}{8} \Rightarrow p = 2q$ but $p \leq q$). Therefore we explore the boundary of $\mathcal{CC}^2(w_1) \cap \mathcal{CC}^5(w_2)$ in order to find the maximum.

- On the line $x = \frac{p}{4}$ we obtain the maximum at $-\frac{p+4y}{8} + \frac{p+2q}{8} = 0 \Rightarrow y = \frac{q}{2}$ giving $Area(V^+(\frac{p}{4}, \frac{q}{2})) = \frac{(p+q)^2}{16}$.

- On the line $y = q - \frac{p}{2}$ we obtain the maximum at $-\frac{x+q-\frac{p}{2}}{2} + \frac{-p+6q}{8} = 0 \Rightarrow x = \frac{p}{4} + \frac{q}{2}$ giving $Area(V^+((\frac{p}{4}+\frac{q}{2}, q-\frac{p}{2}))) = \frac{pq}{4} + \frac{q^2}{16}$, but in order for $(\frac{p}{4}+\frac{q}{2}, q-\frac{p}{2})$ to lie on the boundary of $\mathcal{CC}^2(w_1) \cap \mathcal{CC}^5(w_2)$ it must be the case that $\frac{p}{4} \leq \frac{p}{4} + \frac{q}{2} \leq q - \frac{3p}{4} \Leftrightarrow p \leq \frac{q}{2}$, which is not true since $q \leq \frac{3p}{2}$ so this optimum lies to the right of the area $\mathcal{CC}^2(w_1) \cap \mathcal{CC}^5(w_2)$. Therefore the optimum must lie at the endpoint $(q - \frac{3p}{4}, q - \frac{p}{2})$ and we have $Area(V^+((q - \frac{3p}{4}, q - \frac{p}{2}))) = \frac{pq}{2} - \frac{p^2}{4}$.

- Finally we investigate the boundary $y = x + \frac{p}{4}$ upon which we have $Area(V^+((y - \frac{p}{4}, y))) = -y^2 + (\frac{p}{4} + q)y + \frac{p^2}{8} - \frac{pq}{4}$ achieving a maximum $Area(V^+((-\frac{p}{8}+\frac{q}{2}, \frac{p}{8}+\frac{q}{2}))) = \frac{9p^2}{64} - \frac{pq}{8} + \frac{q^2}{4}$. To check whether $(-\frac{p}{8}+\frac{q}{2}, \frac{p}{8}+\frac{q}{2})$ lies on the boundary of $\mathcal{CC}^2(w_1) \cap \mathcal{CC}^5(w_2)$ it must be the case that $\frac{p}{2} \leq \frac{p}{8} + \frac{q}{2} \leq q - \frac{p}{2} \Leftrightarrow \frac{5p}{4} \leq q$. If $\frac{5p}{4} \geq q$ then the optimum would lie on the endpoint $(q - \frac{3p}{4}, q - \frac{p}{2})$ which we have already explored above.

In order to find the best location b^* of b_1 we must compare each boundary's maximal area. Since the optimum over $y = q - \frac{p}{2}$ is simply the endpoint of $y = x + \frac{p}{4}$, we need only compare the optimum on the boundary $x = \frac{p}{4}$ to the optima upon $y = x + \frac{p}{4}$. Comparing the maximal area upon $x = \frac{p}{4}$ with that upon $y = x + \frac{p}{4}$ given the condition that $\frac{5p}{4} \geq q$:

$$
\begin{aligned}
\frac{(p+q)^2}{16} - \left(\frac{pq}{2} - \frac{p^2}{4}\right) &= \frac{p^2}{16} + \frac{pq}{8} + \frac{q^2}{16} - \frac{pq}{2} + \frac{p^2}{4} \\
&= \frac{5p^2}{16} - \frac{3pq}{8} + \frac{q^2}{16} > 0 \\
&\Leftrightarrow 5p^2 - 6pq + q^2 = (5p - q)(p - q) > 0 \\
&\Leftrightarrow 5p < q \text{ or } p > q
\end{aligned}
$$

so the optimum upon $x = \frac{p}{4}$ is never preferable to the optimum upon $y = x + \frac{p}{4}$ (for $\frac{5p}{4} \geq q$). Since this optimum upon $y = x + \frac{p}{4}$ for $\frac{5p}{4} \geq q$ is the lesser of the optima upon $y = x + \frac{p}{4}$, we can conclude that the optimum over all of $\mathcal{CC}^2(w_1) \cap \mathcal{CC}^5(w_2)$ always lies upon the boundary $y = x + \frac{p}{4}$, and these optima are depicted in Figure 6.4.

Whilst our investigation of every potential placement of b_1 is incomplete, this work satisfies us in that we have seen how Black can play in a non-grid setting, and provides an easy lower bound of Black's best arrangement of $\frac{pq}{2} - \frac{p^2}{4} + \frac{pq}{4} = \frac{3pq}{4} - \frac{p^2}{4}$ when $p \leq q \leq \frac{5p}{4}$ and $\frac{9p^2}{64} - \frac{pq}{8} + \frac{q^2}{4} + \frac{pq}{4} = \frac{9p^2}{64} + \frac{pq}{8} + \frac{q^2}{4}$ when $\frac{5p}{4} \leq q \leq \frac{3p}{2}$, representing the best placements shown

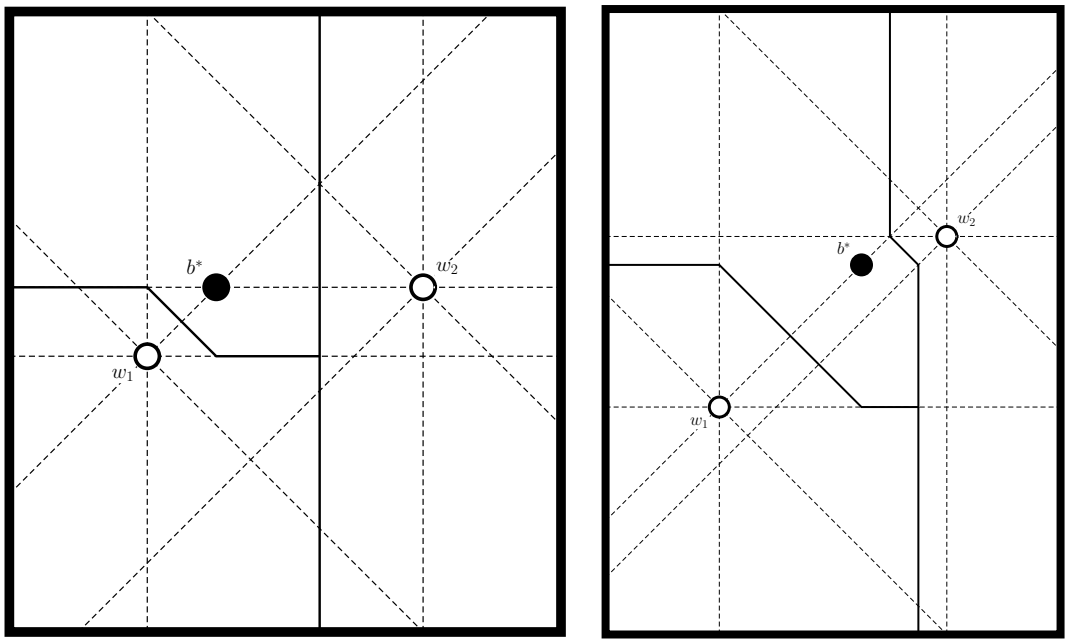

(a) $b^* = (q - \frac{3p}{4}, q - \frac{p}{2}))$ only if $p \leq q \leq \frac{5p}{4}$. (b) $b^* = (-\frac{p}{8} + \frac{q}{2}, \frac{p}{8} + \frac{q}{2})$ only if $\frac{5p}{4} \leq q \leq \frac{3p}{2}$.

Figure 6.4: The best points b^* within $\mathcal{CC}^2(w_1) \cap \mathcal{CC}^5(w_2)$.

in Figure 6.4 along with a simple placement of the second point atop one of White's points in order to steal an untouched half of $V^+(w_i)$ (as outlined in Lemma 4.1.1).

To summarise, we have found the only balanced non-grid non-degenerate arrangement W for $n = 2$ and investigated how Black can respond to such an arrangement.

6.2 The $n = 2$ case with degeneracy

In this section we shall allow degenerate bisectors in the $n = 2$ case. These arrangements take the form (up to reflection) as shown in Figure 6.5.

No matter how we deal with the quarterplanes, by Lemmas 4.1.2 and 4.1.3 the top right quadrant of $V^\circ(w_1)$ must be equal in area to the bottom left quadrant of $V^\circ(w_1)$ and, because the top right and bottom left quadrants of $V^\circ(w_1)$ and $V^\circ(w_2)$ respectively are identical, it must also be equal in area to the top right quadrant of $V^\circ(w_2)$. Therefore $x_1 y_1 = \frac{d^2}{2} = (p - x_1 - d)(q - y_1 - d)$.

Firstly let us try the approach in which the quarterplanes are shared among the points. By Lemmas 4.1.2 and 4.1.3 the top left and bottom right quadrants of $V^\circ(w_1)$ must be equal:

$$\begin{aligned} x_1 \times (d + \frac{(q - y_1 - d)}{2}) = (d + \frac{(p - x1 - d)}{2}) \times y_1 &\Rightarrow x_1(\frac{d}{2} + \frac{q}{2} - \frac{1}{2}y_1) = (\frac{d}{2} + \frac{p}{2} - \frac{1}{2}x1) \times y_1 \\ &\Rightarrow (\frac{q}{2} + \frac{d}{2})x_1 = (\frac{p}{2} + \frac{d}{2})y_1 \\ &\Rightarrow y_1 = \frac{q + d}{p + d}x_1 \,. \end{aligned}$$

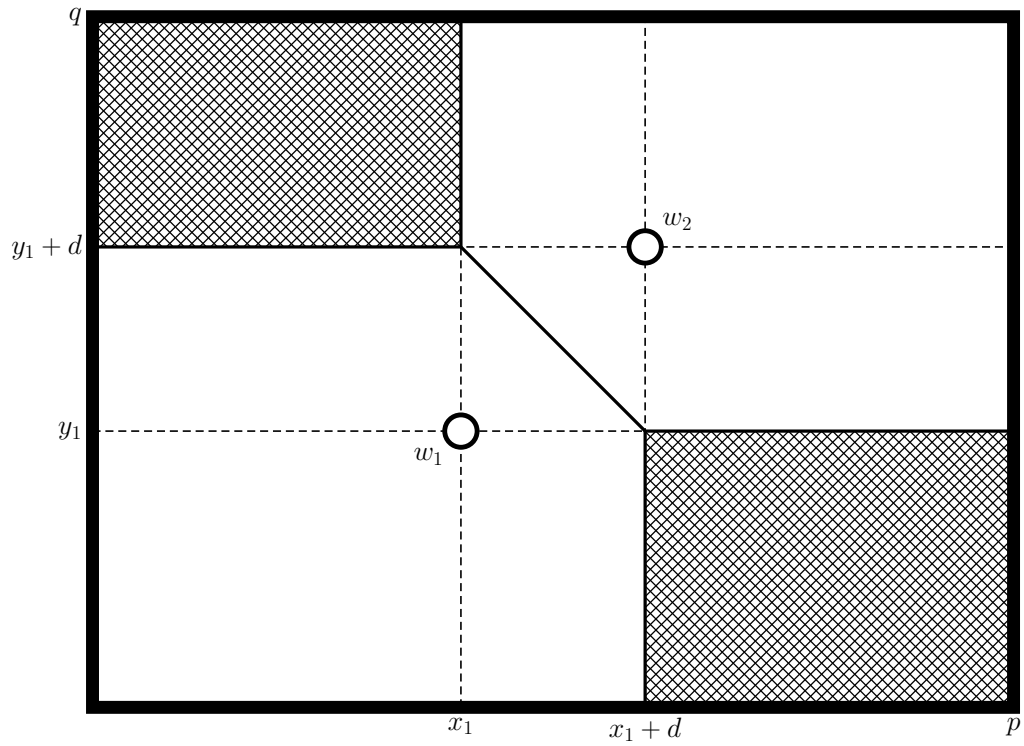

Figure 6.5: White's possible degenerate strategies for $n = 2$.

Analogously the top left and bottom right quadrants of $V^\circ(w_2)$ must be equal:

$$\begin{aligned}(\frac{x_1}{2} + d) \times (q - y_1 - d) &= (p - x_1 - d) \times (\frac{y_1}{2} + d) \\ &\Rightarrow \frac{q}{2}x_1 - \frac{d}{2}x_1 + dq - dy_1 = \frac{p}{2}y_1 - \frac{d}{2}y_1 + pd - dx_1 \\ &\Rightarrow (\frac{q}{2} + \frac{d}{2})x_1 = (\frac{p}{2} + \frac{d}{2})y_1 + d(p - q) \\ &\Rightarrow d(p - q) = 0 \Rightarrow p = q\,.\end{aligned}$$

So there is only a balanced degenerate arrangement (under quarterplane sharing rules) if $\mathcal{P}$ is a square.

Given this condition, $y_1 = \frac{q+d}{p+d}x_1 = x_1$ and $p - x_1 - d = q - y_1 - d$ and since $x_1 y_1 = \frac{d^2}{2} = (p - x_1 - d)(q - y_1 - d)$ it is the case that $x_1 = y_1 = p - x_1 - d = q - y_1 - d = \frac{d}{\sqrt{2}}$. Therefore $d = \sqrt{2}x_1$ and $p = x_1 + d + x_1$ so $p = (2 + \sqrt{2})x_1$. This gives the result $x_1 = \frac{p}{2+\sqrt{2}} = \frac{(2-\sqrt{2})p}{2}$, that the balanced degenerate arrangement W under the sharing rule in a square $\mathcal{P}$ is $w_1 = (\frac{(2-\sqrt{2})p}{2}, \frac{(2-\sqrt{2})p}{2})$ and $w_2 = (\frac{\sqrt{2}p}{2}, \frac{\sqrt{2}p}{2})$ as depicted in Figure 6.6.

Secondly let us use the computational geometry approach, and discard the quarterplanes. By Lemmas 4.1.2 and 4.1.3 the top left and bottom right quadrants of $V^\circ(w_1)$ must be equal: $x_1 \times d = d \times y_1 \Rightarrow x_1 = y_1$. Analogously in $V^\circ(w_2)$, $d \times (q - y_1 - d) = (p - x_1 - d) \times d \Rightarrow q - y_1 - d = p - x_1 - d \Rightarrow p = q$. So there is only a balanced degenerate arrangement (under quarterplane discarding rules) if $\mathcal{P}$ is again a square.

Since these are exactly the same conditions as found when investigating the sharing rule, the arrangement is identical, which is to be expected from Lemma 6.0.1. This gives the result that the balanced degenerate arrangement W under the discarding rule in a square $\mathcal{P}$ is also $w_1 = (\frac{(2-\sqrt{2})p}{2}, \frac{(2-\sqrt{2})p}{2})$ and $w_2 = (\frac{\sqrt{2}p}{2}, \frac{\sqrt{2}p}{2})$ as depicted in Figure 6.6.

In summary, there is only one degenerate arrangement W, irrespective of the degenerate scheme being followed, and this arrangement requires that $\mathcal{P}$ is a square.

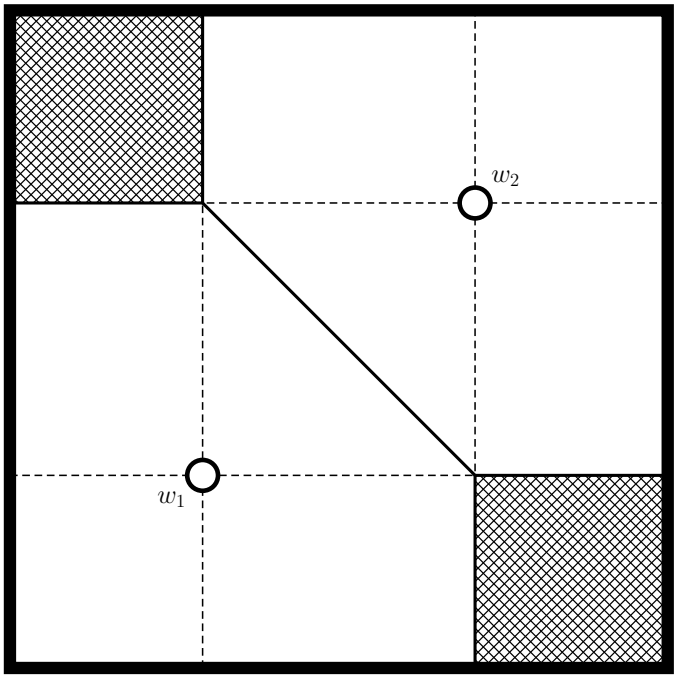

Figure 6.6: White's balanced degenerate arrangement $w_1 = (\frac{(2-\sqrt{2})p}{2}, \frac{(2-\sqrt{2})p}{2})$ and $w_2 = (\frac{\sqrt{2}p}{2}, \frac{\sqrt{2}p}{2})$ for a square $\mathcal{P}$.

6.3 The $n = 3$ case

To tackle the $n = 3$ case we notice that one point $w_1 = (x_1, y_1)$ must contain two corners of $\mathcal{P}$ (so $x_1 = \frac{5p}{6}$ by Lemma 4.2.1) and another point $w_2 = (x_2, y_2)$ must contain another one or two corners. This gives us the two situations shown in Figure 6.7 where the third point $w_3 = (x, y)$ cannot be located in the shaded area (else it would violate the imposed corner conditions of w_1 and w_2). The labelled sections within each figure denote the partitions of structural identity as before, obtained from the configuration lines of w_1 and w_2, and, in Figure 6.7a, the line of equidistance about the upper breakpoint in $B(w_1, w_2)$ to w_1 and w_2 (the importance of which can be seen in Figure 6.8).

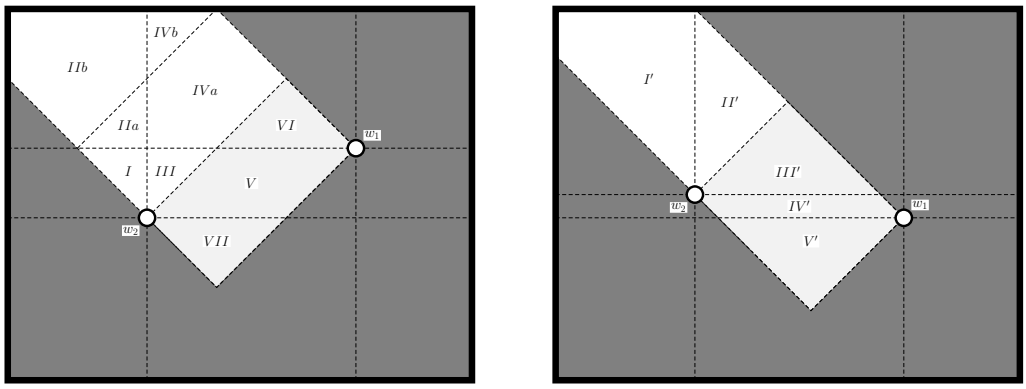

(a) Partition where $y_1 > y_2$.

(b) Partition where $y_1 \leq y_2$.

Figure 6.7: The two partitions of $\mathcal{P}$ for w_3 for $n = 3$.

The Voronoi cells $V^\circ(w_3)$ for w_3 in Sections I, IIa, IIb, III, IVa, IVb, I', and II' are shown in Figure 6.8.

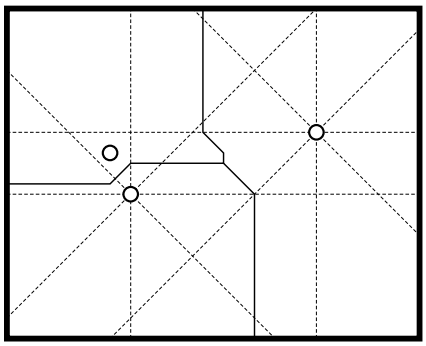

(a) Voronoi cell $V^\circ(w_3)$ for w_3 in Section I.

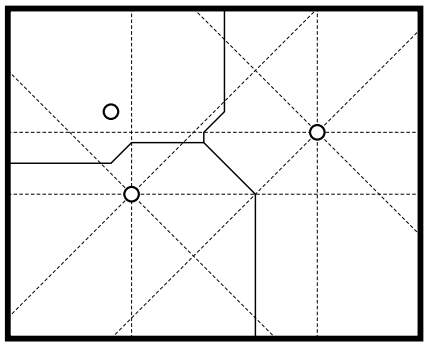

(b) Voronoi cell $V^\circ(w_3)$ for w_3 in Section IIa.

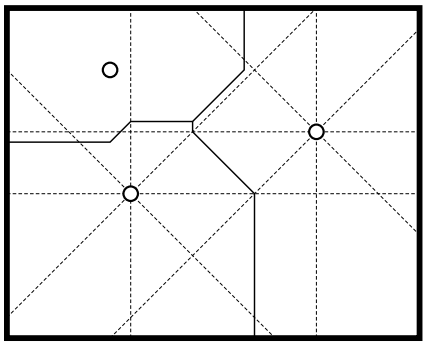

(c) Voronoi cell $V^\circ(w_3)$ for w_3 in Section IIb.

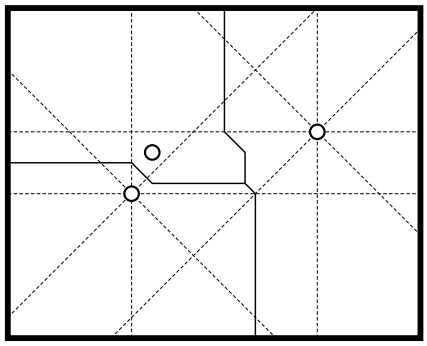

(d) Voronoi cell $V^\circ(w_3)$ for w_3 in Section III.

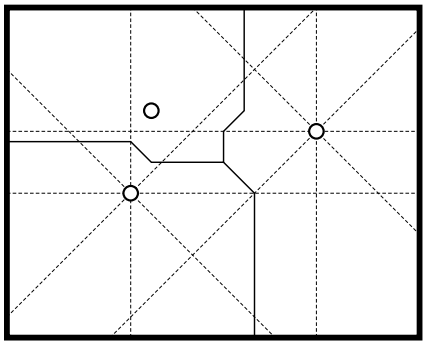

(e) Voronoi cell $V^\circ(w_3)$ for w_3 in Section IVa.

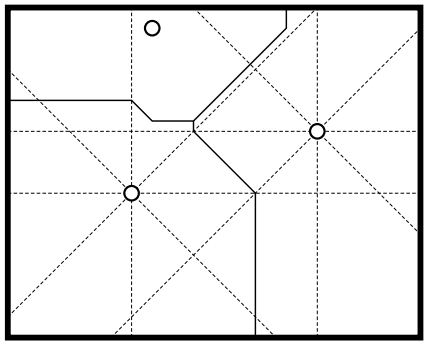

(f) Voronoi cell $V^\circ(w_3)$ for w_3 in Section IVb.

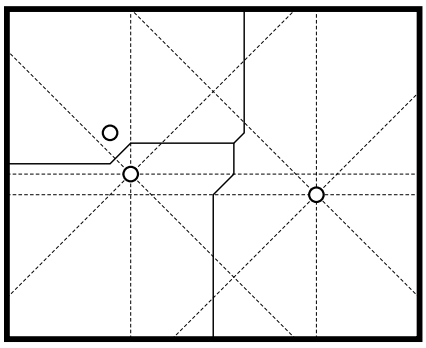

(g) Voronoi cell $V^\circ(w_3)$ for w_3 in Section I'.

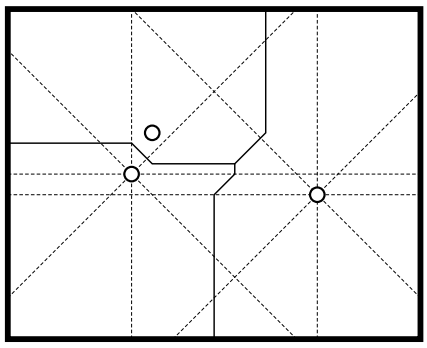

(h) Voronoi cell $V^\circ(w_3)$ for w_3 in Section II'.

Figure 6.8: Voronoi cells $V^\circ(w_3)$ for w_3 in respective sections according to Figure 6.7.

It is useful to note that the Voronoi diagrams for Sections I and II' are identical (merely reflected in the horizontal axis), as are those for Sections III and I'. Therefore we need only consider the Voronoi cells for w_3 in Sections I, IIa, IIb, III, IVa, IVb, and those within the highlighted area.

Firstly we tackle the placement of w_3 within the highlighted areas (Sections V, VI, VII, III', IV', and V'). Within these areas, $V^\circ(w_3)$ does not contain any corners of $\mathcal{P}$ and the vertical through w_3 is fully contained in $V^\circ(w_3)$. This means that it exactly halves $\mathcal{P}$, as to the left is $V^\circ(w_2)$ and the left half of $V^\circ(w_3)$, and to the right is $V^\circ(w_1)$ and the right half of $V^\circ(w_2)$, and by Lemmas 4.1.2 and 4.1.3 this is exactly $\frac{pq}{2}$. Therefore $x_3 = \frac{p}{2}$ and each half of $\mathcal{P}$ is an identical problem (since we must also have $x_2 = \frac{p}{6}$). We will solve the problem in its left-side form as shown, without loss of generality, in Figure 6.9.

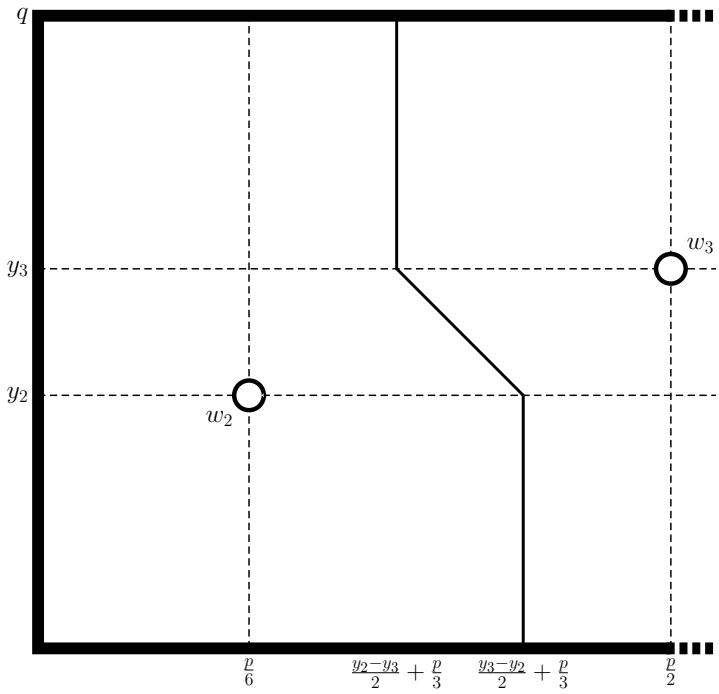

Figure 6.9: Subproblem for one of White's possible strategies for $n = 3$.

We can see that this is in fact identical to the $n = 2$ problem (without including the right half of $V^\circ(w_3)$) where instead we have the width of $\mathcal{P}$ (originally p) being $\frac{2p}{3}$. Using the results from $n = 2$ we know that $y_3 = q - y_2$ and $y_2 = \frac{p}{3}$ is the only solution (for $\frac{2p}{3} \leq q$ which, after rotation, is always satisfied). However, looking at this suggested arrangement shown in Figure 6.10, and $w_1 = (\frac{5p}{6}, \frac{p}{3})$, the top half of $V^\circ(w_3)$ has area

$$\left(q - \left(q - \frac{p}{3}\right)\right) \times \left(\frac{p}{3} + \frac{q}{2} - \left(\frac{2p}{3} - \frac{q}{2}\right)\right) = \frac{pq}{3} - \frac{p^2}{9} = \frac{pq}{6} \Leftrightarrow q = \frac{2p}{3}$$

so this is only balanced if $q = \frac{2p}{3}$ in which case this 'non-grid' arrangement is in fact a grid.

The equations for area symmetry and equal area for arrangements of w_1, w_2, and w_3 within Sections I, IIa, IIb, III, IVa, and IVb are more complex than the theory shown for facilities within the highlighted area, and thus their solutions were sought using a solver (detailed in Appendix A.2). Exactly one balanced arrangement was found within any of these sections: $w_1 = (\frac{5p}{6}, \frac{q}{2})$, $w_2 = (\frac{p}{3}, \frac{3q}{14})$, and $w_3 = (\frac{p}{3}, \frac{11q}{14})$ along with the restrictive condition $p = \frac{36}{49}q$; this is displayed in Figure 6.11.

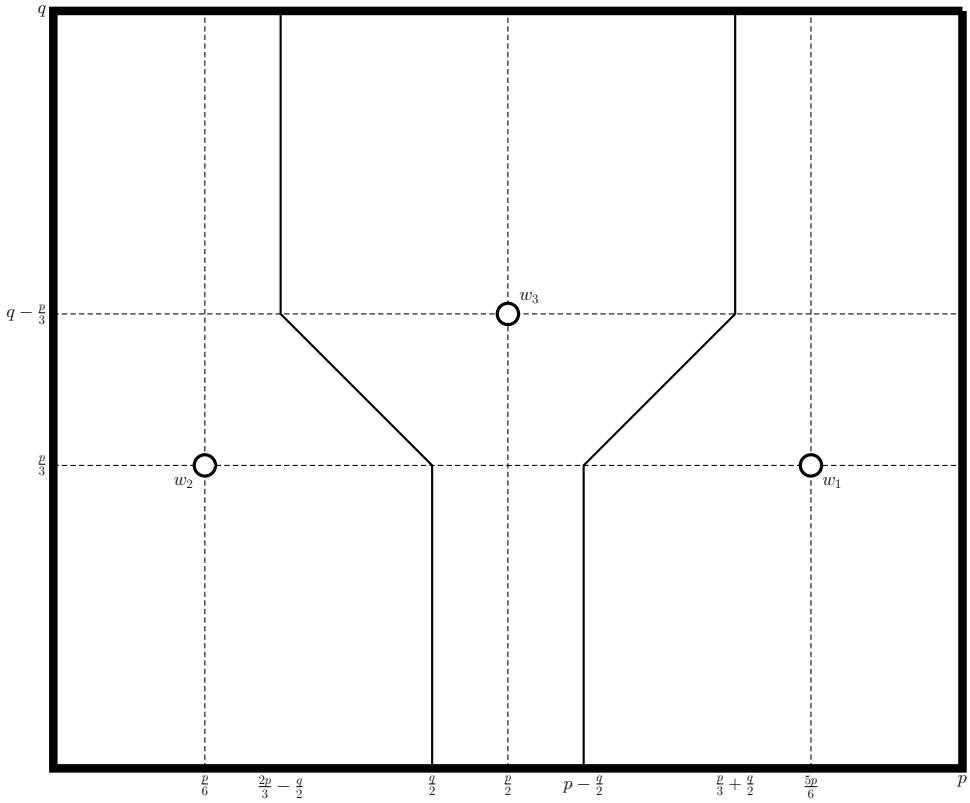

Figure 6.10: White's trial arrangement $w_1 = (\frac{5p}{6}, \frac{p}{3})$, $w_2 = (\frac{p}{6}, \frac{p}{3})$, and $w_3 = (\frac{p}{2}, q - \frac{p}{3})$.

While White may thank their lucky stars that they have been blessed with an arrangement for such a precise aspect ratio of $\mathcal{P}$ (noting that if $p = \frac{36}{49}q$ then $\frac{p}{q} < n$ even with a rotation to swap p and q so, from Chapter 4, there is no such winning grid arrangement for White), unfortunately this non-grid arrangement may not perform so well when considering how best Black can best it. We shall explore all of Black's possible placements and firstly find those which steal an area exceeding $\frac{pq}{6}$ (half of $V^\circ(w_i)$). By the symmetry of White's arrangement we need only consider Black's placement in the bottom half of $\mathcal{P}$, say. All possible placements are represented in Figure 6.12.

To ease calculation, it is worth noting that some areas are futile to explore. Placing $b \in CC^8(w_1)$ restricts $V^+(b)$ to the right half of $V^\circ(w_1)$ so this will never steal more than $\frac{pq}{6}$ (so we can discount Figure 6.12e). Moreover, for $b \in \mathcal{CC}^1(w_2) \cap \mathcal{CC}^7(w_1)$ we can see from Figure 6.12d that, within this region, moving b in a northwest direction will increase the area of $V^+(b)$ so the maximum over this area will occur on $CL^6(w_1)$. Since this is contained in $\mathcal{CC}^1(w_2) \cap \mathcal{CC}^6(w_1)$ (Figure 6.12c) the optimum within $\mathcal{CC}^1(w_2) \cap \mathcal{CC}^7(w_1)$ is no better than that within $\mathcal{CC}^1(w_2) \cap \mathcal{CC}^6(w_1)$ so we need only explore this latter region. The same can be said for how $\mathcal{CC}^5(w_2)$ (Figure 6.12i) is dominated by $\mathcal{CC}^4(w_2)$ (Figure 6.12h), how $\mathcal{CC}^6(w_2) \cap \mathcal{CC}^5(w_1)$ (Figure 6.12j) is dominated by $\mathcal{CC}^7(w_2) \cap \mathcal{CC}^5(w_1)$ (Figure 6.12l), how $\mathcal{CC}^6(w_2) \cap \mathcal{CC}^6(w_1)$ (Figure 6.12k) is dominated by $\mathcal{CC}^7(w_2) \cap \mathcal{CC}^6(w_1)$ (Figure 6.12m), how $\mathcal{CC}^8(w_2) \cap \mathcal{CC}^6(w_1)$ (Figure 6.12o) is dominated by $\mathcal{CC}^1(w_2) \cap \mathcal{CC}^6(w_1)$ (Figure 6.12c) or has its maximum at $\mathcal{CL}^6(w_1)$, and finally how $\mathcal{CC}^8(w_2) \cap \mathcal{CC}^7(w_1)$ (Figure 6.12p) is dominated by either $\mathcal{CC}^8(w_2) \cap \mathcal{CC}^6(w_1)$ (Figure 6.12o) or $\mathcal{CC}^1(w_2) \cap \mathcal{CC}^7(w_1)$ (Figure 6.12d).

Furthermore, comparing Figure 6.12l to Figure 6.12m, one can see that the area lost in $V^+(b)$ through the change in $B(w_2, b)$ is far inferior to the area gained by the change in $B(w_1, b)$ by crossing $\mathcal{CL}^6(w_1)$ so the optimum over $\mathcal{CC}^7(w_2) \cap \mathcal{CC}^6(w_1)$ will exceed that of $\mathcal{CC}^7(w_2) \cap \mathcal{CC}^5(w_1)$ and therefore we need not explore the latter. By the same argument, $\mathcal{CC}^8(w_2) \cap \mathcal{CC}^5(w_1)$ (Figure 6.12n) is dominated by $\mathcal{CC}^8(w_2) \cap \mathcal{CC}^6(w_1)$ (Figure 6.12o). A similar argument can be made for $b \in \mathcal{CC}^8(w_2) \cap \mathcal{CC}^6(w_1)$ (Figure 6.12o). As explained above, the supremum is found on $\mathcal{CL}^6(w_1)$.

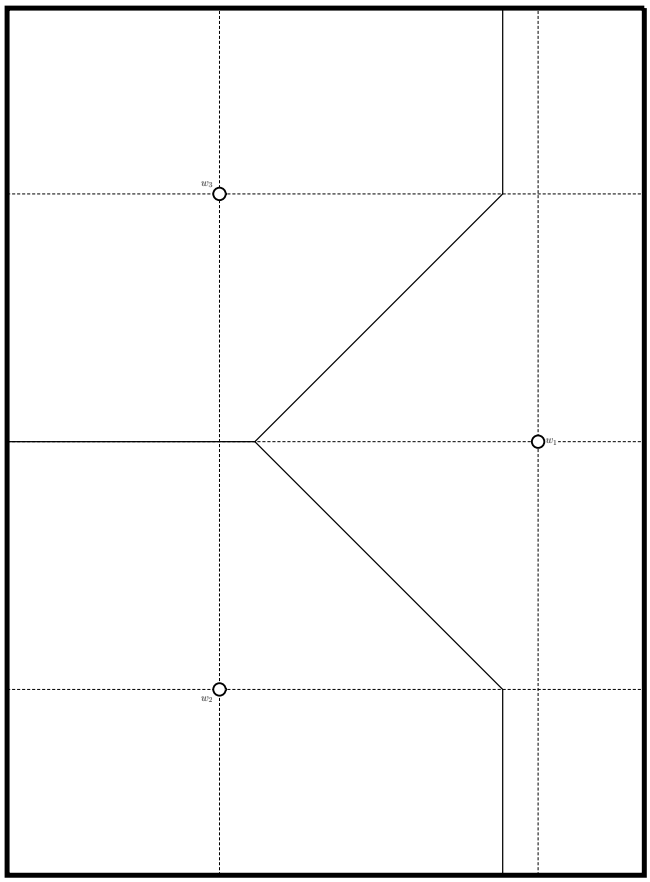

Figure 6.11: White's arrangement $w_1 = (\frac{5p}{6}, \frac{q}{2})$, $w_2 = (\frac{p}{3}, \frac{3q}{14})$, and $w_3 = (\frac{p}{3}, \frac{11q}{14})$ for $p = \frac{36}{49}q$.

Moving northeast along this line will decrease the area due to the worsening of $B(w_2, b)$ from y and below, but increase the area due to the improvement of $B(w_1, b)$. Both bisectors will be shifted by the same amount but the contraction in $B(w_2, b)$ over length of y is much less than the expansion over length $p - x$ of $B(w_1, b)$. Therefore the supremum over $\mathcal{CC}^8(w_2) \cap \mathcal{CC}^5(w_1)$ is found at the intersection of $\mathcal{CL}^1(w_2)$ and $\mathcal{CL}^6(w_1)$, which is also contained in $\mathcal{CC}^1(w_2) \cap \mathcal{CC}^6(w_1)$ (Figure 6.12c) so it is dominated by the latter.

This leads us to the following calculations, where a cell of interest has area greater than $\frac{pq}{6} = \frac{49p^2}{216} = \frac{6q^2}{49}$:

- For $b \in \mathcal{CC}^1(w_2) \cap \mathcal{CC}^5(w_1) \cap \mathcal{CC}^7(w_3)$ we have

$$\begin{aligned}
Area(V^+(b)) &= (\frac{x + \frac{5p}{6} - \frac{q}{2} + y}{2} - \frac{x + \frac{p}{3} - y + \frac{3q}{14}}{2}) \times \frac{y + \frac{11q}{14} + x - \frac{p}{3}}{2} + \frac{1}{2}(\frac{q}{2} - y)(\frac{q}{2} + y) \\
&\quad - \frac{1}{2}(y - \frac{3q}{14})(y + \frac{3q}{14}) - \frac{1}{2}(\frac{x - \frac{p}{3} + y - \frac{3q}{14}}{2})^2 \\
&= (\frac{p}{4} - \frac{5q}{14} + y) \times \frac{y + \frac{11q}{14} + x - \frac{p}{3}}{2} + \frac{1}{2}(\frac{q^2}{4} - y^2) - \frac{1}{2}(y^2 - \frac{9q^2}{196}) - \frac{1}{2}(\frac{x - \frac{p}{3} + y - \frac{3q}{14}}{2})^2 \\
&= \frac{1}{2}(y^2 + xy + (\frac{p}{4} - \frac{5q}{14})x + (-\frac{p}{12} + \frac{3q}{7})y + (\frac{p}{4} - \frac{5q}{14})(\frac{11q}{14} - \frac{p}{3}) \\
&\quad + \frac{29q^2}{98} - 2y^2 - \frac{x^2}{4} - \frac{xy}{2} \frac{y^2}{4} + (\frac{p}{6} + \frac{3q}{28})(x + y) - (\frac{p}{6} + \frac{3q}{28})^2) \\
&= \frac{1}{2}(-\frac{x^2}{4} - \frac{5y^2}{4} + \frac{xy}{2} + (\frac{5p}{12} - \frac{q}{4})x + (\frac{p}{12} + \frac{15q}{28})y - \frac{p^2}{9} + \frac{47pq}{168} + \frac{3q^2}{784}) \\
&= \frac{1}{2}(-\frac{x^2}{4} - \frac{5y^2}{4} + \frac{xy}{2} + \frac{11p}{144}x + \frac{13p}{16}y + \frac{1913p^2}{6912}).
\end{aligned}$$

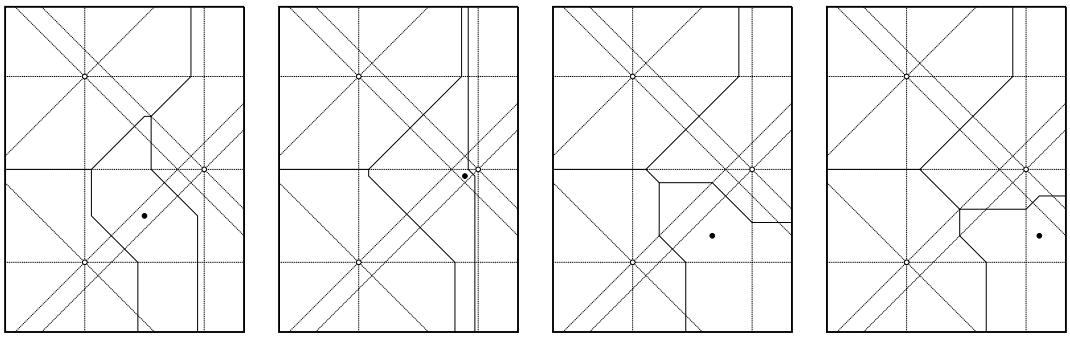

(a) $b \in \mathcal{CC}^1(w_2) \cap \mathcal{CC}^5(w_1) \cap \mathcal{CC}^7(w_3)$ (b) $b \in \mathcal{CC}^1(w_2) \cap \mathcal{CC}^5(w_1) \cap \mathcal{CC}^8(w_3)$ (c) $b \in \mathcal{CC}^1(w_2) \cap \mathcal{CC}^6(w_1)$ (d) $b \in \mathcal{CC}^1(w_2) \cap \mathcal{CC}^7(w_1)$

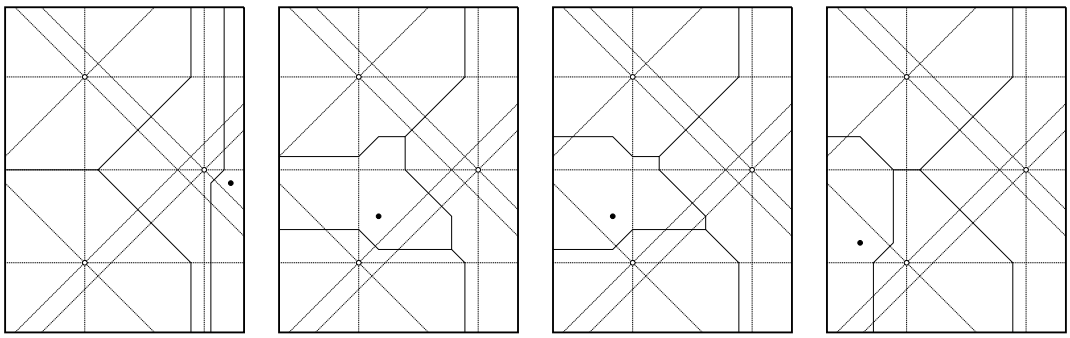

(e) $b \in \mathcal{CC}^1(w_2) \cap \mathcal{CC}^8(w_1)$ (f) $b \in \mathcal{CC}^2(w_2)$ (g) $b \in \mathcal{CC}^3(w_2)$ (h) $b \in \mathcal{CC}^4(w_2)$

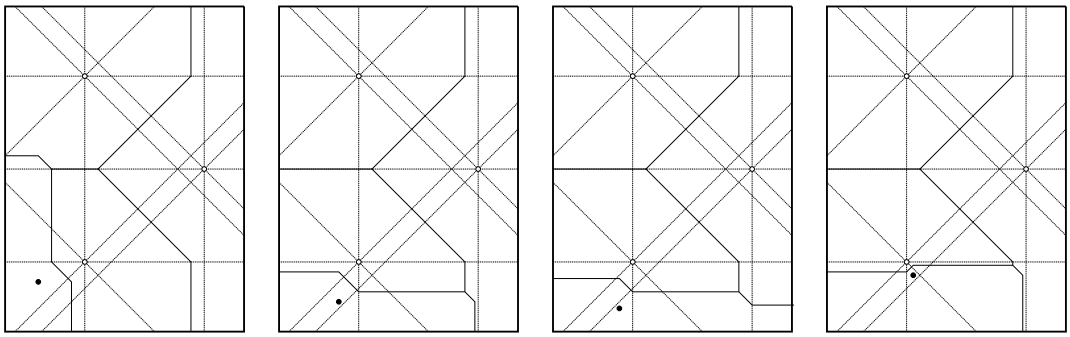

(i) $b \in \mathcal{CC}^5(w_2)$ (j) $b \in \mathcal{CC}^6(w_2) \cap \mathcal{CC}^5(w_1)$ (k) $b \in \mathcal{CC}^6(w_2) \cap \mathcal{CC}^6(w_1)$ (l) $b \in \mathcal{CC}^7(w_2) \cap \mathcal{CC}^5(w_1)$

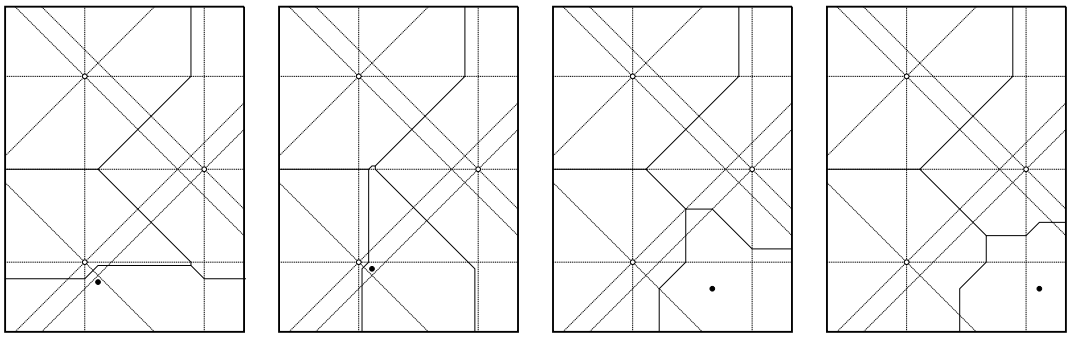

(m) $b \in \mathcal{CC}^7(w_2) \cap \mathcal{CC}^6(w_1)$ (n) $b \in \mathcal{CC}^8(w_2) \cap \mathcal{CC}^5(w_1)$ (o) $b \in \mathcal{CC}^8(w_2) \cap \mathcal{CC}^6(w_1)$ (p) $b \in \mathcal{CC}^8(w_2) \cap \mathcal{CC}^7(w_1)$

Figure 6.12: Voronoi cells $V^+(b)$ for b within the bottom half of $\mathcal{P}$.

The use of gradient methods produces

$$\frac{\delta A}{\delta x} = \frac{1}{2}(-\frac{x}{2} + \frac{y}{2} + \frac{11p}{144})$$
$$\frac{\delta A}{\delta y} = \frac{1}{2}(\frac{x}{2} - \frac{5y}{2} + \frac{13p}{16})$$

which gives the maximum to be $b^* = (\frac{43p}{72}, \frac{4p}{9})$ giving $Area(b^*) = \frac{2489p^2}{10368} > \frac{6p^2}{49}$. For b^* to lie within $\mathcal{CC}^1(w_2) \cap \mathcal{CC}^5(w_1) \cap \mathcal{CC}^7(w_3)$ it must be the case that $\frac{p}{24} \leq x - y \leq \frac{11p}{72}$ which is satisfied with $x - y = \frac{11p}{72}$ so the maximum lies on $y = x - \frac{11p}{72}$ ($\mathcal{CL}^6(w_1)$).

- For $b \in \mathcal{CC}^1(w_2) \cap \mathcal{CC}^5(w_1) \cap \mathcal{CC}^8(w_3)$ we have

$$\begin{aligned} Area(V^+(b)) &= (\frac{x + \frac{5p}{6} - \frac{q}{2} + y}{2} - \frac{x + \frac{p}{3} - y + \frac{3q}{14}}{2}) \times q + \frac{1}{2}(\frac{q}{2} - y)(\frac{q}{2} + y) \\ &\quad - \frac{1}{2}(y - \frac{3q}{14})(y + \frac{3q}{14}) - \frac{1}{2}\frac{2q}{7}(2q - \frac{11q}{14} - \frac{q}{2}) \\ &= (\frac{p}{4} - \frac{5q}{14} + y)q + \frac{1}{2}(\frac{q^2}{4} - y^2) - \frac{1}{2}(y^2 - \frac{9q^2}{196}) - \frac{5q^2}{49} \\ &= -y^2 + qy - \frac{25q^2}{196} \end{aligned}$$

which achieves its maximum at $y = \frac{q}{2}$ giving $Area(V^+((x, \frac{q}{2}))) = \frac{6q^2}{49} \not> \frac{6q^2}{49}$ so this area is not of interest.

- For $b \in \mathcal{CC}^1(w_2) \cap \mathcal{CC}^6(w_1)$ we can easily spot that, whilst remaining within this area, moving $b = (x, y)$ northwest will improve $B(w_2, b)$ above y and $B(w_1, b)$ left of x (leaving the remainders unchanged). Therefore the supremum lies on the line $\mathcal{CL}^6(w_1)$. Hence, for $b = (\frac{5p}{6} - \delta, \frac{q}{2} - \delta)$ on this line,

$$\begin{aligned} Area(V^+(b)) &= (p - \frac{7p}{18}) \times \frac{q}{2} - \frac{\delta^2}{2} - \frac{p}{6} \times \delta - \frac{1}{2}(\frac{q}{2} - \delta + \frac{3q}{14})(\frac{7p}{9} - \delta - \frac{7p}{18}) \\ &= \frac{11pq}{36} - \frac{\delta^2}{2} - \frac{p}{6}\delta - \frac{1}{2}(\frac{5q}{7} - \delta)(\frac{7p}{18} - \delta) \\ &= \frac{11pq}{36} - \frac{\delta^2}{2} - \frac{p}{6}\delta - \frac{1}{2}(\delta^2 - q\delta + \frac{5pq}{18}) \\ &= \frac{pq}{6} + \frac{37p}{72}\delta - \delta^2 > \frac{pq}{6} \Leftrightarrow \delta < \frac{37p}{72} \end{aligned}$$

achieving a maximum at $\delta = \frac{37p}{144}$ at which $Area(V^+((\frac{83p}{144}, \frac{61q}{196}))) = \frac{6073p^2}{20736} > \frac{49p^2}{216}$.

- For $b \in \mathcal{CC}^2(w_2)$ we have

$$\begin{aligned} Area(V^+(b)) &= \frac{x + \frac{5p}{6} - \frac{q}{2} + y}{2} \times (\frac{x - \frac{p}{3} + \frac{11q}{14} + y}{2} - \frac{-x + \frac{p}{3} + y + \frac{3q}{14}}{2}) \\ &\quad + \frac{1}{2}(\frac{q}{2} - y)(\frac{q}{2} + y - 2\frac{-x + \frac{p}{3} + y + \frac{3q}{14}}{2}) - 2 \times \frac{1}{2}(x + \frac{p}{3})(x - \frac{p}{3}) \\ &= \frac{x + \frac{5p}{6} - \frac{q}{2} + y}{2} \times (x - \frac{p}{3} + \frac{2q}{7}) + \frac{1}{2}(\frac{q}{2} - y)(x - \frac{p}{3} + \frac{2q}{7}) - (x + \frac{p}{3})(x - \frac{p}{3}) \\ &= \frac{1}{2}(x + \frac{5p}{6})(x - \frac{p}{3} + \frac{2q}{7}) - (x + \frac{p}{3})(x - \frac{p}{3}) \\ &= \frac{x^2}{2} + \frac{1}{2}(\frac{5p}{6} - \frac{p}{3} + \frac{2q}{7})x + \frac{1}{2}\frac{5p}{6}(-\frac{p}{3} + \frac{2q}{7}) - x^2 + \frac{p^2}{9} \\ &= -\frac{x^2}{2} + (\frac{p}{4} + \frac{q}{7})x + \frac{5pq}{42} - \frac{p^2}{36} \end{aligned}$$

achieving a maximum at $x = \frac{p}{4} + \frac{q}{7} = \frac{4p}{9}$ giving $Area(V^+(\frac{4p}{9}, y)) = \frac{151p^2}{648} > \frac{49p^2}{216}$.

- For $b \in \mathcal{CC}^3(w_2)$ we have

$$Area(V^+(b)) = \frac{x + \frac{5p}{6} - \frac{q}{2} + y}{2} \times \left(\frac{x - \frac{p}{3} + \frac{11q}{14} + y}{2} - \frac{-x + \frac{p}{3} + y + \frac{3q}{14}}{2}\right) + \frac{1}{2}\left(\frac{q}{2} - y\right)\left(\frac{q}{2} + y - 2\frac{-x + \frac{p}{3} + y + \frac{3q}{14}}{2}\right) + 2 \times \frac{1}{2}\left(x + \frac{p}{3}\right)\left(\frac{p}{3} - x\right)$$

  which incidentally is the same formula as for the area for $b \in \mathcal{CC}^2(w_2)$. Since the maximiser of this area is outside $\mathcal{CC}^3(w_2)$ the maximum within this region will lie on $\mathcal{CL}^3(w_2)$, the boundary between the two regions. Upon this line $x = \frac{p}{3}$ we have $Area(V^+(\frac{p}{3}, y)) = \frac{49p^2}{216} \not> \frac{49p^2}{216}$ so this area is not of interest.

- For $b \in \mathcal{CC}^4(w_2)$ we can easily spot that, whilst remaining within this area, moving $b = (x, y)$ northeast will improve $B(w_2, b)$ above y and $B(w_3, b)$ right of x (leaving the remainders unchanged). Therefore the supremum lies on the line $\mathcal{CL}^4(w_2)$. Hence, for $b = (\frac{p}{3} - \delta, \frac{3q}{14} + \delta)$ on this line,

$$Area(V^+(b)) = \frac{p}{3} \times \frac{q}{2} + (\frac{p}{3} - \delta) \times \delta - \delta \times \frac{3q}{14} = \frac{pq}{6} + \delta(\frac{p}{3} - \frac{3q}{14} - \delta) > \frac{pq}{6} \Leftrightarrow \delta < \frac{p}{3} - \frac{3q}{14} = \frac{p}{24}$$

  achieving a maximum at $\delta = \frac{p}{48}$. This gives the supremum solution $b = (\frac{5p}{16}, \frac{45q}{196})$ and area $\frac{1571p^2}{6912} > \frac{49p^2}{216}$.

- For $b \in \mathcal{CC}^7(w_2) \cap \mathcal{CC}^6(w_1)$ we can easily spot that, whilst remaining within this area, moving $b = (x, y)$ northwest will not change the bisector $B(w_1, b)$ expressed in $V^+(b)$ but will improve $B(w_2, b)$ left of x leaving the rightmost horizontal unchanged, while moving northeast will improve $B(w_1, b)$ and $B(w_2, b)$ right of x. Therefore the supremum will be at $(\frac{7p}{18}, \frac{17q}{98})$, the intersection of $CL^5(w_1)$ and $CL^7(w_2)$, at which point

$$Area(V^+(b)) = p \times \frac{3q}{14} - \left(\frac{7p}{18} + \frac{p}{6}\right) \times \left(\frac{3q}{14} - \frac{17q}{98}\right) = \frac{3pq}{14} - \frac{5p}{9} \times \frac{2q}{49} = \frac{169pq}{882} > \frac{pq}{6}\,.$$

As we have seen, there are many locations at which Black can place their point in order to steal more than one sixth of the total area. It is of interest that the maximum area value within each region decreases from Figure 6.12c to 6.12a to 6.12f to 6.12h to 6.12m with $b^* = (\frac{83p}{144}, \frac{61q}{196})$ being the best position across all $\mathcal{P}$, stealing a total area of $\frac{6073p^2}{20736}$, as depicted in Figure 6.13.

This concludes the proof that there is exactly one balanced non-grid arrangement for $n = 3$ if $p = \frac{36}{49}q$, otherwise there are no feasible non-grid arrangements for $n = 3$, and we have found Black's best point for this arrangement.

6.4 The $n = 3$ case with degeneracy

We will now explore non-grid arrangements for $n = 3$ which contain at least one degenerate bisector. For this particular exploration we shall choose that neither (or none) of the points obtains the area contained within a quarterplane section.

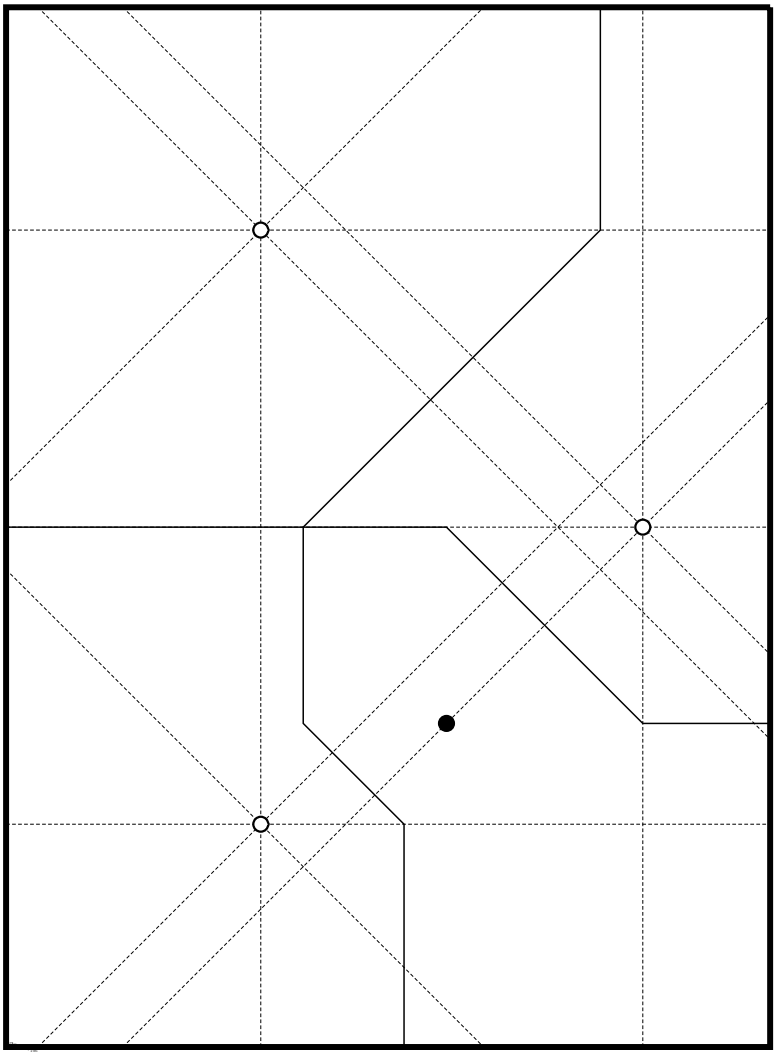

Figure 6.13: White's arrangement $w_1 = (\frac{5p}{6}, \frac{q}{2})$, $w_2 = (\frac{p}{3}, \frac{3q}{14})$, and $w_3 = (\frac{p}{3}, \frac{11q}{14})$ and Black's best point $b^* = (\frac{83p}{144}, \frac{61q}{196})$ for $p = \frac{36}{49}q$.

6.4.1 Three degenerate bisectors

Consider placing three points in turn so that we obtain three degenerate bisectors. For this to occur, each bisector between each pair of points must be degenerate, and so the points must lie on the same diagonal line. After placement of two points (on the same diagonal) then, in order for the third to lie on a diagonal through both points already placed, it is clear that the third point must also be placed on this diagonal, i.e. the three points are collinear. If all three points are collinear on the same diagonal then, without loss of generality (allowing for reflection and rotation), we have the arrangement as depicted in Figure 6.14 where $w_{1_x} \geq w_{1_y}$.

Because the top right and bottom left quadrants of $V^\circ(w_2)$ are both right-angled triangles and must have equal area, the arms of $V^\circ(w_2)$ are all equal, d say. Therefore each cell takes an area $3d^2$. Concentrating on the top half of $V^\circ(w_1)$ we observe that the area is $dw_{1_x} + \frac{1}{2}d^2 = \frac{3}{2}d^2$ so $w_{1_x} = d$, and similarly for the right half of $V^\circ(w_1)$ we obtain $w_{1_y} = d$. The area of the bottom left quadrant of $V^\circ(w_1)$ must equal the area of the top right quadrant of $V^\circ(w_1)$; however, these areas are d^2 and $\frac{1}{2}d^2$ respectively. Therefore there is no balanced arrangement of White's points for $n = 3$ where all points lie on the same diagonal.

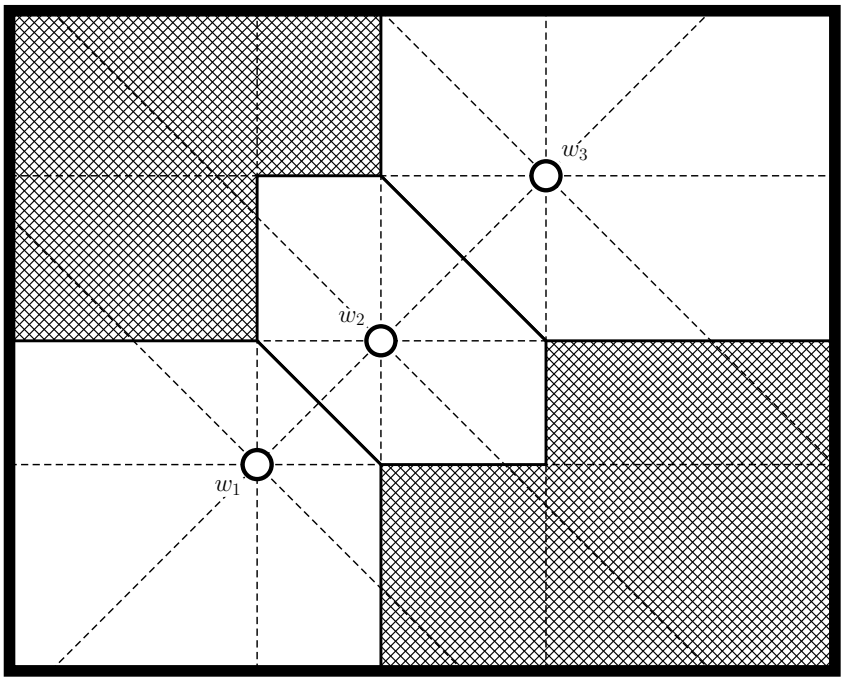

Figure 6.14: Collinear points.

Note that this argument does not rely on the position of the diagonal line upon which the points were positioned relative to $\mathcal{P}$ (the combination of which vertical or horizontal boundaries of $\mathcal{P}$ were intersected by the diagonal line was irrelevant to the outcome of this result so the result holds for any collinear trio of points).

6.4.2 Two degenerate bisectors

If there are exactly two degenerate bisectors, then exactly one white point has degenerate bisectors with both other points (so lie on the same diagonal as each of the other points). Without loss of generality, choose w_3 to be the rightmost vertex of White's three points which contain two degenerate bisectors (if two points are considered the rightmost then reflect in y). Now it is the case that either w_3 is the point involved in two degenerate bisectors or it is not that point, as shown in Figures 6.15a and 6.15b respectively.

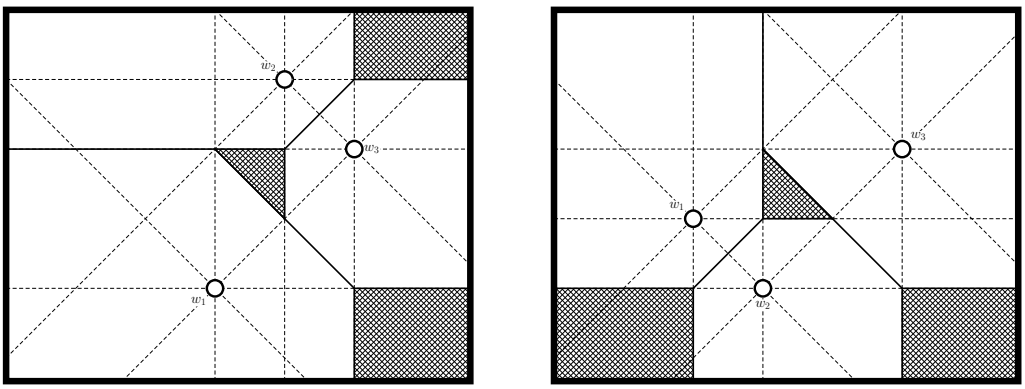

(a) w_3 contributing exactly two degenerate bisectors.(b) w_3 contributing exactly one degenerate bisector.

Figure 6.15: Voronoi diagrams of three points containing two degenerate bisectors.

These are the only two possible arrangements and each one is unique up to a reflection in x. Moreover, these two arrangements are identical up to rotation so we need only explore one of these arrangements. Without loss of generality, let us choose the arrangement as depicted in Figure 6.15b and enforce that w_3 is the topmost vertex (i.e. w_1 cannot be moved higher, else reflect in y).

As we can see from Figure 6.15b, the top left quadrant of $V^\circ(w_2)$ has no greater area than the top right quadrant of $V^\circ w_2$ which in turn has no greater area than the bottom left quadrant of $V^\circ(w_3)$. This, in fact, will always be the case. To see this, firstly let us focus on the top quadrants of $V^\circ(w_2)$. The area of the top left quadrant of $V^\circ(w_2)$ is $\frac{1}{2}(w_{2x} - w_{1x})^2$ while the area of the top right quadrant of $V^\circ(w_2)$ has area $(w_{3x} - w_{2x}) \times (w_{1y} - w_{2y}) - \frac{1}{2}(w_{1y} - w_{2y})^2$. Now, owing to the fact that both w_1 and w_3 lie on the same diagonal as w_2, we have $w_{2x} - w_{1x} = w_{1y} - w_{2y}$ and $w_{3x} - w_{2x} = w_{3y} - w_{2y}$. Therefore the area of the top right quadrant of $V^\circ(w_2)$ can be written

$$\begin{aligned}
(w_{3x} - w_{2x}) \times (w_{1y} - w_{2y}) - \frac{1}{2}(w_{1y} - w_{2y})^2 &= (w_{3y} - w_{2y}) \times (w_{1y} - w_{2y}) - \frac{1}{2}(w_{1y} - w_{2y})^2 \\
&= ((w_{3y} - w_{2y}) - \frac{1}{2}(w_{1y} - w_{2y}))(w_{1y} - w_{2y}) \\
&= (w_{3y} - \frac{1}{2}w_{1y} - \frac{1}{2}w_{2y}))(w_{1y} - w_{2y}) \\
&\geq (\frac{1}{2}w_{1y} - \frac{1}{2}w_{2y}))(w_{1y} - w_{2y}) \\
&= \frac{1}{2}(w_{1y} - w_{2y})^2 \\
&= \frac{1}{2}(w_{2x} - w_{1x})^2 .
\end{aligned}$$

Therefore the top right quadrant of $V^\circ(w_2)$ is greater than or equal to the area of the top left quadrant of $V^\circ(w_2)$. It is easier to simply state that the area of the top right quadrant of $V^\circ(w_2)$ is no greater than the area of the bottom left quadrant of $V^\circ(w_3)$, because these are exactly the same structures apart from the fact that a triangular area is removed from the top right quadrant of $V^\circ(w_2)$ according to the value of w_{1y} compared to w_{3y}.

Now denote the bottom and left arms of $V^\circ(w_3)$ and the right arm of $V^\circ(w_2)$ by $d = w_{3x} - w_{2x} = w_{3y} - w_{2y}$. Comparing the bottom right and the top left quadrants of $V^\circ(w_3)$, we obtain the equation $(p - w_{3x})d = d(q - w_{3y}) \Rightarrow p - w_{3x} = q - w_{3y}$. Comparing the top right and the bottom left quadrants of $V^\circ(w_3)$, we obtain the equation $(p - w_{3x})^2 = \frac{1}{2}d^2 \Rightarrow d = \sqrt{2}(p - w_{3x})$. Therefore the bottom right quadrant of $V^\circ(w_3)$ has area $\sqrt{2}(p - w_{3x})^2$ while the bottom left quadrant of $V^\circ(w_3)$ has area $(p - w_{3x})^2$, even greater still.

However, the top half of $V^\circ(w_2)$ (composed of the top left and top right quadrants) must have the same area as the bottom half of $V^\circ(w_3)$ (composed of the bottom left and bottom right quadrants), yet the former's two constituent quadrants have area no greater than one of the latter's constituent quadrants, and less than the other quadrant. Therefore there is no such balanced point set for $n = 3$ with exactly two degenerate bisectors.

6.4.3 One degenerate bisector

Now it remains to be proven whether or not there exists a balanced area arrangement of White's points containing one degenerate bisector. In order to answer this question we shall explore the placement of w_3 in $\mathcal{P}$ upon diagonal configuration lines of w_1 or w_2, points which are already located in $\mathcal{P}$ producing a non-degenerate bisector.

Without loss of generality we can say $w_2 \in \mathcal{CC}^5(w_1)$, as shown in Figure 6.16. By the symmetry of Figure 6.16, we need only explore the placement of w_3 on the configuration lines $\mathcal{CL}^2(w_1)$, $\mathcal{CL}^4(w_1)$, $\mathcal{CL}^6(w_1)$, $\mathcal{CL}^8(w_1)$, $\mathcal{CL}^2(w_2)$, $\mathcal{CL}^4(w_2)$, $\mathcal{CL}^6(w_2)$, and $\mathcal{CL}^8(w_2)$ contained within the Voronoi cell of w_2, so we can ignore $\mathcal{CL}^2(w_1)$ and $\mathcal{CL}^8(w_1)$. Moreover, it will save us some time to notice that within the rectangle $R(w_2, w_1)$ the Voronoi diagrams resulting from the placement of w_3 on one of the diagonal configuration lines will be identical, so we shall choose to ignore $\mathcal{CL}^6(w_1)$ in $\mathcal{CC}^1(w_2)$. Figure 6.16 depicts every possible structure of an arrangement of three of White's points which includes exactly one degenerate bisector.

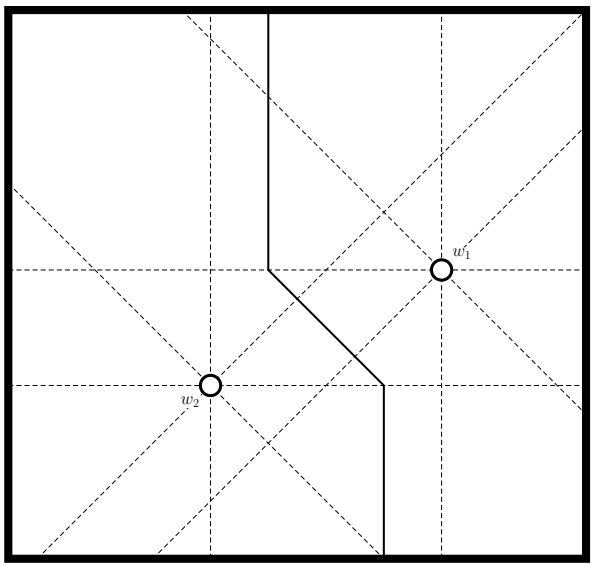

Figure 6.16: Two general points contributing to a non-degenerate bisector.

All possible unique placements of w_3 are represented in Figure 6.17.

Notice that Figures 6.17a and 6.17d have the same structure, as well as Figures 6.17b and 6.17e (they are simply a swap of w_2 and w_3). Figures 6.17c and 6.17i also depict the same structure after a reflection in y, and Figures 6.17h and 6.17j are identical after a rotation of 90°. Therefore we need only explore the arrangements shown in Figures 6.17a, 6.17b, 6.17c, 6.17f, 6.17g, 6.17j, and 6.17k.

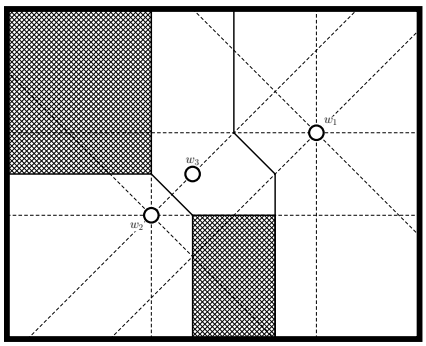

(a) Voronoi cell $V^\circ(w_3)$ for w_3 on $\mathcal{CL}^2(w_2)$.

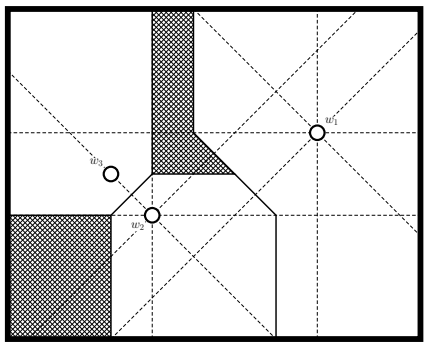

(b) Voronoi cell $V^\circ(w_3)$ for w_3 on $\mathcal{CL}^4(w_2)$ below $\mathcal{CL}^5(w_1)$.

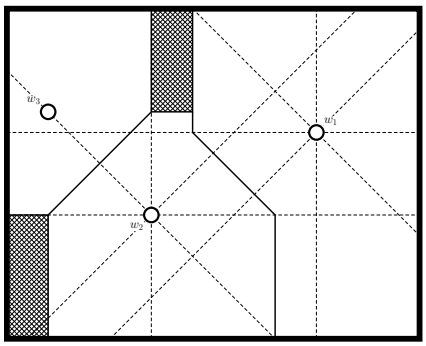

(c) Voronoi cell $V^\circ(w_3)$ for w_3 on $\mathcal{CL}^4(w_2)$ above $\mathcal{CL}^5(w_1)$.

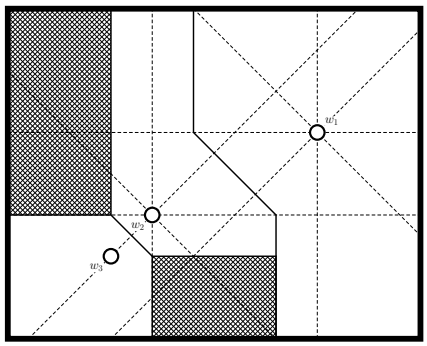

(d) Voronoi cell $V^\circ(w_3)$ for w_3 on $\mathcal{CL}^6(w_2)$.

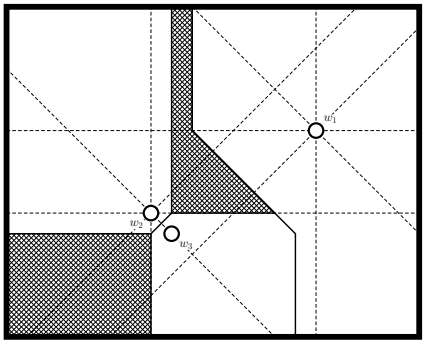

(e) Voronoi cell $V^\circ(w_3)$ for w_3 on $\mathcal{CL}^8(w_2)$ above $\mathcal{CL}^6(w_1)$.

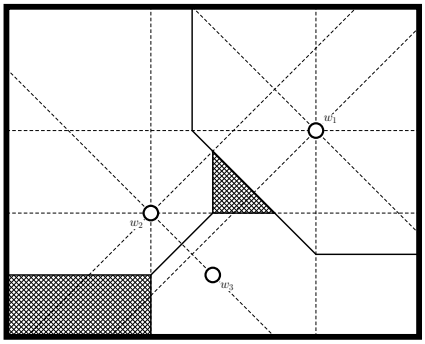

(f) Voronoi cell $V^\circ(w_3)$ for w_3 on $\mathcal{CL}^8(w_2)$ below $\mathcal{CL}^6(w_1)$.

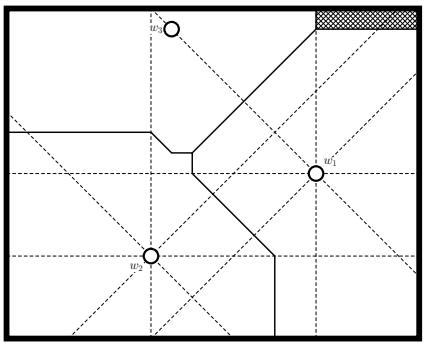

(g) Voronoi cell $V^\circ(w_3)$ for w_3 on $\mathcal{CL}^4(w_1)$ right of $\mathcal{CL}^3(w_2)$.

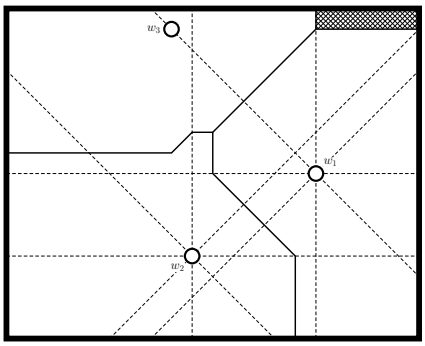

(h) Voronoi cell $V^\circ(w_3)$ for w_3 on $\mathcal{CL}^2(w_1)$ left of $\mathcal{CL}^1(w_2)$.

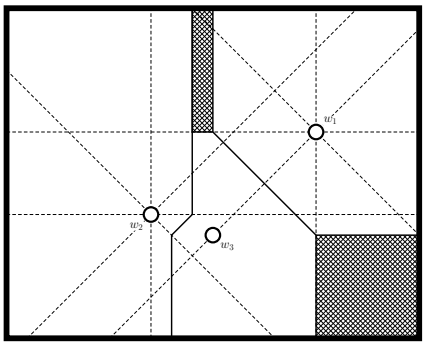

(i) Voronoi cell $V^\circ(w_3)$ for w_3 on $\mathcal{CL}^6(w_1)$ in $\mathcal{CC}^8(w_2)$.

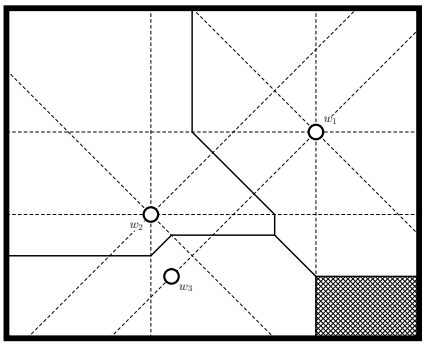

(j) Voronoi cell $V^\circ(w_3)$ for w_3 on $\mathcal{CL}^6(w_1)$ in $\mathcal{CC}^7(w_2)$.

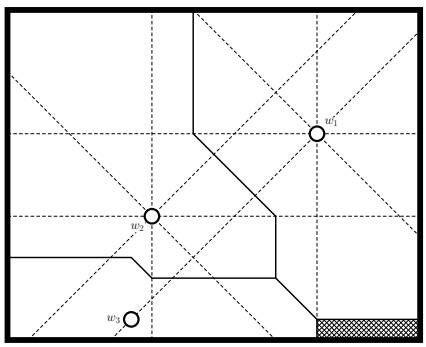

(k) Voronoi cell $V^\circ(w_3)$ for w_3 on $\mathcal{CL}^6(w_1)$ in $\mathcal{CC}^6(w_2)$.

Figure 6.17: Voronoi cells $V^\circ(w_3)$ for w_3 on respective diagonal configuration lines according to Figure 6.16.

Firstly, a common shape found in these arrangements is the rectangle with a corner clipped (for example $V^\circ(w_2)$ in Figure 6.17a). For a cell of this shape, the arms bounding the quadrant containing the clipped corner are always identical in length (being equal to $|w_{ix} - w_{jx}| \equiv |w_{iy} - w_{jy}|$ for some i and j). Both halves of the cell containing this clipped corner have the same shape (a trapezium with two right angles) and also the same width (the distance of the edge between these right angles) – this width being $|w_{ix} - w_{jx}| \equiv |w_{iy} - w_{jy}|$. Therefore, since both halves of the cell must also have the same area, they must also have the same length and so be identical up to a reflection in $y = x$. This means that the quadrant opposite to the quadrant containing the clipped corner must be a square because the arms bounding it are of equal length.

Thus, denoting the length of the arms bounding the clipped corner as d and the length of the other arms as d', we obtain, equating the areas of these opposite quadrants, $\frac{1}{2}d^2 = d'^2 \Rightarrow d = \sqrt{2}d'$.

The trapezium described above also exists outside this shape: for example, in Figure 6.17a the trapezium is also the left half and bottom half of $V^\circ(w_3)$. Therefore the lengths of this cell's arms which bound the trapezium must also be $d + d'$.

Using these workings we shall investigate the abovementioned figures in order to determine whether such a balanced arrangement exists.

Firstly let us explore the arrangement in Figure 6.17a. As already described we have a cell, $V^\circ(w_2)$, resembling a rectangle with a clipped corner, and also the trapezium shape in the left and bottom halves of $V^\circ(w_3)$. Therefore the bottom and left arms of $V^\circ(w_3)$ are d and the top and right arms of $V^\circ(w_3)$ are d'. The bottom left quadrant of $V^\circ(w_2)$ must have the same area as the top right quadrant of $V^\circ(w_3)$ (through the equality of the clipped corner quadrants of both cells), this area being d'^2. Since both bounding arms of the top right quadrant of $V^\circ(w_3)$ are d', this quadrant must also be a square, forcing w_3 to be located on the same horizontal as w_1 in order to have a vertical bisector.

This would cause $V^\circ(w_1)$ to be a rectangle and so $w_{1y} = w_{3y} = \frac{q}{2}$. Therefore the top arm of $V^\circ(w_3)$ would be of length $d' = q - w_{3y} = \frac{q}{2}$, forcing $w_{2y} = d' = \frac{q}{2}$. This would mean $w_{3x} - w_{2x} \equiv w_{3y} - w_{2y} = 0$, so $w_2 = w_3$, which is obviously impossible, not least because the top right and bottom left quadrants of $V^\circ(w_2)$ and $V^\circ(w_3)$ respectively would be non-existent.

The same is in fact true for the arrangement in Figure 6.17b. The rectangle with the clipped corner in this scenario is $V^\circ(w_3)$, and we have the trapezium in the left half of $V^\circ(w_2)$. This forces the bottom arm of $V^\circ(w_2)$ to be d'. Since the area of the top left quadrant of $V^\circ(w_3)$ and that of the bottom right quadrant of $V^\circ(w_2)$ are equal to d'^2, the right arm of $V^\circ(w_2)$ is also d' (because the bottom right quadrant of $V^\circ(w_2)$ is rectangular). This forces the top half of $V^\circ(w_2)$ to be the trapezium shape described, requiring that w_1 and w_2 lie on the same horizontal in order to produce a vertical bisector. This is the situation to which we reduced the arrangement in Figure 6.17a, reflected in x, so there is also no feasible arrangement of the form shown in Figure 6.17b.

At the risk of repeating oneself, the approach for the arrangement in Figure 6.17c is not dissimilar to that utilised for Figure 6.17b. Using identical logic we again see that the right and bottom arms of $V^\circ(w_2)$ are d', forcing the top half $V^\circ(w_2)$ to also resemble the trapezium, again achieved by a vertical bisector between w_1 and w_2, despite the top half being, in general, a different form here compared to that in Figure 6.17b. Therefore there are also no feasible arrangements of this form.

Now we come to the arrangement shown in Figure 6.17f. Focusing still for the time being on $V^\circ(w_2)$ and $V^\circ(w_3)$, we see that the bottom half of $V^\circ(w_2)$ and the left half of $V^\circ(w_3)$ take the trapezium shape. Therefore the bottom and right arms of w_2 and the top and left arms of w_3 have length d and the left arm of $V^\circ(w_2)$ and the bottom arm of $V^\circ(w_3)$ have length d'. Now the top left quadrant of $V^\circ(w_2)$ must have the same area as the bottom right quadrant of $V^\circ(w_3)$ and since these quadrants are both rectangular with one side of length d', the other length of both quadrants (the top arm of $V^\circ(w_2)$ and the right arm of $V^\circ(w_3)$) must be equal, d'' say. In order for this to be the case, $\mathcal{P}$ must be a square since it requires that $p = d' + d + d''$ (calculated from left to right across $V^\circ(w_2)$ and $V^\circ(w_3)$) and $q = d' + d + d''$ (calculated from bottom to top across $V^\circ(w_3)$ and $V^\circ(w_2)$). Thus $w_2 = (d', d + d')$ and $w_3 = (d + d', d')$.

Turning our attention now to $V^\circ(w_1)$ we notice that, in this arrangement, it is $V^\circ(w_1)$ which takes the rectangle with a clipped corner shape; however, the clipped corner here does not

represent the diagonal segment of a degenerate bisector with another point in W. The results hold similarly for $V^\circ(w_1)$ in this case, so the bottom and left arms of $V^\circ(w_1)$ are of equal length, l say, as are the top and right arms of $V^\circ(w_1)$, a length of l' say, and $l = \sqrt{2}l'$. Thus $w_1 = (d + d' + d'' - l', d + d' + d'' - l')$ and the Voronoi diagram is symmetrical about $y = x$.

Now the top half of $V^\circ(w_1)$ has the same area as the left half of $V^\circ(w_3)$. This gives

$$\begin{aligned}(l + l') \times l' = (l + \sqrt{2}l) \times \sqrt{2}l = d \times (\sqrt{2}d + \frac{1}{2}d) = d \times (d' + \frac{1}{2}d)\\ \Rightarrow (2 + \sqrt{2})l^2 = (\frac{1 + 2\sqrt{2}}{2})d^2\\ \Rightarrow 2(2\sqrt{2} - 1)(2 + \sqrt{2})l^2 = (2\sqrt{2} - 1)(2\sqrt{2} + 1)d^2\\ \Rightarrow 2(2 + 3\sqrt{2})l^2 = 7d^2 \Rightarrow l < d\,.\end{aligned}$$

However, $d \leq l$ by construction. The lower arm of $V^\circ(w_1)$ ends at the bisector $B(w_1, w_3)$ so l is the distance from w_3 to any part of the diagonal bisector segment of $B(w_1, w_3)$. The top arm of $V^\circ(w_3)$ cannot extend further than the bisector $B(w_1, w_3)$ will allow so, for $w_3 \in \mathcal{CC}^6(w_1)$, $d \leq l$, before even factoring any interference from w_2. Therefore there cannot be any such balanced arrangement of White's points as depicted in Figure 6.17f.

Unfortunately the remaining arrangements include neither the rectangle with a clipped corner nor the trapezium shape so we cannot benefit from the useful logic derived for these shapes. Tackling the arrangement in Figure 6.17g we can see that the cells $V^\circ(w_1)$ and $V^\circ(w_3)$ have the same structure, reflected in $x = y$. Moreover, the top left quadrant of $V^\circ(w_1)$ is equal in shape and dimension to the bottom right quadrant of $V^\circ(w_3)$. That is, the top arm of $V^\circ(w_1)$ is equal in length to the right arm of $V^\circ(w_3)$ (a length of t say) and the left arm of $V^\circ(w_1)$ has a length equal to that of the bottom arm of $V^\circ(w_3)$ (a length of l say). The fact that the top half of $V^\circ(w_1)$ must have the same area as the right half of $V^\circ(w_3)$ leads us to conclude that the right arm of $V^\circ(w_1)$ has a length equal to that of the top arm of $V^\circ(w_3)$, r say. Due to the fact that the bottom right quadrant of $V^\circ(w_1)$ must have the same area as the top left quadrant of $V^\circ(w_3)$ (since the areas of the top left quadrant of $V^\circ(w_1)$ and the bottom right quadrant of $V^\circ(w_3)$ are equal), and both are rectangular with one side of length r, the bottom arm of $V^\circ(w_1)$ must be the same length, b say, as the left arm of $V^\circ(w_3)$. Hence $V^\circ(w_1)$ and $V^\circ(w_3)$ are in fact identical in structure and dimension, and again we must have a square $\mathcal{P}$ where $p = b + t + r$ (summing arms from left to right across $V^\circ(w_3)$ and $V^\circ(w_1)$) and $q = b + t + r$ (summing arms from bottom to top across $V^\circ(w_1)$ and $V^\circ(w_3)$).

Now the top arm of $V^\circ(w_2)$ must be of the same length as the bottom arm of $V^\circ(w_3)$ since both arms touch the diagonal bisector part of $B(w_2, w_3)$, and similarly the right arm of $V^\circ(w_2)$ must be of the same length as the left arm of $V^\circ(w_1)$, so these arms are all of length l. The top left and bottom right quadrants of $V^\circ(w_1)$ must be of equal area and are both rectangular with one side of length l, so they must also be of equal dimension; the bottom and left arms of $V^\circ(w_2)$ are of equal length, x say. Therefore $w_2 = (x, x)$, $w_3 = (b, p - r)$, and $w_1 = (p - r, b)$, symmetrical about $y = x$, and the square with opposite corners $(0, 0)$ and $(b + t, b + t)$ contains a total of exactly two cells (one whole cell and two half cells), so the area of one cell should total $\frac{(b+t)^2}{2}$.

Using these workings we can input the equations that the halves of the cells would have to satisfy into the solver in MATLAB® as shown in Appendix A.3.1, where it is found to have no solution; no balanced arrangement of White's points as depicted in Figure 6.17g exists.

Now we come to the arrangement shown in Figure 6.17j. Since both arms touch the diagonal segment of the bisector $B(w_1, w_3)$, the bottom arm of $V^\circ(w_1)$ and the right arm of $V^\circ(w_3)$ are the same length, r say. Similarly the top arm of $V^\circ(w_3)$ is of equal length to the bottom arm of $V^\circ(w_2)$, t say, and the left arm of $V^\circ(w_1)$ is of equal length to the right arm of $V^\circ(w_2)$, t' say. Let the left and bottom arms of $V^\circ(w_3)$ have lengths l and b respectively, the top and right arms of $V^\circ(w_1)$ have lengths l' and b' respectively, and the top and left arms of $V^\circ(w_2)$ have lengths d' and d respectively (some of these labelled lengths may only be utilised in the calculations in the appendices). The rectangle with opposite corners $(0, b)$ and $(l + r, q)$ contains one whole cell and two half cells and has area $(l + r)(r + l')$ so the area of one cell is $\frac{(l+r)(r+l')}{2}$.

Owing to the apparent lack of symmetry in this arrangement we resort to MATLAB® in order to determine whether there is a set of arm lengths which satisfy Lemmas 4.1.2 and 4.1.3, as detailed in Appendix A.3.2. The resulting output shows that there is yet again no feasible arrangement of White's points as depicted in Figure 6.17j which satisfies the desired properties.

Finally we tackle the arrangement depicted in Figure 6.17k. Similarly to what was spotted in Figure 6.17g, the cells $V^\circ(w_1)$ and $V^\circ(w_3)$ have the same basic structure, reflected in $y = -x$; however, the result that the bordering quadrants of $V^\circ(w_1)$ and $V^\circ(w_3)$ must be of equal area (a result which led to most of our discoveries) does not appear to be necessarily true in this case. We can nevertheless label the lengths of the arms as we did for the arrangement in Figure 6.17j. That is, the bottom arm of $V^\circ(w_1)$ and the right arm of $V^\circ(w_3)$ are the same length, r say. Similarly the top arm of $V^\circ(w_3)$ is of equal length to the bottom arm of $V^\circ(w_2)$, t say, and the left arm of $V^\circ(w_1)$ is of equal length to the right arm of $V^\circ(w_2)$, t' say. Let the left and bottom arms of $V^\circ(w_3)$ have lengths l and b respectively, the top and right arms of $V^\circ(w_1)$ have lengths l' and b' respectively, and the top and left arms of $V^\circ(w_2)$ have lengths d' and d respectively (again, some of these labels may only be utilised in the calculations in the appendix). The rectangle with opposite corners $(0, b)$ and $(l + r, q)$ contains one whole cell and two half cells and has area $(l + r)(r + l')$ so again the area of one cell is $\frac{(l+r)(r+l')}{2}$.

Beyond this, not much can be said about the relationship between the cells, so we rely upon the MATLAB® code in Appendix A.3.3 to show that there exist no balanced arrangements as depicted in Figure 6.17k.

Note that all of these results hold no matter the location of w_1 and w_2 relative to the boundaries of $\mathcal{P}$, so these results hold for any rectangular $\mathcal{P}$. Therefore there are no balanced degenerate arrangements for $n = 3$ and so we have found the only such arrangements of White's points for $n = 3$ and they are the row (grid) arrangement and the non-grid arrangement shown in Figure 6.11.

6.5 The $n > 3$ case

While the next natural step may be to analyse the $n = 4$ case, one can expect the amount of work required to study this by investigating every structurally independent arrangement (a total enumeration approach) to be, roughly estimating from the amount of work required for the $n = 3$ case, a colossal undertaking. Instead we shall explore how we can use our results from the $n = 2$ and $n = 3$ cases to find non-grid arrangements for $n > 3$.

One approach would be a composition method. For any even n we can divide $\mathcal{P}$ into a horizontal row of equal-sized, equal-proportioned rectangles of dimension $\frac{2p}{n}$ and q and use the non-grid $n = 2$ arrangement (alternating between this and its reflection so that bisectors between rectangles are themselves the vertical dividers) to obtain a balanced non-grid arrangement of n, as shown in Figure 6.18a. Another non-grid arrangement is this very arrangement reflected in the horizontal plane. Note that for these arrangements we require $\frac{2p}{n} \leq q$ and if this is not satisfied we can still construct an arrangement in this way using a simple rotation of the arena as before or a rotation of the $n = 2$ arrangement within the rectangle.

Similarly we can divide $\mathcal{P}$ into a vertical row of equal-sized, equal-proportioned rectangles of dimension p and $\frac{2q}{n}$ and use the $n = 2$ arrangement (alternating between this and its reflection again so that bisectors between rectangles are themselves the horizontal dividers) to obtain a balanced non-grid arrangement of n provided that $p \leq \frac{2q}{n}$, as shown in Figure 6.18b. The reflection in the vertical plane provides yet another arrangement.

Moreover, using these particular arrangements within each block can produce more non-grid arrangements (as described above) for every unique factor F of $\frac{n}{2}$ where $\mathcal{P}$ is divided into a horizontal or vertical row of F identical rectangles within which one of the four arrangements already mentioned can be used.

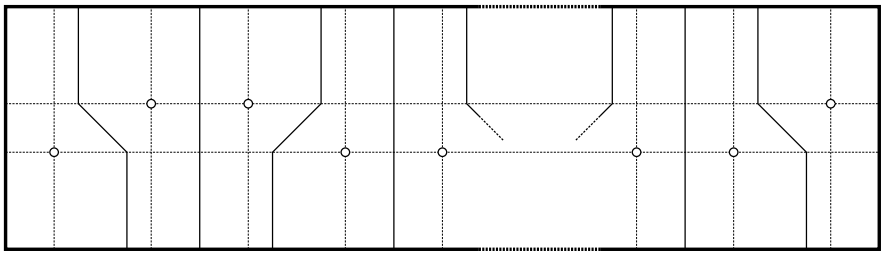

(a) A row of $n = 2$ arrangements.

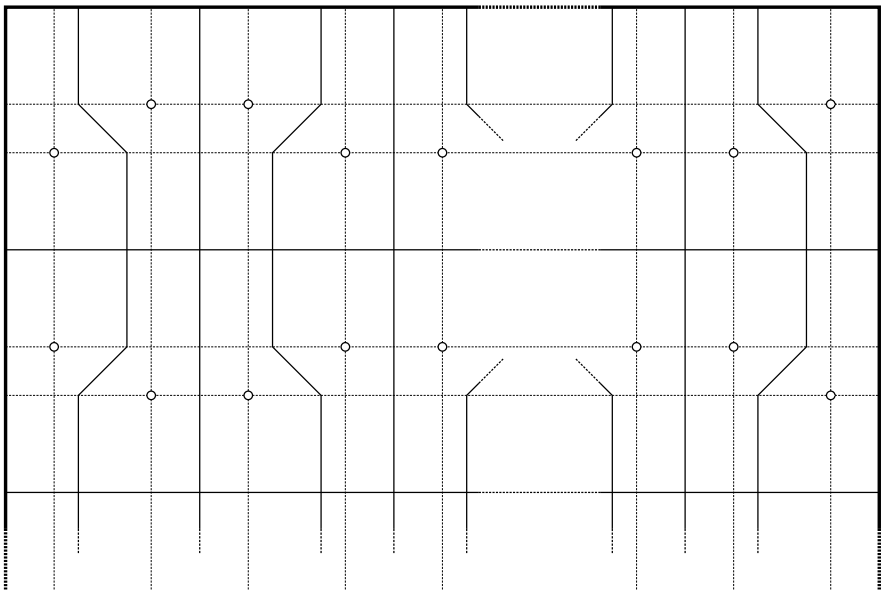

(b) A column of rows of $n = 2$ arrangements.

Figure 6.18: Two possible decomposable extensions of the $n = 2$ arrangement.

Identical arguments can be used to extrapolate the $n = 3$ arrangement for any n divisible by 3. Moreover, any arrangement can contribute to further arrangements for larger n as described if the number of points in the arrangement is a factor of n. We shall call any such arrangement which contains a grid of rectangles within its Voronoi diagram a *decomposable* arrangement.

Furthermore, we may find the $n = 3$ arrangement to be of even more use. We notice an important property of the $n = 3$ design. Since it has been constructed in order to be balanced, the left half of $V(w_1)$ has area $\frac{pq}{6}$. However, since this is symmetrical in $y = \frac{q}{2}$ the top left section of $V(w_1)$ is exactly $\frac{pq}{6}$ and therefore so is every other quarter of $V(w_1)$. This property, along with the geometrical symmetry of its construction, lends itself well to the creation of more, non-decomposable, arrangements.

First let us consider placing an additional point among vertices resembling those in our $n = 3$ arrangement. We could try similarly to attach one point to the left-hand side of the $n = 3$ arrangement (attaching to the right-hand side would be the decomposable $n = 3 + n = 1$ arrangement). This is shown in Figure 6.19.

However, since the quarters of $V(w_2)$ and $V(w_3)$ are not symmetrical, we must relax the y-coordinates of w_2 and w_3 in order to find out if there is a feasible non-grid solution resembling this arrangement. Since the arrangement is symmetrical in $x = \frac{p}{2}$ and $\frac{q}{2}$, once we know the coordinates within the bottom left quadrant of $\mathcal{P}$ we have defined the whole arrangement. Since the Voronoi cells are symmetrical, Lemmas 4.1.2 and 4.1.3 tell us that each quarter of each cell must have an area equal to $\frac{pq}{16}$. This gives us the x-coordinates as noted in Figure 6.19, and the value of y to satisfy these can be found using a solver (as shown in Appendix A.4.1) to obtain the arrangement in Figure 6.20 for any $\mathcal{P}$ satisfying $p = \frac{8}{9}q$.

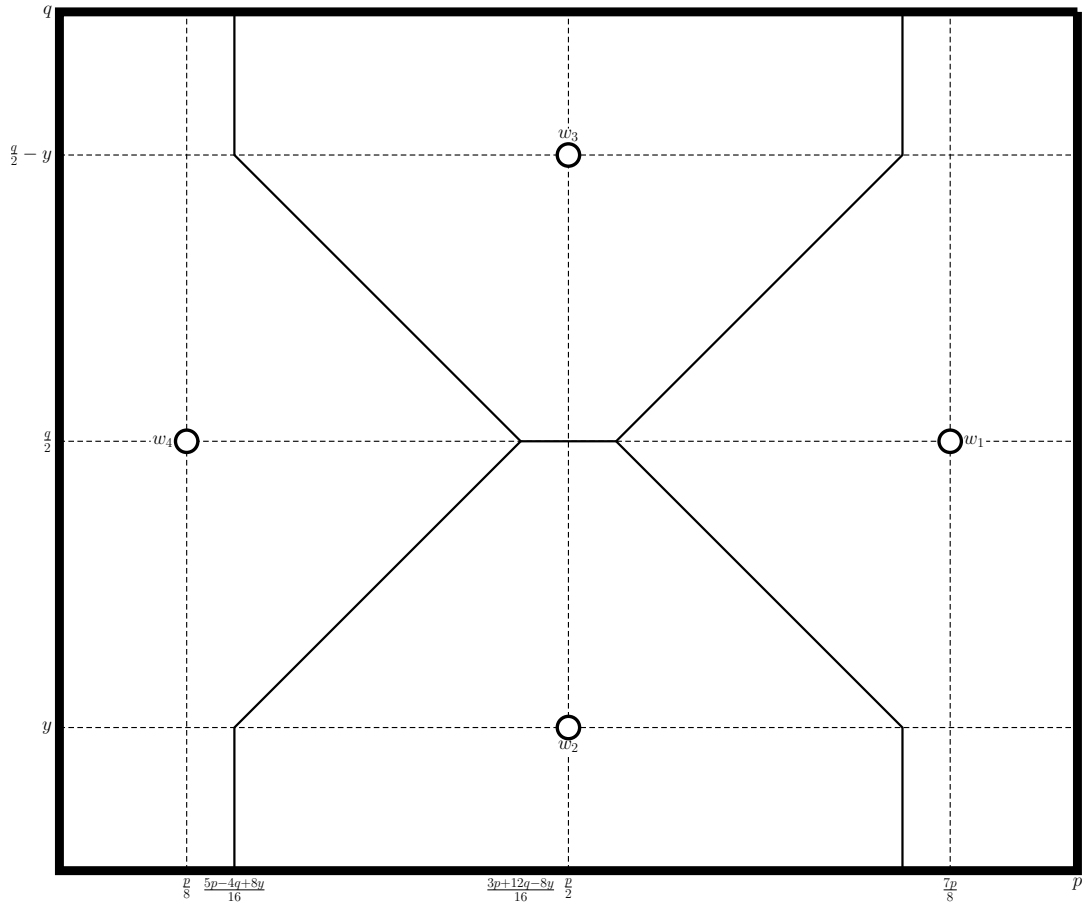

Figure 6.19: White's trial arrangement for $n = 4$.

We may notice that we can exploit the shape of $V^\circ(w_2)$ (and $V^\circ(w_3)$) and the fact that these points are all technically degenerate bisectors to obtain yet another arrangement for $n = 4$. This consists of four $V^\circ(w_2)$-shaped cells, all rotated by different amounts of 90° about $V^\circ(w_2)$'s top vertex, and contained within a square $\mathcal{P}$ (so the quarterplanes are the remaining space) as depicted in Figure 6.21. Note that this arrangement is balanced only under the discard rule, by Lemma 6.0.1.

Both of these $n = 4$ arrangements can clearly be extended to provide an arrangement for any $n \equiv 1 \pmod 3$ (the leftmost point with any number of the arrangement of three points conjoined to the right as shown in Figure 6.22 for the non-degenerate case) and, since each addition adds a length of $\frac{7}{9}q$ or $\frac{5}{6}q$ (for the non-degenerate and degenerate cases respectively) to p's effective length, this arrangement will be balanced if and only if, for $n = 3k + 1$ for $k \in \mathbb{N}$, $p = \frac{7k+1}{9}q$ or $p = \frac{5k+1}{6}q$ (for the non-degenerate and degenerate cases respectively).

On seeing the success of concatenating the $n = 4$ arrangement, we may wonder if the $n = 3$ arrangement can be extended by repeatedly adding an arrangement resembling the $n = 3$ arrangement along a row. Unfortunately this is not the case. As shown in the $n = 3 + 3$ arrangement in Figure 6.23, we would require the aspect ratio of $n = 3$ to be present over the left-side $\frac{p}{2} \times q$ subrectangle and the aspect ratio of $n = 4$ to be present over the right-side $\frac{2p}{3} \times q$ subrectangle. This amounts to both $\frac{p}{2} = \frac{36}{49}q$ and $\frac{2p}{3} = \frac{8}{9}q$ which is not viable.

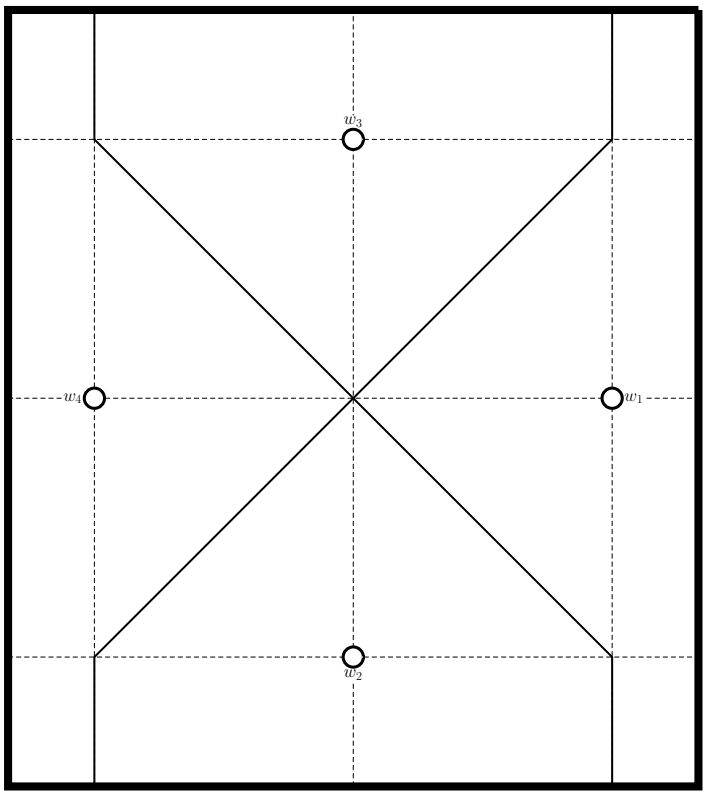

Figure 6.20: White's arrangement $w_1 = (\frac{7p}{8}, \frac{q}{2})$, $w_2 = (\frac{p}{2}, \frac{q}{6})$, $w_3 = (\frac{p}{2}, \frac{5q}{6})$, and $w_4 = (\frac{p}{8}, \frac{q}{2})$ for $p = \frac{8}{9}q$.

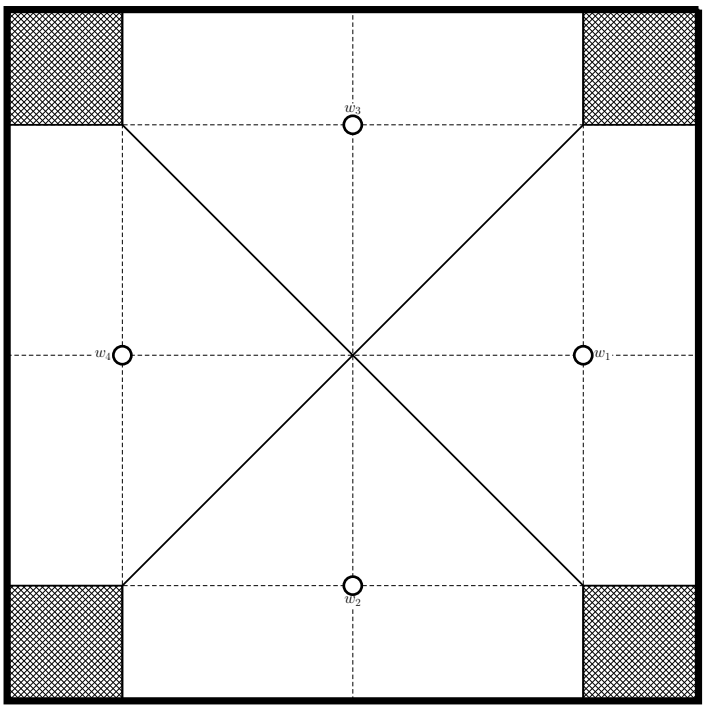

Figure 6.21: White's arrangement $w_1 = (\frac{5p}{6}, \frac{q}{2})$, $w_2 = (\frac{p}{2}, \frac{q}{6})$, $w_3 = (\frac{p}{2}, \frac{5q}{6})$, and $w_4 = (\frac{5p}{6}, \frac{q}{2})$ for $p = q$.

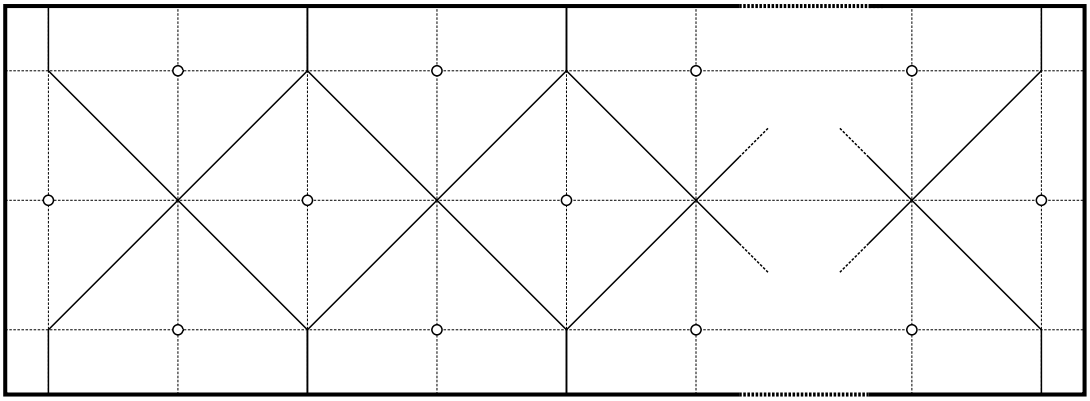

Figure 6.22: A non-grid arrangement for $n \equiv 1 \pmod 3$.

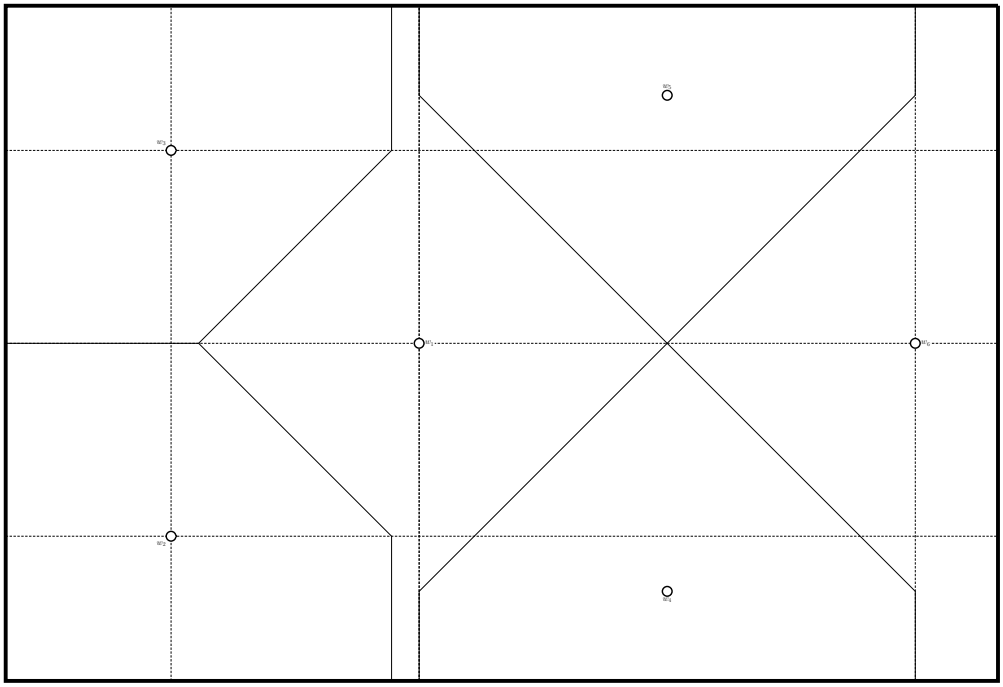

Figure 6.23: A botched attempt to extend the $n = 3$ non-grid arrangement.

Now, for $n = 5$, we shall consider the addition of an extra two points. These two points must both be on the same side of the $n = 3$ arrangement else we would obtain a decomposable $(n = 4) + (n = 1)$ arrangement. Moreover, they cannot be located on the left-hand side of the arrangement as it appears in Figure 6.11 without creating the decomposable $(n = 2) + (n = 3)$ arrangement. We can see this by realising that, in order not to interfere with $V^\circ(w_1)$, these points must lie in $\mathcal{CC}^4(w_2) \cup \mathcal{CC}^5(w_2) \cup \mathcal{CC}^4(w_3) \cup \mathcal{CC}^5(w_3)$. Because of this, only the areas in the left half of $V^\circ(w_2)$ and $V^\circ(w_3)$ will differ from their shape in the $n = 3$ arrangement. But each quarter of $V^\circ(w_2)$ and $V^\circ(w_3)$ must not change its total area. No matter the placement of w_4 and w_5, there will be one quarter cell whose left perimeter is a vertical line and so this quarter cell must be identical to that in the $n = 3$ arrangement. This, though, forces the remainder of this bisector to remove area from the other quarter of the cell, thereby breaking the balanced restraints. Therefore the two points must be located on the right-hand side of the $n = 3$ arrangement.

Because, as explained in the $n = 4$ discussion, each quarter of $V(w_1)$ has identical area, if we reflect over the $n = 3$ board to the left of $x = \frac{5p}{6}$ we obtain a feasible arrangement for $n = 5$ as shown in Figure 6.24. For this arrangement we must have $\frac{p}{2} = \frac{5}{6} \times \frac{36}{49}q \Rightarrow p = \frac{60}{49}q$.

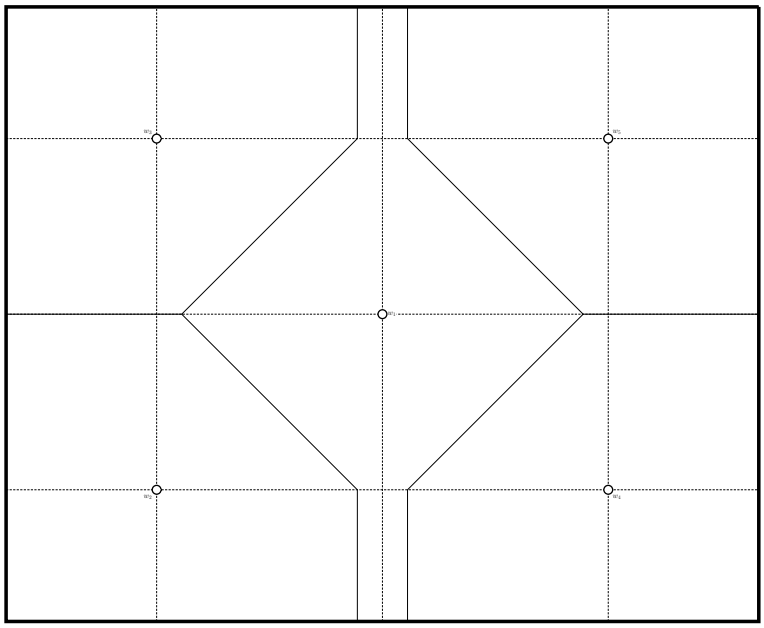

Figure 6.24: White's arrangement $w_1 = (\frac{p}{2}, \frac{q}{2})$, $w_2 = (\frac{p}{5}, \frac{3q}{14})$, $w_3 = (\frac{p}{5}, \frac{11q}{14})$, $w_4 = (\frac{4p}{5}, \frac{3q}{14})$, and $w_5 = (\frac{4p}{5}, \frac{11q}{14})$ for $p = \frac{60}{49}q$.

One may wish to extend this, as was done in the $n = 4$ case, by slotting in the $n = 3$ arrangement to the left of this arrangement, but unfortunately this is not possible as, using identical reasoning to that in the $n = 3 + 3$ argument, this would require $\frac{3p}{8} = \frac{36}{49}q$ from the leftmost (or rightmost) $n = 3$ $\frac{3p}{8} \times q$ subrectangle and $\frac{p}{2} = \frac{8}{9}q$ from the middle $n = 4$ $\frac{p}{2} \times q$ subrectangle which is, again, incompatible.

At this point we may ask if the $n = 3$ arrangement can ever be extended using the $n = 4$ arrangement. For this, both aspect ratios must be satisfied somewhere. That is, for a fixed trial n, $\frac{3p}{n} = \frac{36q}{49}$ must be satisfied within the $n = 3$ arrangement, and $\frac{4p}{n} = \frac{8q}{9}$ must be satisfied within the $n = 4$ arrangement. Alas, these are contradictory, so these arrangements can never coexist within a rectangle.

Finally, for our analysis we shall investigate whether we can adapt the $n = 3$ arrangement to suit a $n = 6$ arrangement. Firstly, all three additional points must lie on the same side of the $n = 3$ arrangement since a solo point on the left of the $n = 3$ arrangement would produce both the $n = 4$ and $n = 3$ arrangements at once (which we know is not possible) and a solo point on the right of the $n = 3$ arrangement would produce a decomposable $n = 5 + 1$ arrangement. Investigating the placement of points to the right of our $n = 3$ arrangement without the formation of the $n = 4$ arrangement, and requiring that at least two points must share a boundary with the rightmost point of the $n = 3$ arrangement, we have the two possibilities as shown in Figure 6.25.

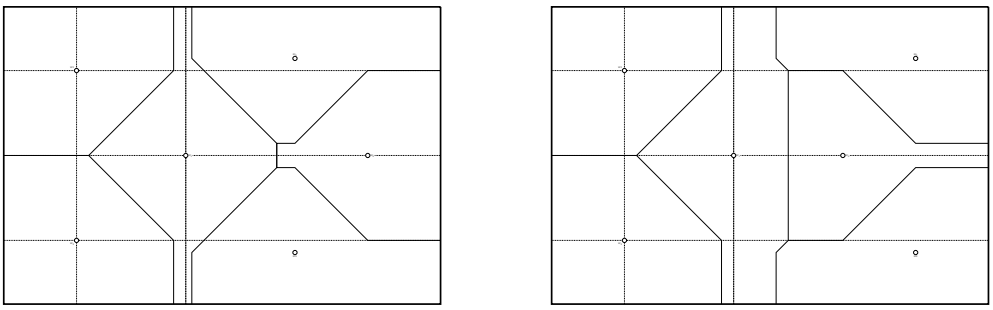

Figure 6.25: The two trial partitions of $\mathcal{P}$ for points to the right of the $n = 3$ arrangement for $n = 6$.

However, as can be seen in Appendix A.4.2, neither of these arrangements is balanced.

At this point the daunting task of finding more balanced non-decomposable arrangements for $n > 3$ may fill us with dismay. But while we await divine inspiration to guide us towards more non-decomposable arrangements, we can comfort ourselves with the following result, summarising some results regarding decomposable arrangements for general n.

Theorem 6.5.1. *For every $n \neq 7$ there exists a rectangle $\mathcal{P}$ and a non-degenerate arrangement W of n points such that W is balanced within $\mathcal{P}$ and no Voronoi cell in $\mathcal{VD}(W)$ is a rectangle.*

Proof. For every $n = 3k + 5l$ with $k, l \in \{0, 1, \ldots\}$, we can construct an arrangement W of n points by combining k blocks of the $n = 3$ arrangement and l blocks of the $n = 5$ arrangement, as shown in Figure 6.26.

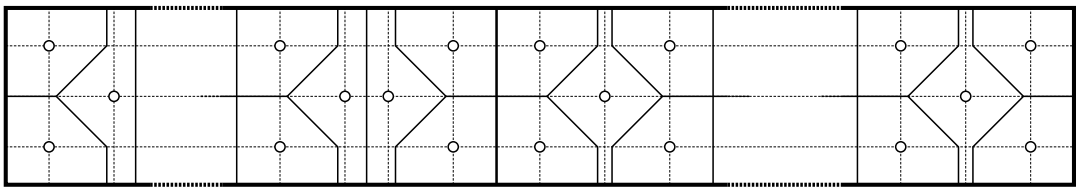

Figure 6.26: An arrangement for $n = 3k + 5l$ for $p = (\frac{36}{49}k + \frac{60}{49}l)q$.

This yields configurations with $n = 3k$ for $k \geq 1$, $n = 3k + 2 = 3(k - 1) + 5$ for $k \geq 1$, or $n = 3k + 1 = 3(k - 3) + 10$ for $k \geq 3$, so we obtain configurations for all $n \geq 8$ and $n = 3, 5, 6$. Since, for every $n = 2k$ with $k \in \{1, 2, \ldots\}$, there also exists an arrangement by combining k blocks of the $n = 2$ arrangement, as shown in Figure 6.18a, we have found an arrangement as desired for every $n \neq 7$. □

Theorem 6.5.1 encapsulates the findings within the chapter. There is a variety of diverse non-grid balanced arrangements for almost any n, and these arrangements can be used as building blocks to create more non-grid balanced arrangements. In addition, we have explored how Black can capitalise upon some of these arrangements.

Chapter 7

Conclusions and Directions for Future Research

This thesis has tackled several open problems in facility location theory and facility game theory. The scenarios considered concern the locating of facilities within an area of continuously distributed demand where distance is measured using the Manhattan metric. Most problems have already been solved for Euclidean distances, highlighting the disparity in research between the two metrics. It is my hope that the thesis draws attention to the exciting additional challenges associated with sculpting solution methods to such problems in the rectilinear plane while exhibiting some creative approaches to their solution, as well as showcasing the beauty of diversity in the intricate structures intrinsic to l_1 Voronoi diagrams.

7.1 Conclusions

The first problems confronted were facility location problems in Chapter 3. Here, given a convex polygonal market region within which n facilities are fixed and a polygonal barrier is situated, we wish to find the optimal location of a new facility so as to optimise some objective. In Section 2.2.1, five problems were suggested for objectives: maximise/minimise the average distance between facilities and customers; minimise the maximum distance between facilities and customers; maximise the area of points for which a prescribed set of facilities is their closest facility; and maximise the area of points, within some predetermined distance of each facility, for which a prescribed set of facilities is their closest facility.

Given that we are considering continuous demand, these objectives are dictated entirely by the Voronoi diagram of the facilities. Pairing this with the Manhattan setting presents our first hurdle: these objectives do not exist in a closed form and instead vary depending on where we consider placing the additional facility. Therefore the objectives can only be optimised if a region is found wherein the new facility produces a Voronoi diagram retaining the same structural properties. Acknowledging this, an algorithm was constructed in Section 3.2 which, for fixed existing facilities and barrier, considers the location of the additional facility restricted within specific regions relative to the existing facilities, barrier, and market region, and we investigated how the Voronoi diagram may change if the location is moved within this space. This approach will ultimately create a partition of the market region into regions within which the objective can be optimised; however, it is unwieldy, unintuitive, and frankly exhausting.

In reaction to the ineffectualities of the algorithm in Section 3.2, an alternative method was offered in Section 3.3. Rather than pursuing the areas in which the objective's formula is maintained, the exact opposite was of interest: what are the lines across which the formula changes? Through this we identified the partition of a convex polygonal market region, within which n facilities are fixed and a polygonal barrier is situated, into convex polygonal cells with the result that the representation of the objective function is preserved for any possible new facility locations in each cell. The partition obtained by Averbakh et al. (2015) for the barrier-free problem was extended by identifying a set of six novel and very dissimilar lines which ensure the preservation of the representation of the objective function by considering

the position of the barrier in relation to the bisector from the barrier-free problem and how its interaction with the bisectors affects the representation of the objective function. These lines were found by exploiting a parametric representation of the objective function when considering its influence from the Voronoi diagram. By this means we were able to prove that polynomial exact algorithms exist for solving the facility location problems with barriers in Section 3.4 by demonstrating how each objective could be assessed, and so optimised, over each partition cell.

Having designed exact algorithms to solve the above facility location problems, we turned our attention to the One-Round Voronoi Game on the rectilinear plane in Chapter 4. Here, one player places n points within a rectangular playing arena followed by the play of another n points by the second player. The player whose points are the closest point for the largest area of the playing arena is crowned the winner.

In order to determine winning strategies for both players, in Section 4.1 we discovered two properties that the first player must ensure that their points obey if they are to win, which we refer to as fairness (Lemma 4.1.2) and local optimality (Lemma 4.1.3). If a player's arrangement of points is both fair and locally optimal then we refer to this arrangement as balanced. A follow-on from these findings was that if the second player could play one point to steal more than $\frac{1}{2n}$ of the playing arena then they could win.

This led to ever stricter classifications of winning arrangements for the first player in Section 4.2 (relating to the horizontal and vertical distances from each point to the perimeter of the area of points for which it is the closest point), ultimately producing the result that the first player can only win if they play their points in a regular row and only if the playing arena is sufficiently wide in relation to its height.

Thus we have resolved the open problem dealing with the One-Round Voronoi Game on the rectilinear plane. We have found cases in which the first player wins and cases in which the second player wins, and have even found optimal strategies for both in the general n game.

A natural extension of the abovementioned work is the One-Round Stackelberg Game on the rectilinear plane. Identically to the One-Round Voronoi Game, two players place points in a rectangular playing arena; however, within this game each player plays to maximise their area captured, not solely to win.

Using the results from the previous chapter, it was found in Section 5.1 that, if all the properties that were found attractive in the Voronoi game were still enforced, the first player should play a regular grid, and it is these arrangements that Chapter 5 explores. Considering firstly the second player's response to their opponent playing a row, we calculated, in Section 5.2, the maximisation of the area stolen from the first player by one point over regions of the playing arena within which the area stolen remains structurally identical. This allowed us both to find the point which steals the most from the first player in Section 5.3.1 and to use this to determine the best response of the second player for even n in Section 5.3.2. We were able to prove that we had found the best response by exploiting the symmetry of one of the second player's singular best points which was not possible for odd n, though an effective (and possibly optimal) response was conjectured.

Analogously to the work done to investigate when the first player plays a row, we then explored in Section 5.4 the maximisation of the areas stolen by one of the second player's points restricted to certain regions if the first player were to play a grid, from where we found the locations which steal the largest area for the second player in Section 5.5.1. These best points, however, were sorely lacking in their ability to suggest successful arrangements for the second player; since they stole a little from a lot of different points of the first player, these best points were lone wolves rather than team players. Therefore in Section 5.5.2 we looked at points resembling those that were useful in Section 5.3.2 (i.e. those positioned closer to one of the first player's points). This allowed us to suggest a similar response for the second player but due to shortcomings in the efficacy of the best singular points these arrangements were not proved to be optimal.

Following this work we wondered how the first player would fare if any of the conditions recommended in Chapter 4 were relaxed. Since the remaining case (i.e. the first player does not play a grid) is incredibly non-restricted we decided to keep the sensible requirement that the first player plays a balanced arrangement, and we ventured into such arrangements in Chapter 6.

In this work we conclusively found all balanced non-grid arrangements for $n = 2$ in Section 6.1 and $n = 3$ in Section 6.3 (even including arrangements producing degenerate bisectors – i.e. involving areas shared between two points – in Sections 6.2 and 6.4). The amount of work to trial all possible non-grid arrangements for $n > 3$ caused us to explore alternative methods to discover non-grid arrangements in Section 6.5, where we used symmetries and concatenations to produce non-grid arrangements for every $n \neq 7$.

We have demonstrated that, beyond grid arrangements, there is a spectrum of balanced arrangements, based on identifying a number of small non-decomposable arrangements that can be concatenated in a strip-like fashion to produce balanced arrangements of size n for almost any $n \in \mathbb{N}$. For every grid arrangement and even some non-grid arrangements we have found the positions, dependent on the aspect ratio of $\mathcal{P}$, of the second player's best point which will steal the largest area from the first player, and have managed to determine the second player's best strategy for the Stackelberg game if the first player plays a row strategy.

7.2 Directions for Future Research

Concerning facility location problems, our derived results are fairly general and can easily be applied to a range of location problems in the rectilinear plane to find exact solutions. The techniques of this thesis are efficacious in proving similar results. The methodology demonstrated for the conditional median and the market share problems should be extendable to the majority of problems in which the objective function is additive, i.e. is the integral of all customers' individual contributions, depending solely on each customer's nearest facility and its location in relation to them. The subproblems over the cells of the derived partitions were solved analytically for the conditional median and the market share problems; however, numerical methods may be required for more complex problems.

There are two further classes of models worth mentioning from the literature where the approach proposed in Section 3.4 may be beneficial. Conditional location problems occur naturally in time-dynamic models (Okabe et al., 2000). Unlike models where all facilities can be constructed simultaneously, in time-dynamic models facilities are constructed not instantaneously but rather in stages, perhaps due to considerations such as limited resources. A typical example of a member of this family of problems is the locating of one new facility per time period as presented in Okabe et al. (2000). A standard goal of these problems is to minimise the total sum of travel times between customers and their closest facility over all time periods.

Finally, as in the case of many of the results proven above, the barrier need not always be convex, and it could be investigated whether it need ever be convex. This work on barrier-constrained facility location problems can also naturally be extended to the multi-barrier problem which would then facilitate the relaxation of a convex market region. The relaxation of the uniform demand assumption was already explored in Byrne (2016) in the barrier-free scenario. However, this was found to be far from a trivial extension as it greatly increases the number of partitioning lines and depends heavily on the degree of the demand function (piecewise polynomial demands were explored) – so much so that current tools cannot find the exact solution for demand beyond a certain specific complexity. A natural extension would be to combine the two results and investigate the problems in the presence of multiple, non-convex barriers where demand is distributed continuously and non-uniformly over a non-convex market region with the hope that the partitioning lines found from each separate problem would be transferable to the joint case.

Additionally, there are still many problems to solve regarding facility location games. Whilst one can guarantee a win in the Voronoi game by a fixed margin, real-world applications rarely allow such exact placements, so it would be interesting to know how this margin varies as a function of the amount that the first player deviates from a row. There are some real-life situations where explicit zoning laws enforce a minimum distance between points; obviously, our results still apply for the limiting case. It seems clear that the second player will be at a serious disadvantage when this lower bound is raised, and this presents an issue which merits closer investigation in future research.

Another important avenue to explore is the adaptation of the game to a polygonal arena (not necessarily rectangular), or one with holes. This will disrupt the power of the symmetric and identically-sized area properties and arm properties that restricted the first player's strategy to playing a regular orthogonal row. In addition to this, it will induce a much more complicated partition since the configuration lines will no longer be the only partitioning lines as the bisectors interact with new corners. A less ambitious and therefore more realistic target would be to play the game with non-uniform demand. After a rebranding of some of our concepts (for example, our equal area and area-symmetric requirements would instead become equal weight and weight-symmetric constraints) it may be that some of our uniform demand results are transferable, and then we could still rely on the geometric comfort that a rectangular playing arena provides.

Perhaps the most tantalising problems deal with the multiple-round game. Our results from Section 4.2 show that for the cases where the first player has a winning strategy, the second player cannot prevent this by any probabilistic or greedy approach: unless the second player blocks one of the first player's key points by placing a point there themselves (which has probability zero for random strategies, and will not happen for simple greedy strategies), the first player can simply play those points as in the one-round game and claim a win. Thus, analysing these key points may indeed be the key to understanding the game.

Stackelberg games also represent an exciting area of study and go some way to answering many interesting and difficult questions. Are there further non-decomposable arrangements? Is it possible to combine them into more intricate two-dimensional patterns rather than just putting together identical strip-based arrangements? Is there some clearer relationship between the feasible degenerate arrangements under the share rule and the discard rule? Beyond that, the biggest challenge is clearly to provide a full characterisation of all balanced arrangements. Furthermore, can we definitively prove that the first player will perform better in the Stackelberg game if they play an arrangement that satisfies the fairness and/or local optimality conditions?

Alongside these questions are the issues of what is the second player's best point, and what is their best arrangement. Even for simple arrangements and small n, these questions are difficult to even begin to approach. This is a new frontier which has not yet been crossed in any metric or any dimension greater than one, and which makes further exploration truly exciting.

References

Abramowitz, M., & Stegun, I. A. (1972). *Handbook of mathematical functions with formulas, graphs, and mathematical tables.* Mineola, NY: Dover.

Ahn, H.-K., Cheng, S.-W., Cheong, O., Golin, M., & van Oostrum, R. (2004). Competitive facility location: the Voronoi game. *Theoretical Computer Science*, *310*(1–3), 457–467.

Aneja, Y. P., & Parlar, M. (1994). Algorithms for Weber facility location in the presence of forbidden regions and/or barriers to travel. *Transportation Science*, *28*(1), 70–76.

Aurenhammer, F., & Klein, R. (2000). Voronoi diagrams. *Handbook of Computational Geometry*, *5*(10), 201–290.

Aurenhammer, F., Klein, R., & Lee, D. T. (2013). *Voronoi diagrams and Delaunay triangulations.* Singapore: World Scientific.

Averbakh, I., Berman, O., Kalcsics, J., & Krass, D. (2015). Structural properties of Voronoi diagrams in facility location problems with continuous demand. *Operations Research*, *62*(2), 394–411.

Bandyapadhyay, S., Banik, A., Das, S., & Sarkar, H. (2015). Voronoi game on graphs. *Theoretical Computer Science*, *562*, 270–282.

Banik, A., Bhattacharya, B. B., Das, S., & Mukherjee, S. (2013). One-round discrete Voronoi game in R^2 in presence of existing facilities. In *Canadian Conference on Computational Geometry (CCCG).*

Barvinok, A. I., Fekete, S. P., Johnson, D. S., Tamir, A., Woeginger, G. J., & Woodroofe, R. (2003). The geometric maximum Traveling Salesman problem. *Journal of the ACM*, *50*, 641–664.

Batta, R., Ghose, A., & Palekar, U. S. (1989). Locating facilities on the Manhattan metric with arbitrarily shaped barriers and convex forbidden regions. *Transportation Science*, *23*(1), 26–36.

Berman, O., & Huang, R. (2008). The minimum weighted covering location problem with distance constraints. *Computers & Operations Research*, *35*(2), 356–372.

Bhadury, J., Eiselt, H. A., & Jaramillo, J. H. (2003). An alternating heuristic for medianoid and centroid problems in the plane. *Computers & Operations Research*, *30*(2), 553–565.

Bischoff, M., & Klamroth, K. (2007). An efficient solution method for Weber problems with barriers based on genetic algorithms. *European Journal of Operational Research*, *177*(1), 22–41.

Byrne, T. (2016). *Conditional facility location problems with piecewise polynomial demand* (MSc dissertation). School of Mathematics, The University of Edinburgh.

Byrne, T., Fekete, S., Kalcsics, J., & Kleist, L. (2021). Competitive location problems: balanced facility location and the one-round Manhattan Voronoi game. In *International Conference and Workshops on Algorithms and Computations (WALCOM) [to appear].*

Byrne, T., Fekete, S. P., Kalcsics, J., & Kleist, L. (2020). Competitive facility location: Balanced facility location and the one-round Manhattan Voronoi game. *arXiv: 2011.13275.*

Byrne, T., & Kalcsics, J. (2020). Conditional facility location problems with continuous demand and a polygonal barrier. *European Journal of Operational Research [under revision].*

Canbolat, M. S., & Wesolowsky, G. O. (2012). On the use of the Varignon frame for single facility Weber problems in the presence of convex barriers. *European Journal of Operational Research*, *217*(2), 241–247.

Cavalier, T. M., & Sherali, H. D. (1986). Euclidean distance location-allocation problems with uniform demands over convex polygons. *Transportation Science*, *20*(2), 107–116.

Cheong, O., Har-Peled, S., Linial, N., & Matousek, J. (2004). The one-round Voronoi game. *Discrete & Computational Geometry*, *31*(1), 125–138.

Choi, J., Shin, C.-S., & Kim, S. K. (1998). Computing weighted rectilinear median and center set in the presence of obstacles. In *International Symposium on Algorithms and Computation (ISAAC)* (pp. 30–40).

Cohen, H. (1993). *A course in computational algebraic number theory.* Berlin: Springer.

Cooper, L. (1963). Location-allocation problems. *Operations Research*, *11*(3), 331–343.

Dearing, P. M., Hamacher, H., & Klamroth, K. (2002). Dominating sets for rectilinear center location problems with polyhedral barriers. *Naval Research Logistics*, *49*, 647–665.

Dearing, P. M., Klamroth, K., & Segars, R. J. (2005). Planar location problems with block distance and barriers. *Annals of Operations Research*, *136*(1), 117–143.

Dehne, F., Klein, R., & Seidel, R. (2005). Maximizing a Voronoi region: The convex case. *International Journal of Computational Geometry & Applications*, *15*(5), 463–475.

Drezner, Z. (1982). Competitive location strategies for two facilities. *Regional Science and Urban Economics*, *12*(4), 485–493.

Drezner, Z. (1995a). *Facility location: A survey of applications and methods.* New York: Springer–Verlag.

Drezner, Z. (1995b). Replacing discrete demand with continuous demand. In Z. Drezner (Ed.), *Facility location: A survey of applications and methods* (chap. 2). New York: Springer–Verlag.

Drezner, Z., & Hamacher, H. W. (Eds.). (2002). *Facility location: Applications and theory.* Berlin Heidelberg New York: Springer–Verlag.

Dürr, C., & Thang, N. K. (2007). Nash equilibria in Voronoi games on graphs. In *European Symposium on Algorithms (ESA)* (pp. 17–28).

Eiselt, H. A., & Laporte, G. (1997). Sequential location problems. *European Journal of Operational Research*, *96*(2), 217–231.

Eiselt, H. A., Pederzoli, G., & Sandblom, C. L. (1985). On the location of a new service facility in an urban area. *Proceedings of the Administrative Sciences Association of Canada*, *6*, 356–372.

Erlenkotter, D. (1989). The general market area model. *Annals of Operations Research*, *18*, 45–70.

Fekete, S. P., Fleischer, R., Fraenkel, A. S., & Schmitt, M. (2004). Traveling Salesmen in the presence of competition. *Theoretical Computer Science*, *313*(3), 377–392.

Fekete, S. P., & Meijer, H. (2005). The one-round Voronoi game replayed. *Computational Geometry*, *30*(2), 81–94.

Fekete, S. P., Mitchell, J. S. B., & Beurer, K. (2005). On the continuous Fermat-Weber problem. *Operations Research*, *53*, 61–76.

Finke, U., & Hinrichs, K. H. (1995). Overlaying simply connected planar subdivisions in linear time. In *Proceedings of the Eleventh Annual Symposium on Computational Geometry* (p. 119–126).

Francis, R. L., & Lowe, T. J. (2019). Aggregation in location. In G. Laporte, S. Nickel, & F. Saldanha da Gama (Eds.), *Location Science* (pp. 537–556). Cham: Springer.

Francis, R. L., & White, J. A. (1974). *Facility layout and locations: An analytic approach.* Englewood Cliffs, N.J.: Prentice Hall.

Gerbner, D., Mészáros, V., Pálvölgyi, D., Pokrovskiy, A., & Rote, G. (2013). Advantage in the discrete Voronoi game. *arXiv preprint arXiv:1303.0523*.

Hakimi, S. L. (1964). Optimal location of switching centers and the absolute centers and medians of a graph. *Operations Research*, *12*, 450–459.

Hamacher, H. W., & Nickel, S. (1995). Restricted planar location problems and applications. *Naval Research Logistics*, *42*(6), 967–992.

Kalcsics, J. (2012). *Location problems on a convex polygon with continuous demand: Characterizing structural properties of voronoi diagrams.* (presentation at ISOLDE XII, Nagoya, Japan)

Katz, I. N., & Cooper, L. (1981). Facility location in the presence of forbidden regions, I: Formulation and the case of Euclidean distance with one forbidden circle. *European Journal of Operational Research*, *6*(2), 166–173.

Kiyomi, M., Saitoh, T., & Uehara, R. (2011). Voronoi game on a path. *IEICE Transactions on Information and Systems*, *94*(6), 1185–1189.

Klamroth, K. (2001). A reduction result for location problems with polyhedral barriers. *European Journal of Operational Research*, *130*(3), 486–497.

Kolen, A. (1981). Equivalence between the direct search approach and the cut approach to the rectilinear distance location problem. *Operations Research*, *29*(3), 616–620.

Küçükaydın, H., Aras, N., & Kuban Altınel, I. (2012). A leader–follower game in competitive facility location. *Computers & Operations Research*, *39*(2), 437–448.

Kusakari, Y., & Nishizeki, T. (1997). An algorithm for finding a region with the minimum total L_1–distance from prescribed terminals. In *International Symposium on Algorithms and Computation (ISAAC)* (pp. 324–333).

Laporte, G., Nickel, S., & Saldanha da Gama, F. (Eds.). (2019). *Location Science*. Springer International Publishing.

Larson, R. C., & Sadiq, G. (1983). Facility locations with the Manhattan metric in the presence of barriers to travel. *Operations Research*, *31*(4), 652–669.

Launhardt, C.-F. (1900). *The principles of location: The theory of the trace. Part I: The commercial trace*. Lawrence Asylum Press, Madras. (A. Bewley, trans., 1900)

Lee, D. T., & Wong, C. K. (1980). Voronoi diagrams in L_1 (L_∞) metrics with 2–dimensional storage applications. *SIAM Journal of Computing*, *9*(1), 200–211.

Lloyd, S. (1982). Least squares quantization in PCM. *IEEE Transactions on Information Theory*, *28*(2), 129-137.

Lösch, A. (1954). *The Economics of Location*. Yale University Press, New Haven. (W.H. Woglom, trans.)

Manne, A. S. (1964). Plant location under economies of scale-decentralization and computation. *Management Science*, *11*, 213–235.

Marucheck, A. S., & Aly, A. A. (1981). An efficient algorithm for the location-allocation problem with rectangular regions. *Naval Research Logistics Quarterly*, *28*, 309–323.

Matisziw, T. C., & Murray, A. T. (2009a). Area coverage maximization in service facility siting. *Journal of Geographical Systems*, *11*(2), 175–189.

Matisziw, T. C., & Murray, A. T. (2009b). Siting a facility in continuous space to maximize coverage of a region. *Socio-Economic Planning Sciences*, *43*(2), 131–139.

Megiddo, N. (1983). Linear-time algorithms for linear programming in R^3 and related problems. *SIAM Journal on Computing*, *12*(4), 759–776.

Mitchell, J. (1992). L_1 shortest paths among polygonal obstacles in the plane. *Algorithmica*, *8*(1), 55–88.

Moore, J. T., & Bard, J. F. (1990). The mixed-integer linear bilevel programming problem. *Operations Research*, *38*(2), 911–921.

Murat, A., Verter, V., & Laporte, G. (2011). A multi-dimensional shooting algorithm for the two-facility location–allocation problem with dense demand. *Computers & Operations Research*, *38*(2), 450–46.

Murray, A. T., O'Kelly, M. E., & Church, R. L. (2008). Regional service coverage modeling. *Computers & Operations Research*, *35*(2), 339–355.

Murray, A. T., & Tong, D. (2007). Coverage optimization in continuous space facility siting. *International Journal of Geographical Information Science*, *21*(7), 757–776.

Newell, F. G. (1973). Scheduling, location, transportation, and continuum mechanics: some simple approximations to optimization problems. *SIAM Journal of Applied Mathematics*, *25*, 346–360.

Okabe, A., & Aoyagi, M. (1993). Spatial competition of firms in a two-dimensional bounded market. *Regional Science and Urban Economics*, *23*, 259–289.

Okabe, A., Boots, B., Sugihara, K., & Chiu, S. N. (2000). *Spatial tessellations: Concepts and applications of Voronoi diagrams*. Chichester, UK: John Wiley and Sons.

Okabe, A., & Suzuki, A. (1987). Stability of spatial competition for a large number of firms on a bounded two-dimensional space. *Environment and Planning A*, *19*(8), 1067–1082.

Oğuz, M., Bektaş, T., & Bennell, J. A. (2018). Multicommodity flows and Benders decomposition for restricted continuous location problems. *European Journal of Operational Research*, *266*(3), 851–863.

Plastria, F. (2001). Static competitive facility location: an overview of optimisation approaches. *European Journal of Operational Research*, *129*(3), 461–470.

Reilly, W. J. (1931). *The law of retail gravitation.* New York, NY: Knickerbocker Press.

Serra, D., & Revelle, C. (1994). Market capture by two competitors: the pre-emptive location problem. *Journal of Regional Science*, *34*(4), 549–561.

Suzuki, A., & Drezner, Z. (1996). The p-center location problem in an area. *Location Science*, *4*(1), 69–82.

Tamir, A., & Mitchell, J. S. (1998). A maximum b-matching problem arising from median location models with applications to the roommates problem. *Mathematical Programming*, *80*(2), 171–194.

Teramoto, S., Demaine, E. D., & Uehara, R. (2006). Voronoi game on graphs and its complexity. In *2006 IEEE Symposium on Computational Intelligence and Games* (pp. 265–271).

von Hohenbalken, B., & West, D. S. (1984). Manhattan versus Euclid: Market areas computed and compared. *Regional Science and Urban Economics*, *14*(1), 19–35.

von Stackelberg, H. (1952). *The theory of the market economy.* Oxford University Press.

Weber, A. (1909). *Theory of the Location of Industries.* University of Chicago Press. (C.J. Friedrich, trans., 1929)

Wei, H., Murray, A. T., & Xiao, N. (2006). Solving the continuous space p-centre problem: planning application issues. *IMA Journal of Management Mathematics*, *17*(4), 413–425.

Weiszfeld, E. V. (1937). Sur le point pour lequel la somme des distances de n points donnés est minimum. *Tohoku Mathematical Journal*, *43*, 335–386.

Wesolowsky, G. O. (1993). The Weber problem: History and perspective. *Location Science*, *1*, 5–23.

Wesolowsky, G. O., & Love, R. F. (1971a). Location of facilities with rectangular distances among point and area destinations. *Naval Research Logistics Quarterly*, *18*, 83–90.

Wesolowsky, G. O., & Love, R. F. (1971b). The optimal location of new facilities using rectangular distances. *Operations Research*, *19*, 124–130.

Wesolowsky, G. O., & Love, R. F. (1972). A nonlinear approximation method for solving a generalized rectangular distance Weber problem. *Management Science*, *18*(11), 656–663.

Xue, G. L., Rosen, J. B., & Pardalos, P. M. (1996). A polynomial time dual algorithm for the Euclidean multifacility location problem. *Operations Research Letters*, *18*(4), 201–204.

Appendix A

MATLAB® code

A.1 MATLAB® code for Section 6.1

We use the MATLAB® inbuilt function `solve` to discover whether there are arrangements which satisfy the equations enforced by Lemmas 4.1.2 and 4.1.3 and to identify them if they exist. For an example of the code producing a solution (or solution set), we have included the code designed to verify the arrangements found in Section 6.1.

```
>> syms y p q positive
>> eqn = [p*y==(q-y)*(p+4*y-2*q)]

eqn =

p*y == (q - y)*(p - 2*q + 4*y)

>> S=solve(eqn, y, 'ReturnConditions', true)

S =

  struct with fields:

              y: [2x1 sym]
     parameters: [1x0 sym]
     conditions: [2x1 sym]

>> S.y

ans =

 q - p/2
     q/2

>> S.conditions

ans =

            p < 2*q
 p < 2*q | 2*q <= p
```

A.2 MATLAB® code for calculations in Section 6.3

This appendix contains the MATLAB® code utilised in the investigation into balanced non-degenerate arrangements for $n = 3$.

A.2.1 Section I

For the arrangement depicted in Figure 6.8a we have the following code.

```
>> syms y x1 y1 x2 y2 p q positive
>> eqnI = [y1*(5*p/6+x1+y-y1)==p*q/3; %Bottom half V(w_1)
x1*(x2-x1+y1+y2)+(x1-x2)^2==p*q/3; %Left half V(w_1)
2*(5*p/6-x1+y-y1)*(x1-x2+y1+y2)-(x1-x2-y1+y2)^2==4*p*q/3; %Right half V(w_1)
x2*(2*q-(x2-x1+y1+y2))==p*q/3; %Left half V(w_2)
(q-y2)*(5*p/6+x2-y+y2)+(y-y2)^2==p*q/3; %Top half V(w_2)
(5*p/6+x2+y-y2)*(x2-x1+y2-y1)+2*(x1-x2)*(x1+x2)==2*p*q/3; %Bottom half V(w_2)
(q-y)*(7*p/6-x2+y-y2)==p*q/3; %Top half V(w)
q*(5*p/6-x1-y+y1)+0.5*(x1-y1-x2+y2)*(2*q+(x2-x1-y2-3*y1)/2)+(y-y2)*(2*q-y-y1)==p*q/3];
                                                                    %Left half V(w)

>> S=solve(eqnI, [y x1 x2 y1 y2 p q], 'ReturnConditions', true)

S =

  struct with fields:

            y: [0x1 sym]
           x1: [0x1 sym]
           x2: [0x1 sym]
           y1: [0x1 sym]
           y2: [0x1 sym]
            p: [0x1 sym]
            q: [0x1 sym]
   parameters: [1x0 sym]
   conditions: [0x1 sym]
```

A.2.2 Section IIa

For the arrangement depicted in Figure 6.8b we have the following code.

```
>> syms y x1 y1 x2 y2 p q positive
>> eqnIIa = [y1*(5*p/6+x1+y-y1)==p*q/3; %Bottom half V(w_1)
x1*(x2-x1+y1+y2)+(x1-x2)^2==p*q/3; %Left half V(w_1)
(x1-x2+y1+y2)*(5*p/6-x1+y-y1)-0.5*(x1-x2-y1+y2)^2==2*p*q/3; %Right half V(w_1)
x2*(2*q-(x2-x1+y1+y2))==p*q/3; %Left half V(w_2)
(q-y2)*(5*p/6+x2-y+y2)==p*q/3; %Top half V(w_2)
(x1+x2)*(x1-x2)-(x1-x2+y1-y2)*(5*p/6+x2+y-y2)/2+(y-y2)^2==p*q/3; %Bottom half V(w_2)
(q-y)*(7*p/6-x2+y-y2)+(y-y2)^2==p*q/3; %Bottom half V(w)
(7*p/6-x2-y+y2)*y-0.5*(x1-x2+3*y1+y2)*(x1-x2-y1+y2)/2==p*q/3]; %Top half V(w)
>> S=solve(eqnIIa, [y x1 x2 y1 y2], 'ReturnConditions', true)

S =

  struct with fields:

            y: [1x1 sym]
```

```
            x1: [1x1 sym]
            x2: [1x1 sym]
            y1: [1x1 sym]
            y2: [1x1 sym]
    parameters: [1x0 sym]
    conditions: [1x1 sym]

>> S.y

ans =

q/2

>> S.x1

ans =

(12*q)/49

>> S.x2

ans =

(12*q)/49

>> S.y1

ans =

(3*q)/14

>> S.y2

ans =

(11*q)/14

>> S.conditions

ans =

49*p == 36*q
```

A.2.3 Section IIb

For the arrangement depicted in Figure 6.8c we have the following code.

```
>> syms y x1 y1 x2 y2 p q positive
>> eqnIIb=[y1*(5*p/6+x1+y-y1)==p*q/3; %Bottom half V(w_1)
x1*(x2-x1+y1+y2)+(x1-x2)^2==p*q/3; %Left half V(w_1)
(x1-x2+y1+y2)*(5*p/6-x1-y+y1)+2*(y-y1)*(y+y1)==2*p*q/3; %Right half V(w_1)
x2*(2*q-(x2-x1+y1+y2))==p*q/3; %Left half V(w_2)
(q-y2)*(5*p/6+x2-y+y2)==p*q/3; %Top half V(w_2)
0.5*(x2-x1+y2-y1)*(10*p/6+x1+x2-2*y+y1+y2)+2*(x1-x2)*(x1+x2)==2*p*q/3; %Bottom half V(w_2)
y*(7*p/6-x1-y+y1)+(y-y1)^2==p*q/3; %Bottom half V(w)
(7*p/6-x1+y-y1)*(q-y)-0.5*(-x1+x2-y1+y2)*(4*q-x1+x2-y1-3*y2)/2==p*q/3]; %Top half V(w)
```

```
>> S=solve(eqnIIb, [y x1 x2 y1 y2], 'ReturnConditions', true)

S =

  struct with fields:

             y: [1x1 sym]
            x1: [1x1 sym]
            x2: [1x1 sym]
            y1: [1x1 sym]
            y2: [1x1 sym]
    parameters: [1x0 sym]
    conditions: [1x1 sym]

>> S.y

ans =

q/2

>> S.x1

ans =

(12*q)/49

>> S.x2

ans =

(12*q)/49

>> S.y1

ans =

(3*q)/14

>> S.y2

ans =

(11*q)/14

>> S.conditions

ans =

49*p == 36*q
```

A.2.4 Section III

For the arrangement depicted in Figure 6.8d we have the following code.

```
>> syms y x1 y1 x2 y2 p q positive
>> eqnIII=[x1*(x2-x1+y2+y1)==p*q/3; %Left half V(w_1)
```

```
y1*(5*p/6+x1+y-y1)==p*q/3; %Bottom half V(w_1)
(x2-x1)*(x1+x2)+0.5*(x1-x2+y2-y1)*(10*p/6+x1+x2+2*y-y1-y2)/2==p*q/3; %Top half V(w_1)
(q-y2)*(5*p/6+x2-y+y2)+(y-y2)^2==p*q/3; %Top half V(w_2)
(2*q+x1-x2-y1-y2)*x2+(x2-x1)^2==p*q/3; %Left half V(w_2)
(5*p/6+x2+y-y2)*(x2-x1-y1+y2)/2-(x2-x1)*(x1+x2)==p*q/3; %Bottom half V(w_2)
(q-y)*(7*p/6-x2+y-y2)==p*q/3; %Top half V(w)
q*(5*p/6-x2+y-y2)-(y-y2)*(y+y2)-0.5*(x1-x2-y1+y2)*(x1-x2+3*y1+y2)/2]; %Left half V(w)
>> S=solve(eqnIII, [y x1 x2 y1 y2], 'ReturnConditions', true)

S =

  struct with fields:

            y: [0x1 sym]
           x1: [0x1 sym]
           x2: [0x1 sym]
           y1: [0x1 sym]
           y2: [0x1 sym]
   parameters: [1x0 sym]
   conditions: [0x1 sym]
```

A.2.5 Section IVa

For the arrangement depicted in Figure 6.8e we have the following code.

```
>> syms y x1 y1 x2 y2 p q positive
>> eqnIVa=[x1*(x2-x1+y2+y1)==p*q/3; %Left half V(w_1)
y1*(5*p/6+x1+y-y1)==p*q/3; %Bottom half V(w_1)
(x2-x1)*(x1+x2)+0.5*(x1-x2+y2-y1)*(10*p/6+x1+x2+2*y-y1-y2)/2==p*q/3; %Top half V(w_1)
(q-y2)*(5*p/6+x2+y2-y)==p*q/3; %Top half V(w_2)
(2*q+x1-x2-y1-y2)*x2+(x2-x1)^2==p*q/3; %Left half V(w_2)
(2*q-x1+x2-y1-y2)*(5*p/6-x2+y-y2)/2+(y2-y)*(2*q-y2-y)==p*q/3; %Right half V(w_2)
(q-y)*(7*p/6-x2+y-y2)+(y2-y)^2==p*q/3; %Top half V(w)
y*(7*p/6-x2-y+y2)-0.5*(x1-x2-y1+y2)*(x1-x2+3*y1+y2)/2==p*q/3]; %Bottom half V(w)
>> S=solve(eqnIVa, [y x1 x2 y1 y2], 'ReturnConditions', true)

S =

  struct with fields:

            y: [1x1 sym]
           x1: [1x1 sym]
           x2: [1x1 sym]
           y1: [1x1 sym]
           y2: [1x1 sym]
   parameters: [1x0 sym]
   conditions: [1x1 sym]

>> S.y

ans =

q/2

>> S.x1
```

```
ans =

(12*q)/49

>> S.x2

ans =

(12*q)/49

>> S.y1

ans =

(3*q)/14

>> S.y2

ans =

(11*q)/14

>> S.conditions

ans =

49*p == 36*q
```

A.2.6 Section IVb

For the arrangement depicted in Figure 6.8f we have the following code.

```
>> syms y x1 y1 x2 y2 p q positive
>> eqnIVb=[x1*(x2-x1+y2+y1)==p*q/3; %Left half V(w_1)
y1*(5*p/6+x1+y-y1)==p*q/3; %Bottom half V(w_1)
(x2-x1)*(x1+x2)+(5*p/6+x1-y+y1)*(x1-x2-y1+y2)/2+(y-y1)^2==p*q/3; %Top half V(w_1)
(q-y2)*(5*p/6+x2+y2-y)==p*q/3; %Top half V(w_2)
(2*q+x1-x2-y1-y2)*x2+(x2-x1)^2==p*q/3; %Left half V(w_2)
(2*q-x1+x2-y1-y2)*(5*p/6-x2-y+y2)/2-((x2-x1-y1+y2)/2)^2==p*q/3; %Right half V(w_2)
(q-y)*(7*p/6-x1+y-y1)-0.5*(x2-x1-y1+y2)*(4*q-x1+x2-y1-3*y2)/2==p*q/3; %Top half V(w)
y*(7*p/6-x1-y+y1)+(y-y1)^2==p*q/3]; %Bottom half V(w)
>> S=solve(eqnIVb, [y x1 x2 y1 y2], 'ReturnConditions', true)

S =

  struct with fields:

            y: [1x1 sym]
           x1: [1x1 sym]
           x2: [1x1 sym]
           y1: [1x1 sym]
           y2: [1x1 sym]
   parameters: [1x0 sym]
   conditions: [1x1 sym]

>> S.y
```

```
ans =

q/2

>> S.x1

ans =

(12*q)/49

>> S.x2

ans =

(12*q)/49

>> S.y1

ans =

(3*q)/14

>> S.y2

ans =

(11*q)/14

>> S.conditions

ans =

49*p == 36*q
```

A.3 MATLAB® code for calculations in Section 6.4

This appendix contains the MATLAB® code utilised in the investigation into balanced degenerate arrangements for $n = 3$.

A.3.1 Figure 6.17g

For the arrangement depicted in Figure 6.17g we have the following code.

```
>> %Figure g
>> syms x t l b r positive
>> eqns = [(x + l)*x == (b + t)^2/4; %Bottom half V(w_2)
l*x + l^2/2 + (t - l)^2/2 == (b + t)^2/4; %Right half V(w_2)
r*(b + t) == (b + t)^2/4; %Right half V(w_1)
(l + r)*t - (t - l)^2/2 == (b + t)^2/4; %Top half V(w_1)
(l + r)*b - (b - x)*(b + x)/2 == (b + t)^2/4] %Bottom half V(w_1)

eqns =

                        x*(l + x) == (b + t)^2/4
```

```
       l*x + l^2/2 + (l - t)^2/2 == (b + t)^2/4
                       r*(b + t) == (b + t)^2/4
         t*(l + r) - (l - t)^2/2 == (b + t)^2/4
 b*(l + r) - ((b + x)*(b - x))/2 == (b + t)^2/4

>> S=solve(eqns, [x t l b r], 'ReturnConditions', true)

S =

  struct with fields:

              x: [0x1 sym]
              t: [0x1 sym]
              l: [0x1 sym]
              b: [0x1 sym]
              r: [0x1 sym]
     parameters: [1x0 sym]
     conditions: [0x1 sym]
```

A.3.2 Figure 6.17j

For the arrangement depicted in Figure 6.17j we have the following code.

```
>> %Figure j
>> syms t l b r t1 l1 b1 d d1 positive
>> eqns = [b1*(r+l1) == (l+r)*(r+l1)/4; %Right half V(w_1)
(t1+b1)*l1 == (l+r)*(r+l1)/4; %Top half V(w_1)
t1*d1 - (d1-l1)^2/2 + (l+r-d-t1)*(r+l1-t-d1) + (l+r-d-t1)^2/2 == (l+r)*(r+l1)/4; %Left half V(w_1)
(l+r)*b == (l+r)*(r+l1)/4; %Bottom half V(w_3)
l*(b+t) - (l+d)*(l-d)/2 == (l+r)*(r+l1)/4; %Left half V(w_3)
r*(b+t) - (l+r-d-t1)^2/2 == (l+r)*(r+l1)/4; %Right half V(w_3)
d*(t+d1) == (l+r)*(r+l1)/4; %Left half V(w_2)
(d+t1)*d1 - (d1-l1)*(d1+l1)/2 == (l+r)*(r+l1)/4; %Top half V(w_2)
(d+t1)*(t-l+d) + (d+l)*(l-d)/2 == (l+r)*(r+l1)/4]; %Bottom half V(w_2)
>> S=solve(eqns, [t l b r t1 l1 b1 d d1], 'ReturnConditions', true)

S =

  struct with fields:

              t: [0x1 sym]
              l: [0x1 sym]
              b: [0x1 sym]
              r: [0x1 sym]
             t1: [0x1 sym]
             l1: [0x1 sym]
             b1: [0x1 sym]
              d: [0x1 sym]
             d1: [0x1 sym]
     parameters: [1x0 sym]
     conditions: [0x1 sym]
```

A.3.3 Figure 6.17k

For the arrangement depicted in Figure 6.17k we have the following code.

```
>> %Figure k
>> syms t l b r t1 l1 b1 d d1 positive
>> eqns = [b1*(r+l1) == (l+r)*(r+l1)/4; %Right half V(w_1)
(t1+b1)*l1 == (l+r)*(r+l1)/4; %Top half V(w_1)
t1*d1-(d1-l1)^2/2+(l+r-d-t1)*t+(l+r-d-t1)^2/2 == (l+r)*(r+l1)/4; %Left half V(w_1)
(l+r)*b == (l+r)*(r+l1)/4; %Bottom half V(w_3)
l*(b+t) == (l+r)*(r+l1)/4; %Left half V(w_3)
d*t-(d-l)^2/2+t1*(l1+r-d1-t)+(l1+r-d1-t)^2/2 == (l+r)*(r+l1)/4; %Top half V(w_3)
t1*t == d*d1; %Top left and bottom right quadrants V(w_2)
(d+t1)*t-(d+l)*(d-l)/2 == (l+r)*(r+l1)/4; %Bottom half V(w_2)
t1*(d1+t)-(d1-l1)*(d1+l1)/2 == (l+r)*(r+l1)/4]; %Right half V(w_2)
>> S=solve(eqns, [t l b r t1 l1 b1 d d1], 'ReturnConditions', true)

S =

  struct with fields:

            t: [0x1 sym]
            l: [0x1 sym]
            b: [0x1 sym]
            r: [0x1 sym]
           t1: [0x1 sym]
           l1: [0x1 sym]
           b1: [0x1 sym]
            d: [0x1 sym]
           d1: [0x1 sym]
   parameters: [1x0 sym]
   conditions: [0x1 sym]
```

A.4 MATLAB® code for calculations in Section 6.5

This appendix contains the MATLAB® code utilised in the investigation into balanced arrangements for $n = 4$ and $n = 6$.

A.4.1 Figure 6.19

For the arrangement depicted in Figure 6.19 we have the following code.

```
>> syms y p q positive
>> eqns = [q*(5*p-4*q+8*y)/16 + (q/2-y)^2 == p*q/4; %Bottom horizontal left
q*(3*p+4*q-8*y)/16 - (q/2-y)^2 == p*q/4; %Left vertical bottom
y*(3*p+4*q-8*y) == p*q] %Bottom horizontal bottom

eqns =

 (q/2 - y)^2 + (q*(5*p - 4*q + 8*y))/16 == (p*q)/4
 (q*(3*p + 4*q - 8*y))/16 - (q/2 - y)^2 == (p*q)/4
                        y*(3*p + 4*q - 8*y) == p*q

>> S=solve(eqns, [y p q], 'ReturnConditions', true)

S =

  struct with fields:
```

```
             y: [1x1 sym]
             p: [1x1 sym]
             q: [1x1 sym]
    parameters: [1x1 sym]
    conditions: [1x1 sym]

>> S.y

ans =

z/6

>> S.p

ans =

(8*z)/9

>> S.q

ans =

z
```

A.4.2 Figure 6.25

For the arrangements depicted in Figure 6.25 we have the following code.

```
>> %n=6 I
>> syms x1 x2 y p q positive
>> eqns = [(x2-5*p/12)*q - ((x2+5*p/12)-(x1+5*p/12-q/2+y))*(y+(y+q/2-x1+x2)/2) == p*q/6;
                                                                    %bottomright V(w_1)
(x1-(x1+5*p/12-q/2+y)/2)*(y+q/2-x1+x2) - ((y+q/2-x1+x2)/2-y)^2 == p*q/6; %left V(w_4)
(p-(x1+5*p/12-q/2+y)/2)*y == p*q/12; %bottom V(w_4)
(p-x1)*(y+q/2-x1+x2) - (2*p-x2-x1)*(x2-x1) == p*q/6; %right V(w_4)
(p-x2)*(q/2-(y+q/2+x1-x2)/2) == p*q/24; %bottomright V(w_6)
(x2-5*p/12)*(q/2-(y+q/2+x1-x2)/2) - (x1-5*p/12)*(x2-x1) == p*q/12]; %bottomleft V(w_6)
>> S=solve(eqns, [x1 x2 y p q], 'ReturnConditions', true)

S =

  struct with fields:

            x1: [0x1 sym]
            x2: [0x1 sym]
             y: [0x1 sym]
             p: [0x1 sym]
             q: [0x1 sym]
    parameters: [1x0 sym]
    conditions: [0x1 sym]

>> %n=6 II
>> syms x1 x2 y p q positive
>> eqns = [(x2-5*p/12)*q - ((x2+5*p/12)-(x1+5*p/12-q/2+y))*(y+(y+q/2-x1+x2)/2) == p*q/6;
                                                                  %bottomright V(w_1)
(x1-5*p/12+q/2-y)*y + ((x1-x2+q/2-y)/2)^2 + (x2-5*p/12)*(q/2-y-x1+x2)/2 == p*q/6;
```

```
                                                                    %left V(w_4)
(p-(x1+5*p/12-q/2+y)/2)*y == p*q/12; %bottom V(w_4)
(p-x1)*(q/2+y+x1-x2) == p*q/6 %right V(w_4)
(x2-5*p/12)*(q/2-y+x1-x2) == p*q/6; %bottomleft V(w_6)
(p-x2)*(q/2-(q/2+y+x1-x2)/2) + 0.5*(x1-x2)^2 == p*q/24]; %bottomright V(w_6)
>> S=solve(eqns, [x1 x2 y p q], 'ReturnConditions', true)

S =

  struct with fields:

           x1: [0x1 sym]
           x2: [0x1 sym]
            y: [0x1 sym]
            p: [0x1 sym]
            q: [0x1 sym]
   parameters: [1x0 sym]
   conditions: [0x1 sym]
```